SEDIMENTOLOGY AND HISTORY OF DEGLACIATION IN THE DRYDEN, ONTARIO AREA, AND THEIR BEARING ON THE HISTORY OF LAKE AGASSIZ

A THESIS
PRESENTED TO
THE FACULTY OF GRADUATE STUDIES
UNIVERSITY OF MANITOBA
IN PARTIAL FULFILLMENT
OF THE REQUIREMENTS FOR THE DEGREE

MASTER OF SCIENCE

TIMOTHY A. WARMAN

MAY 1991

ISBN 0-315-77013-9

SEDIMENTOLOGY AND HISTORY OF DEGLACIATION IN THE DRYDEN, ONTARIO AREA, AND THEIR BEARING ON THE HISTORY OF LAKE AGASSIZ

BY

TIMOTHY A. WARMAN

A thesis submitted to the Faculty of Graduate Studies of the University of Manitoba in partial fulfillment of the requirements of the degree of

MASTER OF SCIENCE

ABSTRACT

During the deglaciation of the Dryden area of northwestern Ontario, long, arcuate end moraines, eskers, isolated fans ("kames") and glaciolacustrine rhythmites were deposited. These deposits are comprised of eight distinct facies; silt-clay rhythmites, sand-clay rhythmites, sand-silt rhythmites, current-bedded sand, pebbly sand, clast-supported gravel, matrix-supported gravel, and matrix supported diamict. Depositional processes were dominated by high and low-density underflows, and gravity flows, with minor wave-reworking in some areas. Paleocurrents in these deposits are almost entirely unidirectional and away from the moraines. Moraines and isolated fans show an upward and distal fining from coarse gravel to fine-grained rhythmites. The vertical distribution of paleo-water depth indicators such as subaerial delta surfaces, wave ripples, and clay sediments suggest that the majority of the moraines and isolated fans were deposited subaqueously. Eskers were deposited both in subglacial meltwater tunnels, and subaqueously at the margins of these tunnels. These features therefore represent subaqueous outwash deposits formed within and at an ice margin standing in Lake Agassiz. Isolated fans are the result of discharge from short-lived glacial meltwater tunnels, while eskers represent discharge within and from the mouths of more stable, long-lived conduits. The laterally continuous end moraines are coalesced fans (and minor deltas) which formed during periods of enhanced meltwater output. These pulses of meltwater are interpreted as penecontemporaneous along the entire margin of the Rainy Lobe, probably discharging through a broad system of bifurcating meltwater conduits. Rhythmites deposited on the distal areas of the fans are interpreted as varves, produced by low-density underflows and vertical settling of clays, during and between the meltwater pulses. The varve record in the Dryden area spans almost 1000 years.

New sedimentological and stratigraphic data from Dryden and elsewhere in northwestern Ontario have permitted a re-interpretation of the deglaciation history of northwestern Ontario. The Fort Frances-Rainy River area was

deglaciated, and the Eagle-Finlayson moraine formed, at approximately 11 ka. Lake Agassiz stood at the Herman level at that time. Retreat of the Rainy lobe from the Eagle-Finlayson moraine resulted in the opening of the Shebandowan or Dog-Kaministikwia outlets to the Superior basin. The Clearwater outlet in Saskatchewan may also have been open during this time. The resultant drop in lake levels and abandonment of the southern outlet marked the start of the Moorhead Phase of Lake Agassiz, and caused exposure of the floor of the lake along the southern margins of the Agassiz basin and formation of the Moorhead Delta at Fargo, North Dakota. The southern Manitoba basin, including Lake Manitoba, and the Dryden area remained inundated by Lake Agassiz. This early Moorhead Phase lake level is not represented by any of the currently recognized and named strandlines, and is here informally referred to as the early Moorhead level. The Dryden area was probably deglaciated, and the Hartman moraine, between 21-64 km to the north, began forming, by about 10.4 ka. The ice may have retreated a further 56 km to the north after 10.4 ka, allowing the Kaiashk eastern outlet to open. However, by about 10.1 ka, the Rainy lobe had readvanced approximately 30 km to form the Lac Seul moraine. The correlative Marquette readvance of the Superior lobe to the Dog Lake-Marks moraine position near Thunder Bay caused the formation of Lake Kaministikwia. Lake Agassiz rose from the Moorhead level to the Norcross level at this time due to closure of the eastern outlets. If it had opened earlier, the Clearwater outlet was also closed by this time. This rise in water level resulted in a transgression in the southern part of the Lake Agassiz basin, and marked the beginning of the Emerson Phase. Lake Kaministikwia was confluent with Lake Agassiz, and flow towards the southern outlet carried red clay throughout northwestern Ontario, resulting in deposition of the red clay marker unit. Ice retreated from the Lac Seul moraine and formed the Sioux Lookout moraine at about 9.8 ka. Downcutting of the southern outlet eventually resulted in a drop in Lake Agassiz to the Campbell level, although water levels remained above the Campbell strandline until at least 9.5 ka. Retreat from the Sioux Lookout moraine resulted in the opening of the eastern outlets of Lake Agassiz, allowing

water to drop below the Campbell level. This marked the beginning of the Nipigon phase, which likely began around 9.4 ka. During this time, northwestern Ontario gradually became subaerially exposed, and the sub-Campbell beaches were formed.

ACKNOWLEDGEMENTS

I would like to thank my supervisor, Dr. Jim Teller, for numerous helpful discussions and comments, and also for his patience. I would also like to thank the other members of my committee, Dr. Norm Halden of the University of Manitoba, and Dr. Harvey Thorleifson of the Geological Survey of Canada, as well as Dave Sharpe, also of the GSC. This thesis would have been a much poorer work without their insight and advice.

This project was funded through a Canada-Ontario Mineral Development Agreement, administered by Dave Sharpe of the GSC, and through an NSERC Operating Grant to Dr. J.T. Teller. Financial assistance while at the University of Manitoba from Kim, and from Mom and Dad is also gratefully acknowledged. Field work was carried out while employed as a summer student at the Geological Survey of Canada by Dave Sharpe and Harvey Thorleifson. Able assistance was provided in the field by Patsy Rossi and Shaun Pelkey.

The support of my friends and fellow grad-students at the University of Manitoba helped me to survive two Winnipeg winters.

Finally, I would like to thank Kim Telford, who helped me in more ways than she can imagine.

TABLE OF CONTENTS

ABSTRACT ii

ACKNOWLEDGEMENTS v

TABLE OF CONTENTS vi

LIST OF FIGURES ix

CHAPTER

1 INTRODUCTION AND METHODOLOGY

1.1 INTRODUCTION 1
1.2 OBJECTIVES 3
1.3 METHODOLOGY 7
1.3.1 FIELD WORK 7
1.3.2 SECTION LOGGING 7
1.3.3 REFLECTION SEISMIC 9
1.3.4 SUBBOTTOM ACOUSTIC PROFILES 9
1.3.5 ROTASONIC DRILLING 11
1.3.6 WATER WELL RECORDS 12
1.3.7 GEOCHEMICAL ANALYSES 12
1.3.8 MINERALOGICAL ANALYSES 13
1.3.9 GRAIN SIZE ANALYSE 15

2 DESCRIPTION OF THE SEDIMENTS

2.1 INTRODUCTION 16
2.2 FACIES DESCRIPTIONS 16
2.2.1 SILT-CLAY RHYTHMITES (FACIES 1) 16
GREY SEQUENCE 16
RED SEQUENCE 23
RHYTHMITE THICKNESS 30
GRAIN SIZE 32
MINERALOGY 32
GEOCHEMISTRY 34
GEOMETRY 42
2.2.2 SANDY RHYTHMITES (FACIES 2) 42
DESCRIPTION 42
RED SEQUENCE 52
GEOMETRY 54

2.2.3 RHYTHMICALLY-BEDDED SAND AND SILT (FACIES 3) 54
DESCRIPTION 54
GEOMETRY 57
2.2.4 NON-RHYTHMIC, CURRENT-BEDDED SAND (FACIES 4) 57
DESCRIPTION 57
GEOMETRY 59
2.2.5 PEBBLY SAND (FACIES 5) 68
DESCRIPTION 68
GEOMETRY 75
2.2.6 CLAST-SUPPORTED GRAVEL (FACIES 6) 75
DESCRIPTION 75
GEOMETRY 79
2.2.7 MATRIX-SUPPORTED GRAVEL (FACIES 7) 82
DESCRIPTION 82
GEOMETRY 82
2.2.8 MASSIVE, MATRIX-SUPPORTED DIAMICT (FACIES 8) 84
DESCRIPTION 84
GEOMETRY 84
2.3 GEOGRAPHIC DISTRIBUTION OF FACIES 84
2.4 VERTICAL FACIES SEQUENCES 87
2.5 LATERAL FACIES SEQUENCES 97
2.6 PALEOCURRENT DATA 99

3 ORIGIN OF THE SEDIMENTS

3.1 FACIES INTERPRETATIONS 105
3.1.1 RHYTHMITES (FACIES 1, 2 & 3) 105
UNDERFLOWS 105
PERIODICITY OF THE UNDERFLOWS 107
RED CLAY RHYTHMITES 111
NOTABLE FEATURES OF THE FACIES 2 SANDY RHYTHMITES 116
3.1.2 CURRENT-BEDDED SAND (FACIES 4) 118
3.1.3 PEBBLY SAND (FACIES 5) 122
3.1.4 CLAST-SUPPORTED GRAVEL (FACIES 6) 123
3.1.5 MATRIX-SUPPORTED GRAVEL (FACIES 7) 126
3.1.6 MASSIVE, MATRIX-SUPPORTED DIAMICT (FACIES 8) 127

4 DEPOSITIONAL ENVIRONMENT AND FACIES MODEL

4.1 DEPOSITIONAL ENVIRONMENT 128
4.2 FACIES MODEL 137
4.3 COMPARISONS WITH OTHER MODELS 141
4.4 FORMATION OF THE ESKERS, KAMES AND MORAINES 144
4.5 POSSIBLE CAUSES AND MECHANISMS FOR MELTWATER DISCHARGE 151

5 HISTORY OF DEGLACIATION AND LAKE AGASSIZ

5.1 INTRODUCTION 155
5.2 CONSTRAINTS ON LAKE AGASSIZ WATER LEVELS 162
5.3 IMPLICATIONS FOR THE CURRENTLY ACCEPTED CHRONOLOGY OF LAKE AGASSIZ 166

6 SUMMARY OF THE DEPOSITIONAL MODEL AND INTEGRATION WITH THE LAKE AGASSIZ MODEL

6.1 SUMMARY OF THE DEPOSITIONAL MODEL 173
6.2 INTEGRATION OF THE DEPOSITIONAL AND LAKE AGASSIZ MODELS 175

REFERENCES CITED 183

APPENDIX

A ANNOTATED GRAPHIC LOGS FOR ALL SECTIONS AND SONIC CORES 194

B DESCRIPTION OF THE SAMPLE SUITE, INCLUDING ANALYSES PERFORMED 238

C GEOCHEMICAL DATA 240

D MINERALOGICAL DATA 253

E GRAIN SIZE DATA 255

LIST OF FIGURES

FIGURE

1-1	Location of study area	2
1-2	Simplified Quaternary geology of the Dryden area	4
1-3	Currently accepted moraine formation model	5
1-4	Seismic, sonar and drill hole locations	10
2-1	Section locations	17
2-2	Facies 1 silt-clay rhythmites at section 87-5	18
2-3	Bioturbation on surface of rhythmites at section 87-5	20
2-4	Carbonate concretions from section 87-5	21
2-5	Concretion beach at section 87-5	22
2-6	Small-scale faulting in rhythmites at section 89-1	24
2-7	Small-scale slumping in rhythmites at section 87-5	25
2-8	Transition from Facies 2 to1 at section 87-24	26
2-9	Red clay rhythmites at section 87-19	27
2-10	Red band on grey laminae at base of redrhythmites (87-24)	29
2-11	Rhythmite thickness plots	31
2-12	Grain size plots	33
2-13	Vertical plots of significant element concentrations	36, 37
2-14	Vertical plots of non-significant element concentrations	38
2-15	Rare Earth Element plots	40
2-16	Sketch of section 89-1	43
2-17	Large-scale slumping in Facies 1 at section 87-20	44
2-18	Facies 1 infilling scours at crest of Hartman moraine (87-11)	45
2-19	Facies 2 sandy rhythmites at section 87-20	46
2-20	Lee-side ripples in Facies 2 at section 87-27	48
2-21	Wave ripples in Facies 2 at section 87-2	49
2-22	Opposing ripples in Facies 2 at section 87-27	50
2-23	Soft-sediment deformation in Facies 2 at section 87-3	53
2-24	Facies 3 sand-silt rhythmites at section 87-24	55
2-25	Flame structures in Facies 3 at section 87-2	56
2-26	Sketch of upper part of section 88-2	58
2-27	Facies 4 sands sandwiched between gravel bodies (87-2)	60
2-28	Facies 4 tabular sand grading into crossbedded channel fill (87-2)	61
2-29	Trough-crossbedding in Facies 4 at section 87-2	62

2-30 Facies 4 tabular sand in lee of gravel bedform at section 87-2 63
2-31 Large-scale foresets at section 88-6 64
2-32 Ripples going up foresets at section 88-6 65
2-33 Scour around boulders at section 88-6 66
2-34 Sketch of lower part of section 88-2 67
2-35 Crossbedding in sands at section 87-11 69
2-36 Ripples in Facies 4 sands at section 88-9 70
2-37 Horizontal bedding in Facies 4 sands at section 88-4 71
2-38 Facies 5 pebbly sands at section 88-4 72
2-39 Horizontal bedding in Facies 5 pebbly sands at section 88-4 73
2-40 Normal grading in Facies 5 pebbly sands at section 88-5 74
2-41 Sketch of section 88-4 76
2-42 Sketch of section 87-23 77
2-43 Facies 6 clast-supported gravel at section 87-2 78
2-44 Imbrication in Facies 6 gravels at section 88-9 80
2-45 Foresets in Facies 6 gravel at section 87-2 81
2-46 Facies 7 matrix-supported gravels at section 88-6 83
2-47 Facies 8 diamict at section 88-2 85
2-48 Red clay distribution in the Dryden area 88
2-49 Graphic drill core logs 89
2-50 Facies 6 gravels over rhythmites at section 88-9 91
2-51 Fining upward sequence at section 87-23 93
2-52 Sketch of section 87-27 94
2-53 Seismic profile 95
2-54 Sonar profile 96
2-55 Slumping in sonar profile 98
2-56 Red clay from north and south of the Hartman moraine 100
2-57 Paleoflow map 102
2-58 Paleoflow comparisons 103
2-59 Opposing paleoflows 104
3-1 Configuration of L. Agassiz & L. Kam at red clay deposition 113
3-2 Outcrop area of Sibley beds 115
3-3 Flow separation figure 119
3-4 Slumping on foresets at section 87-2 120
4-1 Moraine cross-sections 133
4-2 Quaternary geology with topographic contours 134
4-3 Plan view facies model 138
4-4 Morainal banks from various sources 145
4-5 Model of esker and kame formation 147

4-6 Models of moraine formation 149
5-1 Lake Agassiz water level history 156
5-2 Moraine positions and names 157
5-3 Strandline diagram of Teller & Thorleifson (1983) 160
5-4 Constraints on the water level history at Dryden 164
5-5 Revised Moorhead and Emerson Phase water levels 168
6-1 Summary diagram of nw Ontario history, pt. I 176
6-2 Summary diagram of nw Ontario history, pt. II 179
6-3 Summary diagram of nw Ontario history, pt. III 181

CHAPTER 1: INTRODUCTION AND METHODOLOGY

1.1 INTRODUCTION:

As the Laurentide Ice Sheet retreated across northwestern Ontario during the late Wisconsinan, much of its margin was continually in contact with the relatively deep waters of proglacial Lake Agassiz, the largest of several lakes which formed along the southern margin of the ice sheet. Interactions between the lake and the ice sheet would likely have operated in a complex, two-way system with both positive and negative feedback mechanisms.

Isostatic depression of the crust, extensive meltwater production and blockage of northward drainage into Hudson Bay by the ice were responsible for creating Lake Agassiz. The ice sheet formed the northern and sometimes the eastern boundary of the lake, and also controlled the availability of the lake's outlets. The specific outlets used controlled the extent, water depth, and internal flow patterns of the lake.

Lake Agassiz, in turn, would likely have had a strong influence on the dynamics, flow regime and hydrology of the ice sheet. Both Lake Agassiz and the ice sheet would have controlled the nature, distribution and amount of proglacial, and possibly subglacial, sedimentation in the area.

The Dryden-Wabigoon Lake area (Fig. 1-1) was chosen for this study because of the availability of, and easy access to, excellent exposures of sediments representing the sedimentary record of deglaciation in northwestern Ontario.

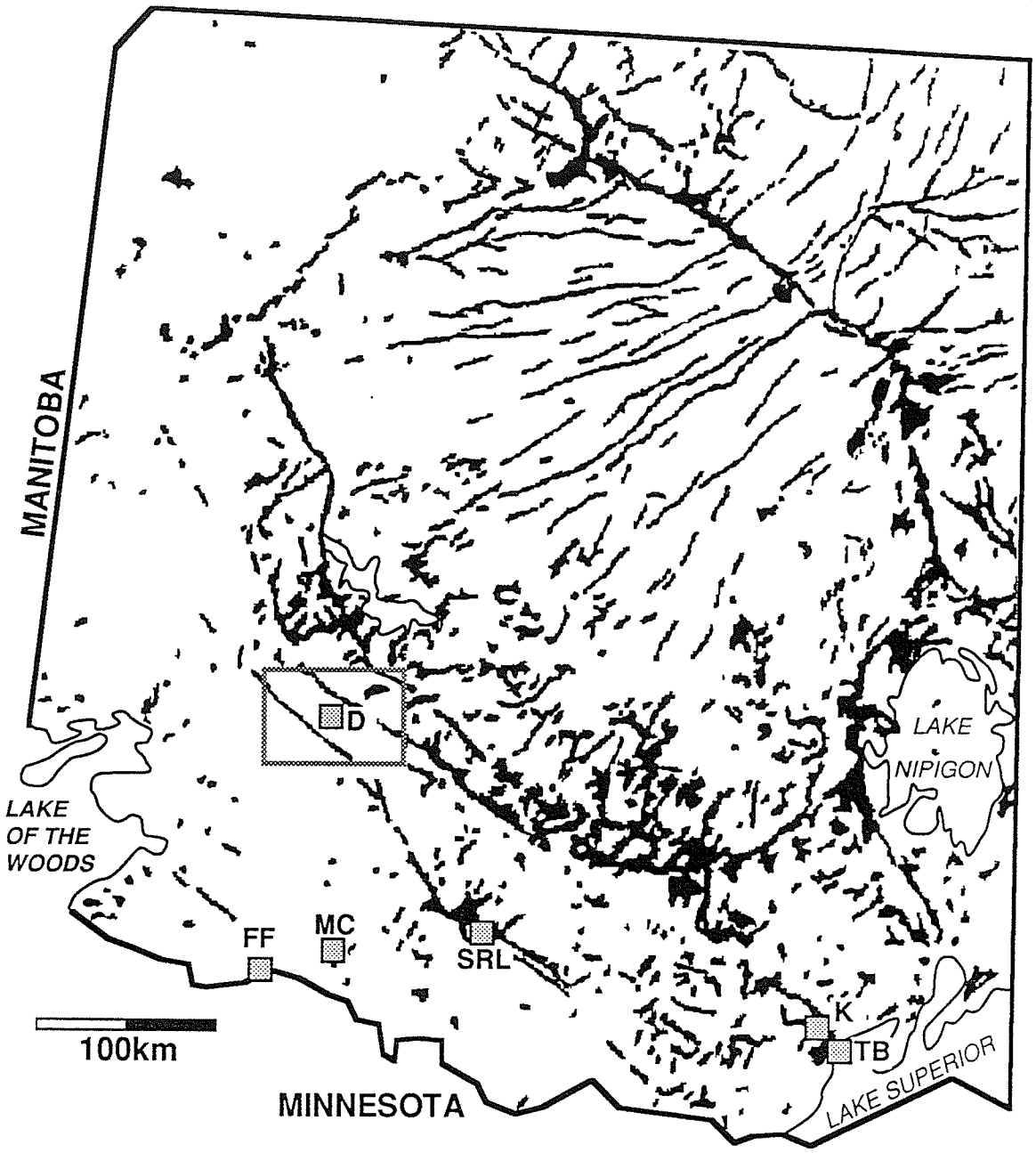

Fig. 1-1 The large-scale pattern formed by sand and gravel bodies in northwestern Ontario, and location of places mentioned in the text. D-Dryden, FF-Fort Frances, MC-Mine Centre, SRL-Steep Rock Lake, K-Kaministikwia, TB-Thunder Bay. The box indicates the study area around Dryden. Note the lobate form outlined by the major end and "interlobate" moraines and the central splayed pattern of major eskers which feed the end moraines (after Sado & Carswell, 1987).

1.2 OBJECTIVES:

The goals of this study were to determine the nature of unconsolidated sediments in the area, to determine the sedimentary processes responsible for these deposits, and to then re-examine the deglaciation history of the area, including the history of Lake Agassiz.

It has been recognized that moraines in the Dryden area (Fig. 1-2) are composed of sorted and stratified materials displaying abundant sedimentary structures indicating deposition by flowing water (Moorhouse, 1941; Satterley, 1946, 1960; Zoltai, 1961, 1965; Cowan, 1987). This differs significantly from the composition implied by most moraine models which tend to envisage moraines as being composed mainly of unstratified, unsorted "till", which has been piled up at a stationary ice margin by slumping, bulldozing, and/or glaciotectonic thrusting (Fig. 1-3)(Oldale & O'Hara, 1984; Thomas, 1984a; Eyles & Eyles, 1984; Mustard & Donaldson, 1987; Powell & Molnia, 1989; Josenhans & Fader, 1989). Thus, a careful examination of the moraines in the area (the Eagle-Finlayson and Hartman moraines) was undertaken.

The relationship between the large, coarse-grained end moraines, and the finer, rhythmically-laminated sediments (rhythmites) associated with them was also examined. These rhythmites had previously been studied by Rittenhouse (1933, 1934), and interpreted as varves. Varve chronologies based on this interpretation have been devised not only for the Dryden area, but for other locations in northwestern Ontario (Antevs, 1951). However, the general interpretation of rhythmically-laminated silts and clays as varves has been

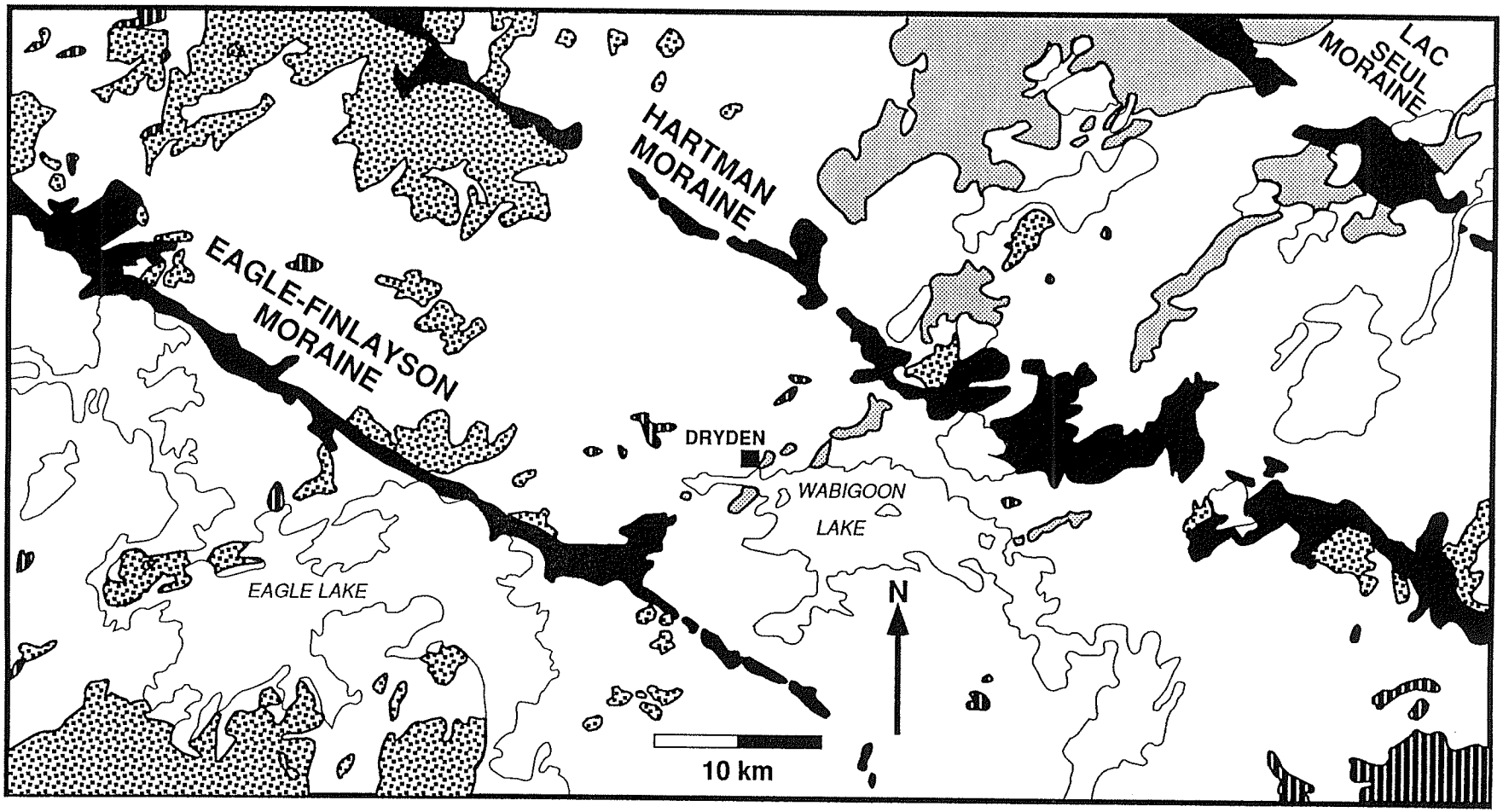

Fig. 1-2 Simplified surficial geology of the study area, after Cowan & Sharpe (1991) and Minning & Sharpe (1991).

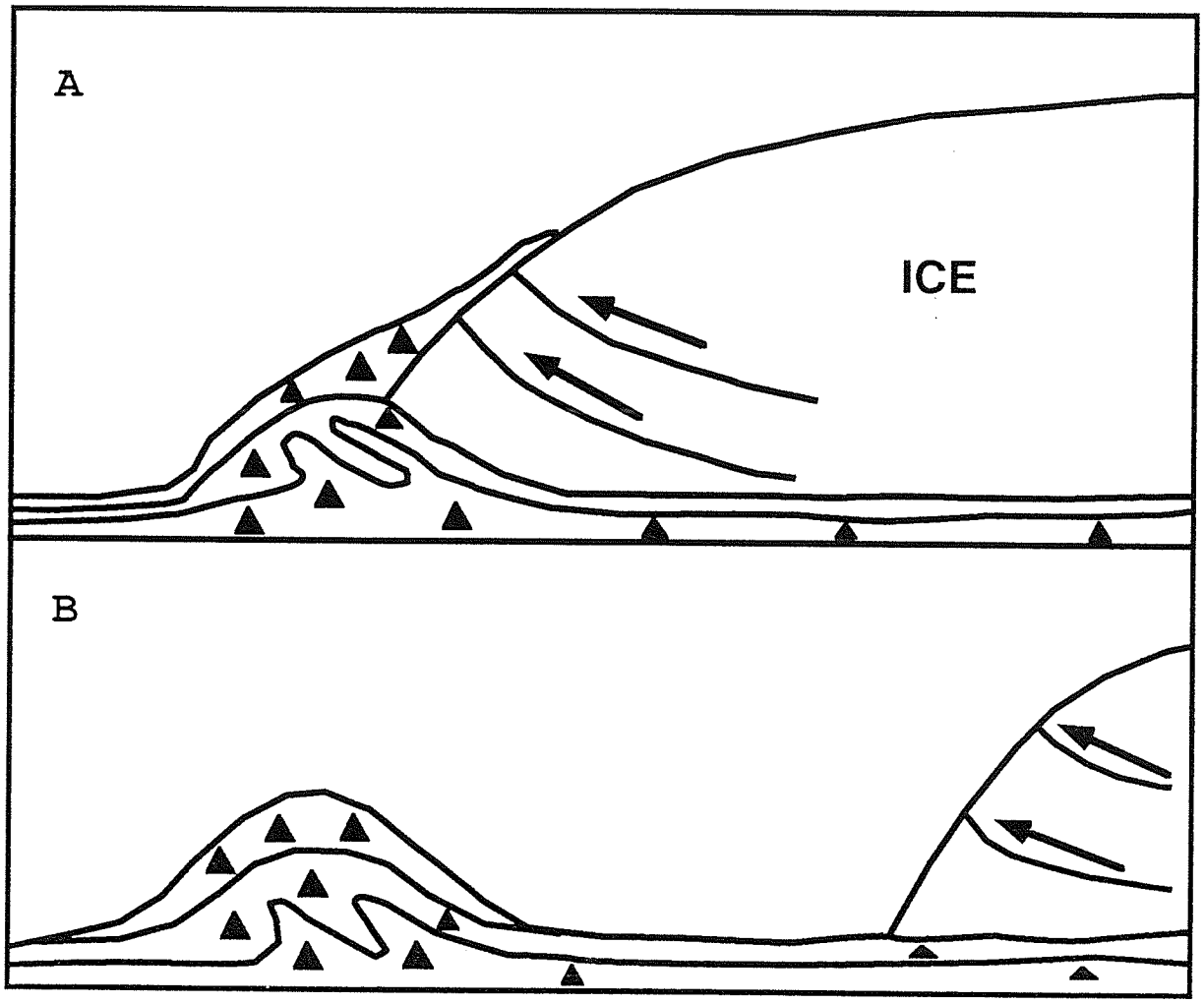

Fig. 1-3 Standard model for the formation of major end moraines. This model has been applied to both subaerial and subaqueous deposits.

challenged (Eyles & Miall, 1984, Lambert & Hsu, 1979), and the Dryden rhythmites therefore required re-examination.

Another problematic aspect of these rhythmites is the presence of a series of unusually thick, red-clay rhythmites in an otherwise monotonous grey-clay rhythmite sequence. These "abnormal" rhythmites were studied by Rittenhouse (1933, 1934) who explained them as being related to the drainage of a higher proglacial lake into the Wabigoon basin of Lake Agassiz. The distinctive red colour of the clays has been attributed to a different provenance by Rittenhouse (1933, 1934) and to a water geochemistry effect by Cowan (1987). The red-clay rhythmites at Dryden have also been correlated with red clay units elsewhere in northwestern Ontario (Antevs, 1951; Zoltai, 1961; Teller & Thorleifson, 1983; Bajc, pers. comm., 1991). By a careful examination and sampling of the red-clay rhythmites, and of red clay units from elsewhere in northwestern Ontario, it was hoped that some of these hypotheses could be tested.

Economic mineral deposits have previously been found in the study area, but large areas still remain unexplored due to the thick cover of proglacial lake deposits. Another problem is the scarcity of diamict units, particularly ones which can be identified as lodgement or meltout tills, since these are the standard sampling mediums for geochemical drift prospecting. An evaluation of the potential for finding buried lodgement tills, or of utilizing the proglacial lake sediments for drift prospecting was attempted.

1.3 METHODOLOGY:

1.3.1 Field Work:

Two months were spent in the study area during the summers of 1987 and 1988. Additional trips were made in the fall of 1987 and 1988, and in the summer of 1989. All navigable roads in the area were traversed by four-wheel drive truck, and most of the shore and islands of Wabigoon Lake, Thunder Lake and Sandybeach Lake (Fig. 1-2) were examined using an inflatable Zodiac boat. Stratigraphic sections were found mainly along wave-cut bluffs in Wabigoon Lake (Fig. 1-2), and in gravel pits and road cuts throughout the study area. An additional trip was made in the summer of 1989 to the Thunder Bay-Kaministikwia area (Fig. 1-1), in order to collect geochemical samples from the basin of proglacial Lake Kaministikwia.

1.3.2 Section Logging:

The use of the facies approach has become fairly standard practice in modern sedimentological studies (Walker, 1984). While developed primarily through work on fluvial and marine sediments, it is equally applicable to sediments of glacial origin, as demonstrated by several recent studies (Eyles and Eyles, 1983, Shaw, 1985).

The term facies has been used in both a genetic and non-genetic sense. Examples of the genetic usage of the term are common in the literature: "esker-delta facies" (Thomas, 1984b); "lower till facies" (Dardis & McCabe, 1983); "delta-front facies" (Cherven, 1984); "interchannel facies" (Cheel & Rust, 1982). However, following the example of Walker (1984), the term facies is now more

commonly used in a strictly non-genetic sense, and this trend will be followed in this study.

The use of a facies approach necessitates the subdivision of lithologies found in the study area into units of similar aspect, which are termed facies. A particular facies is distinguished by "lithological, structural and organic aspects detectable in the field" (de Raaf et al., 1965, in Walker, 1984).

The actual measuring of stratigraphic sections differed in detail and technique, depending on the type of sediments which were exposed. The most detailed measurements were made on sections of silt-clay rhythmites. Here the thicknesses of each silt and clay lamina were recorded on a cash-register tape pinned to a cleaned, vertical face. Each unit boundary of the rhythmites was marked on the tape with a pencil. Care was taken to frequently label silt or clay laminae, in order to avoid missing layers.

For sections of coarser material, which were typically found in active gravel pits, the two-dimensional geometry of the units was first sketched and labelled. Detailed descriptions of each unit were then made, noting sedimentary structures, paleocurrent indicators, grain size and the nature of boundaries. The faces were completely photographed, and the slides were later used to construct accurate, interpreted drawings of the faces.

A total of 32 sections were selected for detailed logging in the study area, and an additional three sections were logged near the towns of Mine Centre and Kaministikwia (Fig. 1-1). Annotated graphic logs of these sections are provided in Appendix A (see Fig. 2-1 for locations).

1.3.3 Reflection Seismic Survey:

A shallow reflection seismic survey was conducted in the study area in the summer of 1988 under the direction of J.A.M. Hunter and S.E. Pullan of the Geological Survey of Canada (GSC). Six seismic lines were run, including two north of the Hartman moraine, and four south of the moraine (Fig. 1-4). All lines were oriented north-south, except for RS-500, which was oriented east-west.

The seismic surveys utilized the "optimum offset" technique developed by the GSC (Gagne et al., 1985). A 12-gauge gun, which fired a 7/8-ounce slug into the ground was used as the source.

The optimum field conditions for the use of this seismic technique are in fine-grained, moist sediments. Because of this, the seismic survey was not run across the coarse-grained, well drained material of the Hartman moraine.

1.3.4 Subbottom Acoustic Profiles:

A series of eleven sub-bottom acoustic (sonar) profiles were run on Lake Wabigoon during the summer of 1988 by L.H. Thorleifson of the GSC (Fig. 1-4). This technique utilized a Raytheon RTT-1000A Portable Survey System with a combined 3.5/7.0 kHz low-frequency penetrating transducer and a 200 kHz high-frequency bottom profiling transducer. Reflections from the high-frequency transducer delineate the sediment-water interface, while those from the low-frequency transducer penetrate and delineate layering in the sub-bottom sediments. The resolution of this system is about 30 cm.

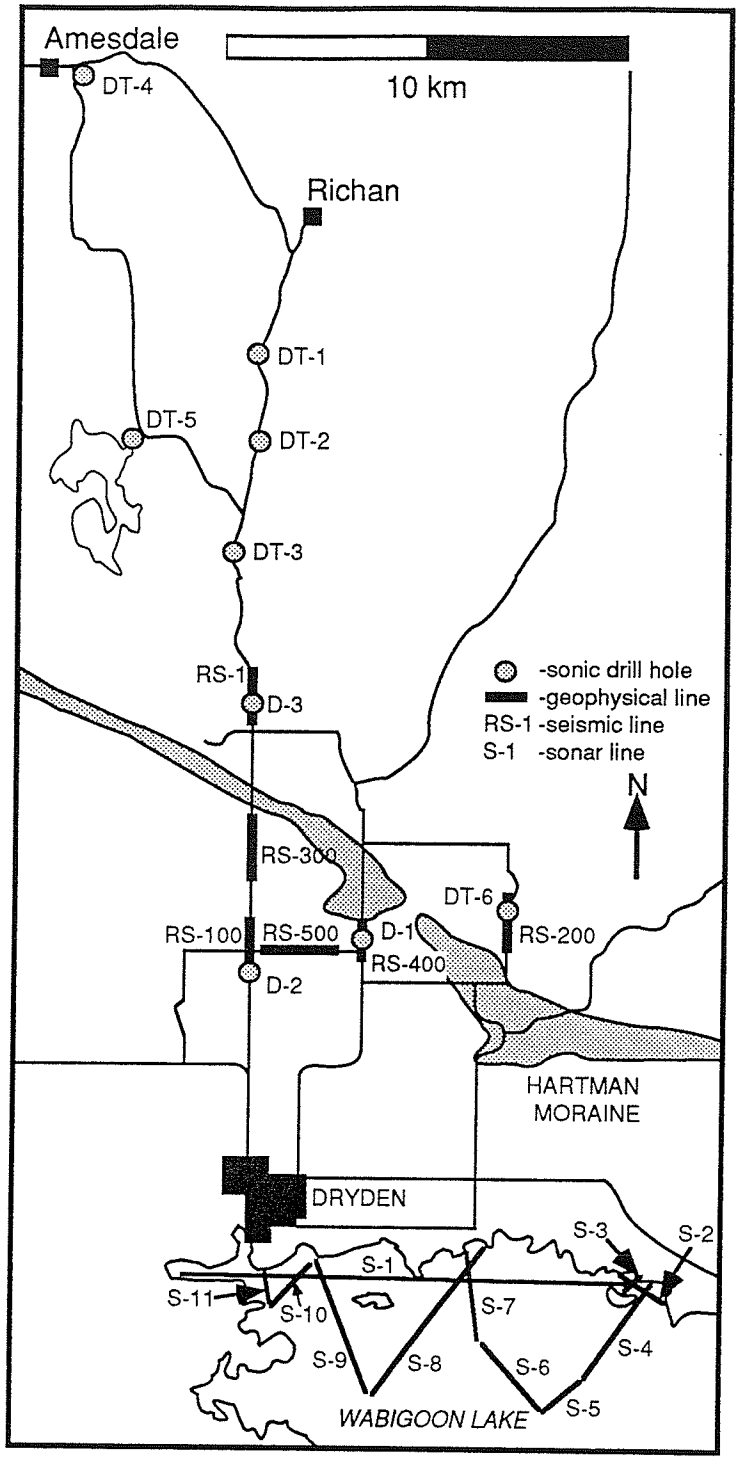

Fig. 1-4 Location of seismic and sonar lines and rotosonic drill holes (D- GSC, DT- J.T. Teller)

The system was mounted in an inflatable Zodiac boat, and navigation was by dead-reckoning between fixed points on shore and on islands. The speed of the boat was kept constant throughout each run.

Sub-bottom profiles in most cases show penetration to bedrock and well-defined bedding of the sediments. Acoustically-opaque zones are present in several profiles. The general explanation for this phenomenon is the presence of nitrogen and methane bubbles in the bottom sediments, which absorb most of the acoustic energy (Edwards & Klassen, 1984, in Larocque, 1987).

1.3.5 Rotasonic Drilling:

A number of rotasonic drill holes were drilled in the summer of 1988 by Midwest Drilling Ltd. of Winnipeg, Manitoba. With this drilling technique, a carbide-tipped, steel core barrel string is drilled into the sediment, and then a carbide-tipped casing string is drilled outside of the core barrel string. This drill utilizes a combination of downhole pressure, rotary motion and ultrasonic vibration to penetrate both unconsolidated sediment and rock.

The core barrel is then withdrawn, and the core is extruded in 1.5m lengths, using water pressure and ultrasonic vibration. Core recovery is generally in the 100% range in fine-grained sediments. However, it can become quite poor in sediments coarser than about medium sand, especially if the sediment is well sorted.

Primary targets for the drilling program were deep, sediment-filled bedrock lows identified from the reflection seismic profiles. These targets produced four fairly long cores, which also allowed interpretation of the seismic

data. A second aim of the drilling program was to attempt to delineate the distribution of the red clay layer north of the Hartman moraine. Cores were collected by J.T. Teller in that area.

Four sonic cores were logged, and their locations are given in figure 1-4 (complete logs are given in Appendix A). Cores were logged at the Ontario Ministry of Northern Development and Mines Core Logging Facility in Kenora, Ontario.

1.3.6 Water Well Records:

Water well records for the study area were obtained from the Ontario Ministry of the Environment in order to provide additional subsurface information. These logs can provide information on elevation, unconsolidated sediment thickness, and depth to bedrock. Though of variable apparent reliability, stratigraphic information was used to obtain general information on the subsurface geometry and distribution of the sediments, particularly the red clay rhythmite unit.

1.3.7 Geochemical Analyses:

In order to test various hypotheses about the nature and source of the red clay rhythmites, samples from several areas were prepared for geochemical, mineralogical and grain-size analysis. A total of 114 samples were collected, including samples from both the red and grey clays in the Wabigoon basin, a few samples of the associated silt laminae, samples of red clay from the Fort Frances area and the Kaministikwia area, and two samples of red lodgement till

from the Thunder Bay area (Fig. 1-1). Details of this sample suite are presented in Appendix B.

Preparation of the samples began with drying of the clays at a temperature of between 60-80° F. This resulted in most of the samples becoming rather hard and brick-like, which necessitated crushing them by hand in a ceramic mortar and pestle. Grain size analyses of crushed and uncrushed samples showed that this did not affect their grain size distribution. The samples were then dry-sieved in stainless steel sieves to a final diameter of less than 3μm. Sub-samples for grain-size analysis were taken before sieving.

Samples for geochemical analysis were sent to Chemex Labs Ltd. in Vancouver, B.C., to be analyzed for a suite of 32 major and trace elements (Appendix B). The samples were digested in aqua-regia, and analysed using an inductively-coupled-plasma (ICP) technique. In addition, the amount of iron present as ferrous oxide was determined by titration. The complete results are given in Appendix C.

A subset of these samples (Appendix B) was also analysed for Rare Earth Elements (REE's), using the neutron activation technique (Appendix C).

1.3.8 Mineralogical Analyses:

Qualitative and semi-quantitative clay mineral analyses were conducted on the clay-sized (< 3.9μm) fraction of 13 samples (Appendix B) using procedures designed by Dr. W.M. Last of the University of Manitoba (Appendix D). Grain-size separation was done by centrifuging, following the method of Tanner and Jackson (1947).

Oriented clay mineral mounts were prepared by allowing an aliquot of the aqueous clay-sized slurry to dry on a petrographic slide using the membrane filter-peel technique of Drever (1973). Each slide was placed in an ethylene glycol environment for 48 hours (Muller, 1967). The glycolated slide was scanned in one direction from 3° to 15° two-theta. Scanning speed was at 0.6° two-theta per minute, with 200 counts per second. Other instrument settings were: 1° beam slit, 0.01 cm detector slit, 1 second measurement constant and a 0.01° step size. After scanning of the glycolated slide, it was heated to 550°C for one hour (Carrol, 1970). The heated slide was run from 3° to 15° two-theta, and from 24° to 27° two-theta.

These x-ray diffraction patterns were used to identify the main clay mineral components and to make semi-quantitative estimates of the relative amounts of the major clay mineral groups present: illite, expandable-lattice clay minerals (which include minerals of the montmorillonite group, vermiculite, expanding chlorites, and various mixed-layer species), kaolinite and chlorite.

Semi-quantitative calculation of the main clay mineral groups was made using a method similar to that described by Biscaye (1965) using the weighting factors of: difference in intensities of the 10 Å glycolated versus heated peaks for the expandable layer clays; four times (4X) the intensity of the 10 Å (glycolated) peak for the illite group; and twice (2X) the 7 Å glycolated peak for kaolinite and chlorite. Qualitative evaluations of the mixed layer components were supplied according to the techniques outlined by Thorez (1975). The weighted peak intensities were summed with the weighted intensity of each

group times 100 and divided by this sum giving the "percentage" of each component.

Although this technique is commonly used for semi-quantitative evaluation of clay minerals, it must be realized that truly quantitative evaluations are not possible in complex clay mineral assemblages without use of very detailed and "non-routine" methods.

1.3.9 Grain Size Analyses:

Grain size analyses were carried out on a suite of 33 samples from the study area and from other areas in northwestern Ontario. A list of the sample suite appears in Appendix B. Complete results are given in Appendix E.

Because of the fine-grained nature of the samples, analyses were carried out using a Micromeritics Sedigraph particle size analyzer. This instrument utilizes an x-ray beam and a moving sample chamber to calculate the equivalent-spherical-diameter distribution of a sample, based on the Stoke's Law equations. The lower grain size limit of this technique is 0.1μm.

CHAPTER 2: DESCRIPTION OF THE SEDIMENTS

2.1 INTRODUCTION:

The sediments found in the area were divided into eight facies, based on their grain size, degree of sorting, and sedimentary structures. Detailed descriptions of all measured aspects of each facies, including their geometry are given here.

This is followed by an attempt to integrate the surficial distribution with the vertical and lateral relationships of the facies, in order to determine their three-dimensional arrangement. This is important, because potentially erroneous estimates of sediment distribution and volume can result from relying strictly on two-dimensional representations such as surficial geology maps, which typically represent only the upper 1 m of sediment.

Finally, a summary of all measured paleocurrent data is presented.

Figure 2-1 shows the locations of sections referred to in the text.

2.2 FACIES DESCRIPTIONS:

2.2.1 Silt-clay Rhythmites (Facies 1):

Grey Sequence:

This facies consists entirely of rhythmically laminated couplets of silt and clay (Fig. 2-2). These couplets consist of a lower silt laminae, overlain by a clay laminae.

The silt laminae may be either massive or finely laminated, and typically show extensive bioturbation throughout, with numerous looping trackways

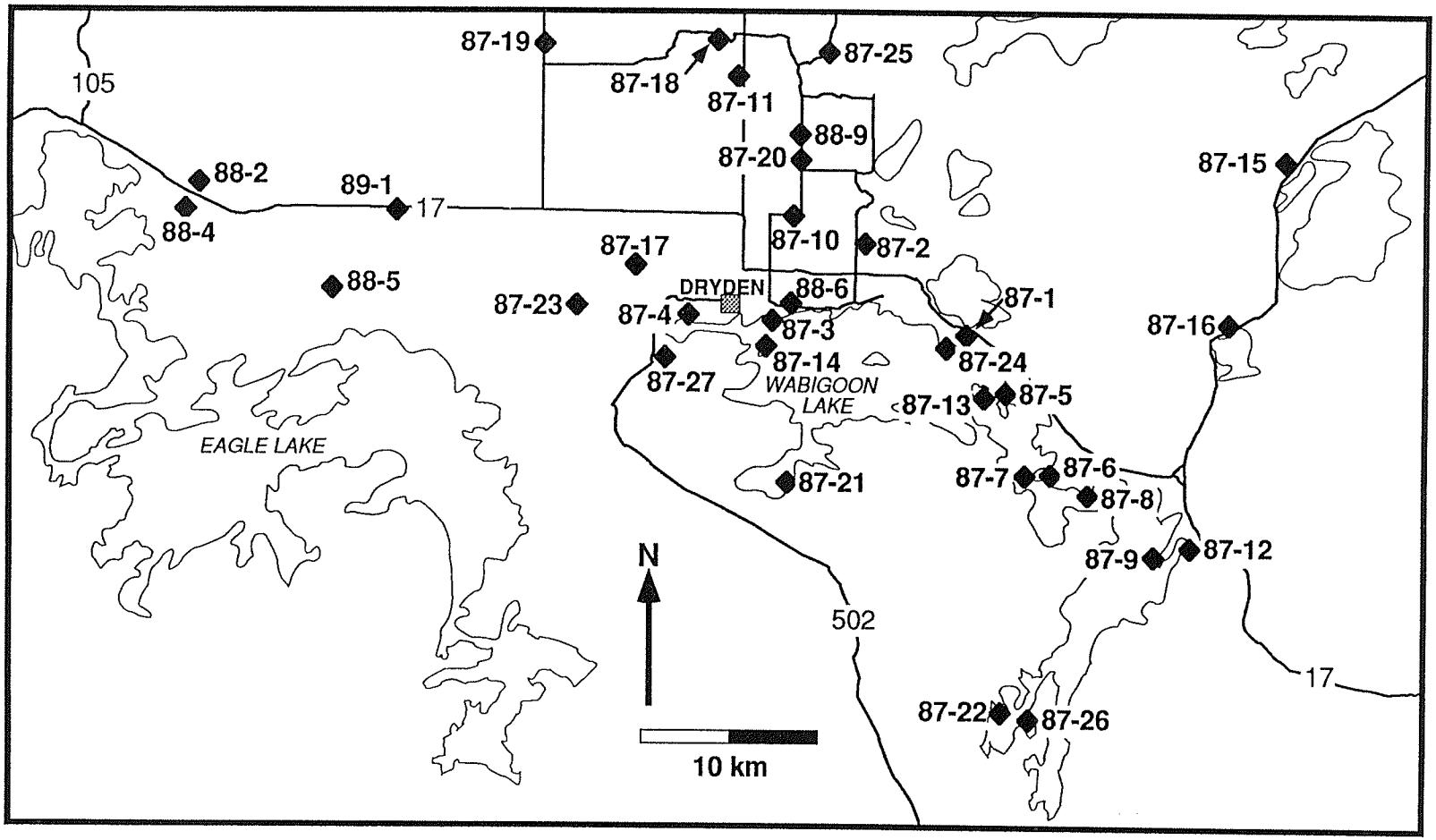

Fig. 2-1 Location of all measured sections in the study area.

Figure 2-2 Facies 1-Rhythmically laminated silts and clays (section 87-5).

visible on its upper surface (Fig. 2-3). The upper and lower boundaries of the silt laminae are usually sharp, and conformable. The grain size of this silt laminae usually falls between 63 and 1 μm (Appendix E). The silts are approximately greyish-white (variable Munsell hue) in colour, although they may have very thin laminae (<1mm) of dark grey (Munsell hue 5Y) or red (Munsell hue 5YR) clay within them. These silt laminae usually range from 0.1 to 1.0 cm in thickness, although they may be as thick as 10.0 cm in some cases.

The clay laminae are generally massive, but occasionally show fine internal laminations. The clays are not usually bioturbated, but burrows in the overlying silts often extend as much as 2-3 mm down into the clay laminae and are infilled with silt. The upper and lower boundaries of the clays are usually sharp and conformable. Clay unit thicknesses are normally in the range from 0.1 mm to 1.0 cm, but may be as large as 10.0 cm. Clay laminae are usually, but not always, thinner than the underlying silt laminae which make up the couplet.

In most outcrops of the Facies 1 rhythmites, platy carbonate concretions, ranging in size from a few millimetres up to 10 or more cm across, can be found in the silt laminae (Fig. 2-4). In some sections there can be hundreds of the larger concretions within two or three square metres of the section face. When these sections are exposed as wave-cut bluffs, there are often residual shingle beaches made entirely of concretions at the base of these bluffs (Fig. 2-5). In the outcrop, these concretions are disk-shaped, often forming single or amalgamated concentric circles in plan view. In some cases, they appear to have completely replaced the silt laminae, while preserving primary structures

Figure 2-3 Subhorizontal trails seen on bedding planes of silt layers in Facies 1 rhythmites (sample from section 87-5).

Figure 2-4 Two pieces of diagenetic carbonate concretion from the Facies 1 rhythmites (samples from section 87-5). These concretions began as nodular forms (some of which can still be seen in the slab on the left), but appear to have coalesced until they have replaced the entire silt lamanae, preserving the bioturbation structures on the former bedding planes. Both slabs are entirely composed of coalesced concretions, and all sediment has been washed off before photographing. Scale (visible at lower right) is in centimetres.

Figure 2-5 Shingle beach at the base of a Facies 1 rhythmite exposure on Lake Wabigoon (section 87-5). The beach is composed entirely of carbonate concretions. Coller and lunchbox at left for scale.

such as bioturbation (Fig. 2-4). They lie parallel to bedding planes, and often show evidence of having caused minor displacement of adjacent beds during their growth. Frequently the nodule-shaped concretions are hollow, and have a jagged surface on their inner shell. The presence of concretions did not appear to show any relationship to position in the stratigraphic sequence, nor to the colour of the clay units.

All of the rhythmite sequences in the study area show minor to abundant small-scale (mm to cm) post-depositional, brittle faulting (Fig. 2-6), and in some cases syndepositional slumping can be recognized (Fig. 2-7).

Outsized clasts are not common; where present, they are pebble-size. These occur individually, and there was no evidence of concentrations of these clasts in any one area, or horizon.

The silt-clay rhythmite facies can have a sharp base where it overlies a local erosional surface or bedrock, or can be gradational where this facies overlies sandy rhythmites (Facies 2)(Fig. 2-8). The upper contact of this facies is normally the present ground surface, although thin (< 1.0 m) pebble gravels (Facies 6) overlie it in a few areas.

Red Sequence:

A notable feature of the Facies 1 silt-clay rhythmite sequence (and rarely, the Facies 2 sand-clay rhythmite sequence) is the presence of a distinctive band of thick, red-clay rhythmites which are found throughout the study area (Fig. 2-9). These red-clay rhythmites have clay laminae which are distinctly reddish-brown in colour (Munsell hue 5YR) in contrast to the overlying and

Figure 2-6 Post-depositional brittle faulting in Facies 1 rhythmites (section 89-1).

Figure 2-7 Syndepositional slumping in Facies 1 rhythmites. Rhythmites above and below slumping are undisturbed. Mottling in silts is due to bioturbation (section 87-5). Scale is in centimetres and is upside down.

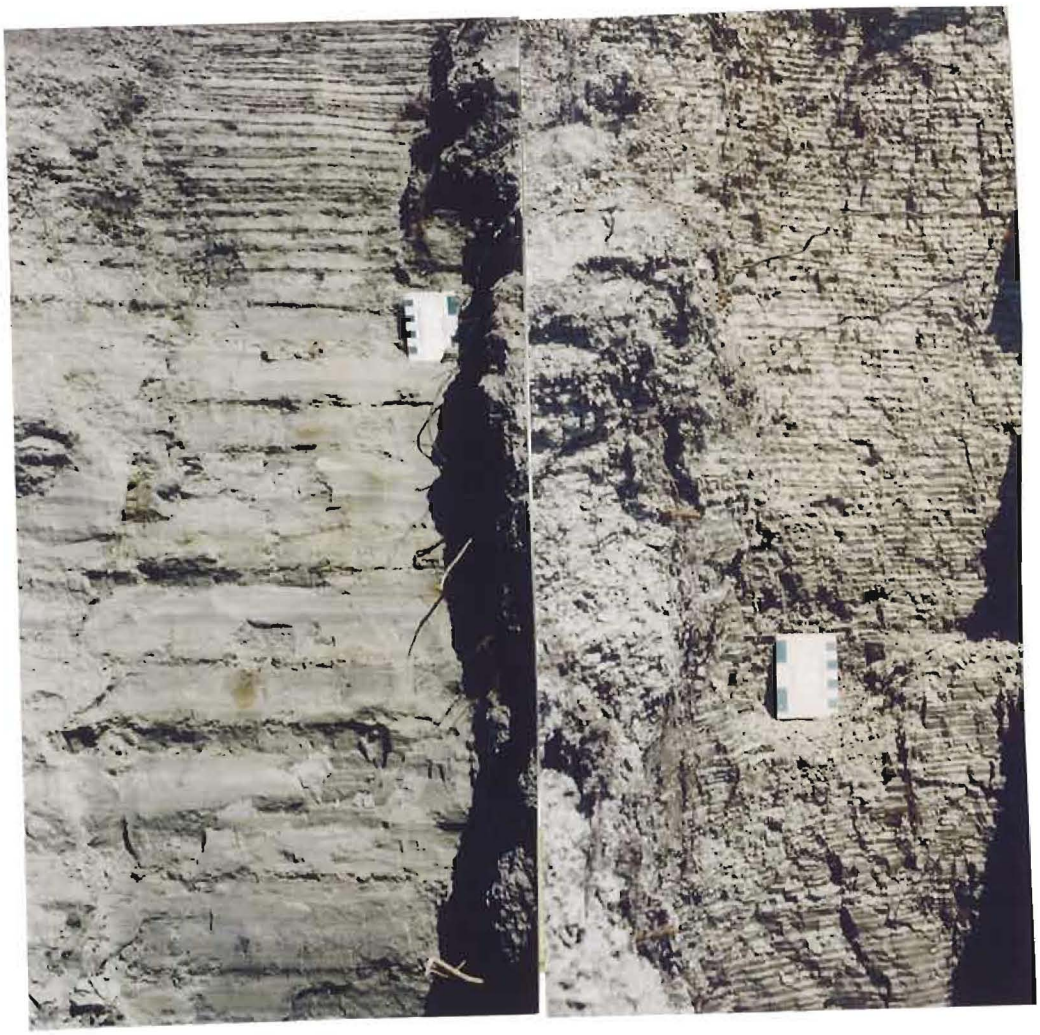

Figure 2-8 Gradational upward transition from Facies 2 sand-clay rhythmites (left) to Facies 1 silt-clay rhythmites (right)(section 87-24). Scale card is 9 cm long.

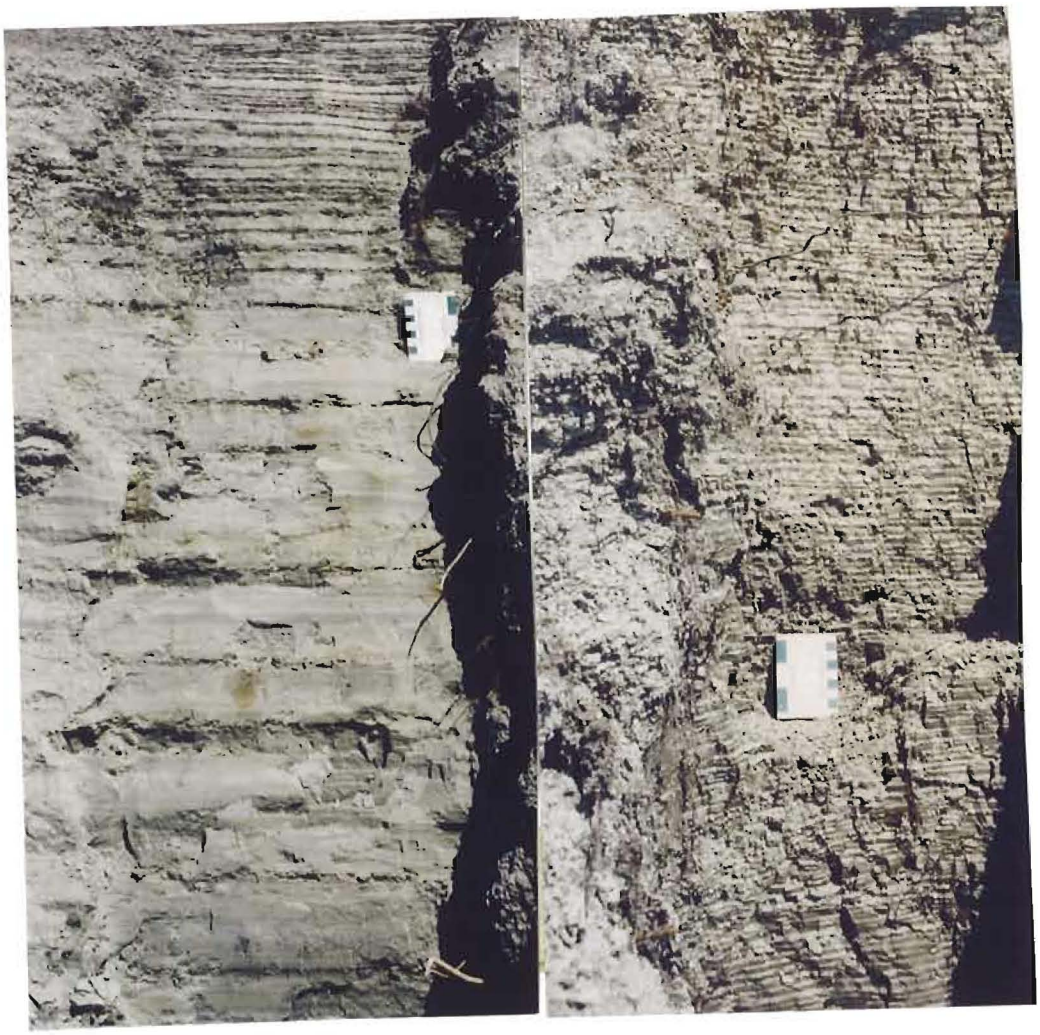

Figure 2-8 Gradational upward transition from Facies 2 sand-clay rhythmites (left) to Facies 1 silt-clay rhythmites (right)(section 87-24). Scale card is 9 cm long.

underlying grey-clay rhythmites whose clay laminae are typically dark grey in colour (Munsell hue 5Y), although these are oxidized to a grey-brown colour (Munsell hue 2.5Y to 5Y) within a few metres of the surface. The number of red-clay rhythmites at any section ranges from 9 to 24, although this exact number is difficult to determine because the upper change from red to grey clay is transitional over 3 to 7 rhythmites. The lower transition from grey to red rhythmites is always abrupt, and the first hint of red clay often appears as a thin (mm scale) laminae of red clay at the top of the uppermost grey clay laminae underlying the first entirely red-clay couplet (Fig. 2-10).

Aside from these differences, these abnormal rhythmites are identical in appearance to the normal, grey-clay rhythmites.

In order to examine the nature and possible origin of the red-clay rhythmites, a number of measurements and analyses were carried out on two representative sections from the Dryden area, as well as on comparative red clay samples from the Kaministikwia area near Thunder Bay and from the Fort Frances area (Fig. 1-1). A sample of the clay portion of each red rhythmite was collected from sections 87-1 and 87-19 (see Appendix B for a detailed description of the sample suite). In addition, the clay portion of several grey-clay rhthymites from above and below the red-clay rhythmites was also sampled (Appendix B). Since it was the clay portion of the red-clay rhythmites which showed the most apparent visual contrast with the grey-clay rhythmites, it was mainly the clay portions which were sampled. However, a few samples of the

Figure 2-10 Thin red clay band on top of grey clay lamina beneath the first completely red clay lamina (section 87-24).

silt portion of the grey-clay and red-clay rhythmites were also collected and analysed. The results of all measurements and analyses are given here.

Rhythmite Thickness:

Measurements from numerous rhythmite exposures in the Dryden area show that the individual red-clay couplets are much thicker than the over- and under-lying grey-clay couplets (Fig. 2-11) (Note that a five-rhythmite-wide smoothing filter has been applied to the data before graphing). This increased couplet thickness is due mainly to a dramatic increase in the thickness of the clay portion of the red-clay couplets, although the silt portion thickens as well (Fig. 2-11).

Overall patterns of clay thickness variation are quite similar in every section. The sudden increase in clay thickness in the red clay rhythmites can be seen in all of the sections. Just below the red clay unit there is a smaller rise and fall in clay thickness, which can also be seen in all of the curves. The clay thicknesses are fairly constant below the red clay unit, although the longer records show a slight increase in laminae thickness towards the base of the measured section (Fig. 2-11).

The silt thickness curves show more variablility than the clay curves, and show somewhat different patterns (Fig. 2-11). The overall pattern is one of a gradual decrease in thickness at the base of the measured section, followed by a gradual increase culminating in the red clay unit.

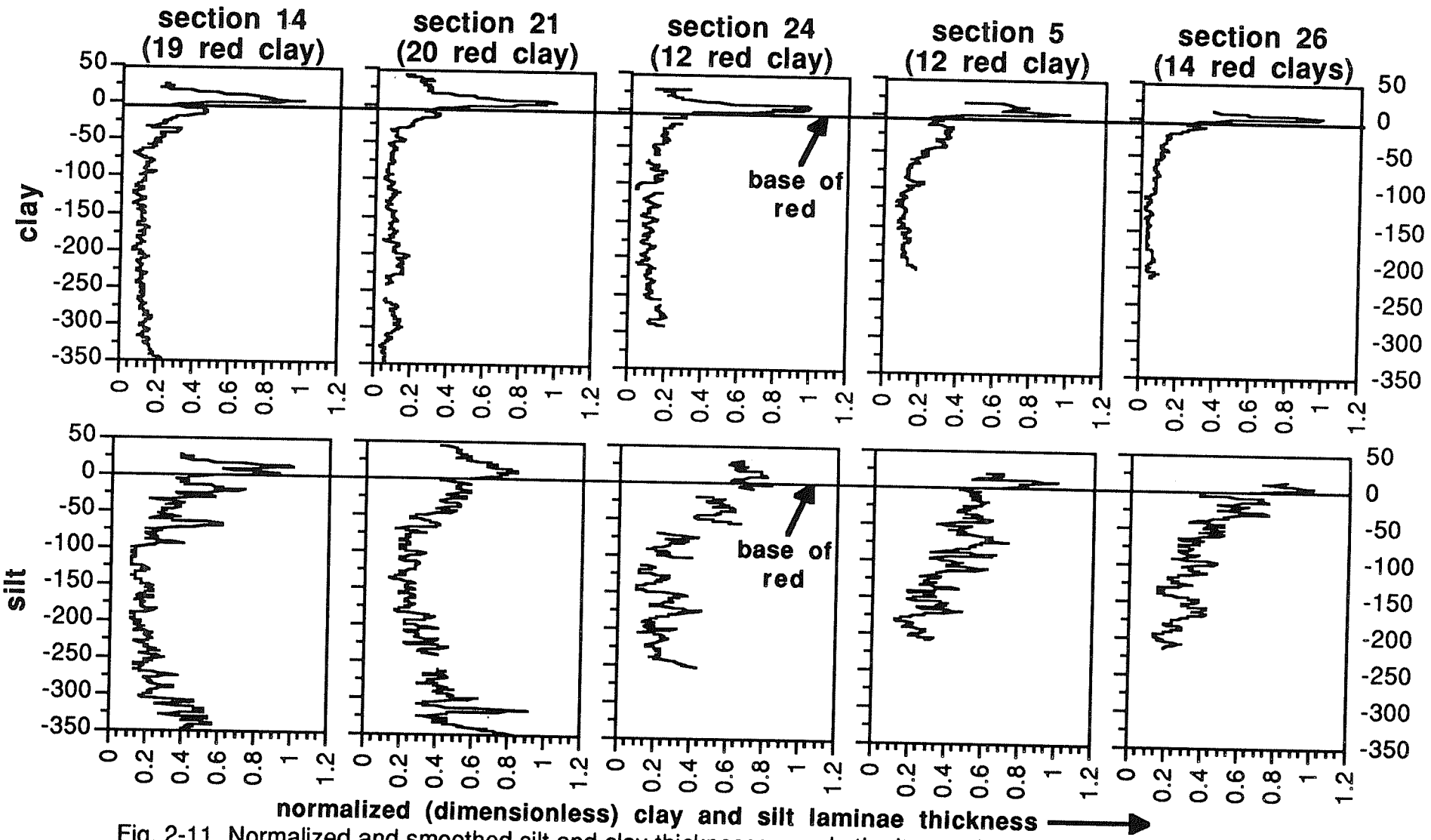

Fig. 2-11 Normalized and smoothed silt and clay thicknesses vs rhythmite number for sections on a 30km transect from NW to SE across the Dryden area (see Fig. 2-1 for locations). Overall, the curves show similar patterns, especially the rapid increase in thickness at the base of the red clay rhythmite unit.

Grain Size:

A suite of 22 rhythmite samples from section 87-19 (see Appendix E) was analysed for grain size using a Micromeritics Sedigraph particle size analyzer. A graphic mean was calculated for each sample from the Sedigraph curves using the method of Folk (1980, p. 41). Figure 2-12 shows that the mean grain size of the clay parts of the couplets is virtually identical for both the red- and grey-clay rhythmites. The differences between the average mean grain sizes of the upper grey clays (0.43μm), the red clays (0.48μm) and the lower grey clays (0.44μm) are much smaller than the variation within each group.

The silt portions of the rhythmites show some variation in grain size, with the silts of the red-clay couplets being somewhat coarser than the silts of the upper and lower grey-clay couplets (average mean grain sizes 3.35, 2.22 and 2.64μm respectively).

As can be seen in Appendix E, the Dryden area red and grey clays are slightly finer than the massive to poorly stratified red clays in the Kaministikwia area (average mean grain size of two samples = 0.60μm). The two red clay samples from the Fort Frances area are quite different in grain size, with graphic means of 0.81 and 0.37μm. The Sedigraph curves indicate that the Fort Frances red clays contain a greater portion of fine (<0.1μm) material than most of the Dryden area clays (10-15% vs 0-10% respectively).

Mineralogy:

Bulk diffractograms on one sample each of the Dryden area red and grey clays was carried out to see if a more comprehensive examination was needed.

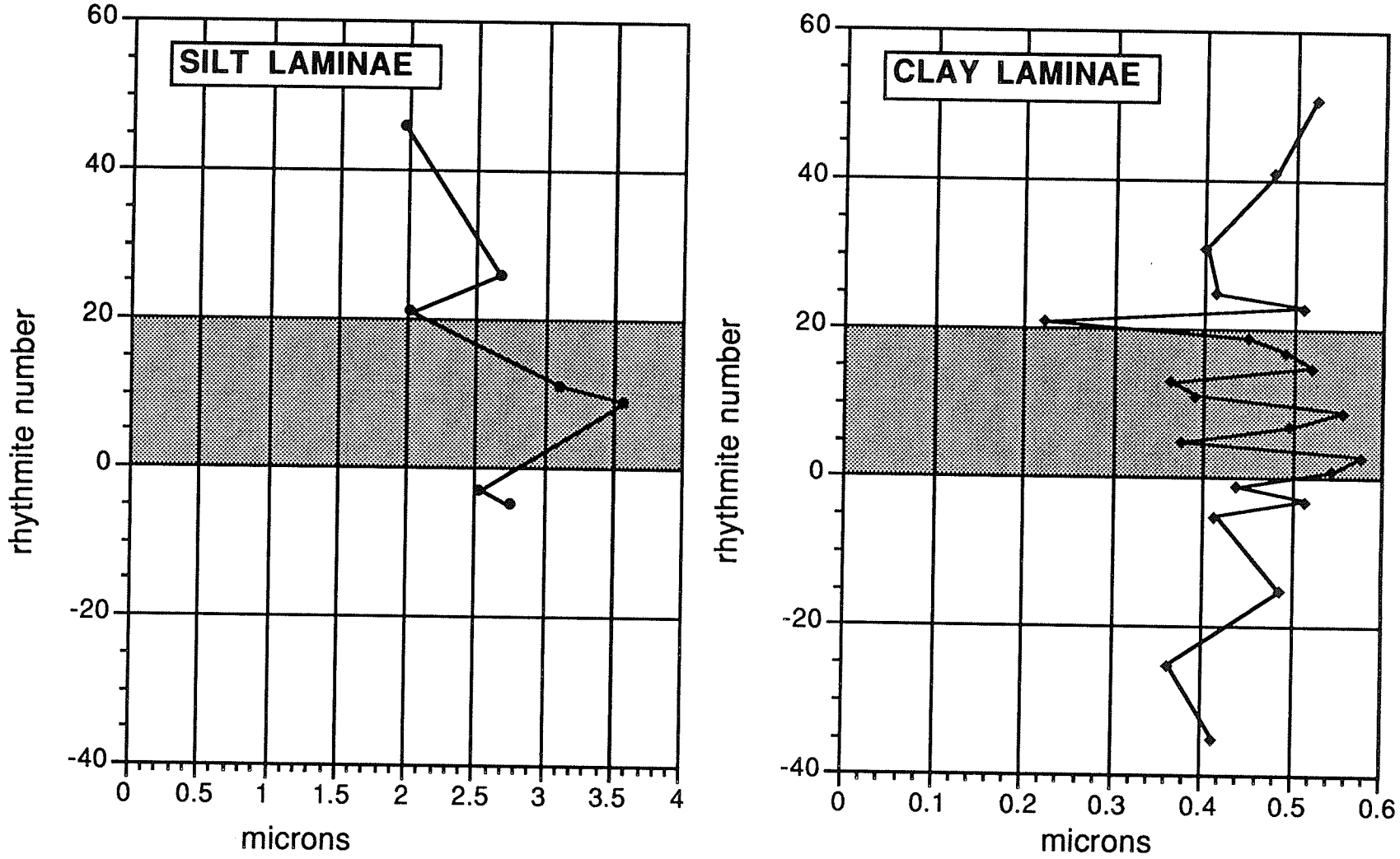

Fig. 2-12 Plot of graphic mean grain size against rhythmite number for section 87-19. The red clay unit is indicated by shading. See Fig. 2-1 for location.

The bulk diffractograms are virtually identical for the red and grey clays, suggesting that there are no significant mineralogical differences between the two samples. This concurs with the findings of Cowan (1987) and W. Coker (unpub. data), that the mineralogy of the red and grey clays is identical, and consists mainly of quartz, with lesser amounts of albite, calcite, dolomite, hornblende and various clay minerals.

Cowan (1987) examined four samples of the Dryden clays and estimated that, based on the relative intensity values from the diffractograms, the red clays had a relatively higher calcite content and lower quartz content than the grey clays (23% vs 13%, and 30% vs 60% respectively).

Semi-quantitative clay mineralogy data calculated by W.M. Last shows no apparent significant differences in clay mineralogy between the Dryden area red and grey clays, although the number of samples examined is insufficient for statistical testing. All samples contain mainly illite (50.6-62.5%), chlorite (15.6-21.8%), and various expanding-lattice clays (18.3-32.9%), along with minor kaolinite (0.0-3.2%) (Appendix D).

Geochemistry:

As an initial examination of the geochemical data from the two representative sections (87-1 & 87-19, see Fig. 2-1), graphs of element concentrations vs. rhythmite number were constructed for each of the major, trace and Rare Earth elements. Visual examination of this graphed data suggested that the Dryden area red clay laminae were geochemically distinct from the grey clay laminae. In addition, visual examination of the raw data

suggested that the red clay samples from the Kaministikwia and Fort Frances areas were geochemically distinct from both Dryden area populations.

In order to test whether or not the populations were truly geochemically distinct, and to see which specific elements were involved, the Student's t-test was used. A comparison of the Dryden area red and grey clays shows that the red clays have statistically higher concentrations of Co, Cu, Fe, Mg, Mn, Na, Ni and Sc, and lower concentrations of Cr, La, Ti, and a lower Fe^{2+}/Fe^{3+} ratio. Figure 2-13 shows vertical plots of these elements through the rhythmites in section 87-19. Even for elements where no statistical differences in concentrations were seen, a vertical plot through the section shows sudden and distinct decreases in concentration at the lower grey-clay rhythmite to red-clay rhythmite transition for Ba, K, Sr, V and Zn (Fig. 2-14).

The silt portion geochemistry shows more variable stratigraphic trends than the clay portion geochemistry (Figs. 2-13 & 2-14). Several of the elements (Ba, Co, Cr, Cu, Fe, K, Mn, Na, Ni, Sc, Ti, V and Zn) show a consistent pattern, with a decrease in concentration in the lower grey rhythmites, and a sharp increase in the red clay rhythmites, which decreases again in the upper grey rhythmites (Figs. 2-13 & 2-14). This pattern is unrelated to the behavior of the clay portion geochemistry, and does not appear to correspond to any physical features (eg. colour) of the rhythmites. The silt portion values for Sr weakly mimic those of the clay portion, while the concentrations of Mg and La show no systematic variations (Figs. 2-13 & 2-14).

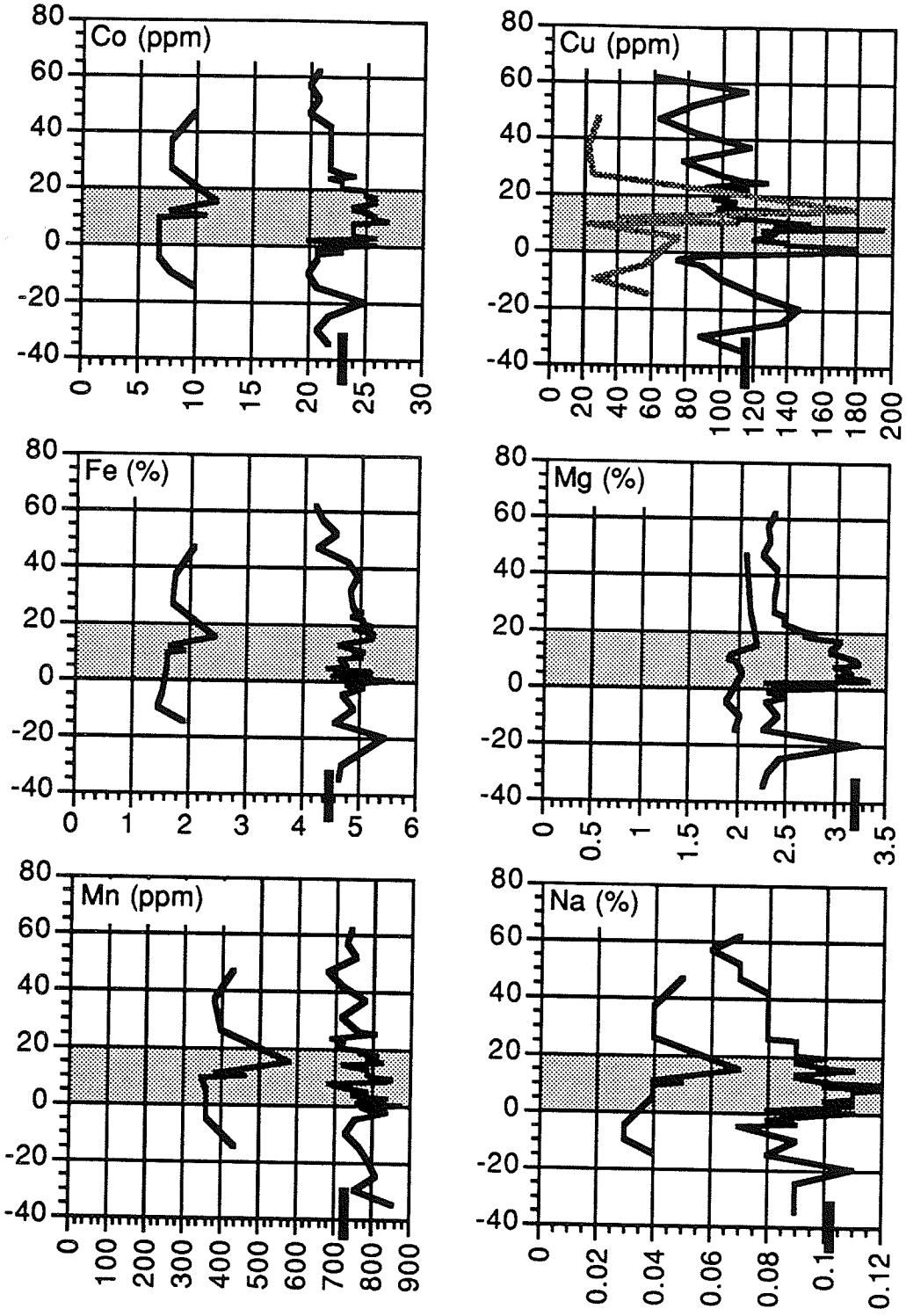

Fig. 2-13 Plots of element concentration vs rhythmite number, showing the geochemical differences between the Facies 1 red clay rhythmites (shaded zone) and the surrounding grey clay rhythmites at section 87-19 near Dryden (see Fig. 2-1 for location). (Con't.on next page).

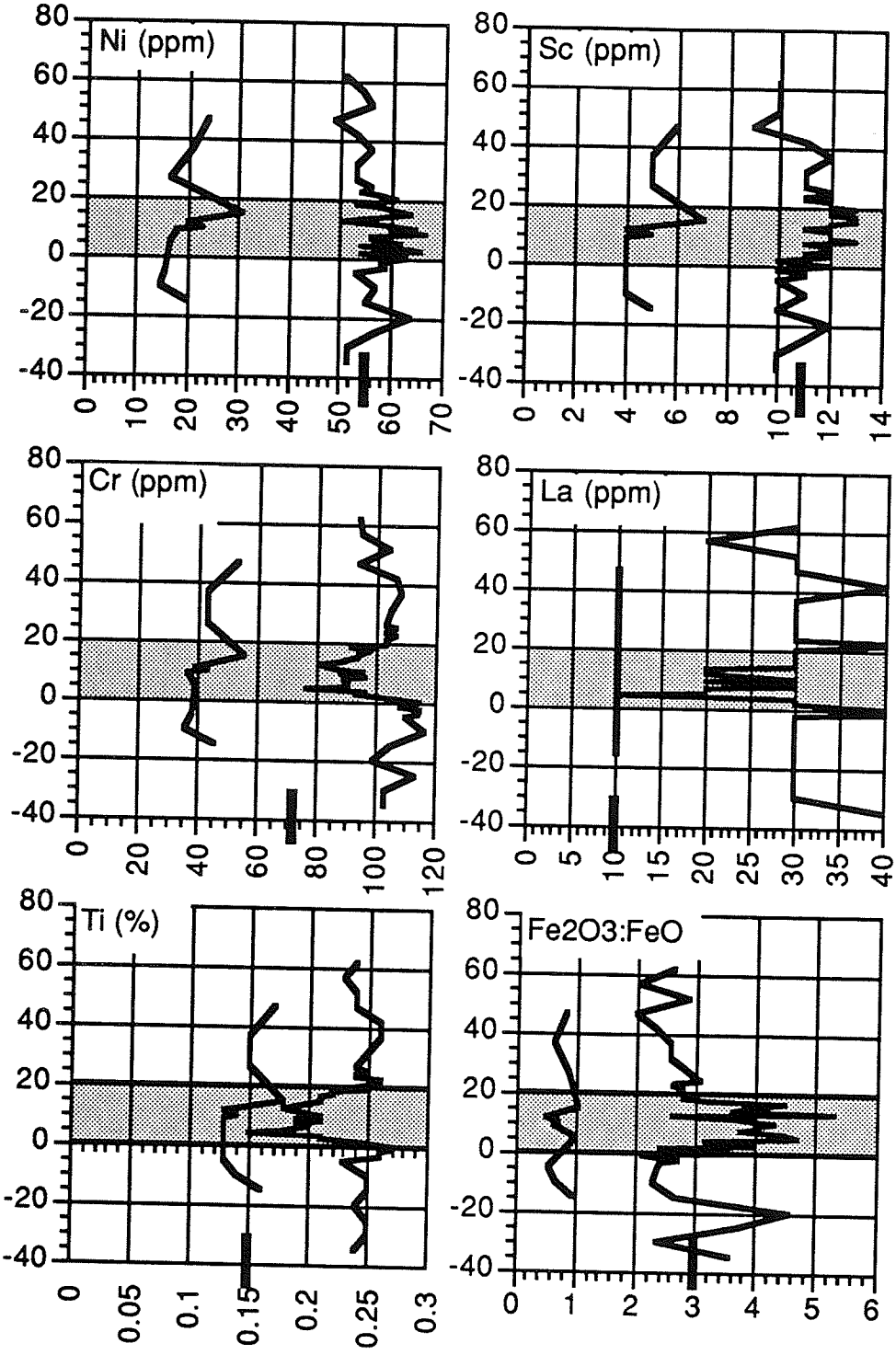

Fig. 2-13 (continued) In all plots, silt is the line on the left, and clay on the right. All elements shown in this figure show statistically significant differences in concentrations between the red and grey clays. The black bars on the x-axis represent average values for the red clays from the Kaministikwia area.

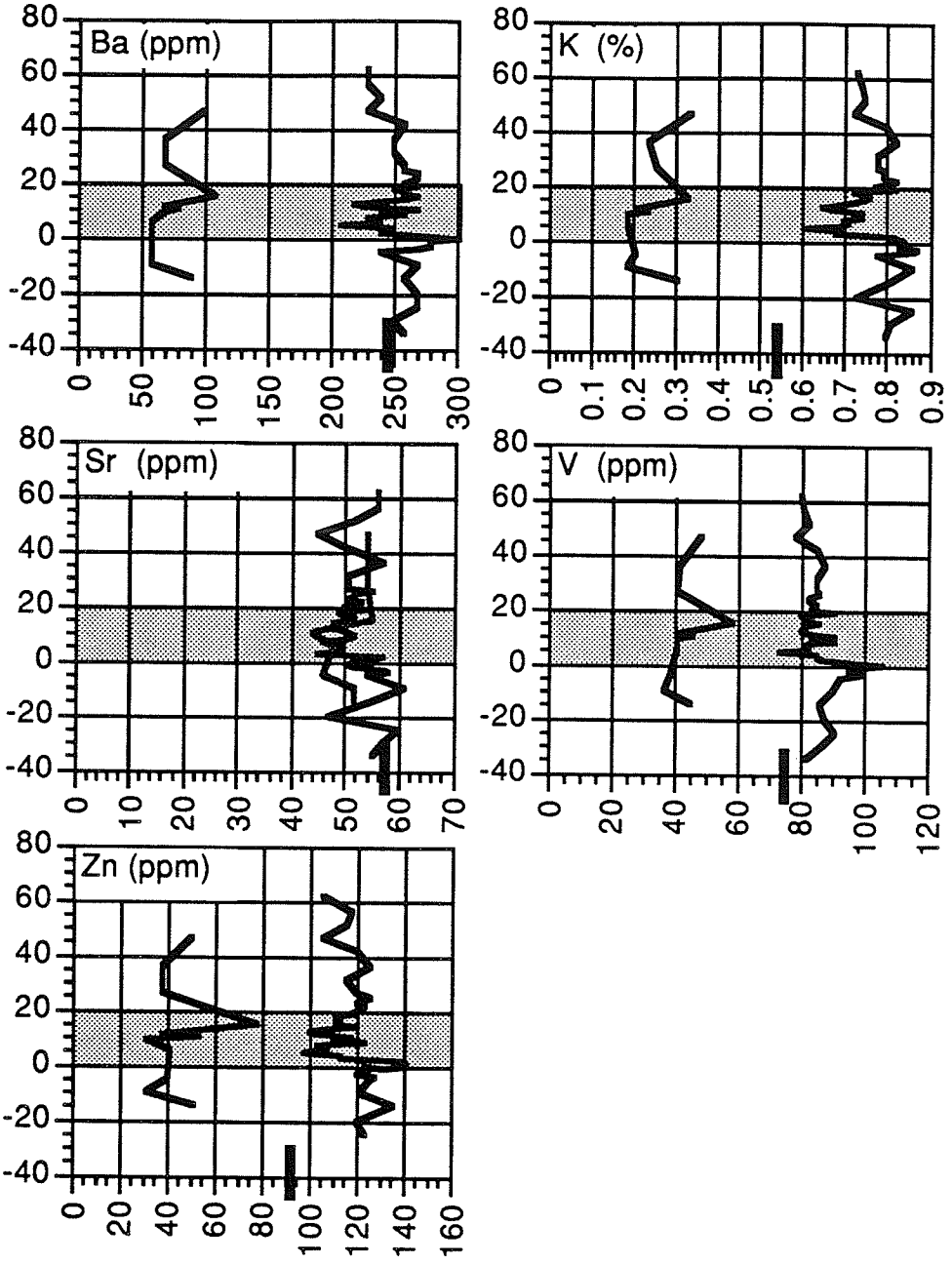

Fig. 2-14 Plots of element concentration vs rhythmite number for the Facies 1 red clay rhythmites (shaded zone) and the surrounding grey clay rhythmites (87-19, Fig. 2-1 for location). The sharp negative shift at the base of the red clay rhythmites is apparent in all of the plots, despite the lack of any statistically significant differences in these element concentrations. In all plots silt is on the left, and clay on the right, except in the Sr plot where silt is the lighter line. Black bars on the x-axes represent average values for the red clays from the Kaministikwia area.

Comparisons between the Dryden area red clays and the Kaministikwia area red clays show fewer differences, although the Dryden area red clays have significantly higher concentrations of Al, Cr, Fe, La, Sc, Ti and Zn, and lower concentrations of Ca, P and Sr.

Relative to the Kaministikwia red clays, the Dryden area grey-clays show statistically higher levels of Cr, K, La, Ti, V, Zn and a higher Fe^{2+}/Fe^{3+} ratio.

Also relative to the Kaministikwia red clays, the Fort Frances red clays show a statistically higher concentration of La and lower concentrations of Ca, Na, Sr, and a lower Fe^{2+}/Fe^{3+} ratio.

The Rare Earth Elements (REE's) are considered to be relatively immobile in surface conditions, and are therefore less susceptible to the effects of lake water chemistry, weathering and soil formation (McLennan, 1989). Analyses for REE's were carried out on a subset of 12 samples from section 87-19 in the Dryden area, and from the Kaministikwia and Fort Frances areas (Appendices B & C).

A chondrite-normalized plot of average REE concentrations for each of the Dryden area red and grey clays, the Kaministikwia red clays and the Fort Frances red clays is shown in figure 2-15. It can be seen that, in general, the REE patterns are very similar to those of most post-Archean, fine-grained rocks (McLennan, 1989). They show a typical depletion of the heavy REE's (HREE's; Gd to Lu) relative to the light REE's (LREE's; La to Sm), and a distinctive negative Eu anomaly. The negative Tb anomaly is probably an artifact of the analytical techniques (S. Preece, Univ. of Toronto, pers. comm. 1990).

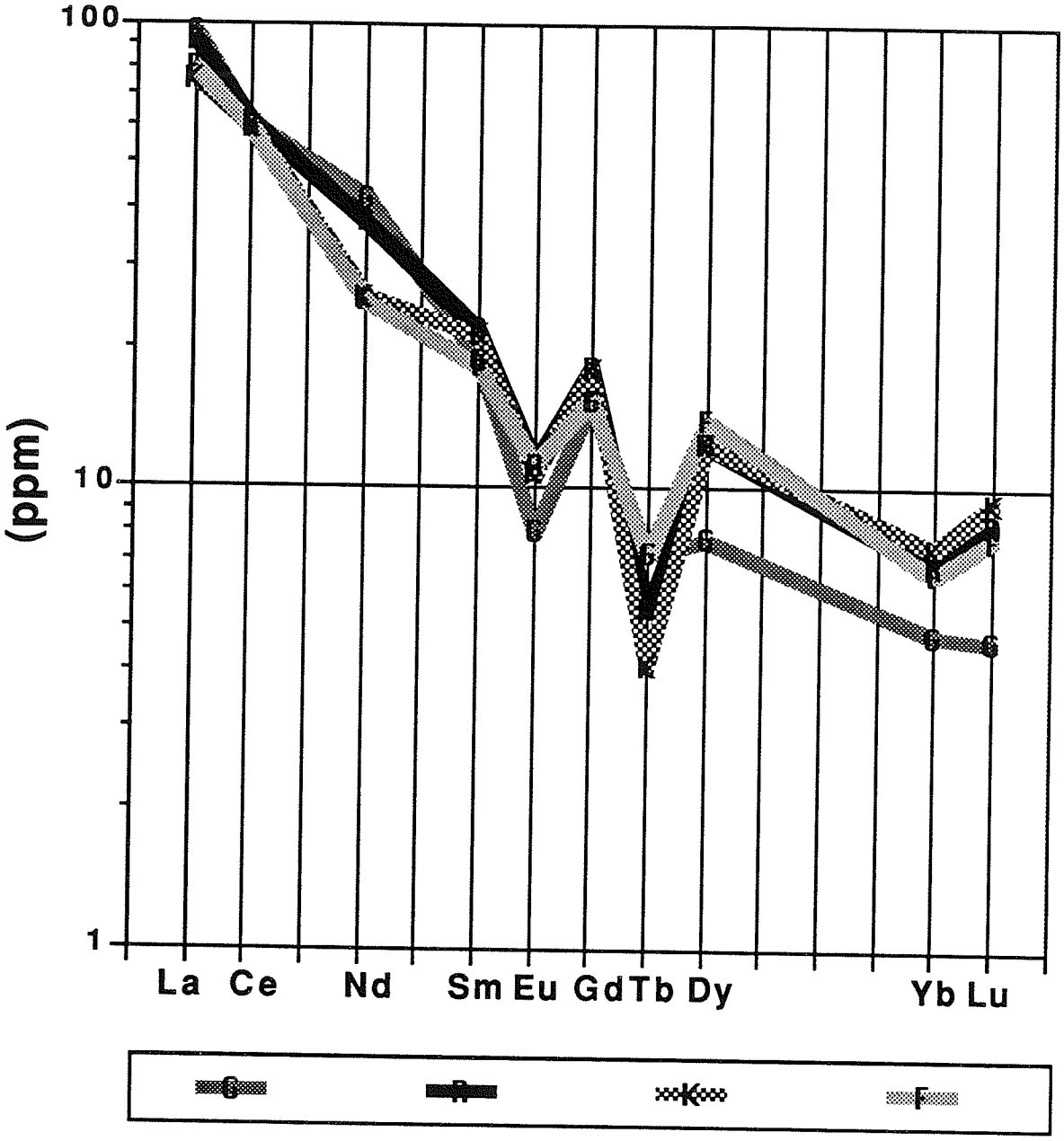

Fig. 2-15 Rare Earth Element plots for the Dryden grey clay (G), Dryden red clay (R), Fort Frances red clay (F) and Kaministikwia red clay (K). Note the greater HREE (Dy to Lu) depletion, and more negative Eu anomaly in the Dryden grey clays.

It is interesting to compare these results with data from a commonly used standard, the post-Archean Average Shale (PAAS) (McLennan, 1989). The extent of the HREE depletion, as measured by the La/Yb ratio, is considerably greater in all of the studied samples (ranging from 14.53 to 20.02) than in the PAAS (9.15). The extent of the Eu anomaly is measured by the ratio Eu/Eu*, where Eu* is the Eu value which would lie along the average slope of the REE curve. This ratio tends to be somewhat smaller in most of the studied samples (ranging from 0.66 to 0.47) than in the PAAS (0.65) (McLennan, 1989).

When the studied samples are compared with each other, it can be seen that the red clay samples from the Dryden area, Kaministikwia, and the Fort Frances area show virtually identical REE patterns, while the Dryden area grey clay samples show a distinctively greater depletion in the heaviest of the REE's (Dy, Yb and Lu) (Fig. 2-15). The La/Yb value for the Dryden area grey clays (20.02) is quite high relative to that of the red clay samples (Dryd. = 13.54; Kam. = 10.19; Ft. Fran. = 12.30). Also, the Eu/Eu* value for the Dryden area grey clays (0.47) is lower than the values for the red clay samples (Dryd. = 0.56; Kam. = .54; Ft. Fran. = .61). It should also be noted that, where the element variation is greatest between the red and grey clays (Nd, Yb, Lu), the values for the Dryden area red clays are intermediate between the Kaministikwia red clays and the Dryden area grey clays.

None of the variations in REE concentrations could be tested statistically due to the insufficient number of samples.

Geometry:

The Facies 1 rhythmites show a very consistent geometry in all of the outcrops examined, regardless of their location. This facies drapes and mantles the underlying lithologies throughout the entire area, and mimics any pre-existing topography (Fig. 2-16). Syndepositional slumping related to such topographic highs can also be recognized in some exposures (Fig. 2-17). Where the facies overlies coarser sediments, the rhythmites may infill and drape scoured channel surfaces (Fig. 2-18). The rhythmites within these channel forms are often quite disturbed.

The thickness of this facies in outcrop never exceeds 5 m, and is usually on the order of 2-3 m.

2.2.2 Sandy Rhythmites (Facies 2):

Description:

Like the Facies 1 silt-clay rhythmites, this facies consists of a sequence of rhythmically bedded couplets. However, these couplets are composed of a lower sand to sandy-silt member capped by an upper clay laminae (Fig. 2-19). Couplet thicknesses are also generally greater than in Facies 1, with the sand member ranging from 1.0-10.0 cm, and the clay member from 0.1-1.0 cm in thickness.

The lower member typically ranges from very fine sandy-silt to medium sand. The dominant sedimentary structures are climbing ripples (A, B and C-type of Jopling & Walker, 1968), and plane laminations. A common sequence within a single bed is from plane laminations in the lower part of the bed to

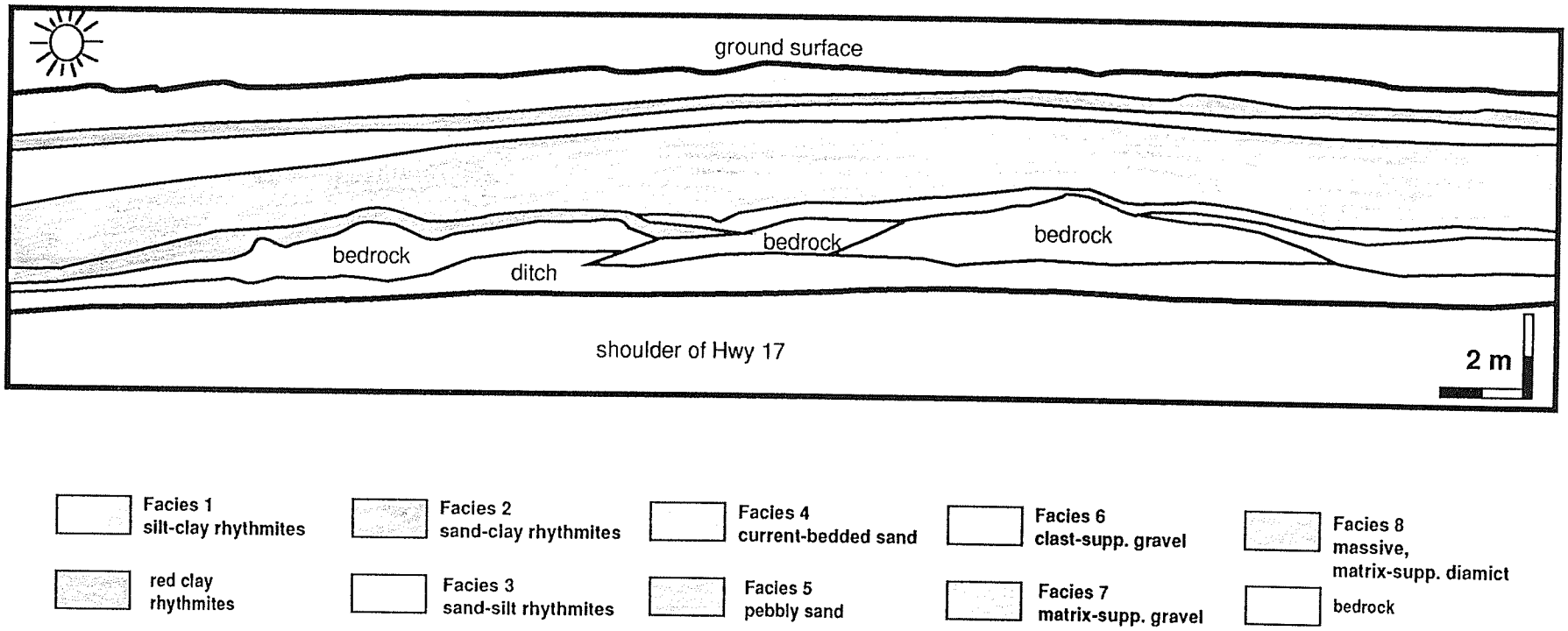

Fig. 2-16 Facies 1, 2 and 3 rhythmites and a thin diamict unit draping a bedrock high. This is a sketch made from photographs of section 89-1. See Fig. 2-1 for location.

Figure 2-17 Syndepositional slumping in Facies 1 rhythmites (section 87-20). Exposed face is approximately 3 m high.

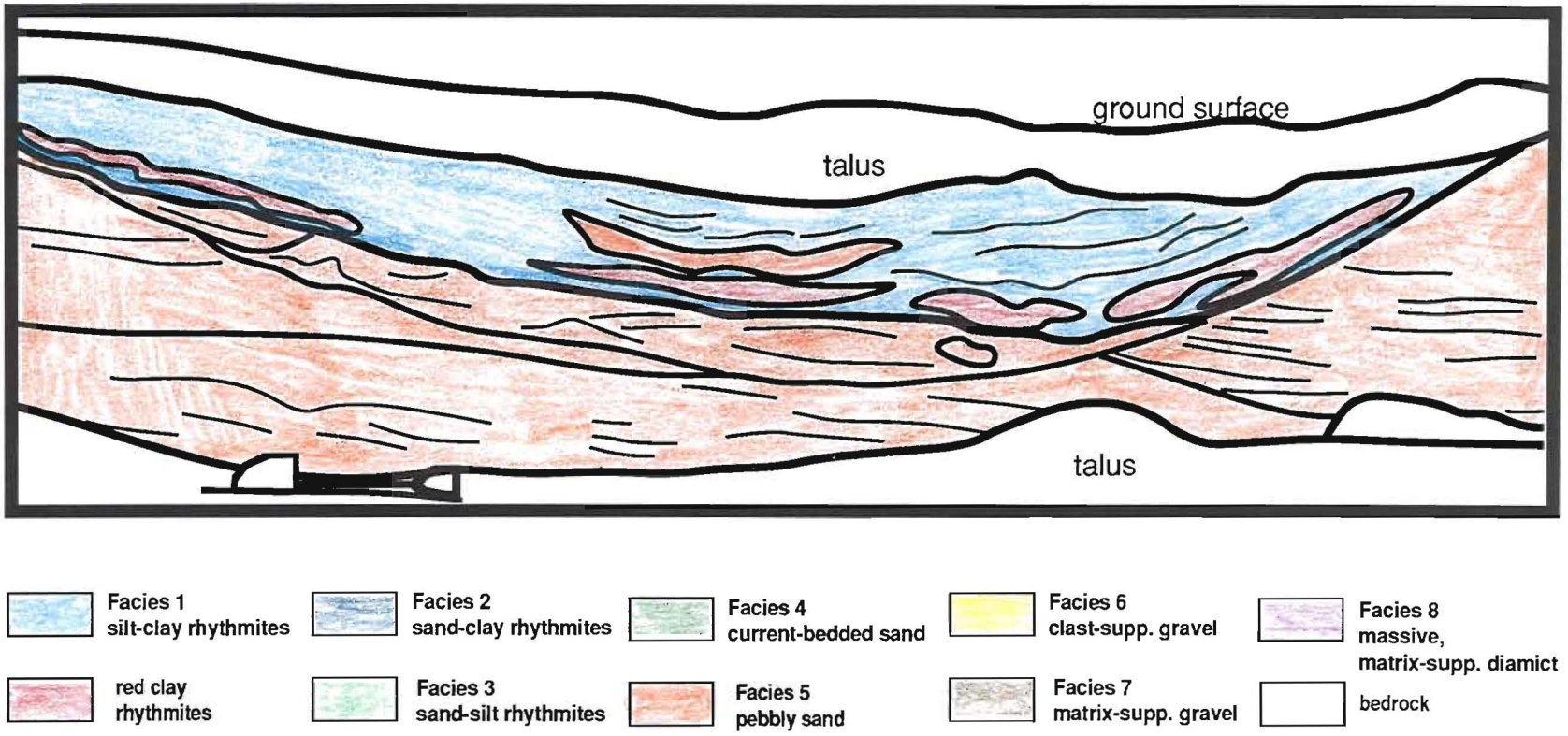

Fig. 2-18 Disturbed Facies 1 rhythmites infilling channel or scour cut into Facies 5 sands at the crest of the Hartman moraine. Note that the red clay rhythmites are present on the moraine crest. This diagram is a sketch made from photographs of section 87-11. Shovel is about 1m long. See Fig. 2-1 for location.

Figure 2-19 Facies 2 sand-clay rhythmites, showing both ripples and sub-horizontal laminations in the sandy part. Note the relatively thin, clayey parts of the couplets (section 87-20). Scale card is graduated in centimetres.

poorly to well-developed climbing ripples in the upper part. In some cases, ripples at the base of a couplet begin to form in the lee of clay-draped ripples of the underlying couplet (Fig. 2-20). Other sedimentary structures present include small-scale trough crossbedding and tabular crossbedding. Where the sand member is horizontally laminated, graded laminations often occur. Both normal (fining-upward) and reverse grading are present, although normal grading is more common.

As a general rule, the thicker the sand member of the rhythmite, the more likely that ripples will be present, and the more well-developed these ripples will be. Typical sand member thicknesses range from 1.0 cm to 10.0 cm, although beds may reach up to 20.0 cm or more. At one location (87-2), a 7cm thick bed of silt, in a 4.5m high section of silt-clay rhythmites, shows evidence of having been re-worked by wave activity (B. Greenwood, pers. comm., 1991). This bed displays non-migrating vortex ripples with an amplitude of 3cm and a wavelength of 10cm, and ripple crests oriented 80-260 degrees (Fig. 2-21). This unit was considered significant, but not widespread enough to merit a separate facies classification.

An unusual sequence of opposing ripples (Fig. 2-22) is seen in the couplets found at one particular outcrop (section 87-27). Each couplet is composed of a number of stacked sets of unidirectional (westward; Fig. 2-22) climbing ripples (sometimes with a thin clay cap) which are overlain erosively by a single set of ripples indicating flow in the opposite (eastward; Fig. 2-22)

Figure 2-20 Close-up of Facies 2 rhythmites. Note the partial erosion of the clay drape at the crest of the ripple near the tip of the tape measure, and the foresets built on the clay drape in the lee of this ripple crest (section 87- 27). Scale at left is in centimetres.

Figure 2-21 Facies 2 rhythmites showing effects of wave modification. Symmetrical, straight-crested wave ripples from section 87-2.

Figure 2-22 Reversing ripples from Facies 2 rhythmites at section 87-27. Note truncation of ripples (at arrow), and opposing foresets (A) built in the lee side (formerly the stoss side) of truncated ripples, all of which are draped with a clay lamina. West is to the right in this photo. Scale is graduated in centimetres.

direction. The entire sequence is then overlain by the clay member of the couplet.

The ripples in section 87-27 appear to be opposed unidirectional ripples rather than bi-directional wave ripples for two reasons. Firstly, the vast majority of the foresets in each couplet indicate paleoflow towards the west, while the eastward foresets comprise only a small portion of the couplet. Secondly, there is no interbedding of the eastward and westward oriented ripples as would be expected with bidirectional wave ripples (Harms et al., 1982; pp. 3-28 to 3-33). The eastward oriented ripples are confined to the tops of the couplets. These two observations indicate that a unidirectional westward flowing current formed the majority of each couplet, followed by an abrupt reversal in paleoflow direction (towards the east) which resulted in erosion of the top of the westward ripple sequence and deposition of the single set of eastward ripples. This was followed by relatively quiet water conditions in which the clay lamina was deposited.

The clay member of the couplet is generally a massive, grey clay lamina ranging between 0.1 and 1.0 cm thick. These laminae drape the underlying sand surface, and may show evidence of having been eroded by the subsequent flow, being thin or absent at the crest of underlying ripples, and generally thicker in the troughs (Fig. 2-22). The lower contacts of these clay laminae are always sharp and conformable.

Commonly within these sequences, there are discrete horizons or zones of moderate to extreme soft sediment deformation, including flame structures,

attached and detached ball and pillow structures and severely convolute bedding (Fig. 2-23). These zones of deformation are frequently capped by an undeformed clay laminae, indicating that quiet water conditions followed a period of deformation. Deformation structures such as flames and folds may be entirely vertical, or may show a preferred orientation (Fig. 2-23), possibly indicating overturning by gravity-induced downslope movement, or by overriding traction currents.

There are also minor internal discontinuities or erosion surfaces within this facies. Outsized clasts are rare, and are always solitary pebble-sized clasts. Overall, this facies tends to display an upward trend of fining grain sizes in the sand member of the couplets, and a decrease in couplet thickness. The upper contact of this facies is gradational where it is overlain by silt-clay rhythmites (Facies 1) and erosional in all other cases.

Red Sequence:

In two of the sonic cores from north of the Hartman moraine (D-3 & DT-6, see Fig. 1-4), there is a zone in which the Facies 2 sand-clay rhythmites are capped by clay laminae which are distinctly red in colour (see Fig. 2-56, p. 95). These laminae are identical to the more common grey clay laminae in all other respects. These red-clay rhythmites appear to be equivalent to the red clay sequence in the Facies 1 silt-clay rhythmites from south of the Hartman moraine.

Figure 2-23 Syndepositional deformation of Facies 2 rhythmites. Note two undeformed zones are separated by a thin undeformed layer, and upper deformed zone is overlain by undeformed clay laminae (section 87-3). Scale card is 9 cm long.

Geometry:

The outcrop-scale geometry of this unit is quite similar to that of the Facies 1 silt-clay rhythmites, in that in areas where it overlies bedrock highs, it appears to drape and mimic the underlying surface (Fig. 2-16).

The unit thickness of Facies 2 in outcrop us usually on the order of 1-4 m.

2.2.3 Rhythmically Bedded Sand and Silt (Facies 3):

Description:

This facies is very similar to the sandy rhythmite facies (Facies 2), except that it lacks clay drapes in its couplets. Instead, the upper member of the couplet is a centimetre-scale massive silt bed which drapes the underlying sand layer (Fig. 2-24). As in the sandy rhythmites, the most common sedimentary structures are climbing ripples and horizontal laminations. In the horizontally-laminated members, both normal and reverse grading are seen, with no clear dominance of one type.

Grain sizes within the lower sandy members range from sandy silts to fine sands, and minor medium sands. These sandy members are typically decimetres to centimetres in thickness, and have sharp to erosional lower contacts. Their upper contacts with the silt drape are always sharp and conformable.

Soft-sediment deformation structures are commonly confined to discrete horizons within the outcrop (Fig. 2-25). Also common are minor, low angle internal disconformities. The upper contact of this facies is typically gradational into silt-clay rhythmites (Facies 1) or sandy rhythmites (Facies 2), otherwise it is

Figure 2-24 Facies 3 sand-silt rhythmites. These rhythmites are conformably overlain at this site by the Facies 2 and 1 rhythmites see in figure 2-8 (section 87- 24). Scale card is 9 cm long.

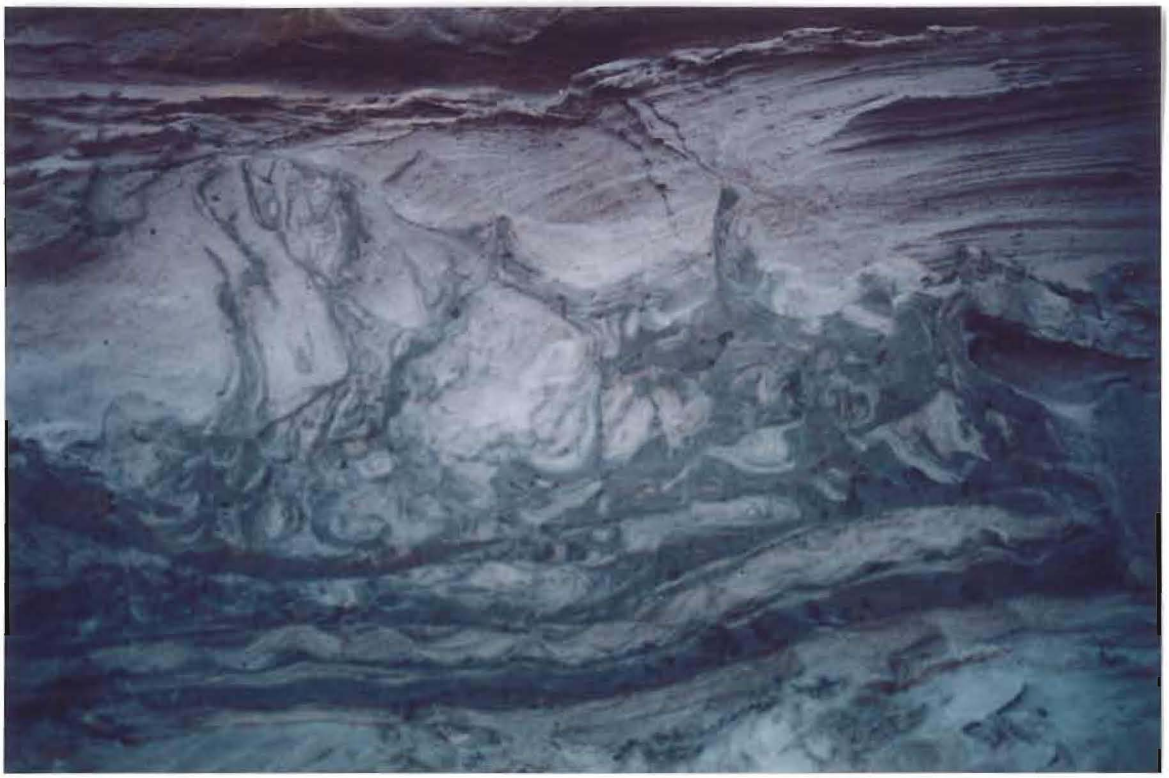

Figure 2-25 Syndepositional deformation in Facies 3 rhythmites. This deformed zone is overlain and underlain by undeformed sediments, and grades laterally into undeformed sediments (section 87-2). Vertical field of view is approximately 80 cm.

erosional. The lower contact of this facies is quite variable, and may be gradational, sharp and conformable, or erosional.

Geometry:

This uncommonly exposed facies normally exhibits a horizontal to subhorizontal attitude (Fig. 2-16). A feature which sets it apart from the finer rhythmically bedded facies is the abundance of channels within which this facies is often found (Fig. 2-26). Within these channels, it is often associated with Facies 4 current-bedded sands.

The unit thickness of the Facies 3 rhythmites in outcrop ranges from 1-2 m.

2.2.4 Non-rhythmic, Current-bedded Sand (Facies 4):

Description:

This facies may be divided into two fairly distinct associations (4A and 4B) based on sedimentary structures, outcrop-scale geometry, and relationship with adjacent facies. However, both associations show some similarity.

In both associations, the units consist mainly of moderately well-sorted fine to coarse sand. These sands typically occur in decimetre- to metre-scale beds, with sharp to gradational lower and upper contacts. These sands are occasionally interbedded with minor granular or pebbly beds, or with silty horizons. These interbeds normally comprise no more than 10% of the outcrop area of this facies, and are generally a few centimetres to decimetres thick. Bedding does not show any rhythmic variation in this facies, and clay laminae

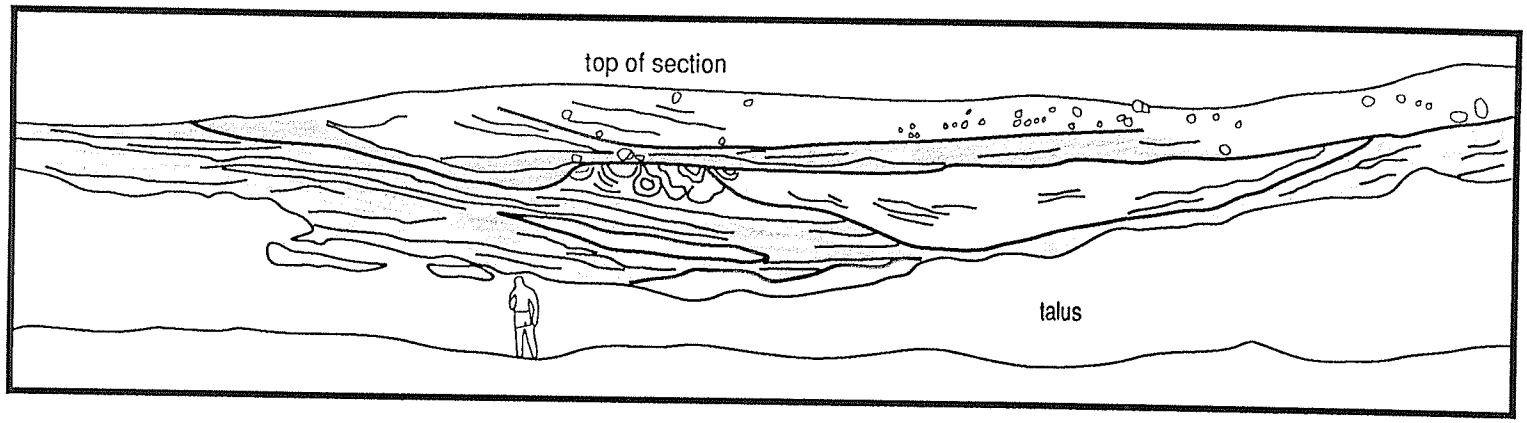

Facies 2
sand-clay rhythmites

Facies 4
current-bedded sand

Facies 6
clast-supp. gravel

Facies 8
massive,
matrix-supp. diamict

Facies 3
sand-silt rhythmites

Facies 5
pebbly sand

Facies 7
matrix-supp. gravel

bedrock

Fig. 2-26 Facies 3 rhythmites infilling a broad, shallow channel on the crest of the Eagle-Finlayson moraine. Note abundant soft-sediment deformation structures. This diagram is a sketch made from photos of the upper part of section 88-2. The figure is approximately 1.75m tall. See Fig. 2-1 for location.

are entirely absent. This facies may have gradational, sharp and conformable, or erosional upper and lower contacts.

Geometry:

Facies association 4A is most commonly found in esker deposits, and consists of a broad (10's to 100's of metres) tabular body of sand, typically 0.5-2.0 m in thickness, which show large-scale, two-dimensional ripples. These are often found between thick units of clast-supported gravels (Facies 6)(Fig. 2-27). These tabular bodies may grade laterally (transverse to measured paleoflow) into thick (2-3 m) trough-crossbedded channel fill sands (Figs. 2-28 & 2-29). These channels are oriented parallel to the esker trend and to the measured paleoflow direction. The tabular sand bodies may also grade parallel to the paleoflow direction (and the esker orientation) into thicker deposits which appear to have been deposited in the lee of large, clast-supported gravel bodies (Facies 6)(Fig. 2-30). In one instance, these sands were interbedded with clast-supported gravels (Facies 6), forming large-scale (3-4 m) foreset beds (Fig. 2-31). Poorly developed ripple forms (Fig. 2-32) and apparent deposition in the lee, and scour around the stoss sides of underlying clasts (Fig. 2-33) was observed.

The 4B association is found most commonly within the end moraines, and occurs as an infill within broad, shallow channels (Figs. 2-26 & 2-34), often in combination with Facies 5 pebbly sands. These channels are always oriented normal to the trend of the moraine, and may be cut into underlying deposits of Facies 4, 5 and 6. Bedding surfaces are normally parallel to the

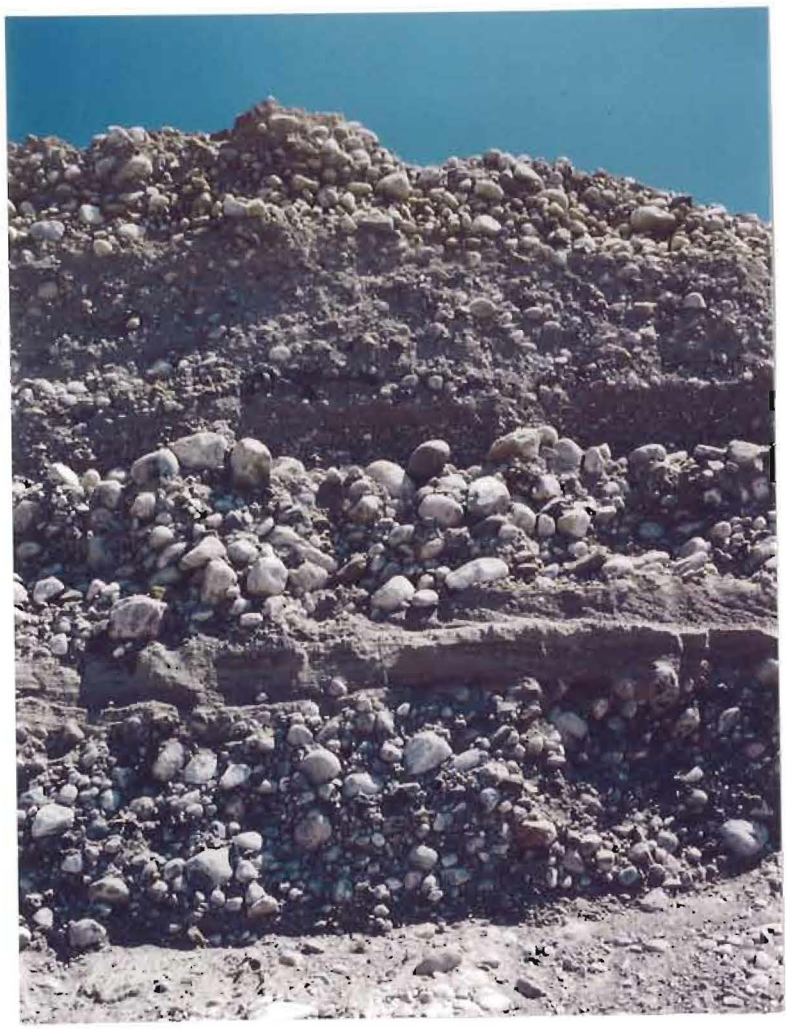

Figure 2-27 Close-up of a broad, tabular Facies 4A sand body sandwiched between clast-supported gravels (Facies 6)(section 87-2). Note both sub- horizontal and tabular crossbedding in the sand. The sand bed in the middle is approximately 20 cm thick.

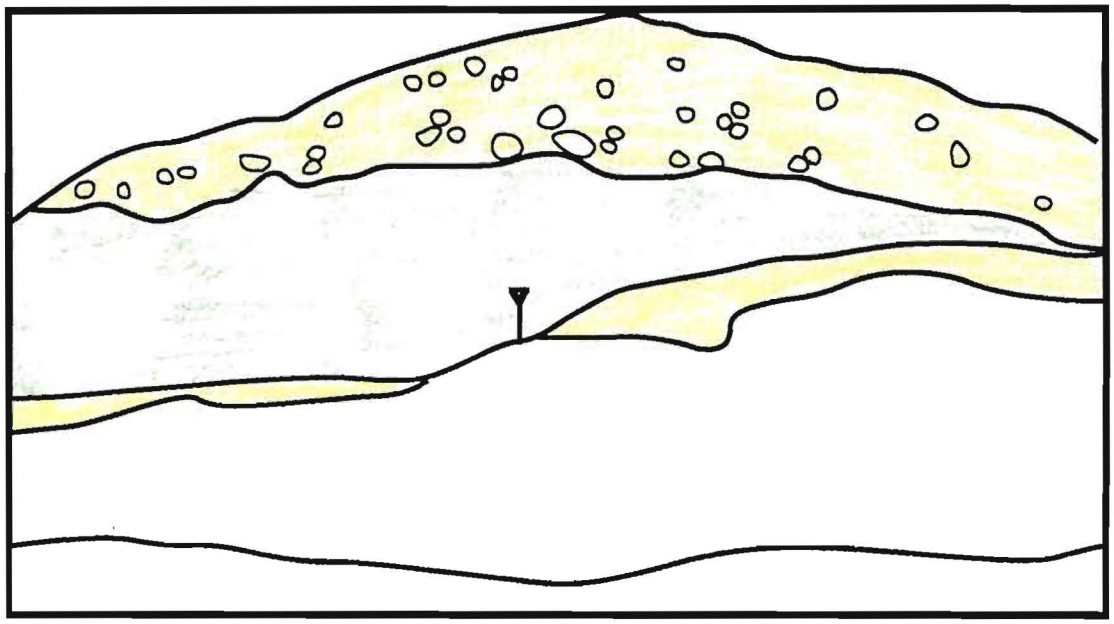

Fig. 2-28 Photograph and sketch of tabular sand body at right grading across the paleoflow direction into large-scale trough crossbedded sandy channel infill at left. Paleoflow is directly towards viewer. Section 87-2, see Fig. 2-1 for locations. Shovel handle is approximately 1m high.

Figure 2-29 Large-scale trough crossbedding in Facies 4 sands (section 87-2, same channel as in figure 2-28). Figure for scale.

Figure 2-30 Thin, tabular sand body (Facies 4)(at left) grading into a much thicker crossbedded unit (at right) in the lee of a large, clast-supported gravel body (section 87-2). Figure for scale.

Figure 2-31 Facies 4 sands interbedded with clast-supported gravels (Facies 6) to form large-scale foreset beds at section 88-6. Figure for scale.

Figure 2-32 Poorly-developed ripples forms which appear to indicate paleoflow up large-scale forest beds seen in figure 2-31 (section 88-6). Flow is from left to right. Scale card is 9 cm long.

Figure 2-33 Foreset beds deposited in the lee of an underlyng boulder indicating paleoflow from left to right, up the large-scale foreset beds seen in figure 2-31 (section 88-6). Notebook is 12 cm wide.

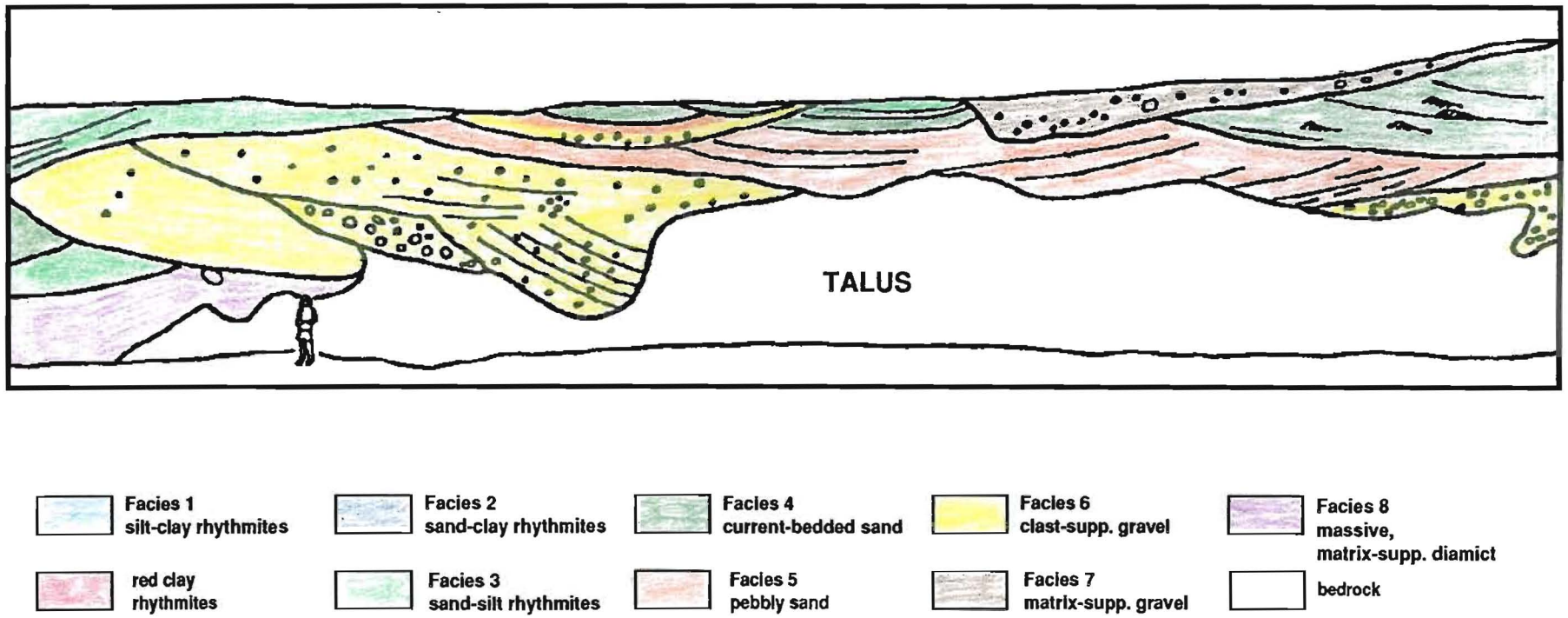

Fig. 2-34 Nested stack of broad, shallow channels infilled with clast-supported gravels, pebbly sands and current-bedded sands on the crest of the Eagle-Finlayson moraine. The section runs parallel to the moraine crest. This is a sketch made from photographs of the lower part of section 88-2. The figure is approximately 1.75m tall. See Fig. 2-1 for location.

channel margins. Channel depth may be up to 4-5 m, and widths can exceed 20 m. These channels are rarely solitary features, and are often part of a series of stacked, erosionally nested channels (Fig. 2-34).

Large- and small-scale, two-dimensional ripples (Figs. 2-35 & 2-36) and sub-horizontal bedding (Fig. 2-37) are most common in the 4B sands. Both large- and small-scale ripples show evidence of climbing and lee-side preservation. Normal and reverse-graded beds are not uncommon, with normal grading predominating.

2.2.5 Pebbly Sand (Facies 5):

Description:

This facies is comprised mainly of medium to coarse sands, containing between 10% and 50% clasts, which are almost always supported by and dispersed in a sandy matrix (Figs. 2-38 to 2-40). The clasts are generally 0.2-2.0 cm in size but may be up to 6.0 cm in diameter.

These pebbly sands may show large-scale, two-dimensional ripples and large-scale trough crossbedding, although horizontal bedding is the most common sedimentary structure (Figs. 2-38 to 2-40). Normal and reverse grading is common in the horizontally stratified units (Fig. 2-40). Bedding is typically on a scale of decimetres to metres. There may be minor (<10%) interbeds of granules or pebbles, or of well sorted,non-pebbly sand. Minor internal erosion surfaces are common, and individual beds may have gradational, sharp and conformable, or erosional upper and lower contacts. The same is true for the facies as a whole.

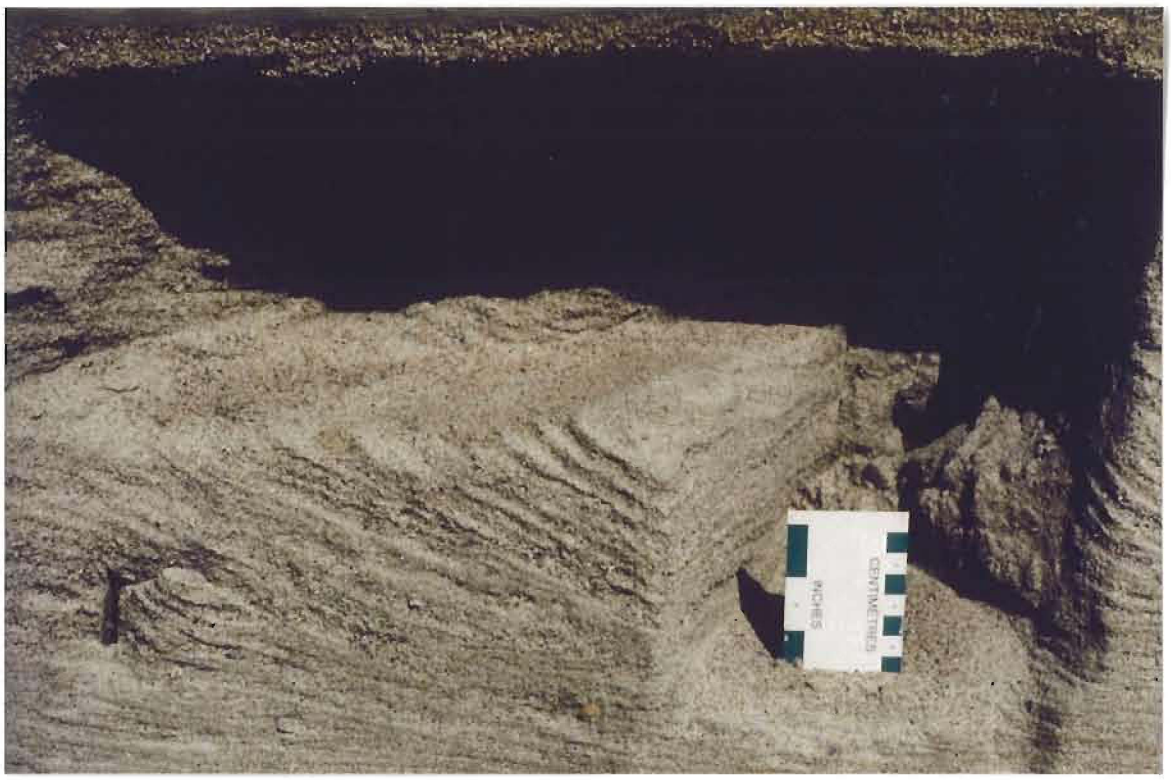

Figure 2-35 Tabular crossbedding in Facies 4 sands (section 87-11). Scale card is graduated in centimetres.

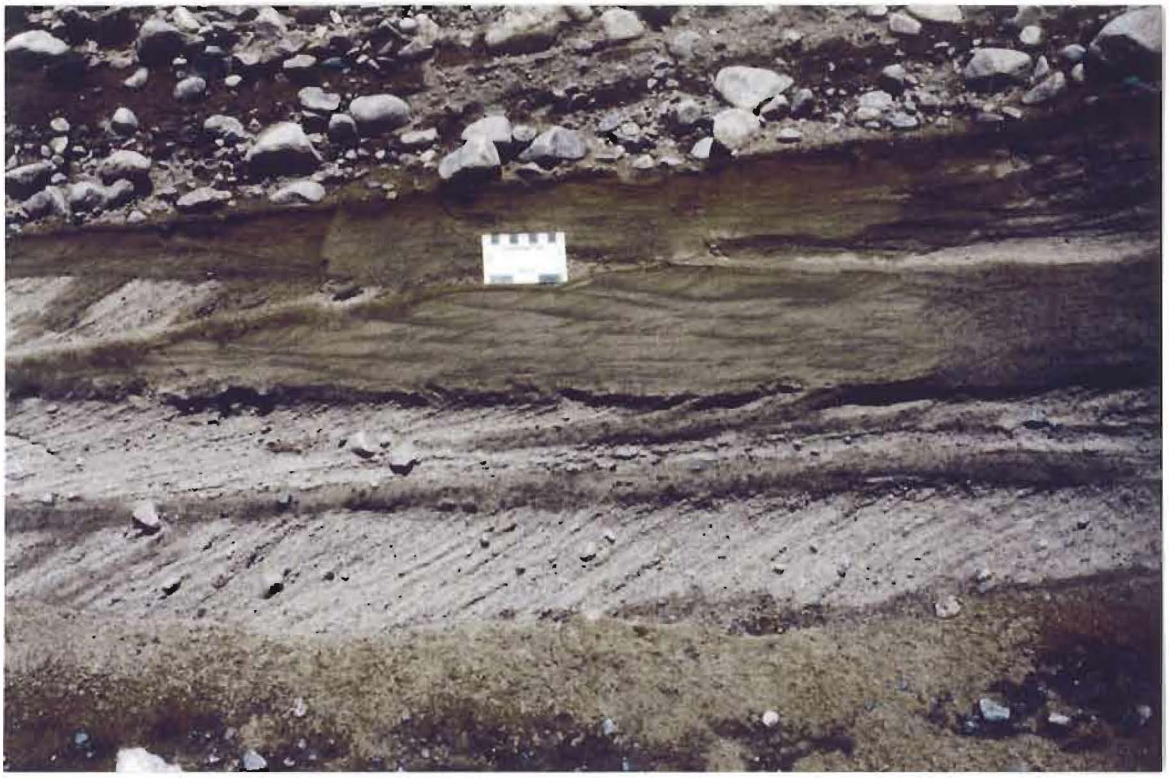

Figure 2-36 Facies 4 sands (darker sands) showing climbing ripples, interbedded with cross-stratified pebbly sands (Facies 5). Scale card is 9 cm long.

Figure 2-37 Sub-horizontal bedding in Facies 4 sands. Note interbeds of Facies 5 pebbly sands (section 88-4). Scale is graduated in centimetres.

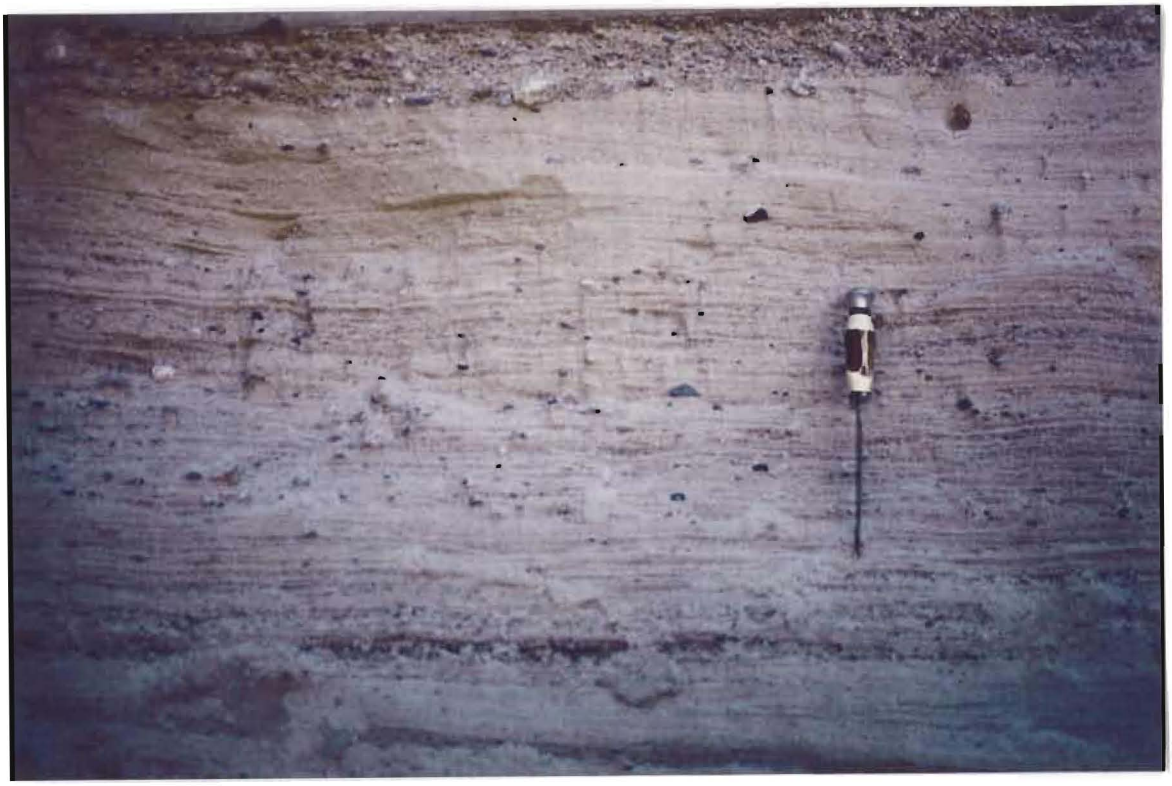

Figure 2-38 Facies 5 pebbly sands. Note that the pebbles are mainly supported by and dispersed in the matrix. A concentration of pebbles along a bedding plane can be seen below the knive (section 88-4). Knife is approximately 25 cm long.

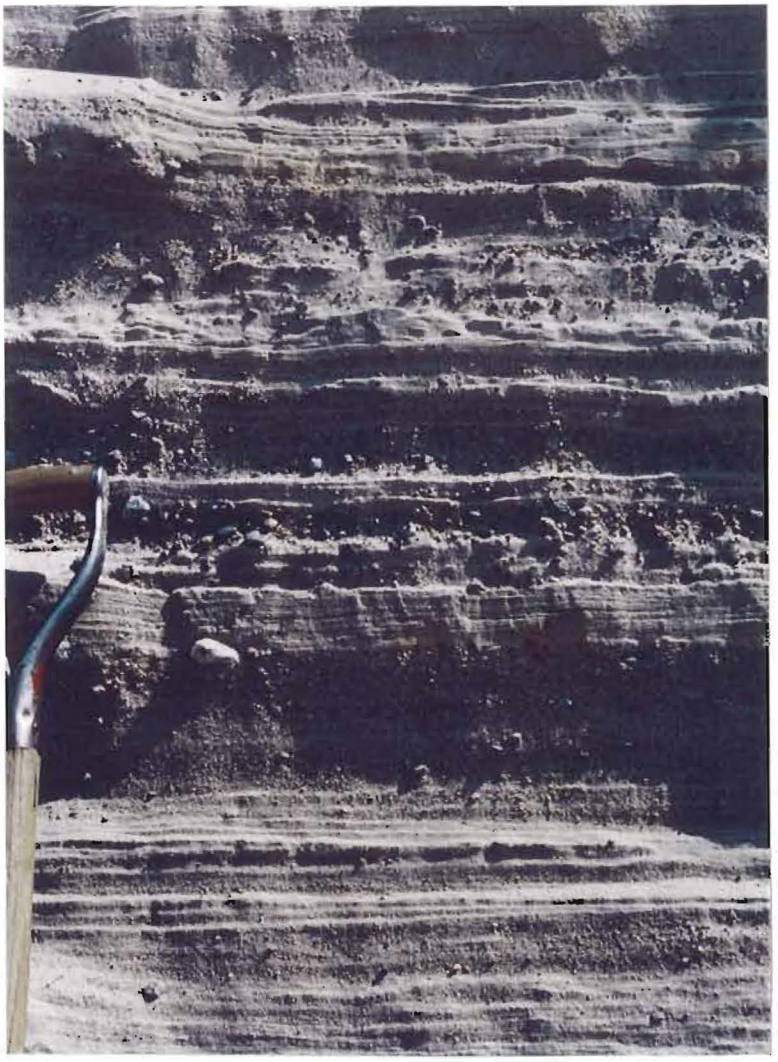

Figure 2-39 Sub-horizontal bedding in Facies 5 pebbly sands (section 88-4). Shovel handle for scale.

Figure 2-40 Normal grading in Facies 5 pebbly sands 9 (section 88-5). Zone in centre is slumped material. Scale is graduated in centimetres.

Geometry:

The Facies 5 pebbly sands form thick (2-10m) infills in broad, shallow, nested channel sets, often in combination with Facies 4B sands (Figs. 2-34, 2-41). These channels are usually quite large, and can be as deep as 10 m and up to 50 m in width. Bedding in the channel infill is parallel to the channel margin (Fig. 2-41). These channels may be eroded into units of Facies 4, or 6, or into other Facies 5 deposits. Within these large channel infills may be smaller-scale erosional surfaces and channels. Overall, a series of these stacked, nested channels may form sequences exceeding 20 m in thickness.

The facies also (but less commonly) forms tabular units of 0.5-2.0 m in thickness, with subhorizontal parallel bedding, particularly when seen in sections oriented parallel to paleoflow (Fig. 2-42). These units are often interbedded with Facies 4 or 6.

2.2.6 Clast-supported Gravel (Facies 6):

Description:

This facies is composed mainly (>50%) of clasts ranging in size from granules to boulders, with most exposures showing clasts in the pebble to cobble range. The distinguishing aspect of this facies is that the majority of clasts are in contact, forming a supporting framework. Clasts are generally moderately sorted, subangular to well rounded and usually display a relatively high sphericity (Fig. 2-43). Maximum clast size observed in the study area was about 50-60 cm. When a matrix is present it is usually poorly sorted and ranges from fine to very coarse sand and granules.

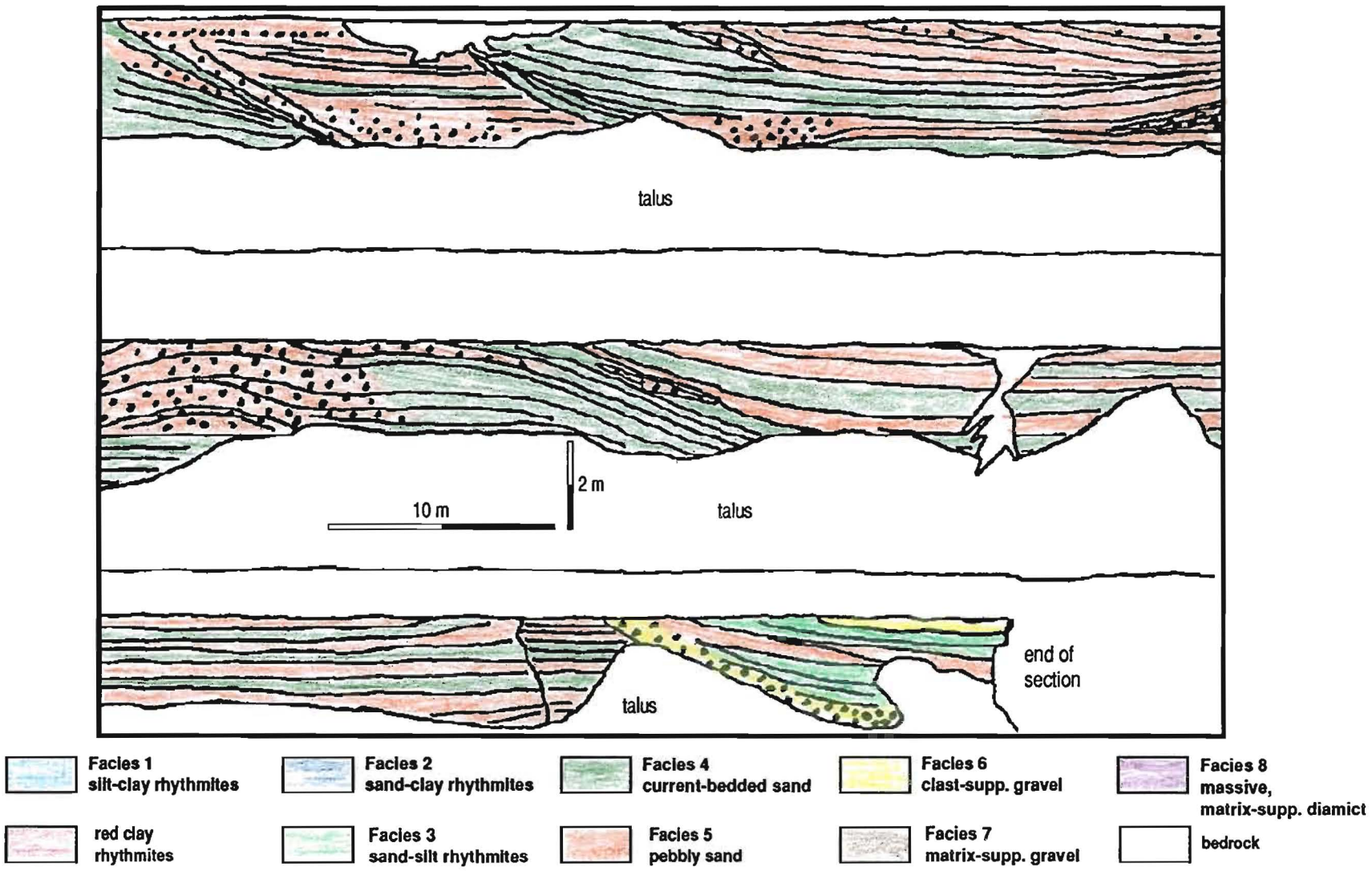

Fig. 2-41 Continuous three part sketch (upper left to lower right) of section 88-4 in the crest of the Eagle-Finlayson moraine. Note the subhorizontal beds of clast-supported gravels, current-bedded sands and pebbly sands infilling broad, shallow channels. Note vertical exageration.

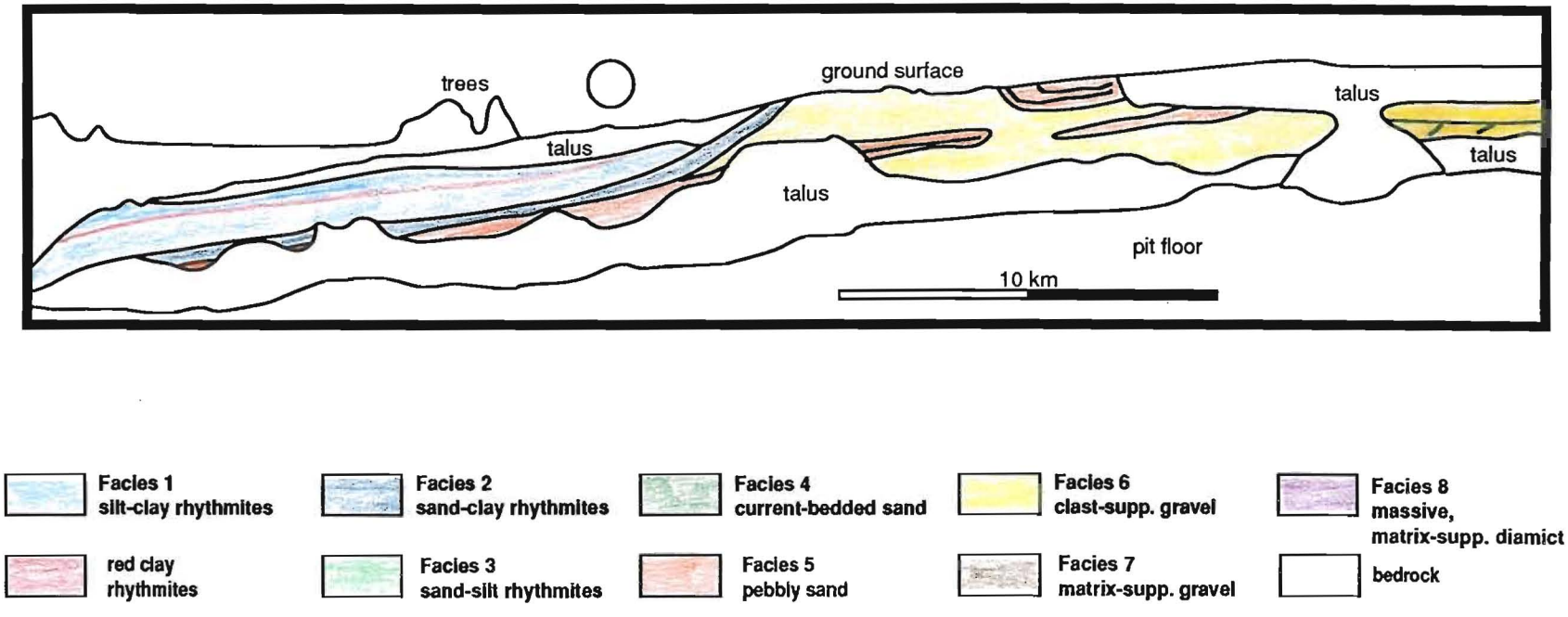

Fig. 2-42 Sketch of section 87-23 showing Facies 5 pebbly sands both in tabular bodies and as channel infilling. This sketch was made from a series of photographs of the section.

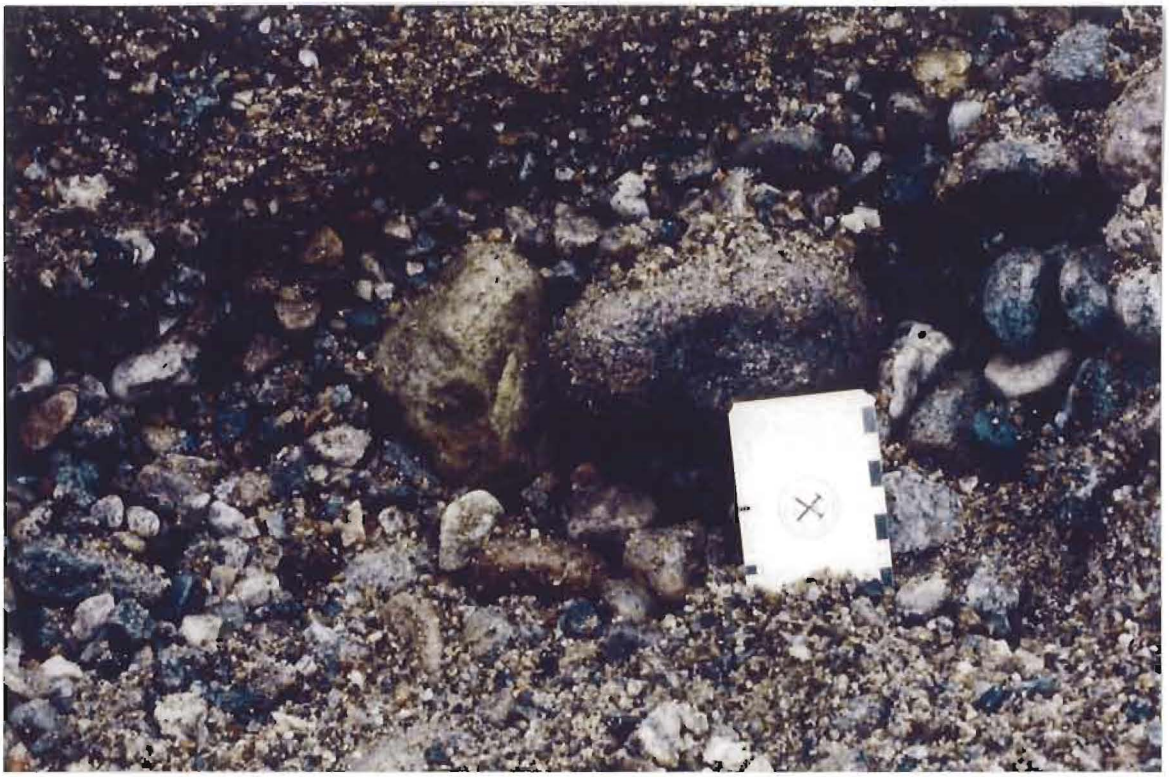

Figure 2-43 Facies 6 clast-supported gravel. Note alternation of open-work and closed-work beds (section 87-2). Scale is graduated in centimetres.

Geometry:

This facies can be subdivided on the basis of geometry, sedimentary structures and clast size into two distinct associations. The most common forms for this facies to take are large tabular bodies (Facies 6A, Fig. 2-27), usually found within esker and kame landforms. These bodies are typically 1 - 5 m in thickness, and may extend for several hundred metres in a direction normal to paleoflow and 100 m or more parallel to paleoflow. The gravels generally are massive to slightly imbricated (Fig. 2-44), and the gravel bodies may have an angled face on their downflow end (Fig. 2-30).

These large gravel bodies may also display well developed foreset beds 1-3 m in height, visible due to grain size variations (Fig. 2-45), or due to interbedding with current-bedded sands (Fig. 2-31). Clasts in the Facies 6A gravels are generally in the cobble to boulder size range. The other occurrence of this facies (Facies 6B) is confined to the end moraine landforms, and appears as infills in large, broad, shallow channels up to 6 m in depth and 45 m in width. These are often nested and stacked (Fig. 2-34), and cut into underlying sediments of Facies 3 through 8. Bedding is parallel to channel margins, and internal discontinuities are not uncommon. A common feature of Facies 6B is an overall normal grading in the clast sizes, although not in the matrix. Clast sizes in the Facies 6B gravels are generally in the pebble to cobble range.

This facies ranges in overall thickness from 1.0 m to > 5.0 m, and usually has an erosional base and a gradational, sharp and conformable, or erosional upper surface.

Figure 2-44 Imbrication in Facies 6 clast-supported gravel (arrowed). Flow was from right to left (section 88-9) Red notebook near base of exposed gravel in centre of photo is 21 cm long.

Figure 2-45 Well-developed foreset beds in Facies 6 clast-supported gravel, defined by variations in grain sizes and alternations of open-work and closed-work beds (section 87-2). Scale card (centre-left, circled) is 9 cm long.

Clast-supported gravels may also appear as relatively thin (10 - 25 cm), isolated beds within sands or pebbly sands (Facies 4 and 5). These generally have little or no matrix and an irregular upper surface.

2.2.7 Matrix-supported Gravel (Facies 7):

Description:

This facies consists of subangular to subrounded clasts ranging in size from pebbles to 90.0 cm boulders. The feature which distinguishes this facies from the Facies 6 clast-supported gravels is the lack of contact between the majority of clasts. Most clasts are completely supported in a matrix of poorly-sorted medium sand to small (<2.0 cm) pebbles (Fig. 2-46). These gravels are generally massive, although rare indistinct stratification, normal grading of the clasts, and/or poorly-developed imbrication may be seen. This facies differs from the Facies 5 pebbly sands in that the average clast size is much greater, and the clasts form more than 50% of the deposit.

Geometry:

This not a particularly common facies in the study area, and was observed at only three locations. It always occurs at the top of sections, and has an erosive base. It may occur as either a flat-lying tabular body (Fig. 2-46), or it may have a channelized base (Fig. 2-34). Unit thicknesses range from 1-3 m.

Both the upper and lower contacts of this facies are erosional. The thickness of this facies ranges from approximately 1.0 m to > 4.0 m.

Figure 2-46 Facies 7 matrix-supported gravel overlying and truncating large-scale forest beds at section 88-6. Shovel for scale.

2.2.8 Massive, Matrix-supported Diamict: (Facies 8):

Description:

This facies is a poorly sorted admixture of clay and silt, with only minor sand, and a few clasts ranging from pebble to boulder size (Fig. 2-47). In the only exposure of diamict in the study area, clast sizes range up to 60 cm in size and the majority are not in contact, being supported entirely by the matrix. There is no apparent imbrication of the clasts.

The matrix is generally massive, but deformed, remnant sedimentary structures such as ripples and horizontal laminations were observed. Within this facies, there are also minor interbeds of horizontally bedded sand up to 30 cm in thickness.

Geometry:

This facies was observed in only one outcrop and in the bottom of several sonic cores, and is generally not well exposed. It appears to be at least 3 m thick (Fig. 2-34), but the geometry of the unit is unknown. It is known to overlie Facies 6B clast-supported gravels at least 3 m thick, and is itself erosively overlain by Facies 2 sand-clay rhythmites and Facies 6B clast-supported gravels. It does not appear to be laterally extensive.

2.3 GEOGRAPHIC DISTRIBUTION OF FACIES:

From the surficial geology maps of Cowan & Sharpe (1991) and Minning & Sharpe (1991) (Fig. 1-2), and from the geology seen in outcrops, it can be seen that the various facies show marked differences in their geographic distributions. Deposits of the coarsest facies (Facies 4 through 7) are quite

Figure 2-47 Facies 8 matrix-supported diamict, overlying sandy beds at section 88-2 (see also Figure 2-34). Knife handle is 10.5 cm long.

restricted, and can be divided into three distinct types, based on their orientation and geometry.

The first and most prominent type of coarse deposit forms a long, thin, arcuate ridge oriented **transverse** to regional ice-flow (Fig. 1-2). This type of deposit has been termed an end moraine by previous workers in the area (Rittenhouse, 1934; Satterly, 1943; Zoltai, 1961; Cowan & Sharpe, 1991; Minning & Sharpe, 1991), and this terminology will be maintained in this thesis. There are three such end moraines within the study area, and these are referred to (from south to north) as the Eagle-Finlayson, the Hartman and the Lac Seul moraines (Fig. 1-2).

A second, and less well-defined coarse deposit forms a long, semi-continuous body oriented **parallel** to regional ice-flow, which usually forms a link between two adjacent moraines (esker deposits of Fig. 1-2). These deposits often form discontinuous ridge-like topographic highs, which appear to be analogous to the beaded eskers of Banerjee and McDonald (1975). Several of these bodies occur in the study area, but were not noted by previous workers, and are not formally named.

The third type of coarse-grained deposit occurs as a relatively large, isolated mound or hill. These forms have been referred to as kames by Satterley (1943) and Zoltai (1961), and as isolated fans by Cowan (1987) (Fig. 1-2). These deposits are generally located in areas between the end moraines and away from the esker deposits.

In contrast to the restricted distribution of the coarse facies, the finer, rhythmically bedded facies (Facies 1 through 3) are quite widespread throughout the study area (Fig. 1-2). These sediments, especially the finer silt-clay rhythmites of Facies 1, form a laterally extensive blanket which drapes the underlying lithologies. In outcrop, these rhythmically bedded sediments are seen to drape underlying bedrock highs, mimicking and subduing the pre-existing topography. Rhythmically laminated sediments are most common and thickest in-between the moraines and away from the esker and kame deposits, but in some cases they drape these topographically higher deposits as well. The most common gaps in the blanket of rhythmic sediments are caused by extreme bedrock highs with steep flanks, that are barren of all sediment.

Of particular interest is the distribution and extent of the red clay rhythmite unit within the Facies 1 and 2 rhythmite sequences. The distribution noted by Zoltai (1967)(Fig. 2-48) is essentially correct, except that he places the northern boundary of the red clay at the Hartman moraine. New exposures, and information from the sonic cores and from water well logs allow this limit to be better defined (Fig. 2-48). It appears that the actual boundary of the red clay unit is somewhere between the Hartman and Lac Seul moraines.

2.4 VERTICAL FACIES SEQUENCES:

Throughout the entire study area there is an overall fining-upward trend in the sedimentary sequence, which can be seen both in outcrop and in sonic drill cores (Fig. 2-49). On the scale of an individual outcrop or drill hole

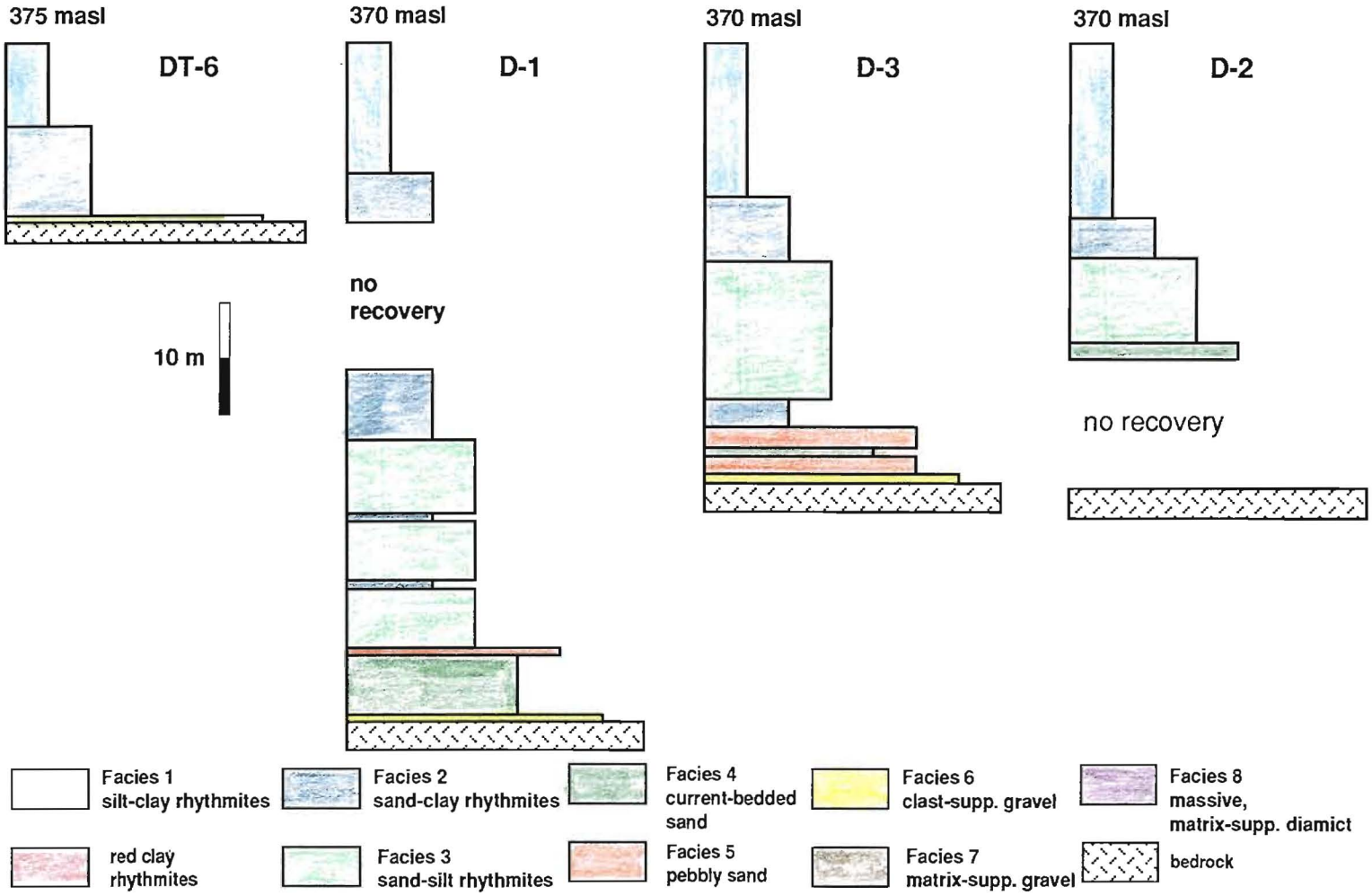

Fig. 2-49 Simplified logs of rotasonic drill cores from the study area (see Fig. 1-4 for locations). Elevation at top of the cores is given in metres above sea level (masl) Note the overall fining-upward trend in all of the cores.

however, smaller sequences may show either fining and coarsening upwards cycles.

Within the three end moraines, the vertical sequences normally start with a core of coarse (cobbly to bouldery) clast-supported gravels with rare diamicts. Commonly overlying these are finer clast-supported gravels and current-bedded pebbly and non-pebbly sands. Deposits of pebbly sands can be quite extensive, as is the case on the crest of the Eagle-Finlayson moraine near Vermillion Bay.

In many cases, this sequence from coarse gravels to pebbly and non-pebbly sands forms the entire morainic deposit, particularly on the Eagle-Finlayson moraine. However, it is not uncommon to find the finer, rhythmic sediments of Facies 1 through 3 draped on top of the moraines. Quite commonly these finer sediments drape and infill large (metre scale) channels or chutes on the surface of the coarser sediments. The finer sediments which are found on or near the moraine crests normally show a higher degree of disturbance and slumping than those deposited away from the moraine. Generally the contact between the coarse sediments forming the core of the moraine and the finer draping sediments appears to be abrupt rather than continuous in nature. In one exposure, badly disturbed sand-silt and sand-clay rhythmites actually underlie a 2-m-thick deposit of clast-supported gravels on the crest of the Hartman moraine (Fig. 2-50).

Within the esker and kame deposits, there is also a core of coarse clast-supported gravels (but without diamicts) overlain by relatively thin deposits of

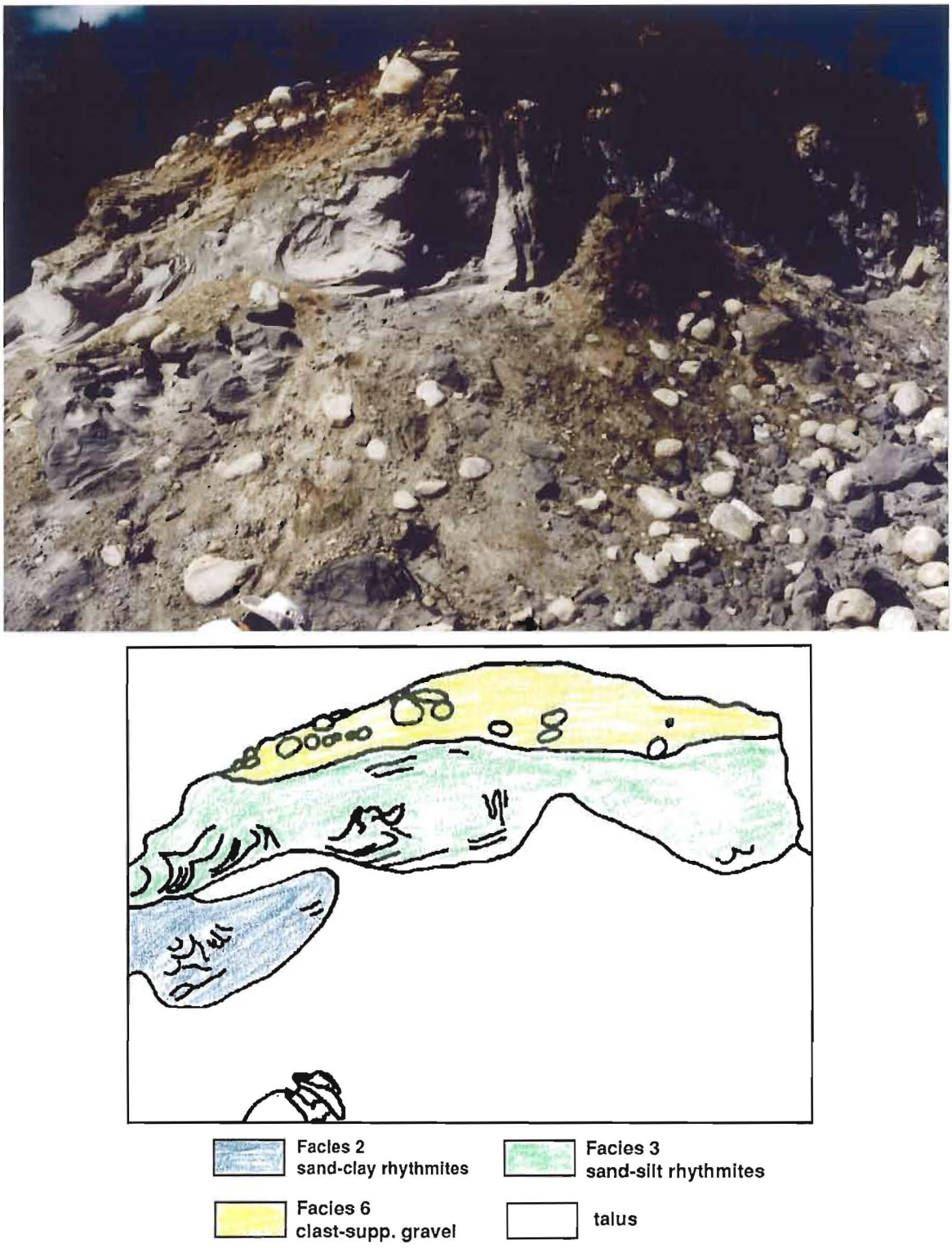

Fig. 2-50 Photograph and sketch showing disturbed Facies 2 and 3 rhythmites overlain by Facies 6 clast-supported gravels on the crest of the Hartman moraine (section 88-9). Figure for scale.

finer gravel, and current-bedded pebbly and non-pebbly sand. However, frequently overlying this is a fining upwards sequence of rhythmically bedded sediments (ie. from Facies 3 through to Facies 1). Unlike the moraine sequences, this entire sequence from clast-supported gravel to silt-clay rhythmites is usually gradational, or shows only minor discontinuities (Figs. 2-51 & 2-52). The majority of the esker and kame structures are entirely or almost entirely draped by finer rhythmically bedded sediments. Because the surficial geology maps of Cowan & Sharpe (1991) and Minning & Sharpe (1991) represent only the upper 1 m of sediment, the number of esker and kame deposits within the study area may be greatly under-represented.

On both the proximal and distal sides of the Hartman moraine, the sedimentary sequences seen in the sonic drill cores and in reflection seismic profiles show some interesting features. The sonic cores reveal a continuous fining upwards sequence from a thin basal diamict and/or pebbly to non-pebbly sand, through thick rhythmically laminated sediments of Facies 3, 2 and 1 (Fig. 2-49; see Appendix A for detailed logs).

Interestingly, the geophysical profiles (Figs. 2-53, 2-54) show that the bedrock topography is much more extreme than the current surface topography, and that this is due to infilling of deep (up to at least 65 m) bedrock lows, mainly by thick deposits of fine-grained, rhythmically-bedded sediments. The lowermost units of the sedimentary infills appear to have been "ponded" in these lows, and it is only the uppermost reflectors which seem to drape the adjacent bedrock highs (Fig. 2-53).

Figure 2-51 Conformable sequence from clast-supported gravel through current-bedded sand, overlain by Facies 3, 2 and 1 rhythmites in an isolated fan (kame) deposit (section 87-23). Notebook is 21 cm high.

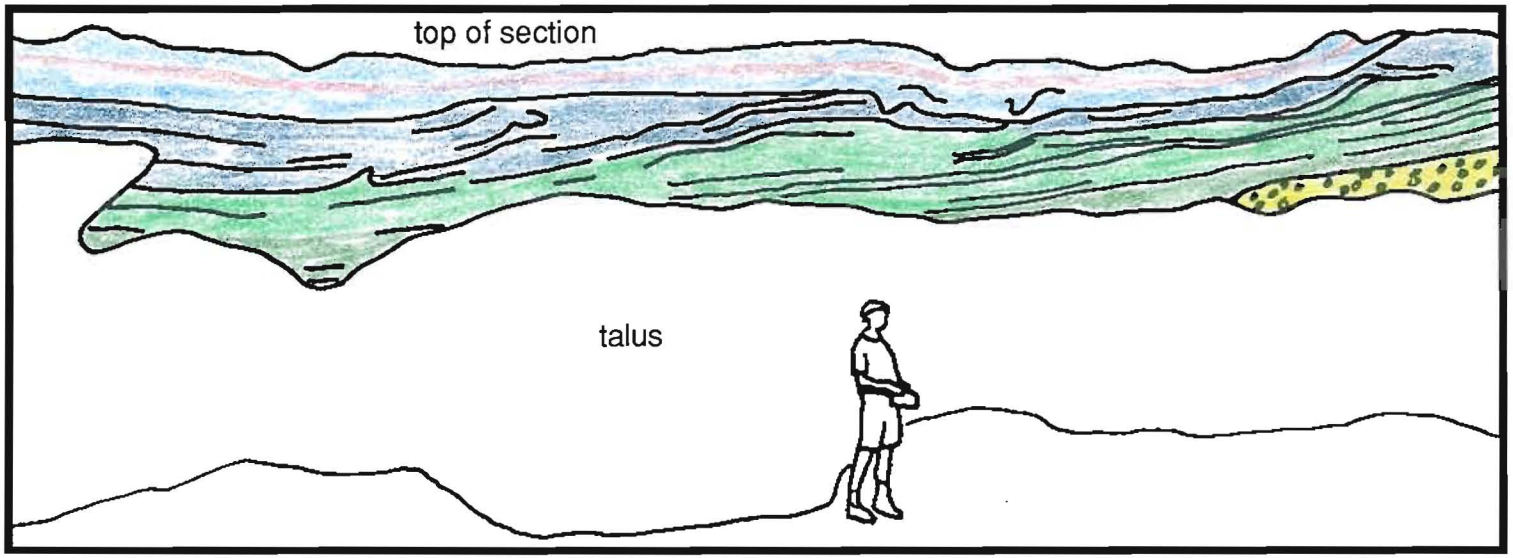

Facies 1 silt-clay rhythmites
Facies 2 sand-clay rhythmites
Facies 4 current-bedded sand
Facies 6 clast-supp. gravel
Facies 8 massive, matrix-supp. diamict
red clay rhythmites
Facies 3 sand-silt rhythmites
Facies 5 pebbly sand
Facies 7 matrix-supp. gravel
bedrock

Fig. 2-52 Sketch of section 87-27 showing a conformable sequence from clast-supported gravel through pebbly sands and current bedded sands into facies 3, 2 and 1 rhythmites. This section is from an esker between the Hartman and Eagle-Finlayson moraines, with paleoflow from right to left. This sketch was made from photos of the section. See Fig. 2-1 for location.

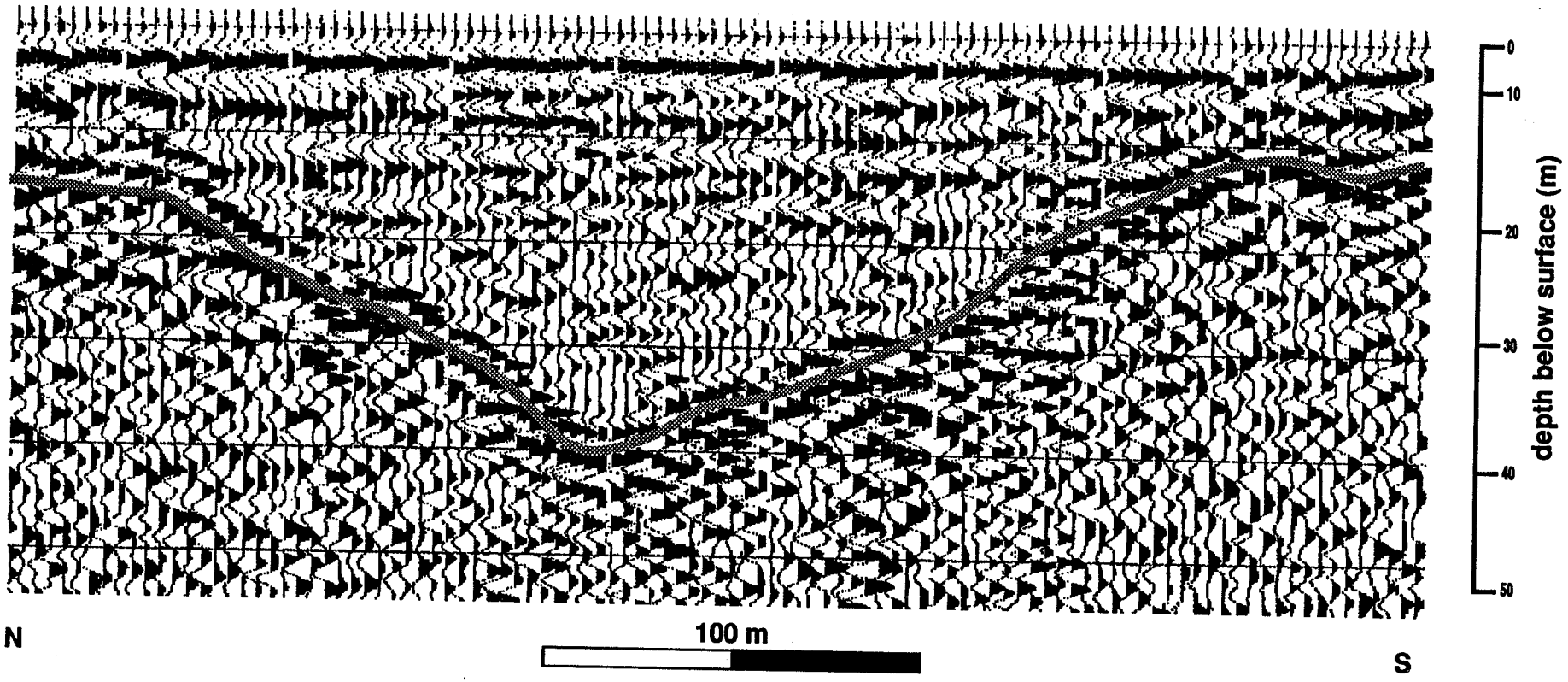

Fig.ure 2-53 Seismic profile from in front of the Hartman moraine (portion of line 100, see Fig. 1-4 for location). Note horizontal reflectors, some of which appear to end abruptly against the sides of the bedrock valley. Sonic hole D-2 was drilled in the middle of this bedrock valley.

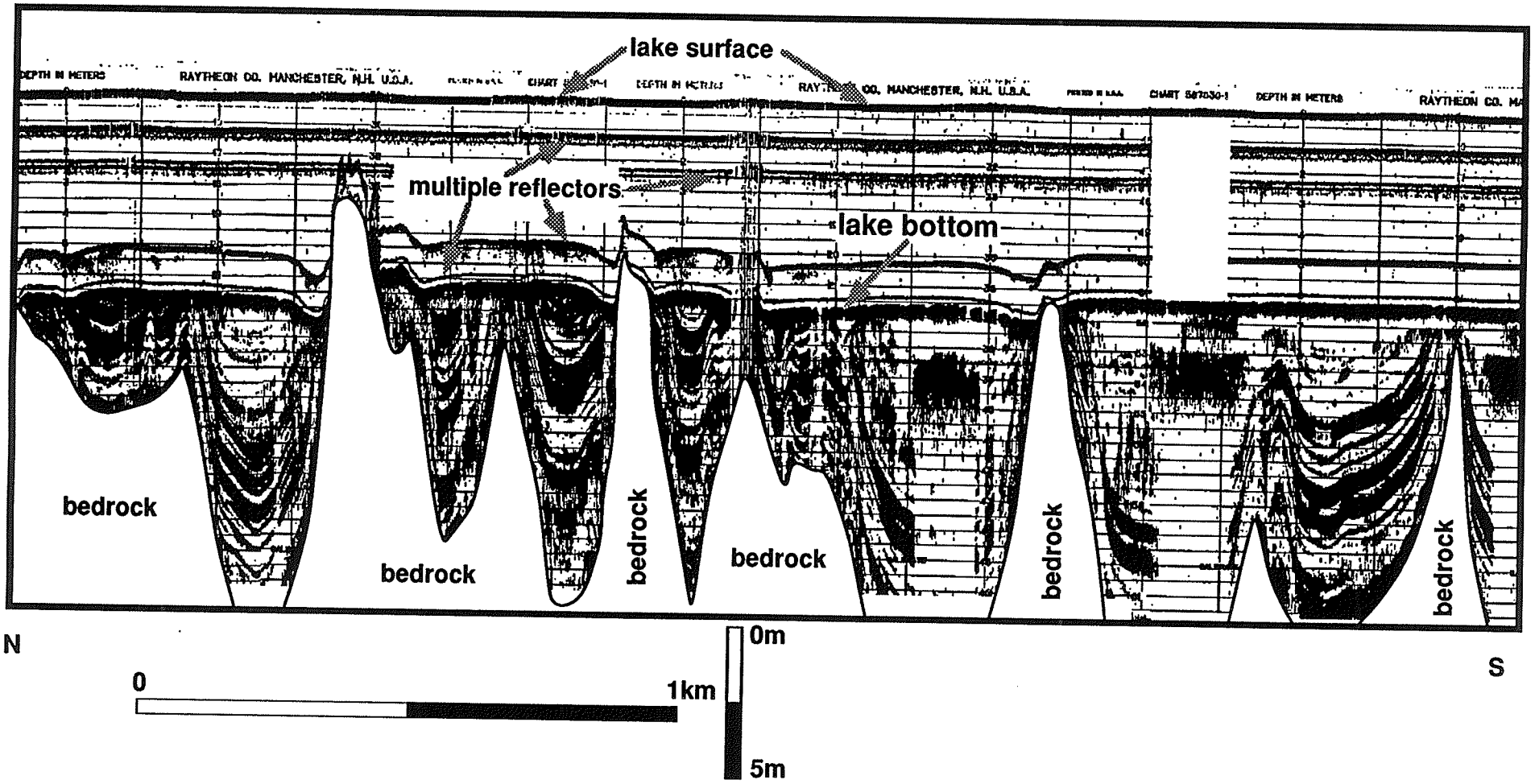

Fig. 2-54 Sonar profile from Wabigoon Lake (portion of line 8, see Fig. 1-4). Note sediments draping the underlying bedrock topography, and sediment units thickening in the topographic lows. Based on extrapolation from surface outcrops, the sediments are probably Facies 1, 2 and 3 rhythmites. Reflectors within the bedrock have been deleted.

These bedrock lows appear to be oriented approximately east-west, since there is much more relief exhibited on the north-south seismic lines, than on adjacent, transversely oriented east-west lines. The trend of the valleys thus appears to parallel the east-west regional bedrock strike.

In the intermoraine areas, away from the esker and kame landforms, the vertical sequence is dominated by Facies 1 silt-clay rhythmites. These may overlie sand-clay and rarely sand-silt rhythmites, or they may lie directly on bedrock.

Sub-bottom sonar profiles from beneath Lake Wabigoon show that the sediments in the intermoraine areas drape the underlying bedrock topography (whose relief frequently exceeds 15 m) and infill bedrock lows (Fig. 2-54). The units between the reflectors appear much thicker over the deepest parts of the bedrock lows, and gradually become thinner and sometimes pinch-out against bedrock highs (Fig. 2-54).

In some cases, irregularities in the reflectors can be seen at the base of bedrock highs, often associated with a local thickening of the units (Fig. 2-55).

Like the areas closer to the moraines, the bedrock lows in the intermoraine areas appear to trend east-west, paralleling the bedrock strike.

2.5 LATERAL FACIES SEQUENCES:

Because the determination of lateral facies sequences would have required large, laterally continuous sections, or numerous sonic drill holes, much less is known about this aspect of the sediments in the study area. Nevertheless, Walther's Law suggests that the overall fining trend that is seen

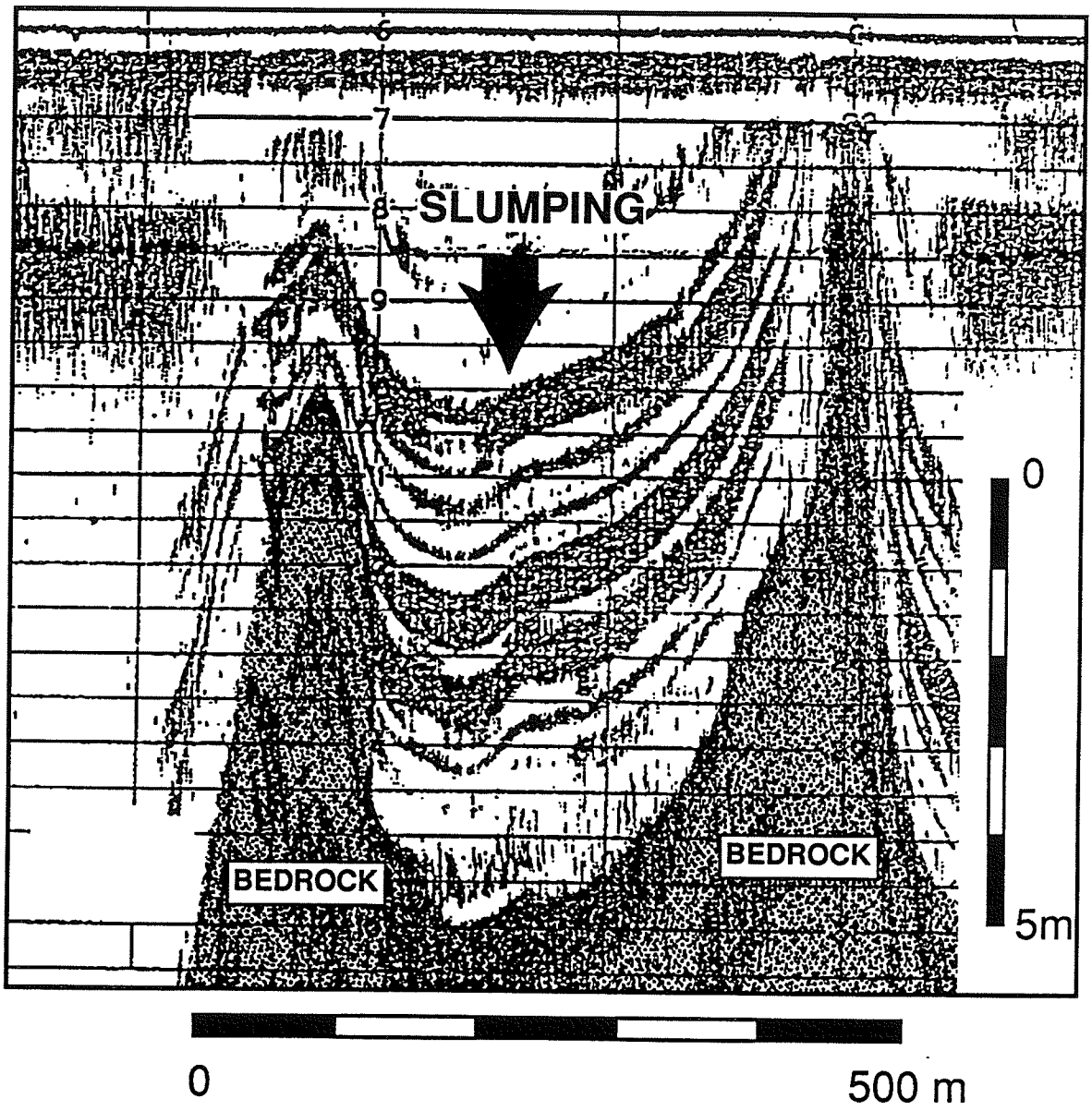

Fig. 2-55 Probable slump structure in rhythmites at the base of a bedrock high, seen in a sonar profile of Lake Wabigoon.

vertically throughout the area is also developed distally away from the moraines, eskers, and kames.

Sonic drill cores provide evidence for lateral transitions in the rhythmites. Where the red clay is present in drill cores from north of the Hartman moraine (see DT-6, D-3, Appendix A), the red clays form the clay portion of Facies 2 sand-clay rhythmites (Fig 2-56). In the holes drilled south of the Hartman moraine (D-1, D-2, Appendix A), and in all outcrops south of the moraine, the red clays are found in the Facies 1 silt-clay rhythmites (Fig. 2-56). This seems to indicate that the Facies 2 sand-clay rhythmites are somewhat more ice-proximal equivalents of the finer-grained Facies 1 silt-clay rhythmites.

The rhythmic bedding of the sand-silt rhythmites of Facies 3, and their gradational, vertical transition through Facies 2 into Facies 1 rhythmites, suggest that these too are higher energy, lateral equivalents of both the sand-clay and silt-clay rhythmites.

These fine-grained rhythmites and the coarser-grained sediments (Facies 4-7) of the moraines, kames and eskers all lie stratigraphically below the red clay unit. This suggests that there may be a continuous transition between the coarse and fine-grained sediments.

2.6 PALAEOCURRENT DATA:

Paleocurrent measurements were taken from a variety of sedimentary structures, including ripples, tabular crossbeds, large-scale foreset beds, and other dipping surfaces. Overall, these measurements shows a clear paleoflow trend toward the southwest, parallel to the regional iceflow patterns and the

Figure 2-56 Red clay (arrowed) capping Facies 2 sand-clay rhythmites in sonic core (left) from north of the Hartman moraine (hole DT-6). Scale is graduated in centimetres. Compare with red clay in Facies 1 rhythmites (right) from south of the Hartman moraine (section 87-19). Scale is 9 cm long.

trends of the esker deposits, and perpendicular to the moraine trends (Fig. 2-57).

A comparison of data from different structures at single sites shows that ripples, tabular crossbeds and large-scale foreset beds all reflect approximately the same paleoflow directions (Fig. 2-58) The largest range usually occurs within the ripple measurements.

Paleoflow data from ripples at site 87-27, just southwest of Dryden, (see Fig. 2-1 for location) show a distinct bimodal pattern (Fig. 2-59). This is due to the presence of the opposing-flow ripples in the Facies 2 rhythmites at this location.

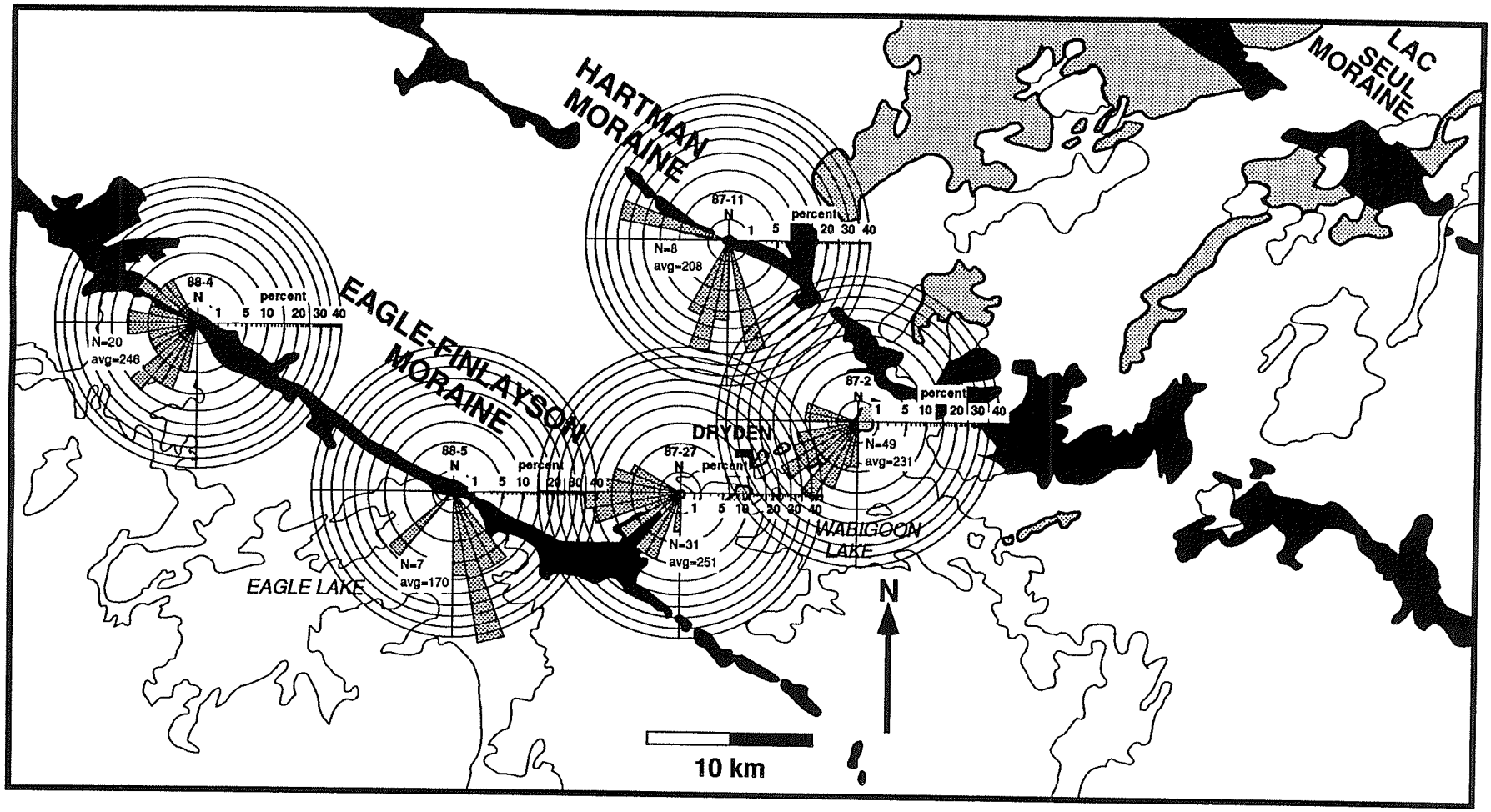

Fig. 2-57 Paleocurrent data from selected sites in the Dryden area (site numbers appear withing the inner ring of the rose diagrams). These data show strong south to southwestward flow trends, parallel to regional iceflow and eskers, and perpendicular to moraines. Note opposing paleoflows have been ommitted from section 87-27. Otherwise, data includes all measurments from each site.

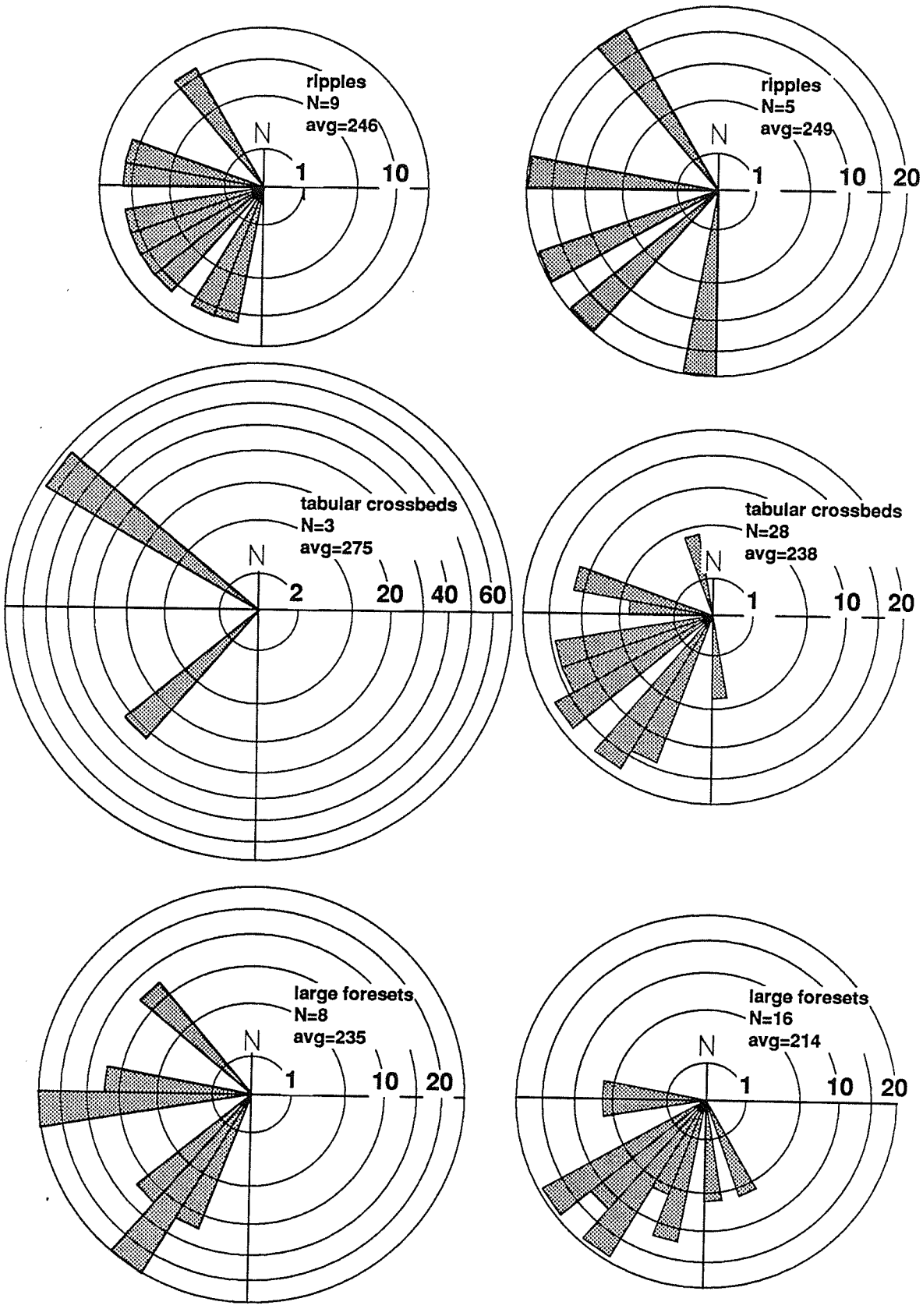

Fig. 2-58 Comparison of paleoflow data from various bedforms for sites in an end moraine (88-4) and an esker (87-2). Scale of rose diagrams is in percent.

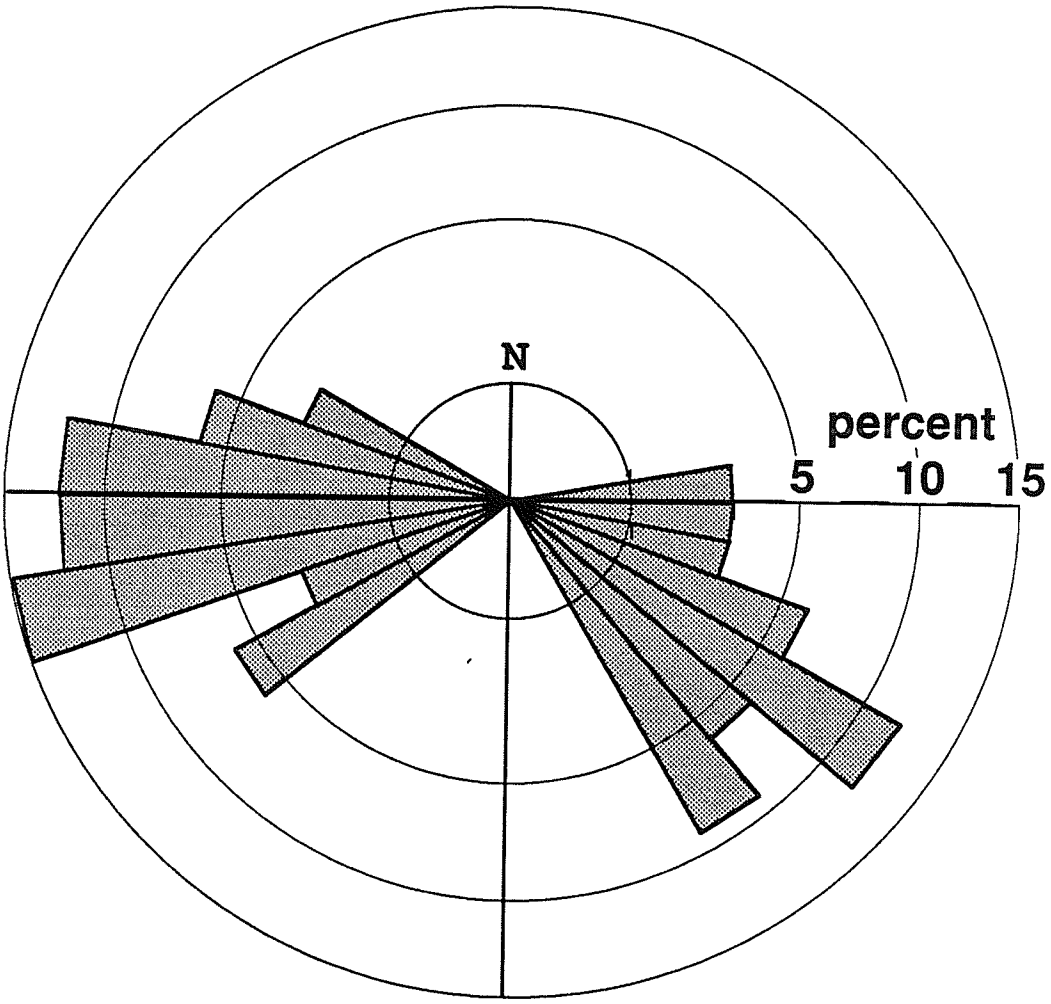

Fig. 2-59 Bimodal paleocurrent directions seen in ripples in section 87-27 (see Fig. 2-22). N=33.

CHAPTER 3: ORIGIN OF THE SEDIMENTS

3.1 FACIES INTERPRETATIONS:

3.1.1 Rhythmites (Facies 1, 2 & 3):

Underflows:

The Facies 1, 2 and 3 rhythmites are interpreted as deposits of the same depositional processes, because of their common, rhythmically-stratified form, and the gradational nature of their lateral and vertical contacts.

The coarse-grained portions of all the rhythmites were deposited by low-density, quasi-continuous underflow currents. Ripples, climbing ripples and occasional erosional bases seen in the Facies 2 and 3 rhythmites confirm the presence of traction currents, and argue against deposition by vertical settling from over- or interflows (Smith & Ashley, 1985; Keunen, 1951). Thickening of the rhythmite facies in bedrock lows, as seen on the seismic and sonar profiles (Figs. 2-53 & 2-54) also supports an underflow, rather than an over- or interflow interpretation, as underflows tend to be channeled into topographic depressions.

The clay portion of the Facies 1 and 2 rhythmites confirms a subaqueous depositional setting, which is necessary for an underflow interpretation. The clay portion was deposited by vertical settling under quiescent conditions of clays carried into the lake by under-, over- and/or interflow currents, and represents periodic cessation of underflow activity (Gustavson, 1975).

Keunen (1951) suggested that rhythmites like the ones in the study area, deposited by a combination of sediment-laden underflows and vertical settling from over- and interflows, should be common in proglacial lakes. Gustavson (1975) actually measured quasi-continuous underflow currents in proglacial Malaspina Lake in Alaska, and documented rhythmites very similar to the ones in the Dryden area, in cores and exposed sections in and around Malispina Lake. A combined underflow and over/interflow mechanism has been suggested for similar rhythmite deposits ranging in age from Quaternary to Proterozoic (Henderson, 1988; Deimer, 1988; Mustard & Donaldson, 1987; Smith & Ashley, 1985; Ashley, 1975; Saunderson, 1975).

Differences between the three rhythmite facies can be attributed entirely to variations in the strength and continuity of the underflow currents. The fining trend in the grain size of the coarse portion of the rhythmites, from coarsest in Facies 3, to finest in Facies 1 suggests a high- to low-energy transition, representing a proximal to distal transition relative to the ice margin, both in time and space (Gustavson, 1975). A relatively higher energy environment is suggested by the commonly channelized geometry of the Facies 3 rhythmites. The lack of a clay portion in the Facies 3 rhythmites suggests that the underflows which deposited this facies operated continuously, or that the currents were powerful enough to completely erode previously deposited clays. The presence of occasional clay clasts in the coarse portion of the couplets (seen in sonic cores), which may represent roll-ups or rip-ups, seems to favour the latter hypothesis. The absence of traction structures in the coarse portion of

the Facies 1 rhythmites may be due to the extensive bioturbation, or more likely, to the lower velocity and tractive power of the most distal underflow currents.

The underflow currents probably originated at or near the mouths of subglacial meltwater tunnels. Underflows may also have been generated by slumping of sediment from the ice surface, although the lack of dropstones in the rhythmites sediments suggests the ice margin contained relatively little debris. Shoreface processes probably contributed little sediment to the rhythmites, as the only shore of the lake in the study area probably was formed by the ice margin. Neither does wave action appear to have played more than a minor role in the deposition of the rhythmites, as wave-induced sedimentary structures are almost entirely lacking, and the largely undisturbed nature of these fine-grained sediments argues for water depths below effective wave base.

Periodicity of the Underflows:

Given the preceding depositional interpretation, the rhythmic stratification in the deposits represents periodic waxing and waning of underflows in a proglacial lake. Figure 2-11 shows a plot of the **relative** vertical variations in both clay and silt thicknesses from several, widely spaced sites in the Wabigoon basin. These sites are located along the shores of Lake Wabigoon, and include the longest available records from the study area.

It does not seem possible to correlate individual couplets between sections. However, the overall patterns of thickness variation are fairly consistent from section to section, especially in the longer, more complete

records. This suggests that there is a systematic, basin-wide control on sedimentation patterns, although it does not resolve the periodicity of the rhythmites.

The patterns of silt thickness variations offer some insights into changes in sedimentation rates in the area (Fig. 2-11). The longer silt thickness curves show an initial decrease in thickness, which may relate to either retreat of the ice margin, or diminishing meltwater and sediment output from the ice (or both). This decrease is followed by a gradual increase which culminates in the red clay unit. This suggests that deposition of the red clay was accompanied by either a readvance of the ice margin, or an increase in meltwater and sediment output (or again, both). However, this increase in silt sedimentation begins before the actual red clay deposition.

The clay thickness curves show considerably less variation, although there is a slight initial decrease in clay thicknesses which mirrors the increase in silt thickness (Fig. 2-11). The increase in clay thickness in the red clay unit is quite sudden and dramatic (as is the change in colour). Thus, the colour change to red clay was accompanied by a sudden increase in clay sedimentation rates.

Periodic underflows affecting an entire basin may be generated by a number of processes. These can include relatively short-lived, recurring storms which cause higher meltwater and sediment output from the glacier due to heavy rainfall on the ice, and possible slumping of lake sediments due to higher wave energies. Underflows may also be generated by annual, diurnal, or irregular variations in the melting of the ice sheet.

The length of time represented by each rhythmite is suggested by the nature of the bioturbation seen in the Facies 1 rhythmites. Bioturbation in this facies is confined almost entirely to the silt portion of the couplets. The only bioturbation seen in the clay layers comes in the form of burrows which originate in the silt layers, and extend only for a short distance into the adjacent clay layer. The implication is that the burrowing organisms were present in the sediment only during, or immediately after the period of silt deposition, and were absent during clay deposition.

A possible reason for this is that the bioturbation may have been caused by the burrowing instar of some type of arthropod, which metamorphosed to a free-swimming or flying form before deposition of the clay unit began. This metamorphosis normally occurs on a yearly cycle, suggesting that these deposits are varves. The bioturbation seen in this facies is very similar to traces produced by chironomid larvae (Duck & McManus, 1984; Morrison, 1987; Duck & McManus, 1987), which do undergo a seasonal metamorphosis. Virtually identical trace fossils have been found in both the Lake Superior (Teller & Mahnic, 1988) and the Lake Nipigon (Lemoine, 1989) basins to the east of the Wabigoon basin. It was noted by Lemoine (1989) that the Lake Nipigon trace fossils were confined to the silt layers, and a seasonal metamorphosis of burrowing arthropods was also suggested.

If the periodicity of couplet deposition were less than a year (eg. due to diurnal, or episodic melting variations or random storms), it is difficult to explain why the bioturbation is confined to the silt portion of the couplets. If the

periodicity was longer than a year, it is again difficult to imagine what happened to these arthropods during deposition of the clay.

Thus, it is concluded that the Facies 1 rhythmites are varves. Since the Facies 2 and 3 rhythmites are interpreted as higher energy equivalents of the Facies 1 rhythmites, this implies that they are also varves. While there is no direct proof of this, it is strongly suggested by their common rhythmic stratification, and by the continuous lateral and vertical transitions between these facies. In addition, the thicknesses of the Facies 2 clay portions (0.1 to 1.0 cm) are comparable to those of the Facies 1 rhythmites, suggesting a similar amount of time for deposition.

A yearly periodicity would exclude the possibility that the couplets are individual turbidites produced by random, short-lived, slump-generated underflows, as suggested by several authors (Smith & Ashley, 1985; Eyles & Miall, 1984; Lambert & Hsu, 1979). It would also appear to exclude other random causes such as storms and irregular warm periods over the glacier, or non-annual processes such as diurnal melting. This is in agreement with the interpretation made by Rittenhouse (1933, 1934).

One problem that arises from this interpretation is the extremely fine-grained nature of the clay portion of the rhythmites. The mean grain size for these clays is approximately 0.4 μm (see Appendix E), and the maximum settling velocity for grains of this size under ideal (Stokes Law) conditions is approximately 0.01 m day^{-1} (Smith & Ashley, 1985, their Table 3). Using a conservative estimate of a 65 day glacial melt season, this leaves 300 days per

year for these clays to settle from suspension. Even under ideal conditions, they would settle only about 3.0 m in this period of time. However, there are numerous clay laminae in the rhythmite sequences that exceed 1.0 cm in thickness, and some that are up to 10.0 cm in thickness. If, as the nature of the bioturbation suggests, the couplets are annual deposits, some factor must have resulted in enhanced settling rates.

Smith & Syvitski (1982) have shown that fecal pelletization of suspended silt and clay particles in a modern glacier-fed lake by pelagic copepods can produce particles which have settling velocities of between 80 and 400 m day^{-1}. Given that a pelagic fauna can exist in a modern glacier-fed lake, and that a benthic fauna clearly existed in the Facies 1 sediments in the study area, it does not seem unreasonable to suggest that a pelagic fauna may also have been present in the study area during deposition of the Facies 1 rhythmites. However, it was not possible to find a reference in the literature confirming the ability of an ice-contact lake to support a pelagic fauna. Nevertheless, it is suggested that pelletization by pelagic fauna can explain the anomalous thicknesses of the clay portions of the varved Facies 1 sediments.

Red Clay Rhythmites:

Data presented in Chapter 2 demonstrates that the red-clay rhythmites in the Dryden area are distinct from the surrounding grey-clay rhythmites in their colour, thickness, and geochemistry. It is difficult to explain such differences by syndepositional lakewater chemistry variations, and they are also unlikely to be due to post-depositional diagenetic or weathering effects. The most probable

explanation is a different provenance for the red clays, as has been suggested by previous workers (Zoltai, 1961; Rittenhouse, 1934). Zoltai (1961) suggested that the Dryden area red clays were produced by a mixing of the local Dryden area grey clay with red clay derived from the drainage basin of proglacial Lake Kaministikwia near Thunder Bay, which was formed by the Marquette readvance of the Superior Lobe (Fig. 3-1). This would also explain the increased clay sedimentation rates associated with the red clays.

Figures 2-13 & 2-14 show that, where a sharp geochemical change is seen at the lower grey clay to red clay transition, the change is normally in the direction of the Lake Kaministikwia values, and is never in the opposite direction. This strongly supports Zoltai's (1961) mixing hypothesis. That the geochemical variations do not always reflect a simple mixing between the two sources is not unexpected, and suggests that other sources outside the Lake Kaministikwia basin may have affected the Dryden area red clays.

Figures 2-13 & 2-14 also show that, in general, the effect of the influx of Lake Kaministikwia material is strongest in the lowermost red clay rhythmites and tends to die out upward. This may reflect decreasing input of Lake Kaministikwia red clay into the Dryden area with time. Alternatively, it may mean that the Lake Kaministikwia red clay was brought into the study area in a single "pulse", and was gradually removed from the water column by vertical settling.

The geochemistry of the silt portion of the Dryden area rhythmites does not, in general, show the same stratigraphic patterns as the clay portion geochemistry. There is also no apparent colour difference between the silt

Fig. 3-1 Configuration of Lake Agassiz and Lake Kaministiwia at the time of red clay depositon. Both lakes were probably confluent at the Agassiz Norcross level. Blockage of the eastern Agassiz outlets by Superior lobe ice, resulted in westward flow from Lake Kaministikwia, which carried the red clay plume into eastern Lake Agassiz. Known areas of red clay in northwestern Ontario are stippled (after Thorleifson, 1983).

portions of the grey clay and red clay rhythmites. This may be due to a much smaller influx of silt-sized material from the Lake Kaministikwia basin. Alternatively, it may be due to the underflow origin of the silt portions of the rhythmites, which would provide much less opportunity for mixing with extrabasinal material during deposition.

The actual red colour of the red clay is not due to the absolute amount of Fe in the clay, nor can it be completely explained by the $FeO:Fe_2O_3$ ratio, since there is considerable overlap in this ratio between the grey and red clays. It would appear that some more complex geochemical effect, probably involving several elements is responsible for the colour of the red clays.

An important question is the bedrock provenance of the red clay. The most probable bedrock sources are the red beds of the Proterozoic Sibley Group (Keele, 1924), which outcrop in the Thunder Bay area (Fig. 3-2 ; Franklin et al., 1980). Glacial erosion of these redbeds probably produced the red clay found not only in the Lake Kaministikwia lacustrine sediments, but also in the distinctive red tills observed in the area of the Lake Kaministikwia basin by the author, and by Thorleifson (1983) and Zoltai (1963).

While there are no detailed geochemical data available for the Sibley Group red beds, their geographical proximity to the Lake Kaministikwia basin, and their striking red colour make them the most likely candidate for the bedrock source of the red clays (Keel, 1924).

Transport of the red clay into the Dryden area, and the rest of northwestern Ontario probably occurred when Lake Kaministikwia drained

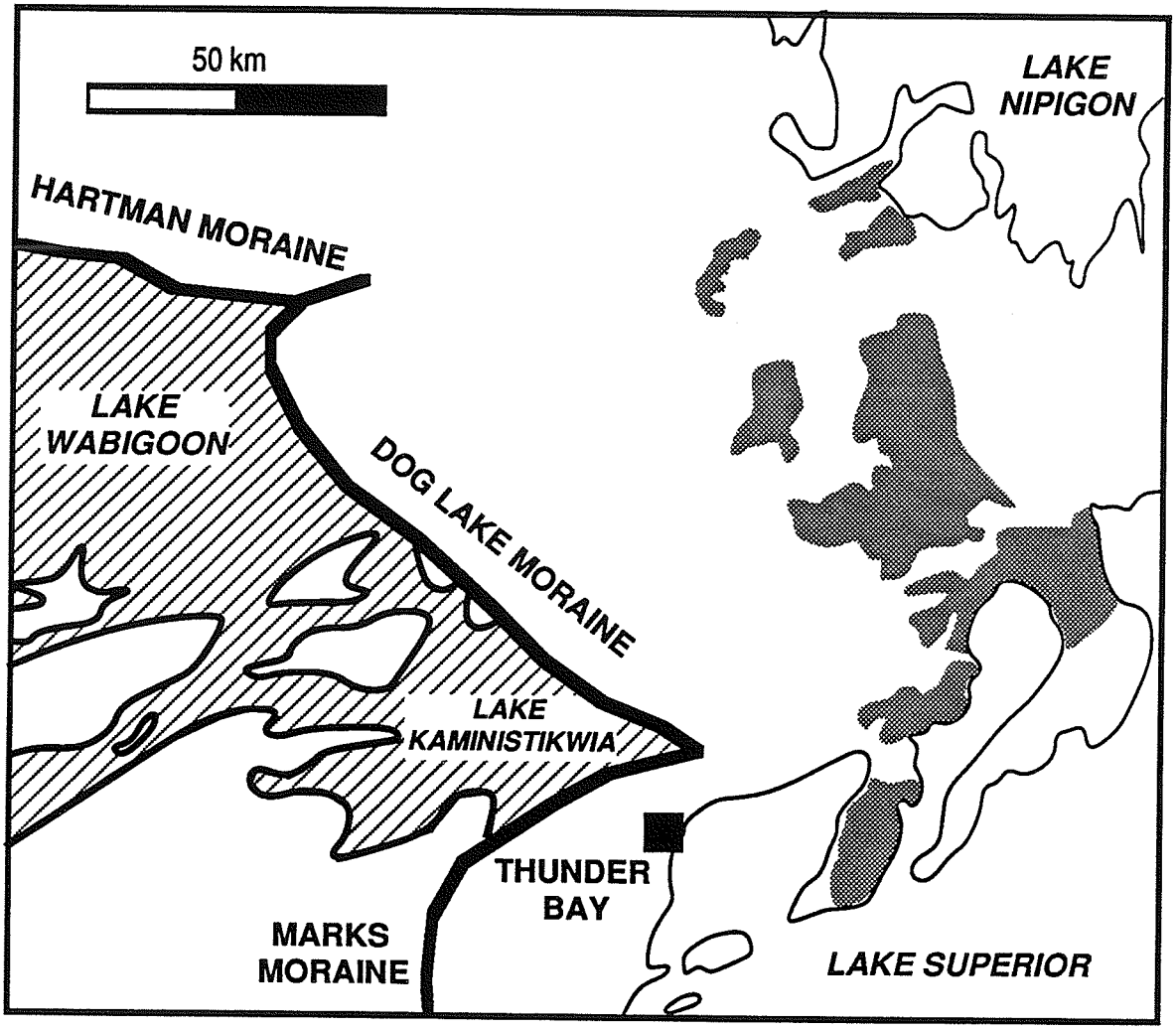

Fig. 3-2 Outcrop of the Proterozoic Sibley Group (stippled) and their relationship to the former position of Lake Kaministikwia (after Franklin et al., 1980).

westward into, or was confluent with Lake Agassiz (Thorleifson, 1983; Zoltai, 1961).

The ultimate igneous bedrock source of the clay sediments in the Dryden area probably controls their REE geochemistry, as the REE's are relatively immobile under near-surface conditions. As was discussed in Chapter 2, the Dryden area grey clays show a more fractionated REE pattern (higher La:Yb and Eu:Eu* values) than the red clays from the Dryden area, and from elsewhere in northwestern Ontario. This suggests the source rocks of the Dryden area grey clays and the red clays had different fractionation histories. However, it is probably impossible to determine the ultimate igneous source or sources for either of the clay types.

The data presented in Chapter 2 also demonstrates a relatively close geochemical affinity between the Fort Frances red clay samples and the Lake Kaministikwia red clays. It is assumed that the Fort Frances red clays, like the Dryden area red clays, were produced by mixing of locally-derived clays with the exotic Lake Kaministikwia red clays.

Notable Features of the Facies 2 Sandy Rhythmites:

An interesting feature observed at one particular site (87-27, see Fig. 2-1 for location) is the presence of apparently opposing ripple foresets at the tops of many of the sandy portions of the Facies 2 rhythmites (Fig. 2-22, described in Chapter 2). Paleoflow measurements from this site show that the flows were almost 90° opposed, with no intermediate orientations (Fig. 2-59). This argues against the opposing ripples being due to an exposure oriented transversely to

a wide fan of paleoflows. Interestingly, this type of return-flow ripple was also present, but apparently not noticed, in glacial Lake Hitchcock sediments in Massachusetts described by Gustavson, Ashley and Boothroyd (1975, their Fig. 11).

As discussed in Chapter 2, these are not wave ripples. They represent a distinct, 180 degree reversal in flow direction just before underflow activity ceases. Given that these rhythmites are interpreted as varves, this cessation presumably occurred at the end of the glacial melt season. This phenomenon has been described from a number of turbidite deposits (Pickering & Hiscott, 1985) and has been explained by Pantin and Leeder (1987) as the result of "solitons", or solitary waves created at the current/water interface of an underflow current which has encountered a significant obstruction. These solitary waves move back up the flow, and can cause a localized reversal in flow direction as they pass, provided flow in the initial direction has waned sufficiently. Since this feature is locally restricted in the study area, it may be explained by the underflow encountering a buried block of ice, or an esker or kame deposit.

An apparent flow reversal caused by antidunes is unlikely, since antidunes represent very high flow velocities which would not be expected at the end of the glacial melt season.

The presence of a wave re-worked bed interbedded with silt-clay rhythmites at section 87-2 indicates that this particular site (at about 400 m.a.s.l.) was shallow enough to allow occasional wave energy to impinge on the bottom,

but deep enough to allow frequent deposition of clay laminae. However, it is difficult to determine the exact depth without knowing the period of the waves which formed the ripples (B. Greenwood, pers. comm., 1991).

3.1.2 Current-bedded Sand (Facies 4):

In the 4A facies association, the planar to crossbedded sand sheets found between or on top of Facies 6 gravels are interpreted as either upper or lower flow regime flat beds and lower flow regime large scale 2-d ripples (Harms et al., 1982). These sands moved along the tops of large gravel bodies (see Facies 6, this chapter) during periods of relatively lower flow velocities (Shaw, 1985; Boothroyd & Ashley, 1975) within, or at the mouths of, subglacial meltwater channels.

Where these sands were carried over the tops of these gravel bodies and down the lee faces, the deposits they produced depended on whether or not the current velocity was high enough to cause flow separation in the lee of the underlying bedform (Allen, 1980, in Walker, 1984, Fig. 3-3). If flow separation occurred (Fig. 3-3), the sands formed steeply dipping, parallel bedded foresets which show poorly developed, but convincing evidence of return flow up the lee face of the gravel body (Figs. 2-31, 2-32 & 2-33). Fluctuations in the flow produced the interbedding of sand and gravel foresets seen at site 88-6 (Fig. 2-31).

If flow separation did not occur, the large scale ripples continued to migrate down the lee face (Fig. 3-3), probably experiencing frequent slumps due to the near angle of repose bedding surface (Fig. 3-4).

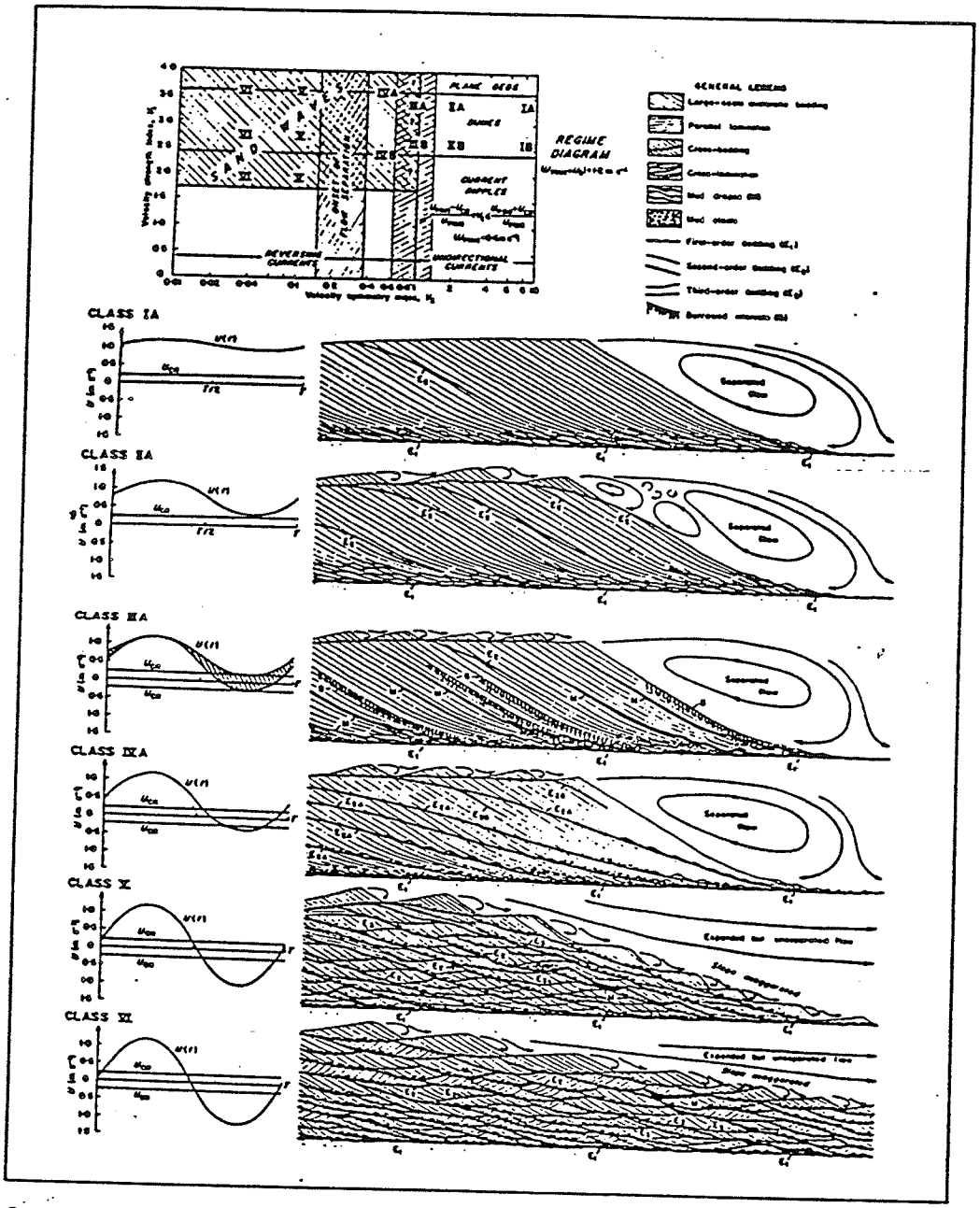

Regime diagram, and predicted categories of sand wave and dune internal structure. Note that the six classes are defined by the time/velocity asymmetry (or symmetry). Classes I to IV have large foresets (commonly with reactivation surfaces, E_3) and flow separation, but classes V and VI have much lower slopes on the "steep" side, and no flow separation. From Allen, 1980.

Figure 3-3 Foreset geometry developed with and without flow separation over the bedform (from Allen, 1980, in Walker, 1984, p. 161).

Figure 3-4 Slump structure in crossbedded sands seen in Fig. 2-30 (section 87-2). Field of view is approximately 60 cm high).

The trough crossbedded channel fills were formed by the migration of 3-d large ripples (dunes and megaripples), moving in channels between the large gravel bodies (Boothroyd & Ashley, 1975) in the subglacial meltwater conduits.

The second association of this facies (Facies 4B) forms infills within large, broad, shallow channels. Sedimentary structures are dominated by sub-parallel bedding, and small- and large-scale two-dimensional ripples. Evidence of stoss-side preservation and climbing in both large and small ripples suggests that both traction and suspension processes were occurring simultaneously (Jopling & Walker, 1968). These (4B) types of sedimentary structures appear to be best explained by deposition from density underflow (turbidity) currents (Jopling & Walker, 1968; Lowe, 1982; Walker, 1984). The lack of massive beds, or dish structures is evidence for low-density underflow currents, while the presence of inversely graded beds, and the association of this facies with Facies 5 pebbly sands (see Facies 5, this chapter) suggests that high-density underflow currents also played a role in the deposition of the Facies 4B sediments. The quasi-continuous nature of underflow currents in a glacial setting may have precluded the deposition of massive beds, which are regarded as the waning stage deposits of high-density underflow currents (Lowe, 1982). Lowe (1982) has suggested that there is a continuum from high- to low-density currents, in that the deposition of the high-density suspended load leaves behind a residual low-density flow carrying material finer than about medium sand. Given the available evidence, it seems likely that both high- and low-density underflow currents were active in this environment.

The Facies 4B current-bedded sands are clearly higher energy deposits than those of the Facies 1, 2 or 3 rhythmites. It is suspected that the Facies 4B sands are simply the more proximal equivalents of these rhythmically-stratified facies. The lack of rhythmic bedding in the current-bedded sand facies may be due to flows that were continuous over the entire year, and/or were energetic enough to erode any finer-grained sediments deposited during periods of lower flow velocity.

3.1.3 Pebbly Sand (Facies 5):

This facies is quite common in the study area, and is found in all of the coarse sediment deposits. The characteristic features of this facies are the dispersion of clasts within a medium to coarse sand matrix, the abundant sub-parallel stratification, and the presence of normal and reverse grading and occasional traction current structures.

Their most common occurrence is as thick (2-10 m) infills in broad, channels up to 10m deep and 50m wide. Where crossbedding is present in this Facies it indicates unidirectional current flow, and there are no sedimentary structures such as wave ripples or hummocky cross-stratification which are strongly indicative of wave action. These pebbly sands also show a close association with Facies 4 sands, all of which were deposited by unidirectional flows, and lack any evidence of wave activity. These features do not support an interpretation of these sediments as beach or shoreface deposits.

The features found in the Facies 5 pebbly sands are thought to be diagnostic of deposition from density-modified grain flows or traction carpets,

produced by a deceleration of high-density underflow currents (S_2 division of Lowe, 1982; Hein, 1982; Farquharson et al., 1984).

The larger clasts are buoyed-up in the matrix during transport by "...strong grain interactions and high dispersive pressures" (Hein, 1982, pg. 283), and are frozen in place by rapid deposition. This can result in the formation of reversely graded beds. The association with tractional high-density underflow currents is supported by the presence of minor tabular and trough crossbedded pebbly sand units. These crossbedded units may correspond to the S_1 division of Lowe (1982).

3.1.4 Clast-supported Gravel (Facies 6):

The large, massive to indistinctly stratified gravel bodies of Facies association 6A are typically found within esker and kame features. This unit is interpreted as part of a large-scale longitudinal or transverse bar, similar to bars found in gravelly braided rivers. These types of bars are described by Harms et al. (1982) as being composed of massive to diffusely bedded cores, possibly with shallowly to steeply-dipping foresets on the downstream ends. Well developed angle of repose foresets are indicative of transverse bars, while low-angle foresets are more common on longitudinal or diagonal bars (pg. 617). Both of these types of structures are seen in several localities within the study area.

This interpretation is supported by the studies of Banerjee & McDonald (1975) and Deimer (1988). The latter author cited evidence which suggests that common alternations of openwork and closed-work gravels represent

fluctuating flows (Frostick et al, 1984; Fraser and Cobb, 1982; both in Deimer, 1988).

An alternative hypothesis considered for some of these gravel bodies is that they are small, subaerial Gilbert deltas. This is suggested by the presence of 2-3m high, near-angle-of-repose crossbedding in two exposures within esker landforms in the study area (Figs. 2-31 & 2-45). As the foresets themselves provide no evidence for or against a deltaic origin, they must be examined in light of their stratigraphic context.

If these foresets did represent a prograding, gravelly Gilbert delta, they might be expected to be overlain by topset beds indicative of deposition in a gravelly braided stream environment. In one exposure the foresets are truncated and overlain by a thick, matrix-supported gravel unit (Facies 7, Fig. 2-46), a facies which is considered to be incompatible with a braided stream environment (Rust & Koster, 1984; Harms et al., 1982). This suggests, but does not prove that a Gilbert delta model may not be applicable.

In the second exposure, the foresets are overlain by coarse, massive gravels which could be topset deposits. However, in this large, three-dimensional outcrop, these foresets are seen to have lateral equivalents both along the paleoflow direction, and across it. These include 3m deep channels filled with trough crossbedded Facies 4 sands, and massive, tabular bodies of Facies 6 clast-supported gravels. These lateral facies variations suggest an interpretation of these foresets as braided stream-type bars rather than Gilbert

deltas, as delta foresets should thin laterally into finer lacustrine sediments (Walker, 1984).

In addition, the morphology of the esker deposits, which form local topographic highs standing above the surrounding lacustrine rhythmites, suggests that if these deposits were deltas, they must have been ice-contact deltas. However, the apparent lack of post-depositional deformation (ie. ice-collapse structures) in any of the extensive exposures of these deposits argues against their having been supported by ice at any time.

The finer (cobble to pebble size) gravels of Facies association 6B occur mainly as complete or partial channel fills within the end moraines. These deposits tend to show characteristic sub-parallel stratification and normal and reverse grading. These finer gravels closely resemble the deposits of gravelly, high-density underflow currents described by Lowe (1982, R_{2-3}, S_1 divisions) and Hein (1982). The sediments were likely transported within a highly concentrated traction carpet, and in suspension at the base of the underflow current, and deposited rapidly as the flow velocity decreased. These deposits would be the higher energy equivalents of the Facies 5 pebbly sands.

Cowan (1987) has noted that the end moraines in the study area show evidence of minor wave reworking of their surfaces. The confinement of the Facies 6B gravels to broad, shallow, nested channels and the complete lack of wave-produced sedimentary structures in these or the surrounding deposits argues against them being beach or shoreface deposits. However, in one section (88-2) in the crest of the Eagle-Finlayson moraine, there is a 1.5m thick

gravel and sand unit at the top of the section (Fig. 2-26) which truncates the underlying channels. This unit may be due to wave reworking. Overall however, wave reworking does not appear to have significantly altered the internal structure of the moraines.

3.1.5 Matrix-supported Gravel (Facies 7):

In all but one occurrence this facies is thought to be an artificial deposit, produced by mixing of the soil horizon with underlying units during gravel pit operations. The one natural deposit of matrix-supported gravel is found within an esker landform, overlying and truncating the sand and gravel foresets of a large gravel bar (section 88-6, Fig. 2-46).

Saunderson (1977) pointed out that a matrix-supported gravel implies contemporaneous deposition of a wide range of grain sizes by a common mechanism. He argued that these characteristics could be produced by deposition from "..a sliding bed inside a subglacial tunnel during full-pipe flow" (pg. 633).

The mechanism he proposed involved movement of the entire bed of the channel by the combined action of water being driven laterally through the bed, and shear stress imparted to the surface of the bed by the overlying flowing water. Sorting within such a sliding bed would be negligible, and relatively large clasts would be transported easily due to the buoyant effect of the finer matrix (Carter, 1975; Middleton & Southard, 1984).

A more conventional interpretation for a matrix-supported conglomerate is that it represents deposition from a debris-flow (Miall, 1978, in Smith, 1985;

Fisher, 1982, 1984; Nemec & Steel, 1984). While this is a possibility, its occurrence within an esker landform tends to support a subglacial tunnel origin. In addition, several authors have suggested that debris flow deposits should **lack** an erosive lower contact (Fisher, 1982, 1984; Nemec & Steel, 1984).

3.1.6 Matrix-supported Diamict (Facies 8):

This facies is interpreted as the product of a slump-generated debris flow. The sorted nature of the matrix (little material coarser than fine sand), and the presence of some disturbed laminations and ripples in the matrix suggest that these sediments had previously been deposited by fluvial processes, and had not been transported a great distance. Failure of these previously deposited sediments may have been caused by any number of factors including high pore water pressures due to rapid deposition, loading of coarse-grained sediments onto finer sediments, ice collapse, or iceberg calving. The source of the debris flow may have been sediments deposited on the moraine, or on the ice surface.

A lodgement till origin is unlikely, given the restricted nature of the deposit, and the remnant sedimentary structures. The interbeds of horizontally-bedded sand, and the overlying and underlying Facies 5 gravels suggest that fluvial processes of some type were occurring contemporaneously with the slumping.

CHAPTER 4: DEPOSITIONAL ENVIRONMENT AND FACIES MODEL

4.1 DEPOSITIONAL ENVIRONMENT:

The coarse-grained sediments (Facies 4-7) in the study area are confined to moraines, kames and eskers, all of which are glacial or glaciofluvial landforms. These sediments show evidence of having been deposited by flowing water, and the dominant paleocurrents are unidirectional (away from the ice margin) and parallel to the former ice flow. These sediments therefore represent proglacial and/or englacial/subglacial outwash. The close association of the rhythmite facies (Facies 1, 2 & 3) with these outwash sediments suggests that these rhythmites are glaciolacustrine deposits formed in a proglacial lake. Rhythmites of virtually identical appearance are found in numerous other proglacial lakes, both ancient and modern (Ashley, 1975; Gustavson, 1975; Gustavson et al., 1975).

Three possible environments of deposition for the coarse grained, proglacial outwash sediments (comprising the kames and moraines) are envisioned: a broad, ice-marginal subaerial braid plain; a series of individual and coalesced, ice-contact glaciolacustrine deltas; and/or a series of individual and coalesced subaqueous outwash fans.

The subaerial braid plain is a common environment in modern proglacial settings (Boothroyd & Ashley, 1975; Rust & Koster, 1984; Smith, 1985). They form broad, low relief plains which can cover wide areas, and often terminate in

proglacial lakes (Fraser & Cobb, 1982; Smith, 1985; Eyles & McCabe, 1989). They typically show little lateral facies variation except over considerable distances (Rust & Koster, 1984; Boulton, 1986).

Most of the coarse deposits in the study area are concentrated in narrow, ice-marginal moraines and kames, so rapid loss of competence in standing water is indicated. This is further evidenced by the rapid lateral transition from the coarse morainal sediments to fine-grained subaqueous rhythmites.

The narrow spatial distribution of the coarse-grained sediments, notably within the moraines, does not fit a broad braid plain model, and this model is therefore rejected. The two remaining alternatives are a series of individual and coalesced ice marginal deltas or subaqueous fans. The main difference between these two models is whether the deposits aggraded to lake level or were entirely subaqueous. This is often difficult to determine. Aggradation to lake level is usually accompanied by progradation of the delta into the lake. Subaqueous fans, on the other hand, probably would not undergo significant progradation, since the zone of flow expansion and loss of competence would not prograde with the structure, as it does on a delta. The combination of aggradation to lake level and progradation in deltas is commonly identified by the presence of a characteristic, coarsening upward sediment sequence with pro-delta muds (rhythmites in this case) at the base. These are overlain by large-scale foreset beds, which are in turn, erosionally overlain by coarser, flat-lying topset beds. This type of sequence has been documented from numerous areas

(eg. Gustavson et al., 1975; Shaw, 1975; Miall, 1984; Smith & Ashley, 1985; McCabe & Eyles, 1988; Fyfe, 1990; Postma, 1990) .

None of the exposures in the Hartman or Eagle-Finlayson moraines, or in the kame landforms, showed evidence of topset beds. However, since the subaerial portion of a delta is a relatively minor component, and is most easily modified by wave action, the lack of topset beds does not, by itself, rule out a deltaic environment.

The stratigraphic sequences in and immediately in front of the moraines and kames in the Dryden area generally show a fining upward, rather than a coarsening upward sequence. In all available moraine and kame outcrops, and the cores from immediately in front of the Hartman moraine, there is an overall fining upward sequence from gravels and sands into rhythmites. While many of the contacts in the moraine and kame sequences are erosional, there do not appear to be any major, regionally-extensive unconformities, and the sequences are considered to be generally continuous. In addition, the stratigraphically-continuous drill cores also show a fining upward sequence. There is no evidence of a coarsening upward sequence anywhere in or in front of the moraines or kames.

A comprehensive facies model for subaqueous fans does not really exist, although a review of the literature suggests that they posses a number of diagnostic features:

> 1) a generally continuous, upward-fining sequence from a core of massive, clast-supported gravels, through fine gravels and sands, and finally into a lacustrine/marine sequence of rhythmically-laminated

sands, silts and clays or in some cases a coarse, fossiliferous beach deposit (eg. Rust & Romanelli, 1975; Rust, 1977; Sharpe, 1988)

2) rapid lateral facies transitions from coarse, high-energy deposits to very fine material (Boulton, 1986; Sharpe, 1988; Rust, 1989)

3) the deposits of subaqueous fans always form a positive relief feature which stands above the surrounding area (eg. Rust & Romanelli, 1975; Rust, 1977; Thomas, 1984b; Deimer, 1988; Burbidge & Rust, 1988)

4) sedimentary sequences are dominated by sediments indicative of deposition by sediment-gravity flows (McCabe et al., 1984; Kaszycki, 1987; Henderson, 1988; Deimer, 1988)

5) sediments finer than fine gravels are often found infilling broad, symmetric, shallow channels, with bedding parallel to the channel margins (McCabe et al., 1984; Deimer, 1988).

6) steep-sided channels filled with massive to vaguely- stratified sand, and often containing intact blocks of laminated sand are common (Rust, 1977; Cheel & Rust, 1982; Sharpe, 1988)

All of these diagnostic features can be found in moraine and kame outcrops throughout the study area, with the possible exception of the massive sand-filled channels.

Structurally, for deltas to form topographically-high ridges (ie the moraines and kames), they must be ice-contact deltas, supported on their proximal side by the ice margin. Subaqueous fans are thought to be free-standing forms which do not normally require a supporting ice margin (Banerjee & McDonald, 1975; Gustavson and Boothroyd, 1987). However, there is no evidence in any of the exposures in the study area of any significant disturbance or faulting which could be attributed to the collapse of supporting ice (cf. McDonald & Shilts, 1975), or to thrusting caused by fluctuations in

position of the ice margin. It is possible that this may be due to the limited number of exposures in the coarse-grained deposits, although the exposures that were available were quite large.

Fyfe (1990) has studied the very similar Salpausselka I moraine in southern Finland, and has suggested that it too is a glacial outwash structure. She has shown that the deltaic portions of the Salpausselka I moraine are generally wider and relatively flat topped, with abundant kettle holes, while the subaqueous portions tend to be narrow with more rounded tops and lacking kettle holes (Fig. 4-1). This characteristic morphology of proglacial deltas has also been noted by McCabe and Eyles (1988).

The Hartman and Eagle-Finlayson moraines are mainly narrow bodies with rounded tops, and lacking kettle holes (Fig. 4-1), and are more characteristic of subaqueous fans. Portions of the Hartman moraine in the southeast part of the study area, however, occur at a higher elevation, and have a broader, flat-topped morphology with abundant kettle holes (Fig. 4-1), indicating that at least some of the Hartman moraine aggraded to lake level. Unfortunately there were no exposures in this area.

Information on specific paleo-water levels is probably the best way of determining if a structure is a delta or a subaqueous fan (Fyfe, 1990; Rust, 1989; Deimer, 1988; Rust & Romanelli, 1975). The broad, flat-topped, portion of the Hartman occurs above the 440 m contour (Fig. 4-2). Kettle holes on the Hartman moraine are largely restricted to areas above the 430 m contour (Cowan & Sharpe, 1991). Thus the geomorphic evidence suggests water levels

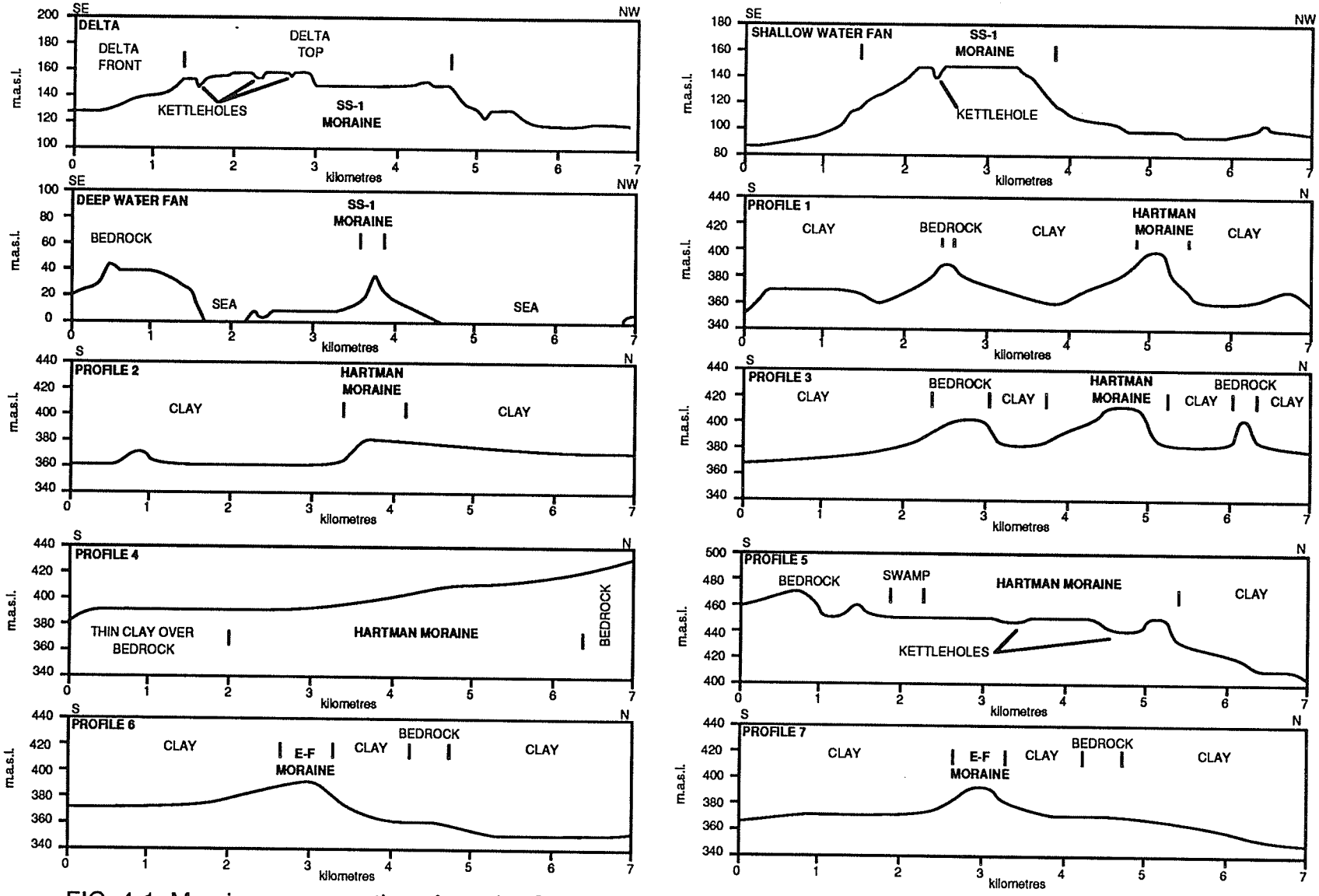

FIG. 4-1 Moraine cross-sections from the Salpausselka 1 (SS-1) moraine in Finland (Fyfe, pers. comm. 1990) and from the Hartman and Eagle-Finlayson moraines in the Dryden area. Proximal side of moraines is always on the right. Locations of Dryden sections are shown in Fig. 4-2.

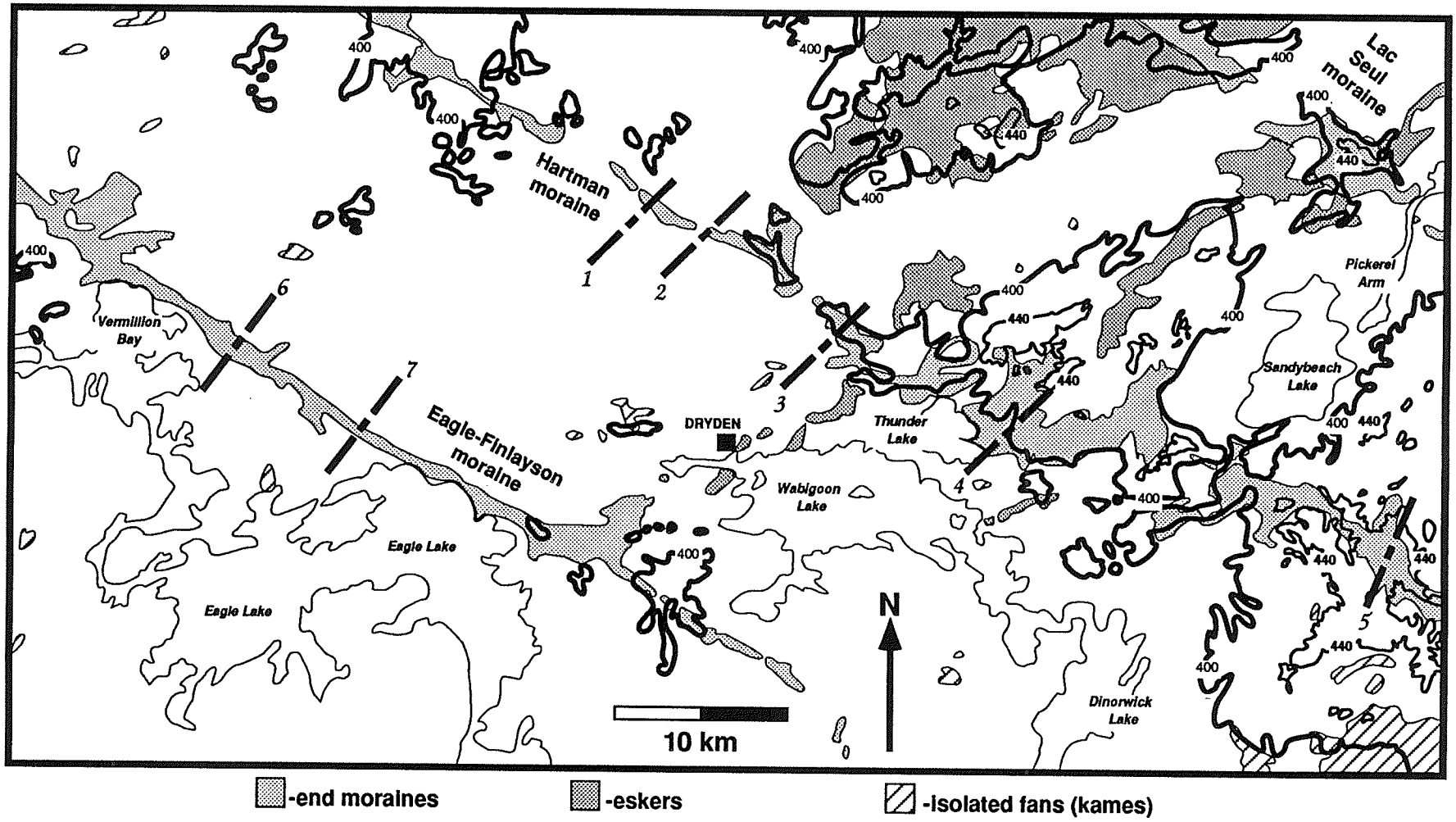

Fig. 4-2 Map showing the major fans, moraines and eskers in the Dryden area, and their relationship to elevation. Most parts of the moraines and eskers, and all of the isolated fans are below the 400 m contour. Portions of the Hartman moraine in the southeast part of the study area rise above the 440 m contour, and are probably deltaic in origin. The dashed, numbered lines give the locations of the cross-sections shown in Fig. 4-1.

of around 430-440 metres above sea level (masl) during construction of the Hartman moraine. As the Eagle-Finlayson moraine (in the study area) is everywhere below 410 masl, and is narrow, round-topped, and devoid of kettle holes, it is assumed that similar water levels existed during its formation.

Additionally, in section 87-2, a sequence of Facies 2 and 3 sandy rhythmites contains minor wave-rippled sands and silts at an elevation of approximately 400 masl. This indicates concurrent underflow activity and occasional (probably storm) wave reworking of the sediment (B. Greenwood, pers. comm. 1991). As Lake Agassiz has a maximum fetch to the northwest of between 900-1100 km, wave energies would likely have been high and storm wave base fairly deep. Thus, the sedimentological evidence is again roughly in agreement with the geomorphic and stratigraphic evidence for water levels of approximately 440 m. Since the rhythmites at section 87-27 form the subaqueously deposited portion of a beaded esker (discussed below) located between the Hartman and Eagle-Finlayson moraines, indicated water levels reflect a time in-between the deposition of the two moraines.

Overall, the sedimentological and paleo-water level evidence seems to favour the Eagle-Finlayson moraine, and most of the Hartman moraine, having been formed entirely subaqueously (as subaqueous fans), probably in water depths of around 440 masl. Since all kames in the Dryden area occur below 400 masl, these are presumed to be (isolated) subaqueous fans as well. Only a portion of the Hartman moraine in the southeastern part of the study area likely

aggraded to lake level, and thus, it is the only true delta in the study area (Fig. 4-2).

It is widely acknowledged that eskers are often composed both of sediment deposited within a glacial meltwater conduit, and sediment deposited at the mouth of the conduit as a tunnel-mouth subaqueous fan or delta (Banerjee & McDonald, 1975; Rust & Romanelli, 1975; Saunderson, 1975 and refs. therein; Hebrand & Åmark, 1989). Conduit sediments may be deposited in a super-, en-, or subglacial conduit. A super- or englacial tunnel environment is unlikely for the esker deposits observed in the Dryden area, as no evidence of post-depositional collapse was seen in any of the excellent esker exposures. A tunnel-mouth, subaerial delta environment is also unlikely, as none of the eskers sit above 410 masl. Esker deposits formed subaqueously at the mouth of subglacial tunnels should show a rapid, downstream fining from coarse gravels into lacustrine silts and possibly clays (Banerjee & McDonald, 1975; Saunderson, 1975). This is seen at esker sections 87-2 and 87-27, but not at 88-6, suggesting that the first two sites represent tunnel-mouth fans, while the latter site represents a subglacial tunnel environment. Site 88-6 also shows massive, matrix-supported gravel overlying and truncating large sand and gravel foresets (see Facies 7). This type of deposit is thought to be restricted to subglacial conduits which experience tunnel-full flow conditions (Saunderson, 1977).

The presence of tunnel-mouth deposits in an esker landform implies that at least some component of the esker is a time-transgressive deposit, and that the entire esker was not simply deposited in a single event within a subglacial

conduit (Banerjee & McDonald, 1975). These tunnel-mouth fans, although not laterally confined by the ice, could still have formed significant topographic highs (and therefore esker ridges), since rapid flow expansion and loss of competence would have resulted in most of the coarse sediment load being deposited in the immediate vicinity of the tunnel mouth (Rust & Romanelli, 1975; Banerjee & McDonald, 1975; Saunderson, 1975; Deimer, 1988).

Because only three extensive exposures were available in the esker landforms (and probably in the same esker system), this interpretation may not be generally applicable to all esker landforms and deposits in the study area.

4.2 FACIES MODEL:

The ice-marginal subaqueous outwash fan model shown in figure 4-3 can be applied to almost all of the sediments found in the study area, including the rhythmites. The exceptions are the areas of sandy diamict mapped by Cowan & Sharpe (1991) and Minning & Sharpe (1991) (Fig. 1-2), and the portion of the Hartman moraine interpreted as a deltaic deposit (Fig. 4-2). Because of the complete lack of exposures in either of these deposits, they are not considered further in this facies model.

The subaqueous outwash fan (Fig. 4-3) consists of several depositional zones. Boundaries between these zones are gradational, and would probably migrate as glacial meltwater discharge varied. These zone are interpreted as follows:

1) Zone 1 consists of the subglacial conduit. This represents the highest energy environment on the fan, and is roughly analogous to the braided river

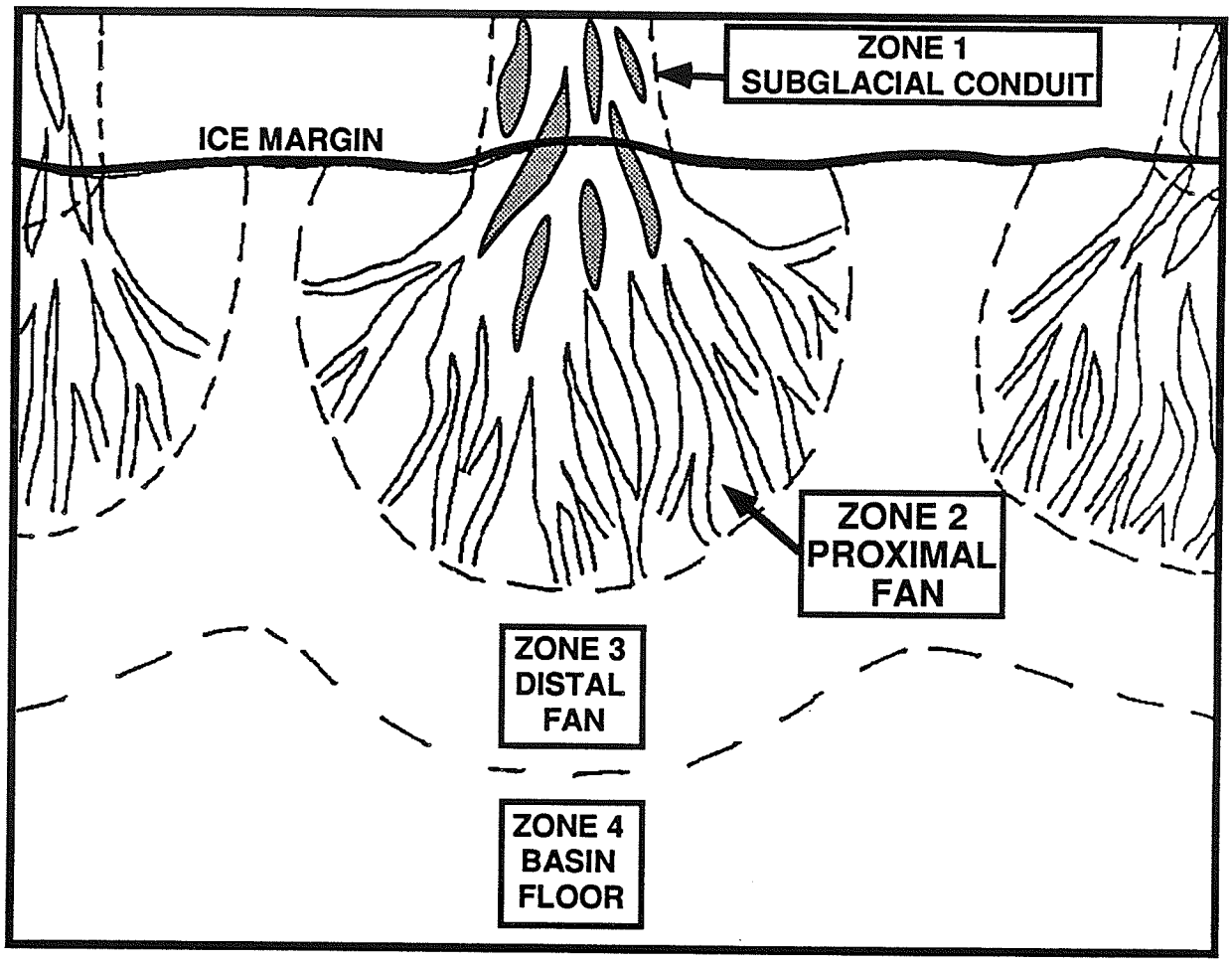

Fig. 4-3 Plan view of idealized subaqueous fan model. Zone 1, the conduit, is dominated by current bedded sands deposited in channels between large gravel bars (shaded), and by matrix-supported gravels representing tunnel-full conditions. Zone 2, the channelized inner fan, represents a transition between river-type fluid-gravity flows and sediment-gravity flows. Finer clast-supported gravels and pebbly sands deposited by high-density underflow currents are the dominant sediment types within the channels, while Facies 2 & 3 sandy rhythmites are found in abandoned channels and interchannel areas. Zone 3, the unchannelized outer fan, is dominated by the low-density underflow current deposits of the Facies 2 & 3 rhythmites. Zone 4, the basin floor, is dominated by low-density underflows during the melt season, and by vertical settling of clays from suspension during the winter. This produces the Facies 1 silt-clay rhythmites.

system traditionally envisioned for the formation of an esker (Banerjee & McDonald, 1975; Saunderson, 1975). Deposition was largely from river-type traction currents. Conduit deposits typically form the core of an elevated ridge (esker) oriented NE-SW and transverse to the former ice margin.

Both longitudinal and transverse gravel bars were deposited during peak flow periods. Deposition between peak flow periods is represented by Facies 4A planar and trough-crossbedded sands, deposited on the bar tops, and in channels between the bars.

The single deposit of Facies 7 matrix-supported gravel (Fig. 2-46) found within an esker ridge at site 88-6 is likely a "sliding-bed deposit", formed by extremely high flow velocities in the conduit (Saunderson, 1977). Saunderson assumed that this type of deposit represented tunnel-full conditions in the conduit, but since conduits in the Dryden area discharged below lake level, they must have been continuously filled with meltwater. Meltwater discharge in Zone 1 was likely year-round (cf. Gustavson, 1975).

2) Zone 2 represents a hydrodynamic transition from river-type fluid flows to sediment gravity flows, probably due to rapid flow expansion. Rapid settling of coarse-grained suspended sediment occurs at the subglacial conduit mouth. Sediments in this zone are characterized by the deposits of high-density turbidity currents (Facies 4B, 5 and 6B sands, pebbly sands and gravels). The concentration of these sediments in broad, shallow channels suggests a channelized fan surface analogous to the channelized mid-fan environment of Walker (1978 in Walker, 1984). Channelized Facies 3 (sand-silt) rhythmites

represent deposition from low-density turbidity currents on the more distal portions of the channelized zone, or in proximal zones during periods of lower discharge. Lowe (1982) has suggested that there should be a proximal to distal transition from high-density to low-density turbidity currents.

Channel abandonment and switching, combined with vertical aggradation in the channels probably resulted in the vertically-stacked sequences of nested channels which are common in the study area. No evidence of lateral channel migration was seen.

3) Zone 3 represents the unchannelized lower portion of the subaqueous fan, and is dominated by the low-density turbidity current deposits of the Facies 2 (sand-clay) and 3 (sand-silt) rhythmites. These low-density turbidity currents did not significantly erode the underlying beds, resulting in their largely sheet-like, unchannelized geometry. The presence of silt and clay laminae within these rhythmites suggests that the reduced winter output of glacial meltwater resulted in currents which died out before they reached this portion of the fan.

The only evidence for wave activity in the study area comes from an unchannelized portion of a fan which forms part of an esker between the Eagle-Finlayson and Hartman moraines (section 87-2). At this location, wave energy reworked fine sand and silt that was originally deposited by underflows, producing straight-crested sinusoidal wave rippled silts and sands interbedded with climbing-rippled fine sands and silts.

The flat-lying beds filling deep bedrock lows, which can be seen on the seismic and sonar profiles (Figs. 2-53 & 2-54), were likely deposited on an unchannelized lower fan environment.

4) Zone 4 is the basin floor area in the distal region of the fan. Sedimentation in this zone was likely dominated by relatively weak, quasi-continuous underflows during the glacial melt season, which deposited the silt component of the Facies 1 silt-clay rhythmites. During the winter when meltwater output was reduced, underflow activity lower, and the lake possibly frozen, vertical settling from suspension dominated, depositing the clay component of the rhythmites. Benthic organisms appear to have been active during deposition of the silt component, but were absent during deposition of the clays.

4.3 COMPARISON WITH OTHER MODELS:

This facies model is similar to those developed for other ice-marginal subaqueous fan deposits (both Quaternary and older) from other areas (eg. Rust & Romanelli, 1975; Shaw, 1985; Mustard & Donaldson, 1985). Not surprisingly however, differences do exist between the study area and other localities and some of these differences will be briefly examined here.

Diamicts are typically seen in other subaqueous outwash deposits, and are usually explained as products of slumping and debris flows from unstable portions of the fan or from the ice margin itself (eg. Mustard & Donaldson, 1987; McCabe et al., 1987; Visser et al., 1987). Alternatively they may represent tills deposited by earlier glacial advances or retreats, especially when they are

found at the base of the sequence (eg. McCabe et al., 1984; Burbidge & Rust, 1988). Diamicts may also result by the dumping of sediment from debris-rich icebergs (ice-rafting), or from overhanging or floating ice-shelves (McCabe et al., 1987; Thomas, 1984). Dropstones in laminated sediments are also considered characteristic of ice-rafting.

The scarcity of diamicts and dropstones within the sediments in the Dryden study area suggests that these types of processes were not significantly active here. In any subaqueous fan setting, where a glacier margin is fronted by a large body of water, calving rates will likely be extremely high, and iceflow is likely to be extensional (Burbidge & Rust, 1988). This would discourage upward shearing within the ice sheet, and prevent debris from being carried into the upper portions of the ice margin, where it could slump into the basin. Icebergs that calved from the upper portions of the glacier would be debris-poor, and would not contribute much iceberg rafted debris. Thus the sediment source for debris flows and dropstones in most subaqueous fans likely comes from the lower portions of the ice sheet. In the study area, this debris was presumably removed and reworked by subglacial meltwater.

Slumping and mixing of rapidly deposited, unstable fan sediments can also produce diamicts, and this appears to have occurred to a certain extent (Facies 8). However the steep-sided, massive sand filled channels that are considered diagnostic of slumping in subaqueous outwash deposits (Rust, 1977) were not seen at all in the study area. This does not mean that these

deposits are not present, since outcrops in the lower fan portions were not abundant in the study area.

The degree to which the subaqueous outwash fan is channelized is quite variable among various facies models. Examples range from totally unchannelized (Shaw, 1985; Thomas, 1984b), through fans with only slump-generated channels (Rust, 1988; Sharpe, 1988) to fans with abundant, meltwater-derived channels (Burbidge & Rust, 1988; Cheel & Rust, 1982). It is clear from exposures in the Eagle-Finlayson moraine (Figs. 2-26 & 2-34) that meltwater-cut channels are common, at least in the more proximal areas of the subaqueous fans. Rust and Romanelli (1975) suggested that these types of channels were cut by powerful meltwater flows at the peak of the glacial meltwater season. No channels were seen which could be attributed to slumping, although this may be due to a lack of outcrop.

The deposits within the study area generally lack faulting or other disturbances which can be attributed to the melting of buried ice blocks, or to the collapse of supporting ice walls. These features appear to be common in other subaqueous fan deposits (eg. Sharpe, 1988; Deimer, 1988; Kaszycki, 1987). This implies that the meltwater tunnels were subglacial rather than englacial, and were not floored by ice (cf. Gustavson & Boothroyd, 1987, their Fig. 9C). Furthermore, it suggests that these conduits were quite broad, with high width to height ratios, and were therefore less susceptible to marginal collapse when the surrounding ice melted or was calved away. Pfirman and Solheim (1989) described a 200-m-wide meltwater tunnel at the margin of a

tidewater glacier in Svalbard. The tunnels in the Dryden area may have been on the scale of tunnel valleys described elsewhere in the literature, which range from 180 m to over 2.0 km in width (Wright, 1973; Mooers, 1989; Eyles & McCabe, 1989).

It appears from a review of the literature that sandy and gravelly subaqueous fans like those in the Dryden study area are end members in a continuum of ice marginal deposits. At the other end of this spectrum are the diamict-dominated morainal banks of Powell and Molnia (1989), while intermediate types are described by McCabe et al. (1984) and Mustard and Donaldson (1987) (Fig. 4-4). The controlling factor on this continuum appears to be the amount of meltwater being discharged at the ice margin, with subaqueous fans representing high meltwater discharge. In addition, the nature of ice flow at the margin may also be a controlling factor. The presence of the large proglacial Lake Agassiz in the Dryden area would have promoted extensional flow near the ice margin. Compressional flow near the margin would tend to cause upward shearing of basal debris, concentrating wet, poorly-sorted debris on the surface of the ice. This material would be prone to slumping, resulting in abundant debris-flow diamicts at the ice margin.

4.4 FORMATION OF THE ESKERS, KAMES AND MORAINES:

Meltwater would have been carried toward the ice margin in a series of subglacial meltwater tunnels. Where these tunnels entered Lake Agassiz, flow expansion occurred, resulting in deposition of a subaqueous outwash fan or a delta, depending on the elevation of the tunnel mouth relative to the lake

1

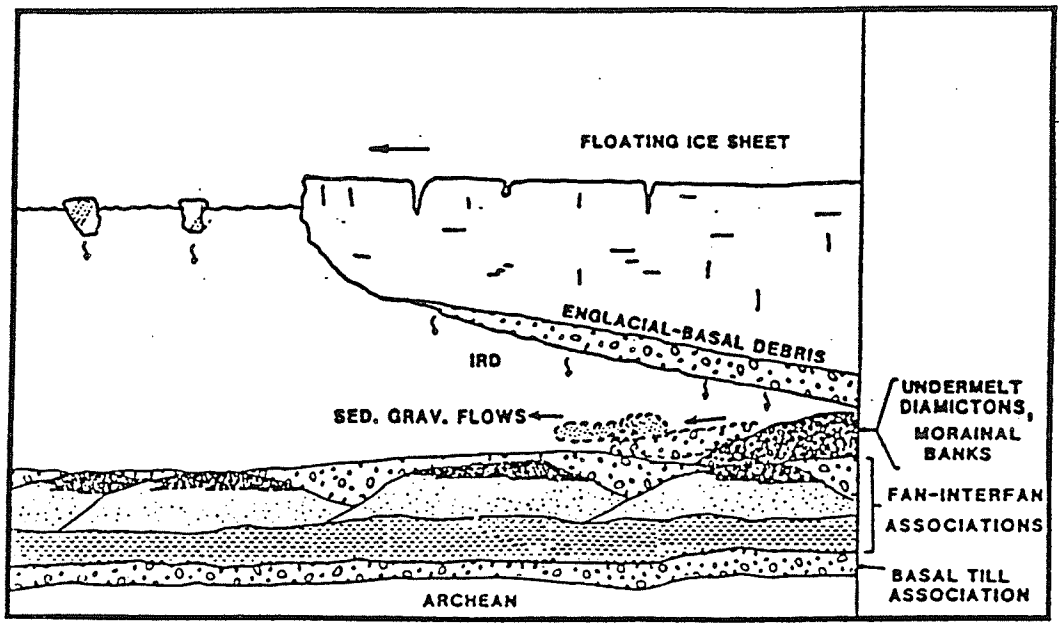

2

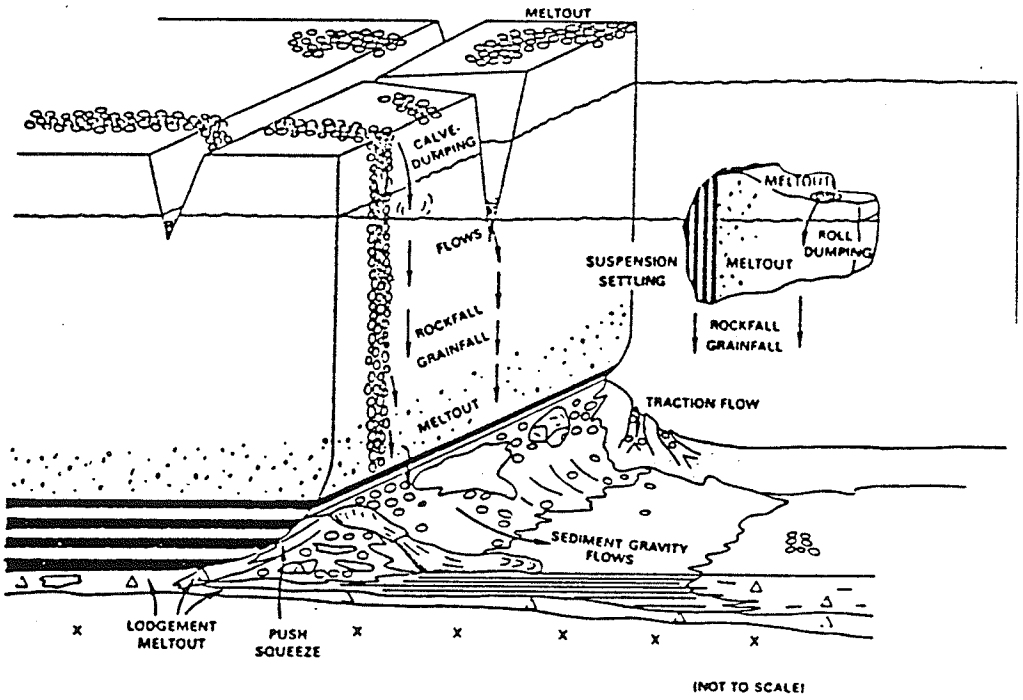

Figure 4-4 Mechanisms proposed for the formation of morainal banks and similar structures by A) Mustard and Donaldson (1987) and B) Powell and Molnia (1989).

surface. If, as discussed previously, water levels in the study area were above most of the deposits, they represent subaqueous fans. Isolated subaqueous fans (kames) formed when a meltwater tunnel was abandoned before significant ice marginal retreat had occurred (Fig. 4-5A).

When a meltwater tunnel remained in use as the ice margin retreated, the zone of coarse sediment deposition retreated with it. This resulted in the formation of an esker, consisting of an iceflow-parallel ridge (Fig. 4-5B), with subglacial tunnel sediment at its core, overlain by a fining upward sequence of subaqueous fan sediments. These fans, although not laterally confined by the ice, would still have formed significant topographic highs, since rapid flow expansion and loss of competence would have resulted in most of the coarse sediment load being deposited in the immediate vicinity of the tunnel mouth (Rust & Romanelli, 1975; Banerjee & McDonald, 1975; Deimer, 1988).

The formation of the end moraines in the Dryden area clearly seems to have occurred through a process similar to that which formed the esker and kame landforms, that is, the deposition of subaqueous outwash fans (and deltas in the case of the moraines) along the margin of the ice. It is relatively simple to envisage individual esker and kame deposits as the products of meltwater discharge from individual subglacial meltwater conduits. It is more difficult to imagine the meltwater source of a moraine which is continuous for hundreds of kilometres along the former ice margin.

The lack of evidence for overriding of the moraines in the study area (Cowan, 1987; this study) and the lack of observed glaciotectonic disturbance

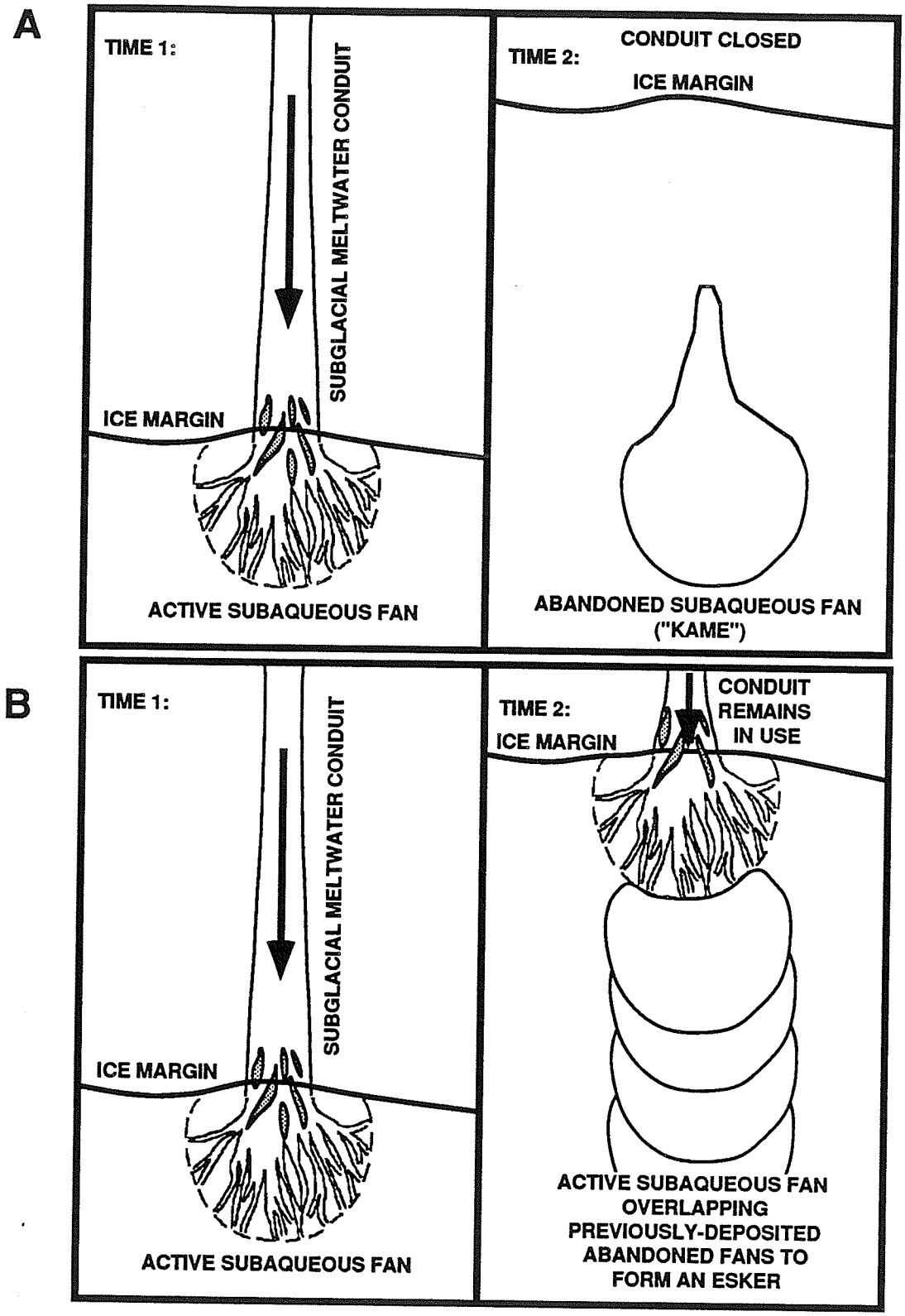

Figure 4-5 Model for the formation of isolated fans ("kames") and eskers in the Dryden area. A) Single, short-lived meltwater conduit creates a single, isolated fan. B) A longer-lived meltwater conduit creates an esker, comprised of overlapping fans, as the ice retreats.

within the moraines argues that: a) the moraines are unlikely to represent multiple readvances of the ice margin to the same point; b) the ice margin was essentially stationary during whatever period of time was required to construct a particular moraine.

Individual moraines may be composite, time-transgressive structures, formed by laterally migrating meltwater tunnels at a stationary ice margin (Fig. 4-6A). This process requires that either meltwater discharge was dramatically increased and the meltwater tunnels migrated rapidly, or, if meltwater discharge did not increase, that the ice margin remained stationary for a considerable (but unknown) period of time.

Alternatively, the moraines may be single, contemporaneous structures, formed by meltwater discharging along the entire margin of the Rainy Lobe, either from closely-spaced subglacial conduits (Fig. 4-6B) or from a short-lived, sheet-like subglacial meltwater flow of the type envisaged by Shaw (1983) and Shaw and Kvill (1984). Either case would seem to require a dramatic increase in the discharge of meltwater during moraine formation, as there is no evidence of a closely spaced conduit network existing in the areas in-between the moraines (ie. between moraine-forming events) (Fig. 1-2).

These multiple working hypotheses can, to a limited extent, be tested. Whether or not the meltwater discharge increased, if the moraines are the products of laterally migrating meltwater conduits, they should consist of a series of stacked and overlapping fans, with the later-constructed fans deposited on top of the finer-grained sediments of the adjacent, earlier-formed

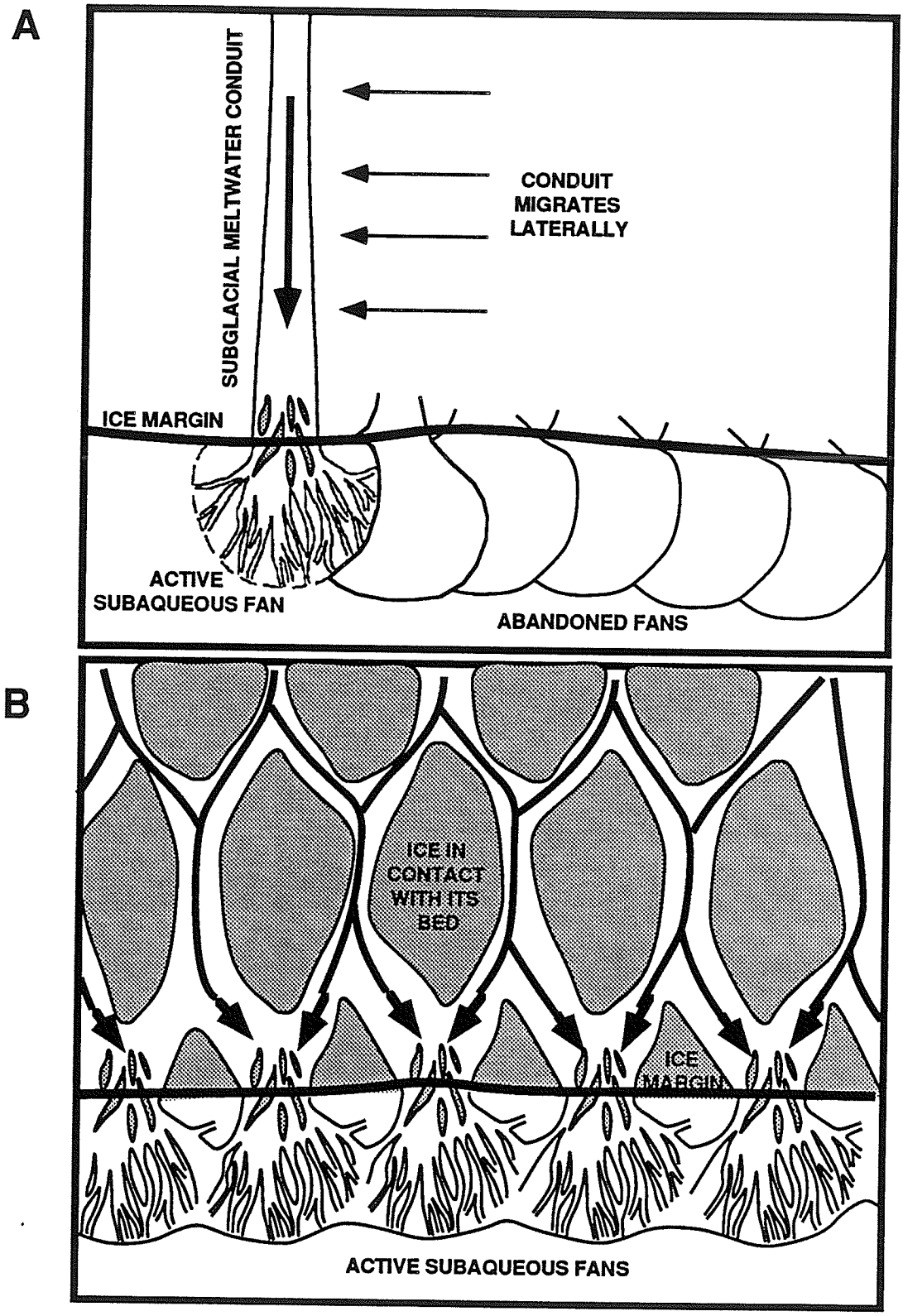

Figure 4-6 Alternative models for the formation of the end moraines in the Dryden area. A) A composite, time-transgressive moraine is formed by laterally migrating meltwater tunnels, which deposit a series of overlapping subaqueous fans. B) A penecontemporaneous moraine is built by discharge from closely-spaced meltwater conduits. Arrows indicate meltwater flow.

fans (Fig. 4-6A). This would produce numerous complex, fining and coarsening upwards sequences with coarse Zone 1 or 2 sediments overlying finer-grained Zone 3 and 4 sediments. In the entire study area there is only one exposure where this occurs (Fig. 2-50) and this is near the crest of the Hartman moraine. This deposit is probably explained by later wave erosion and slumping of the moraine crest as the lake level fell for the final time. The bulk of the exposures in the study area show no evidence of non-contemporaneous, overlapping fan deposition.

In addition, if the moraines were formed gradually by the lateral shifting or switching of meltwater tunnels, without an increase in meltwater discharge, some mechanism would have been required to stabilize the ice margin for a considerable period of time. A climatic deterioration has been suggested as a mechanism by Saarnisto (1974). However, such a climatic deterioration probably would have been accompanied by a decrease in the amount of meltwater delivered to the ice margin. Given a lower meltwater (and therefore sediment) discharge, a relatively long stabilization of the ice margin would have been necessary to form the thick, laterally-continuous moraine deposits. However, the narrowness of the moraines and lack of any glaciotectonic disturbance within the morainic sediments would require a remarkable lack of marginal fluctuation during a long, climatically-induced stillstand.

The climatic evidence from palynological investigations in Minnesota and northwestern Ontario shows no evidence of climatic reversals, with the exception of one site (Rattle Lake) located just south of the Eagle-Finlayson

moraine (Bjorck, 1985). Bjorck noted that a decrease in the abundance of ash and elm pollen from approximately 11.1 ka to 10.2 ka seems to indicate a climatic deterioration, but is not conclusive. This time period seems too long to account for the formation of any one moraine, and is shorter than the time period spanned by formation of all the moraines.

The relatively simple, fining upward sedimentary sequence observed within and immediately in front of the moraines in the Dryden area (see Section 2.4) suggests that individual moraines are single, contemporaneous deposits (Fig. 4-6B). If this is correct, then a mechanism and a cause for discharging meltwater and sediment simultaneously along the entire margin of the Rainy Lobe must be sought.

4.5 POSSIBLE CAUSES AND MECHANISMS FOR MELTWATER DISCHARGE:

If a significant increase in the discharge of subglacial meltwater did occur, bifurcation and enlargement of subglacial tunnels near the ice margin might have been required to accommodate this increased meltwater flow, resulting in the delivery of water and sediment along a broad region of the ice margin simultaneously. Such a mechanism has been proposed for the Hartman and Eagle-Finlayson moraines by Sharpe and Cowan (1990) and for similar moraines in Finland (Fyfe, 1990) and Poland (Ruszcyzynska-Szenijch, 1982). Shaw (1983) and Shaw and Kvill (1984) have proposed that subglacial tunnel expansion may be unable to keep pace with a sudden, catastrophic increase in subglacial meltwater discharge, leading to a sheet-like subglacial meltwater

flow which they suggest may be tens to hundreds of kilometres wide (thickness is not specified). There is no evidence from the Dryden area either for or against tunnel or sheet flow, although only subglacial tunnel flow has been observed in modern glaciers.

A review of the literature suggests two possible causes for such an increase in the discharge of subglacial meltwater. Studies of the 1982-1983 surge of the Variegated Glacier in Alaska by Raymond (1987), and Kamb (1987), have shown that, prior to, and during surging of the glacier, marginward flow in the basal meltwater system is retarded and lateral dispersion of the meltwater flow is enhanced, due to the development of a linked cavity/orifice drainage system. This results in increased basal water pressure in the glacier, which, in turn, reduces basal shear stresses and enhances sliding of the ice (Bindschaldler, 1983), which ultimately causes the glacier to surge.

Zoltai (1965) noted that overridden rhythmites north of the Lac Seul moraine suggest a readvance (surge?) of approximately 30 km to the Lac Seul moraine position, prior to the actual formation of this moraine. However, neither the Lac Seul moraine, nor any other of the Dryden area moraines show any evidence of having been overridden by readvancing ice (Cowan, 1987). This would seem to indicate that, while moraine formation in the Dryden area may have been preceded by surging, the surging ended before the actual increase in meltwater discharge that is thought to have formed the moraines.

This is in agreement with the observations of Kamb et al. (1985), who described the termination of the 1982-1983 surge of the Variegated Glacier as

being "...accompanied by a particularly spectacular flood" (p. 475). The marginward release of glacial meltwater from a linked cavity system was suggested by Fyfe (1990) as a mechanism for delivering meltwater and sediment simultaneously along a large portion of the Scandinavian Ice Sheet, resulting in the formation of the Salpausselka I moraine in Finland, although Fyfe did not relate the release of meltwater to the end of a surge event.

A second possible cause for increased meltwater discharge has been suggested by Sharpe and Cowan (1990). They note that Teller and Thorleifson (1983) have documented several drops in the level of Lake Agassiz due to the opening of eastern outlets by the retreating Superior lobe of the ice sheet. A drop in the level of Lake Agassiz would result in an oversteepening of the potentiometric englacial meltwater surface, and an increase in the relative hydraulic head within the ice sheet. This would lead to a drawdown of glacial meltwater as the glacial hydrologic system re-equilibrated to this lowered base level, resulting in increased meltwater discharge at the ice margin. Sharpe and Cowan (1990) argued that this increased meltwater discharge resulted in the formation of the Dryden area moraines, and that each moraine corresponded to a drop in lake level caused by the opening of a new, lower eastern outlet.

This mechanism is partially analogous to the re-equilibration moraine concept of Hillaire-Marcel et al. (1981), who maintain that the Sakami moraine in Quebec is due to a pause in ice-marginal retreat as the surface profile of the ice sheet re-equilibrated to the lowered level of the proglacial water body. Perhaps both a pause in ice-marginal retreat, and an increase in meltwater

discharge would result from a lowered proglacial lake level. This would allow both increased time for moraine sedimentation, and higher sedimentation rates.

It is difficult to determine if either of these mechanisms (surging followed by rapid meltwater ejection vs lake level drop followed by a halt in retreat and hydraulic gradient steepening) was responsible for the formation of the four major moraines in and around the Dryden area. An examination of the timing of deglaciation and Lake Agassiz water levels (Chapter 5) suggests that either one or both of these mechanisms may have been operative.

CHAPTER 5: HISTORY OF DEGLACIATION AND LAKE AGASSIZ

5.1 INTRODUCTION:

The history of Lake Agassiz in the southern regions is divided into two periods of relatively high water levels (the Lockhart and Emerson Phases) separated by a period of relatively low water levels (the Moorhead Phase)(Fig. 5-1: Fenton et al., 1983). The Lockhart Phase is thought to have ended around 11.0 ka, with the Moorhead Phase lasting around 1,100 years until the start of the Emerson Phase at around 9.9 ka (Teller & Thorleifson, 1983).

The position of the margin of the Rainy and Superior Lobes controlled the availability of outlets, which in turn controlled the level of the lake. Drainage through the relatively high southern outlet during a time of maximum isostatic depression resulted in high lake levels during the Lockhart Phase (Fenton et al, 1983; Teller & Thorleifson, 1983).

As Elson (1967) described, the main low water level episode of Lake Agassiz (the Moorhead Phase) was due to the opening of the lower eastern outlets to Lake Superior. This was caused by retreat of the Rainy Lobe north of the Sioux Lookout moraine position and possibly as far north as the Whitewater moraine position, and withdrawal of the Superior Lobe from the Superior basin (Fig. 5-2)(Teller & Thorleifson, 1983).

The existence of the low water Moorhead Phase is based on an unconformity first noted in the Rainy River area by Johnston (1915) and Elson

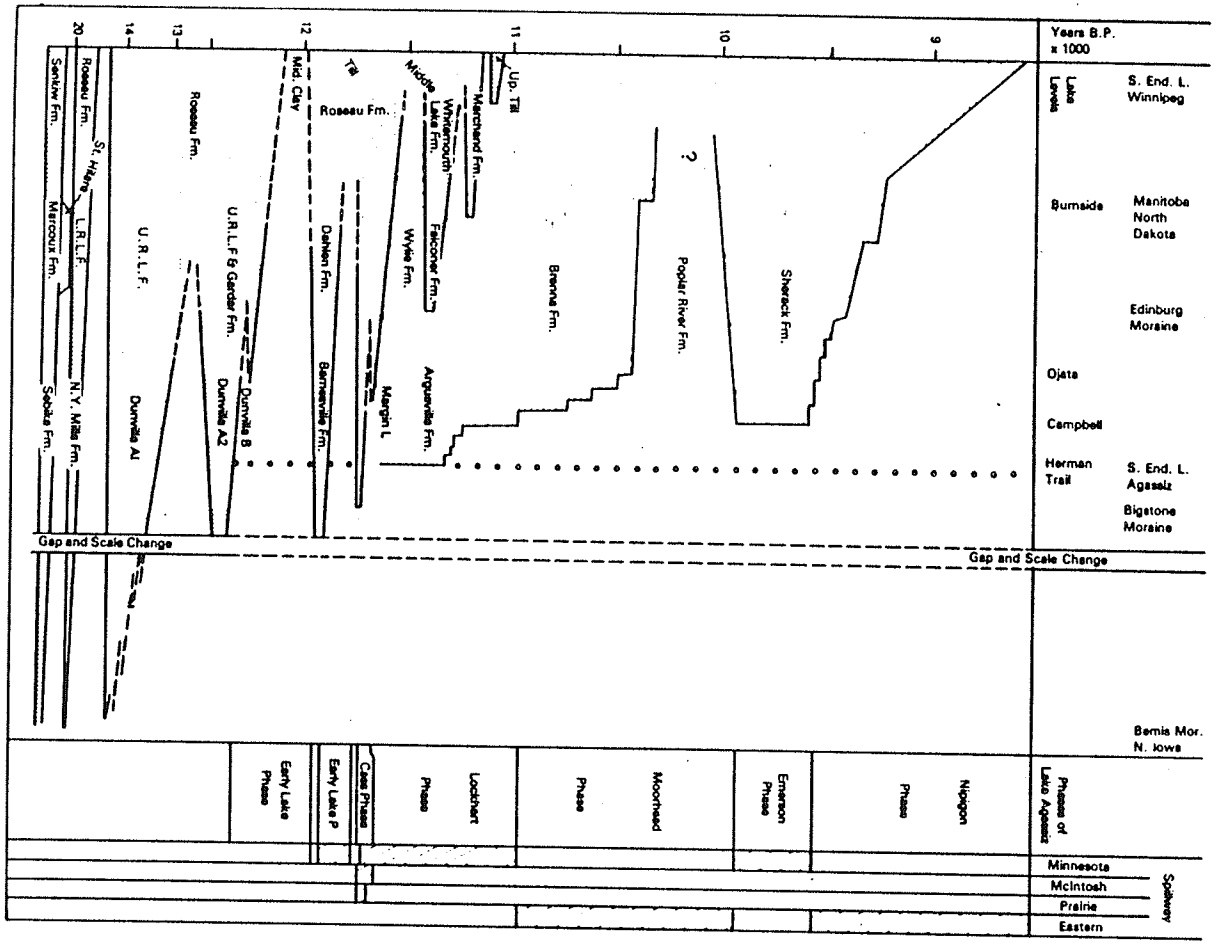

Figure 5-1 The most up to date Lake Agassiz chronology (Fenton et al., 1983, p. 53).

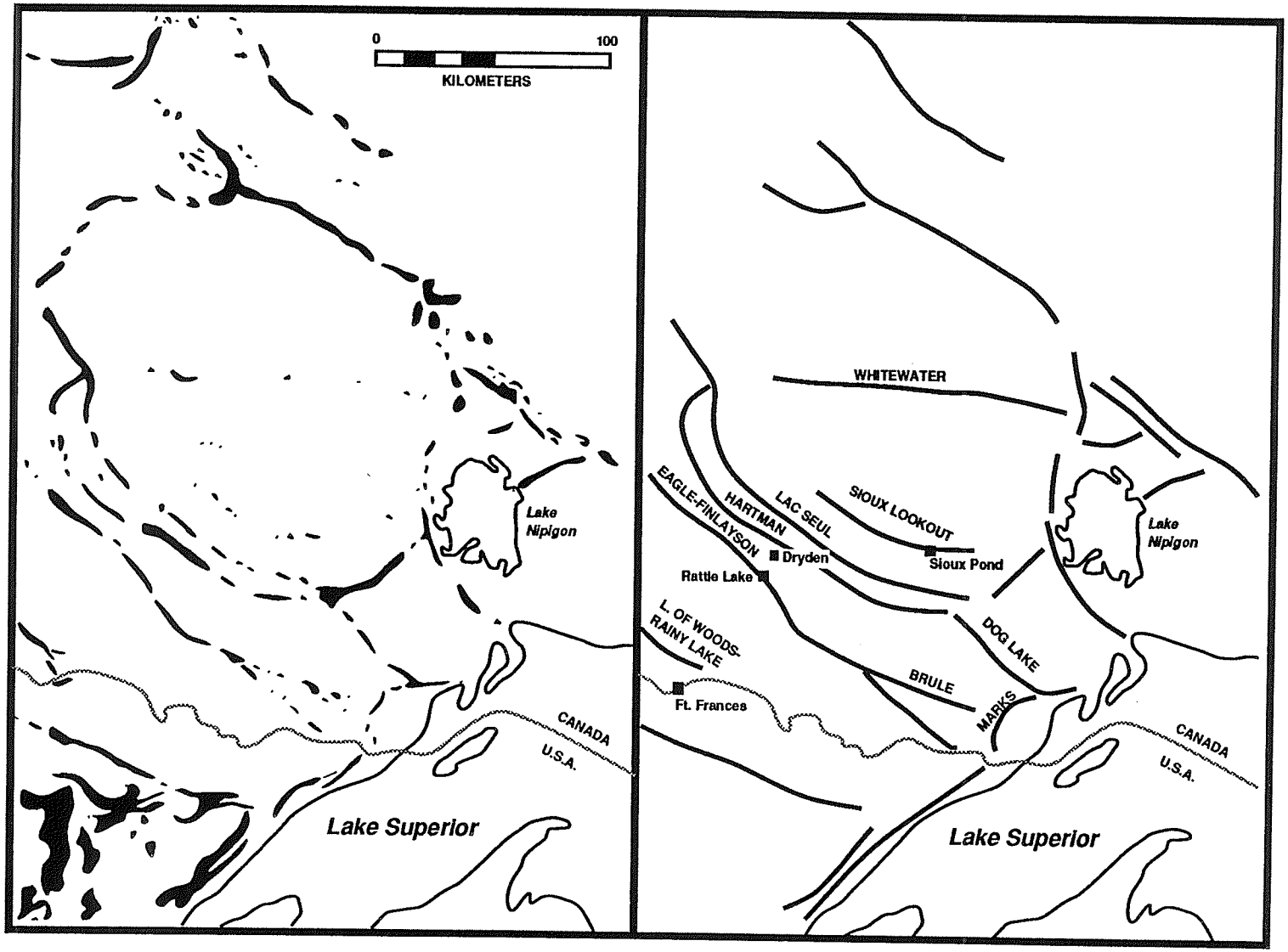

Fig. 5-2 Moraine features in northwestern Ontario (after Teller & Thorleifson, 1983).

(1967), and later documented in North Dakota and Minnesota (Harris et al., 1974; Arndt, 1975; Arndt, 1977; Clayton et al., 1982). Radiocarbon dates obtained from wood at sites where a physical unconformity can be observed in North Dakota, Manitoba, Minnesota and Ontario, range from 10.96 ka to 9.9 ka (Elson, 1967; Harris et al., 1974; Bajc, 1987; Broecker et al., 1989). Nielsen et al. (1982) also present a date obtained from mollusc shell fragments of 11.4 ka from Moorhead Phase alluvium below Emerson Phase sediments near Rainy River. This date was corrected to 11.0 ka, to compensate for contamination by older carbon.

The northward extent of the Moorhead unconformity is uncertain. Teller (1976) stated that "no unconformity or fluvial unit has been recognized at any of the contacts in (the area along the Red River in) Manitoba, as it has been over much of North Dakota and Minnesota" (pg. 38). Teller and Last (1981) have suggested the unconformity may be present in the modern Lake Manitoba basin (which is approximately 20-30 m higher than the area along the Red River), based on the presence of zones of blocky structure and low moisture content in cores. Radiocarbon dates supporting this interpretation are on disseminated organic material in the cores, and were corrected for the presence of pre-Quaternary organic matter (Nambudiri et al., 1980).

Workers in northwestern Ontario have not found evidence of the Moorhead unconformity within the Lake Agassiz basin north of the Fort Frances-Rainy River area (Rittenhouse, 1934; Antevs, 1951; Zoltai, 1961; Elson, 1967; this study).

Johnston (1946) constructed the first strandline diagram for Lake Agassiz, using measured elevations mainly from the southern and western parts of the basin. Updated strandline diagrams were drawn by Elson (1967) and Thorleifson (1983)(Fig. 5-3), but were not much different from the original.

Based on these strandline diagrams, various workers have attempted to assign water levels (which are named after the beaches and other strandline features they produced) to various phases in the history of Lake Agassiz. The Herman levels have been assigned to the Lockhart phase, while Moorhead phase water levels have been placed anywhere from the Ojata level (Fenton et al., 1983) to as low as The Pas or Gimli levels (Teller & Last, 1981). Regardless of the exact Moorhead Phase water levels, the radiocarbon dates discussed previously require that the level of Lake Agassiz fell below the southern outlet between approximately 11.0-9.9 ka. The Moorhead Delta at the southern end of Lake Agassiz apparently formed during this time (Arndt, 1977). Any water levels below the Campbell level would have required the opening of one or more of the eastern outlets to Lake Superior (Fig. 5-3)(Teller & Thorleifson, 1983), and/or the Clearwater outlet to the Arctic Ocean in Saskatchewan (Elson, 1967). The Ojata level would have required opening of one of the lower Kopka Series outlets, while the Pas or Gimli levels would have required opening of the lowest Pikitigushi outlet (Fig. 5-3)(Teller & Thorleifson, 1983). Moorhead Phase water levels are important to this study, because Ojata or lower levels would have resulted in complete subaerial exposure of the Dryden area.

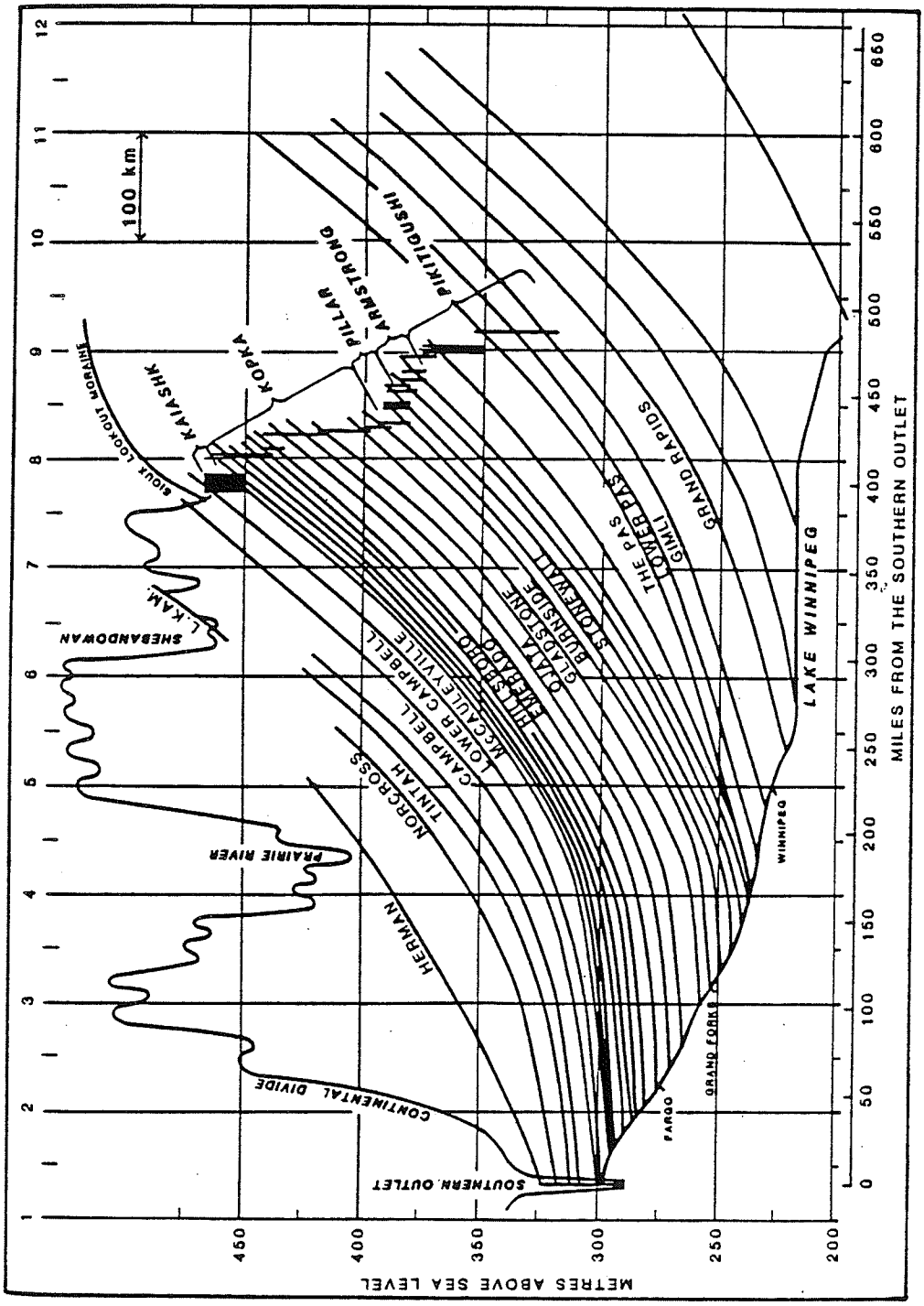

Figure 5-3 Strandline diagram of Teller and Thorleifson (1983, p. 266).

Thorleifson (1983) has argued that the assignment of the Ojata water level to the Moorhead Phase is incorrect. He states that the lower northward gradient on its isostatically deformed surface (lower than that of the Emerson Phase Campbell level)(Fig. 5-3) is more consistent with a younger Nipigon Phase age, since declining isostatic rebound requires that strandline age is proportional to gradient. This, of course, assumes that the isostatic rebound history of the Agassiz basin during the final deglaciation was not punctuated by periods of isostatic depression. In addition, Thorleifson (1983) maintains that none of the radiocarbon dates used as evidence for a Moorhead Phase age for the Ojata level (W-723, TAM-1, I-5213, W-900 & W-1005) can be related with any certainty to the actual Ojata beach. Neither can the Ojata beach be physically traced to the Moorhead delta at the south end of Lake Agassiz, which formed during the Moorhead low water phase (Arndt, 1977; Steve Moran, pers. comm. 1989).

Most workers have concluded that Lake Agassiz rose to the Campbell level during the Emerson Phase (Elson, 1967; Fenton et al., 1983; Bajc, pers. comm. 1991) although Thorleifson (1983) favoured a rise above the Campbell to the Norcross level, and Johnston (1915) suggested the level may have been as high as the uppermost Herman strandline. In any case, the rise from Moorhead to Emerson Phase levels has been interpreted as a result of a readvance of the Superior and Rainy lobes (Marquette readvance) which blocked the eastern outlets to Lake Superior (Teller & Thorleifson, 1983). The

Rainy Lobe is thought to have readvanced as far as the Hartman moraine at about 9.9 ka (Nielsen et al., 1982; Teller & Thorleifson, 1983).

It must be stressed that all of the strandline diagrams that have been constructed for Lake Agassiz are somewhat speculative, since few beaches can be traced north of the international boundary with any confidence, and no beaches can be traced from the eastern and southeastern side of the basin into northwestern Ontario (Elson, 1967; Steve Moran, 1989, pers. comm.).

5.2 CONSTRAINTS ON LAKE AGASSIZ WATER LEVELS:

The interpretation of the sedimentary record of deglaciation at Dryden (presented in Chapters 3 and 4), and evidence from areas elsewhere in the Lake Agassiz basin, have a bearing on the chronology of Lake Agassiz water levels. This section will attempt to present these facts and interpretations in a logical sequence, and then discuss the specific implications of each one. This will be followed by a more general discussion of the currently accepted chronology of Lake Agassiz water levels.

1) *Fact:* The Moorhead unconformity is radiocarbon dated from approximately 10.9 ka to 9.9 ka at sites in North Dakota, Minnesota and northwestern Ontario (Elson, 1967; Harris et al., 1974; Nielsen et al,. 1982; Bajc, 1987; Broecker et al., 1989). *Implication:* Lake Agassiz fell below the southern outlet between 10.9 ka and 9.9 ka (Fig. 5-3).

2) *Fact:* The red clay marker unit in northwestern Ontario directly overlies Moorhead Phase alluvial sediment radiocarbon dated as young as 10.05 ka (Bajc, 1987). In addition (as discussed in Chapter 3) deposition of the red clay

unit is contemporaneous with the existence of the short-lived proglacial Lake Kaministikwia, which was formed by the Marquette readvance of the Superior Lobe (Fig. 3-1). This readvance is radiocarbon dated at approximately 10.0 ka (Clayton, 1983; Drexler et. al., 1983). *Implication:* The age of the red clay unit is roughly 10.0 ka (Fig. 5-4).

3) *Fact:* The longest varve records at Dryden show approximately 400 pre-red varves conformably overlying coarse, ice-proximal Facies 2 and 3 rhythmites (Fig. 2-11). *Implication:* Dryden was deglaciated at 10.4 ka. Thus, the only Lake Agassiz outlets lower than the southern outlet, which were available during the early Moorhead Phase (prior to 10.4 ka) were those located south of the Dryden ice margin. These are the Shebandowan and Dog-Kaministikwia eastern outlets (Zoltai, 1967; Teller & Thorleifson, 1983), and the Clearwater western outlet (Elson, 1967). The alternative to this scenario is that the eastern outlets of Lake Agassiz to Lake Superior were in fact opened prior to 10.4 ka, and that a subsequent readvance to some position south of Dryden removed all evidence of pre-10.4 ka lacustrine sedimentation (including sediment deposited in the deep bedrock lows examined by the sonic cores). However, if such a pre-10.4 ka readvance went to or beyond the Eagle-Finlayson moraine (which seems probable), all eastern outlets would have been blocked, and drainage would temporarily have been returned to the southern outlet. This would require that two Moorhead Phase unconformities exist in North Dakota, in order to explain the presence of an unconformity with dates younger than 10.4 ka.

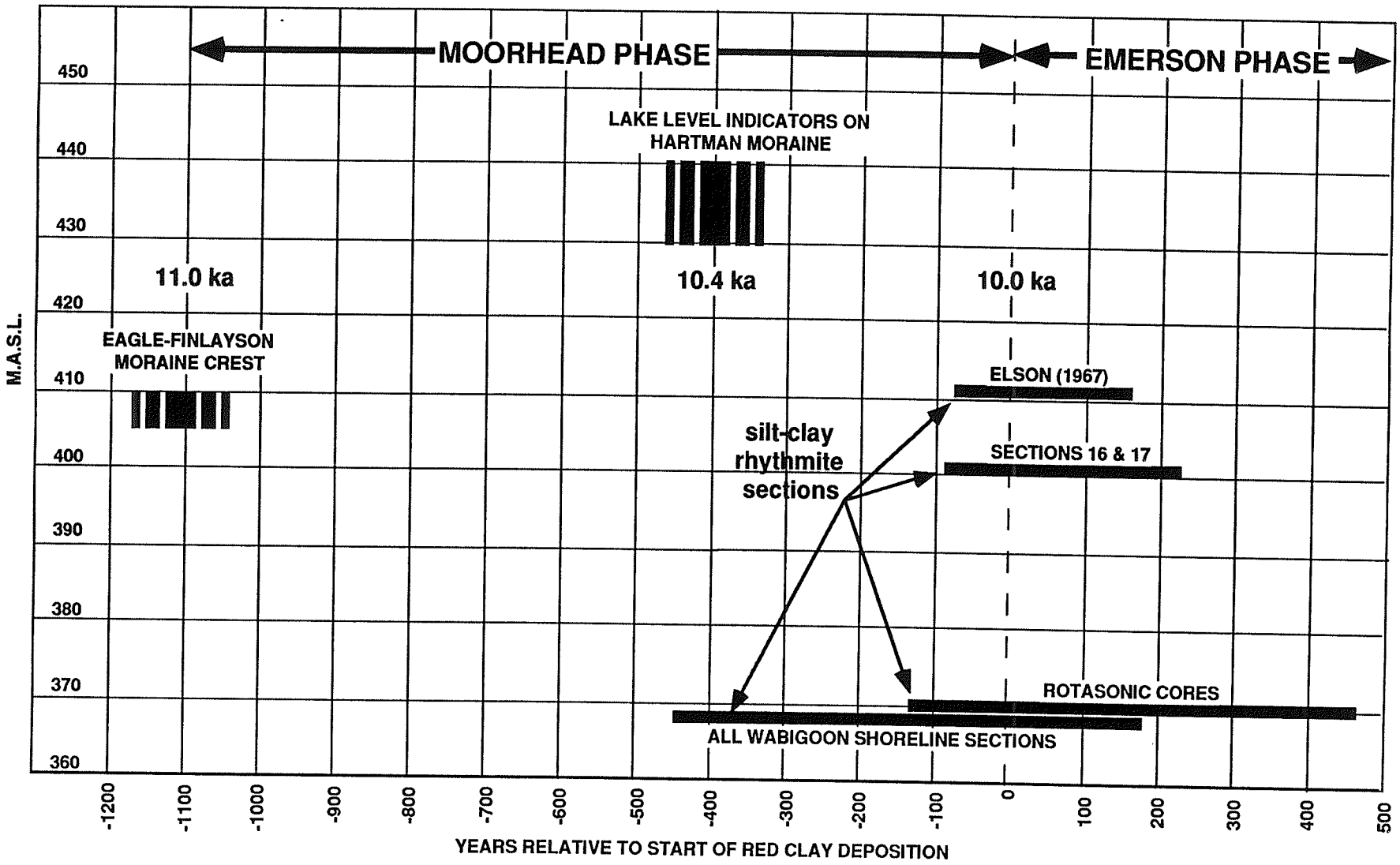

Fig. 5-4 Constraints on the level of Lake Agassiz at Dryden during the Moorhead and Emerson Phases. See text for details.

4) *Fact:* The Hartman moraine is older than the red clay unit, since it stratigraphically underlies it. The thicker and coarser rhythmites which occur in several Dryden area rhythmite sequences approximately 400 varves below the red clay unit (Fig. 2-11) probably correspond to the formation of the Hartman moraine. *Implication:* The Hartman moraine was formed at roughly 10.4 ka (Fig. 5-4).

5) *Interpretation:* The transition of the Hartman moraine from a narrow, round-topped, unkettled morphology to a broad, flat-topped, kettled morphology at approximately 430-440 masl implies a water level of 430-440 masl at Dryden at the time of the Hartman moraine.*Implication:* The water level of Lake Agassiz at Dryden was 430-440 masl at 10.4 ka (Fig. 5-4).

6) *Interpretation:* The lower silt portions of the rhythmites in the Dryden area show a thickening and coarsening trend which culminates in the red clay rhythmites and then dies out above them (Fig. 2-11). This is presumed to represent an increase in meltwater output from the ice margin, and/or a readvance of the ice. Also, the northern limit of the red clay unit lies between the Hartman and Lac Seul moraines (Fig. 2-48). *Implication:* Formation of the Lac Seul moraine by increased meltwater output is correlative with the red clay marker unit, and is dated at 10 ka.

7) *Fact:* There are no unconformities within a sequence of approximately 400 pre-red clay, and 457 post-red clay varves at Dryden at an elevation of approximately 370 masl. *Implication:* Lake Agassiz did not fall below 370 masl at Dryden in late Moorhead or early Emerson time (10.4-9.5 ka)(Fig. 5-4). Thus,

during this time, no eastern outlet of Lake Agassiz lower than the Kaiashk outlet could have opened (Fig. 5-3).

8) *Fact::* A section identified by Elson (1967) contains 67 pre-red clay and 145 post-red clay rhythmites at Dryden at an elevation of 411 masl. *Implication:* Lake Agassiz did not fall below 411 masl at Dryden between approximately 10.06 ka and 9.85 ka (early Emerson Phase)(Fig. 5-4). Thus, the Kaiashk outlet was closed by 10.06 ka.

5.3 IMPLICATIONS FOR THE CURRENTLY ACCEPTED CHRONOLOGY OF LAKE AGASSIZ:

The facts and interpretations discussed in the previous section are at odds with the currently accepted chronology of fluctuations in the water level of Lake Agassiz, particularly with respect to the Moorhead Phase.

That the Moorhead low water Phase occurred is undeniable, given the sedimentological evidence from North Dakota, Minnesota and the Fort Frances area of Ontario. Several radiocarbon ages from these areas date this low water phase as occurring between approximately 10.9 and 9.9 ka. However, if the evidence and interpretations from the Dryden area are accepted, then the water levels (Ojata or The Pas/Gimli) which have been assigned to this low water phase are incorrect; specifically, they are too low.

If only the Shebandowan, Dog-Kaministikwia and Clearwater outlets of Lake Agassiz were available prior to 10.4 ka, the three potential early Moorhead Phase water planes produced by joining these three outlets with a level just below the Fort Frances unconformity (dated at up to 10.8 ka) and the

Moorhead Delta (dated at up to 10.9 ka), are all significantly steeper than any of the currently identified strandlines save perhaps the Herman (Fig. 5-5A). Only the water plane produced by the Shebandowan outlet satisfies the interpretation of a 440 masl water level at the Hartman moraine at 10.4 ka (Fig. 5-5A). A late (post-10.4 ka) Moorhead Phase water plane which joins the Kaiashk eastern outlet with the Moorhead Delta can be drawn, without falling below the lower limits of 370 masl at Dryden (the level of the continuous late Moorhead Phase varve sequences) or 325 masl at Fort Frances (the lowest occurrence of the unconformity)(Fig. 5-5B). This water plane is also steeper than any of the currently identified strandlines except the Herman. The highest elevations of the Emerson Phase red clay unit at both Fort Frances and Dryden, are at or above the projected Campbell strandline (Fig. 5-5C). This suggests that water rose above the Campbell level during the Emerson Phase.

An alternative hypothesis is proposed in which the Herman strandline represents the main Lockhart Phase water level and the steeper, newly added and unnamed strandlines in Figure 5-5 represent (respectively) the theoretical (now eroded or buried) early (5A) and late (5B) Moorhead phase levels. The Norcross strandline represents the later Emerson phase high level, which resulted from the advance of Marquette ice into the Superior basin. All strandlines lower than the Norcross are assigned to the later Emerson and Nipigon Phases, as proposed by Thorleifson (1983). The Lake Agassiz outlets in this model are the southern outlet during the Lockhart Phase, the Shebandowan, Dog-Kaministikwia and/or Clearwater outlets during the early

Figure 5-5 Strandline diagrams for the A) early Moorhead, B) late Moorhead, and C) Emerson Phases of Lake Agassiz. Possible water levels for the early and late Moorhead Phases as constrained by data discussed in the text, are shown. Diagram after Johnston (1946) with additional data from Zoltai (1965), Elson (1967), Arndt (1977), Teller & Thorleifson (1983), Cowan (1987) and Bajc (pers. comm., 1991).

LEGEND

- measured strandline elevations of Johnston (1946)
- strandlines of Johnston (1946)
- projected strandlines (beyond last measured elevation) of Johnston (1946)
- waterplanes constrained by data from this study
- Moorhead Delta, Fargo, ND
- Moorhead Unconformity, Fort Frances, Ont.
- 430-440 masl water level on the Hartman moraine, Dryden
- outlets of Lake Agassiz
- rhythmite elevations pertaining to Lake Agassiz water levels

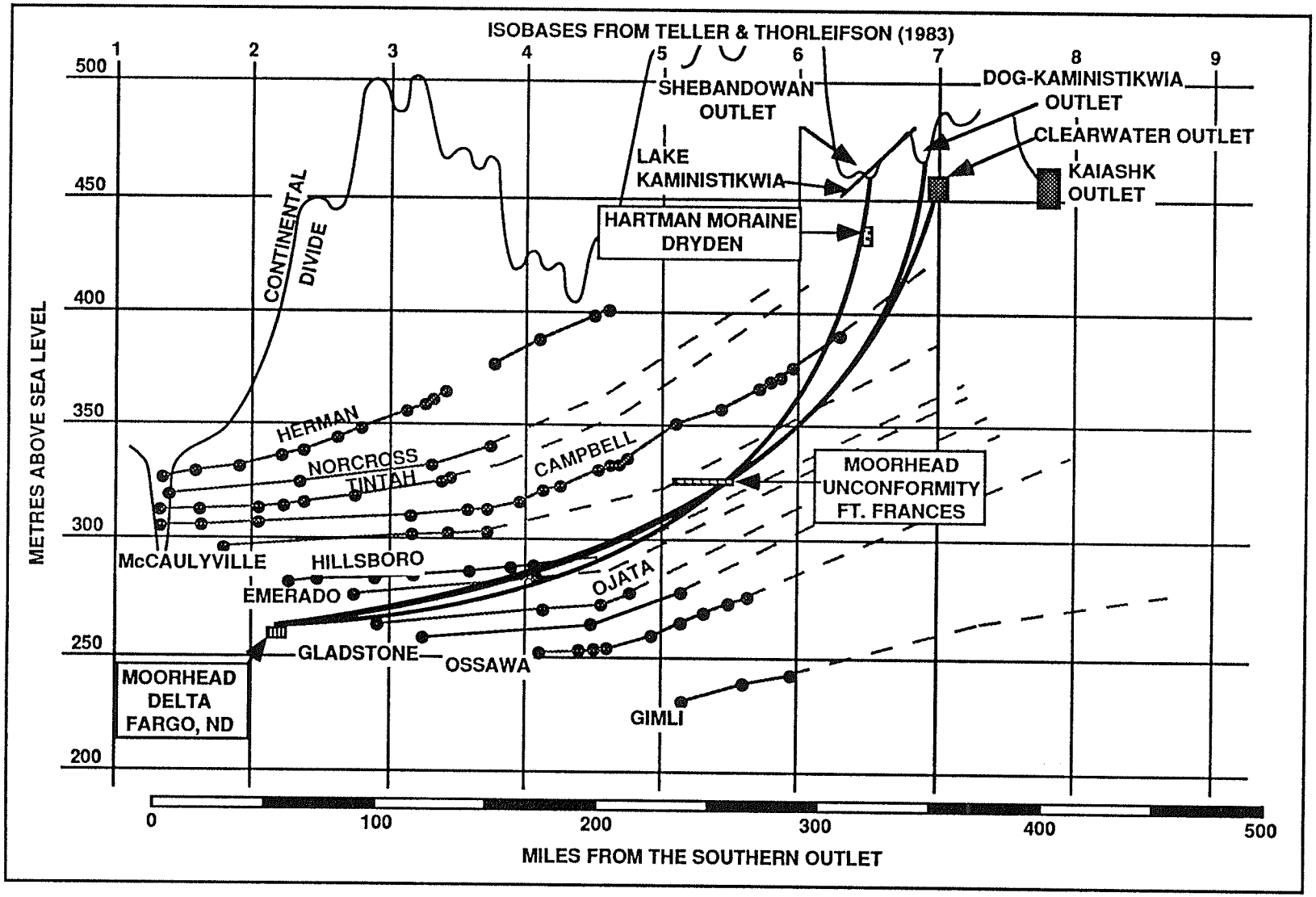

A) EARLY MOORHEAD PHASE (PRE-10.4 ka)

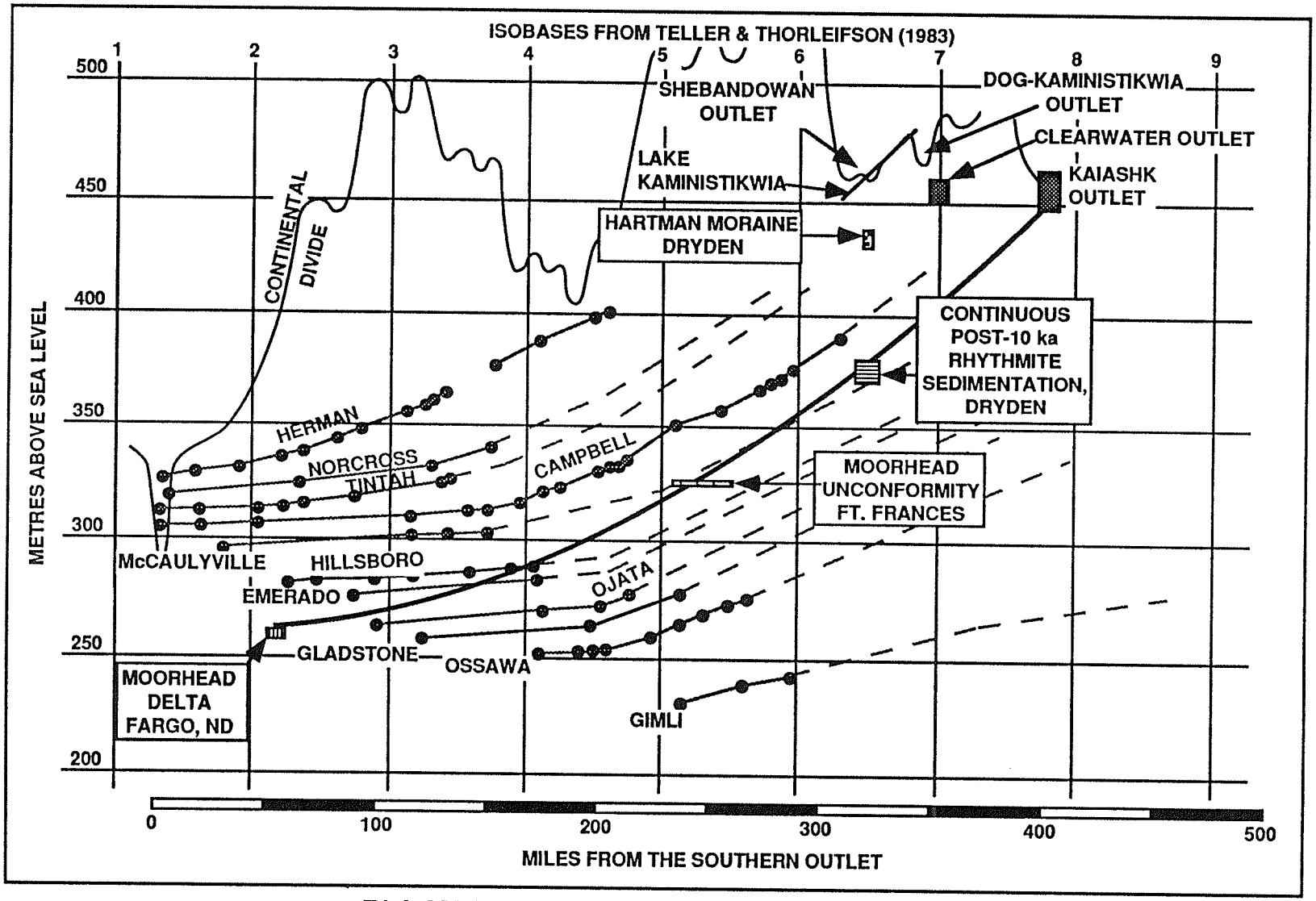

B) LATE MOORHEAD PHASE (POST-10 ka)

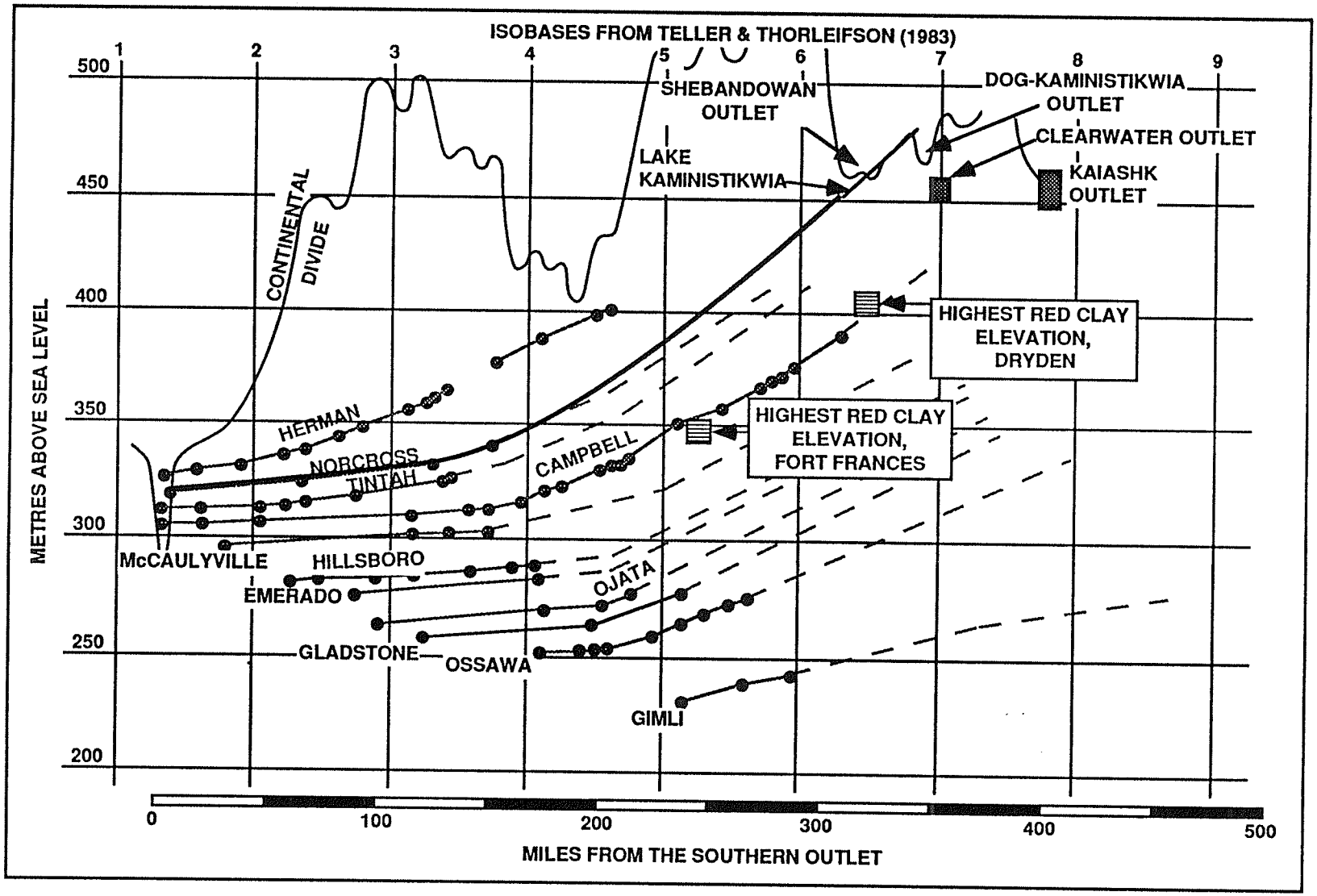

C) EMERSON PHASE (POST 10.06 ka)

Moorhead Phase and the Kaiashk outlet during the late Moorhead Phase (post-10.4 ka). Downcutting of the southern outlet during the Emerson Phase resulted in a drop from the Norcross to the Campbell levels (Fig. 5-3), and opening of the Kaiashk and lower eastern outlets initiated the Nipigon Phase and produced the sub-Campbell strandlines (Thorleifson, 1983).

This hypothesis differs in its assumptions from the currently accepted chronology of Lake Agassiz, only in that it assumes that the Dryden area was not deglaciated prior to 10.4 ka. Interpretations regarding the apparent water level at the time of formation of the Hartman moraine affect only which of the Shebandowan, Dog-Kaministikwia or Clearwater outlets were opened during the early Moorhead Phase. This alternative hypothesis resolves the apparent inconsistency between the slope of the currently identified strandlines and their assigned ages (Thorleifson, 1983), while still permitting eastward drainage of Lake Agassiz during the Moorhead Phase. However, it does not explain why the southern outlet appears to have been more rapidly eroded during the Emerson Phase than during the Lockhart Phase.

Because this alternative hypothesis is at odds with the currently accepted chronology of Lake Agassiz water levels, it clearly requires further testing before it can be accepted as more than an additional working hypothesis. However, this hypothesis does not appear to be seriously contradicted by the available evidence from the Dryden area, or from elsewhere in the Lake Agassiz Basin.

CHAPTER 6: SUMMARY OF THE DEPOSITIONAL MODEL AND INTEGRATION WITH THE LAKE AGASSIZ MODEL

6.1 SUMMARY OF THE DEPOSITIONAL MODEL:

The deglaciation of northwestern Ontario produced a series of large, arcuate end moraines and associated eskers and isolated fans (kames), composed of sorted glaciofluvial deposits. Detailed study of two of these moraines, the Hartman and Eagle-Finlayson, and of related deposits, reveals that the sediment types, their internal architecture, and sedimentary structures cannot be explained in terms of processes associated with push moraines, morainal banks, or other traditional end moraine diamict accumulations.

The moraines and isolated fans show an overall fining upwards cycle from coarse gravels in their core through pebbly sands, current-bedded sands, and coarse to fine-grained rhythmites. This fining trend occurs rapidly, both vertically and distally from the moraine cores. Paleocurrent indicators, large scale bedforms, and broad, shallow scour and fill channels provide evidence for the presence of powerful, unidirectional meltwater currents which flowed NE to SW, parallel to ice flow and away from the ice margin. Sedimentary structures and the rapid lateral fining trends indicate rapid flow expansion in these currents.

These features suggest that the moraines represent coalesced subaqueous outwash fans and minor deltas, formed at an ice margin which fronted in a large lake, during periods of enhanced meltwater and sediment

output. The vertical distribution of features such as subaerial depositional surfaces, shoreline indicators, wave ripples and clay deposits suggests lake levels of approximately 440 masl at the time of deposition of the Hartman moraine, and somewhat higher than 410 masl for the Eagle-Finlayson moraine to the south.

The eskers probably represent former meltwater tunnels which delivered water and sediment to the ice margin. These eskers were formed by a combination of sediments deposited within the tunnels, and at the mouths of the tunnels. Short-lived tunnels likely formed the isolated subaqueous fan deposits (kames).

The rhythmically-stratified sediments of Facies 1, 2 and 3 are interpreted as annual deposits or varves, produced by low-density underflows during the glacial melt season, and vertical settling of clays during the winter. The thicker and coarser rhythmites of Facies 3 may represent a more ice-proximal fan environment and/or a higher energy environment caused by increased meltwater output associated with construction of the moraines.

A distinctive band of red clays in the rhythmite sequence can be correlated both visually and geochemically with similar bands of red clay throughout northwestern Ontario. This red band forms an important stratigraphic marker bed. The source of this red clay was probably the Precambrian red beds found in the drainage basin of glacial Lake Kaministikwia, near Thunder Bay, Ontario, based on visual and geochemical similarities, and paleogeographic reconstructions. The red clay was carried into the Lake Agassiz basin when

Lake Kaministikwia and Lake Agassiz became confluent during the Emerson Phase of Lake Agassiz.

6.2 INTEGRATION OF THE DEPOSITIONAL AND LAKE AGASSIZ MODELS:

New sedimentological and stratigraphic data from Dryden and elsewhere in northwestern Ontario, as well as additional radiocarbon dates from the Fort Frances area (Bajc, 1987), have permitted a re-interpretation of the deglaciation history of northwestern Ontario.

The Fort Frances-Rainy River area was deglaciated, and the Eagle-Finlayson moraine formed, at approximately 11 ka (Fig. 6-1). This date is based on the fact that retreat from the Eagle-Finlayson moraine is required in order to open the eastern outlets at the start of the Moorhead Phase of Lake Agassiz at 10.9 ka (Chapter 5). This date agrees with the radiocarbon date on disseminated organics from Rattle Lake, located just in front of the Eagle-Finlayson moraine (Bjorck, 1985). The area south of the ice front during the formation of the Eagle-Finlayson moraine was inundated by the Lockhart phase of proglacial Lake Agassiz, which stood at the Herman level at that time (Fig. 6-1).

It does not appear that the formation of the Eagle-Finlayson moraine was related to a sudden drop in the level of Lake Agassiz and a resultant steepening of the glacial and hydrologic potentiometric surfaces. Instead, the cause of the increased meltwater output was probably internal to the ice sheet and may have

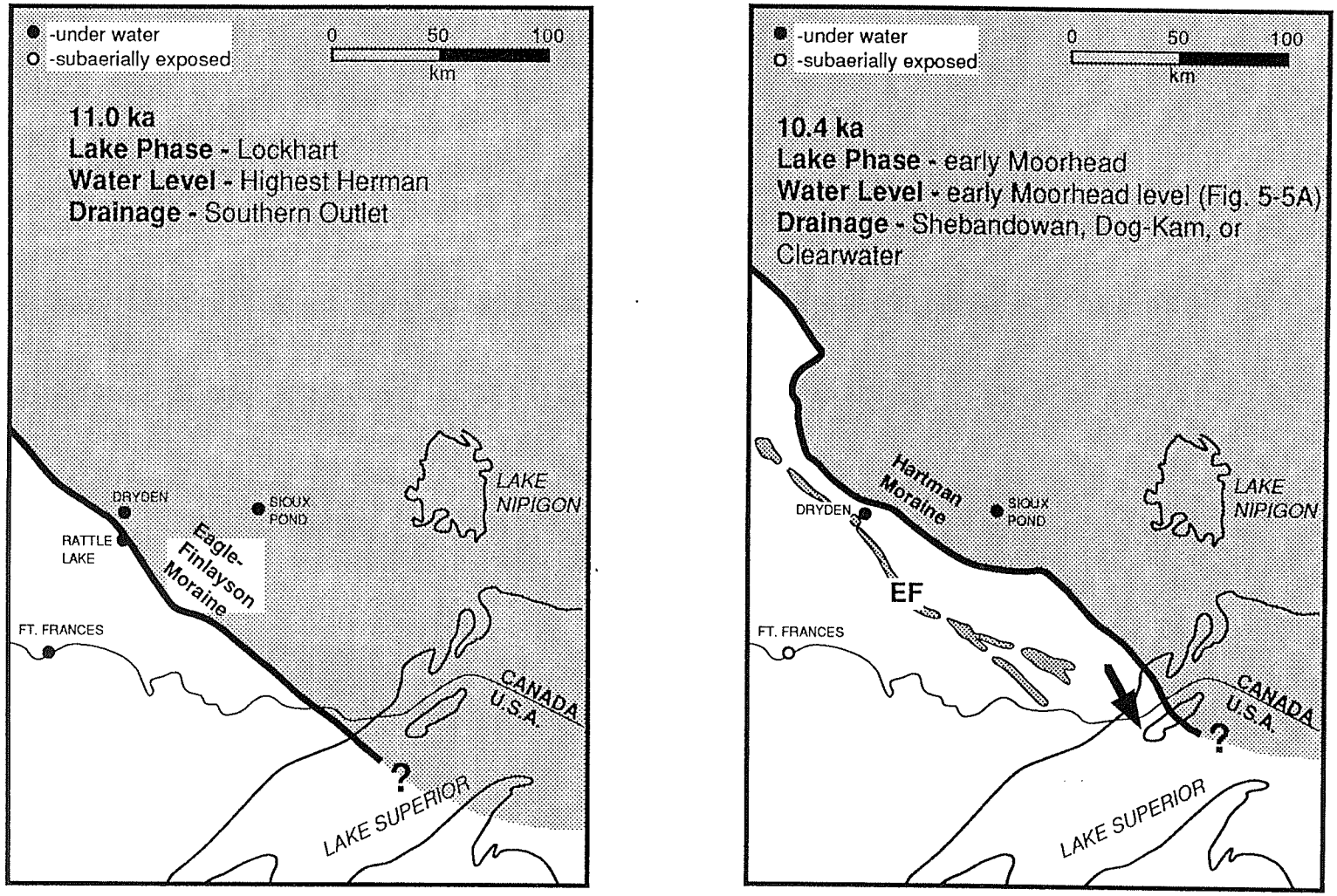

Fig. 6-1 Early deglaciation and lake level history for northwestern Ontario. Ice cover is stippled. Probable drainage arrowed. EF=Eagle-Finlayson moraine.

been related to a surging event, although no evidence for a surge or readvance was seen in the Dryden area.

Retreat of the Rainy lobe from the Eagle-Finlayson moraine, and the opening of the Shebandowan and/or Dog-Kaministikwia eastern outlets to the Superior basin (Zoltai, 1967; Teller & Thorleifson, 1983), and/or opening of the Clearwater outlet in Saskatchewan resulted in a drop in lake levels and abandonment of the southern outlet. This also resulted in exposure of the lake floor in the southern margins of the Agassiz basin (Arndt, 1977), and formation of the Moorhead Delta at Fargo, North Dakota (Arndt, 1977). The Dryden area was probably deglaciated, and the Hartman moraine began forming, by 10.4 ka (Fig. 6-1), based on the varve chronology discussed in Chapter 5. If the estimate of the time of the deglaciation of Dryden is incorrect, the Rainy Lobe may have retreated an unknown distance north (opening the Kaiashk or lower eastern outlets) by this point, and then readvanced over the Dryden area, re-zeroing the varve record. However, this is considered unlikely (Chapter 5).

As with the Eagle-Finlayson moraine, the formation of the Hartman moraine was not apparently associated with a drop in the level of Lake Agassiz, and no evidence for a surge or readvance was seen.

The Lake Manitoba basin, and the Dryden area remained under relatively deep water during the early Moorhead Phase. The early Moorhead Phase water level, which permitted subaerial exposure at Fargo and Fort Frances, while maintaining relatively deep water at Dryden and Lake Manitoba, is not represented by any of the currently recognized strandlines (Fig. 5-5A).

After approximately 10.4 ka, the Rainy Lobe may have retreated northward far enough to open the Kaiashk eastern outlet to Lake Superior (Fig. 6-2), forming the possible late Moorhead water level shown in figure 5-5B. However, by 10.06 ka (Chapter 5), the Rainy lobe had readvanced, closing the Kaiashk outlet, and forming the Lac Seul moraine (Fig. 6-2). Evidence for this readvance comes from overridden lacustrine rhythmites north of the Lac Seul moraine (Zoltai, 1961), and the fact that the Hartman moraine appears to be truncated, at least at its western end, by the Lac Seul moraine (Fig. 5-4).

Here, unlike with the Eagle-Finlayson and Hartman moraines, there is evidence for both a rapid drop in the level of Lake Agassiz and a surge or readvance related to the formation of the Lac Seul moraine.

The correlative Marquette readvance of the Superior lobe to the Dog Lake-Marks moraine position caused the formation of Lake Kaministikwia west of Thunder Bay (Zoltai, 1965), which eventually became confluent with Lake Agassiz.

Lake Agassiz rose from the late Moorhead level (Fig. 5-5B) to the Norcross level at this time due to closure of the Kaiashk, Dog-Kaministikwia and Shebandowan eastern outlets. If the Clearwater outlet had been opened during the Moorhead Phase, it too must have been closed by this time in order to allow deposition of the red clay unit in the eastern Agassiz basin. This rise in water level resulted in a transgression in the southern parts of the Lake Agassiz basin, which marked the beginning of the Emerson Phase. Lake Kaministikwia was confluent with Lake Agassiz (Fig. 6-2), and flow towards the southern outlet

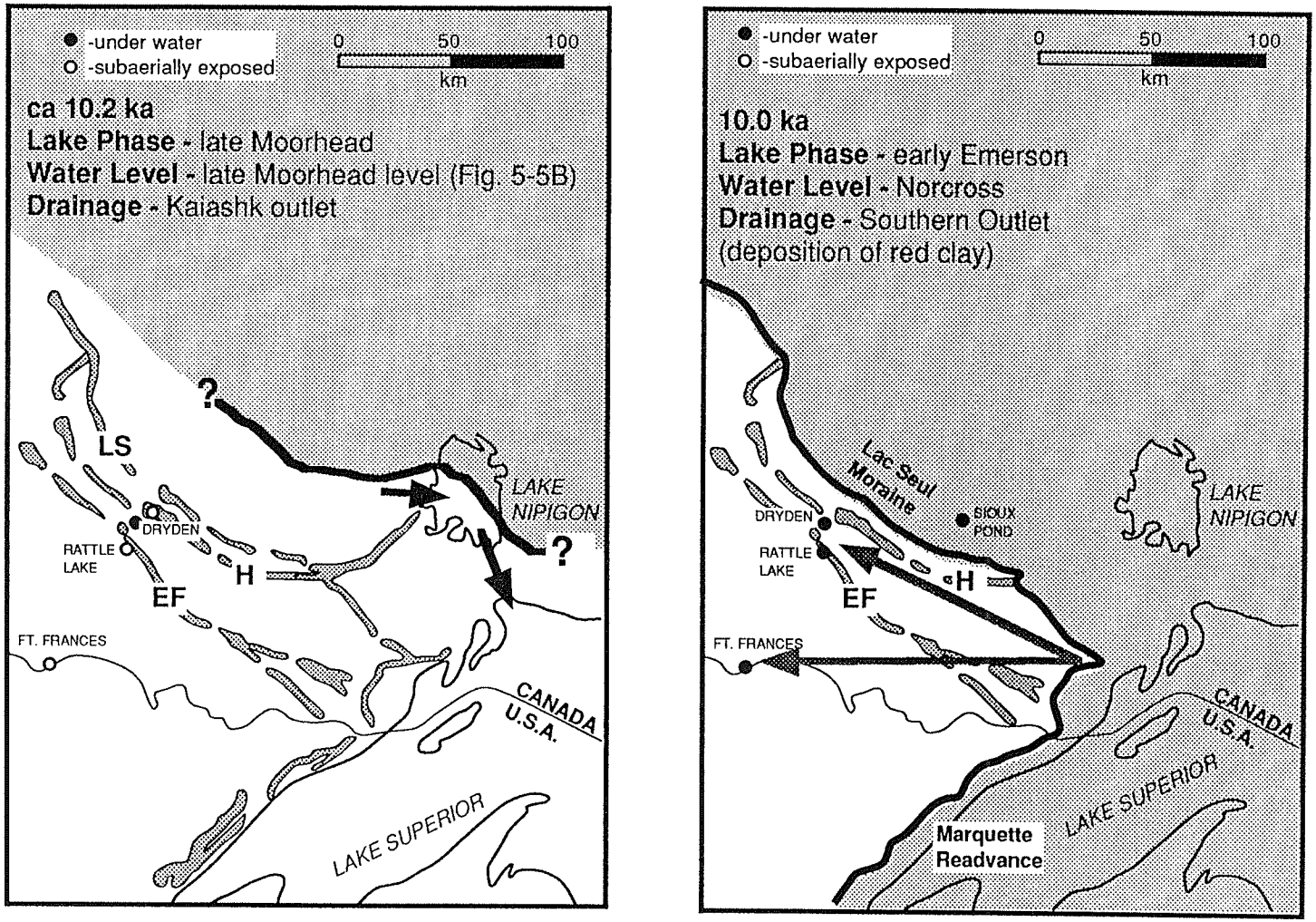

Fig. 6-2 Deglaciation and lake level history for northwestern Ontario following retreat from the Hartman moraine. Ice cover is tippled. Lake Kaministikwia influx into Lake Agassiz is shown by arrows. H=Hartman moraine, LS=Lac Seul moraine.

carried red clay throughout northwestern Ontario, resulting in deposition of the red clay marker unit.

The ice eventually retreated northward from the Lac Seul moraine and formed the Sioux Lookout moraine (Fig. 6-3) at about 9.9 ka, based on the radiocarbon date from Sioux pond, located on top of the moraine (Bjorck & Keister, 1983). Little information is available regarding this moraine forming event. Downcutting of the southern outlet eventually resulted in a drop in Lake Agassiz to the Campbell level (Thorleifson, 1983), although the varve record from the Dryden area indicates that water levels remained above the Campbell strandline until at least 9.57 ka, 430 years after deposition of the red clay ceased.

Retreat from the Sioux Lookout moraine resulted in the opening of the eastern outlets of Lake Agassiz, allowing the water levels to drop below the Campbell level. This marked the beginning of the Nipigon phase, which likely began around 9.5 ka, based on the Dryden varve record. During this time, northwestern Ontario gradually became subaerially exposed, and the sub-Campbell beaches were formed.

Overall, it does not seem possible at this time to determine the exact cause of moraine formation in northwestern Ontario. A drop in the level of Lake Agassiz does not seem to be indicated for the formation of the Eagle-Finlayson or Hartman moraines, although the Lac Seul moraine may have formed after opening of the Kaiashk outlet, an event which would have resulted in a rapid fall in lake level. No evidence was found to indicate surging or readvance to the

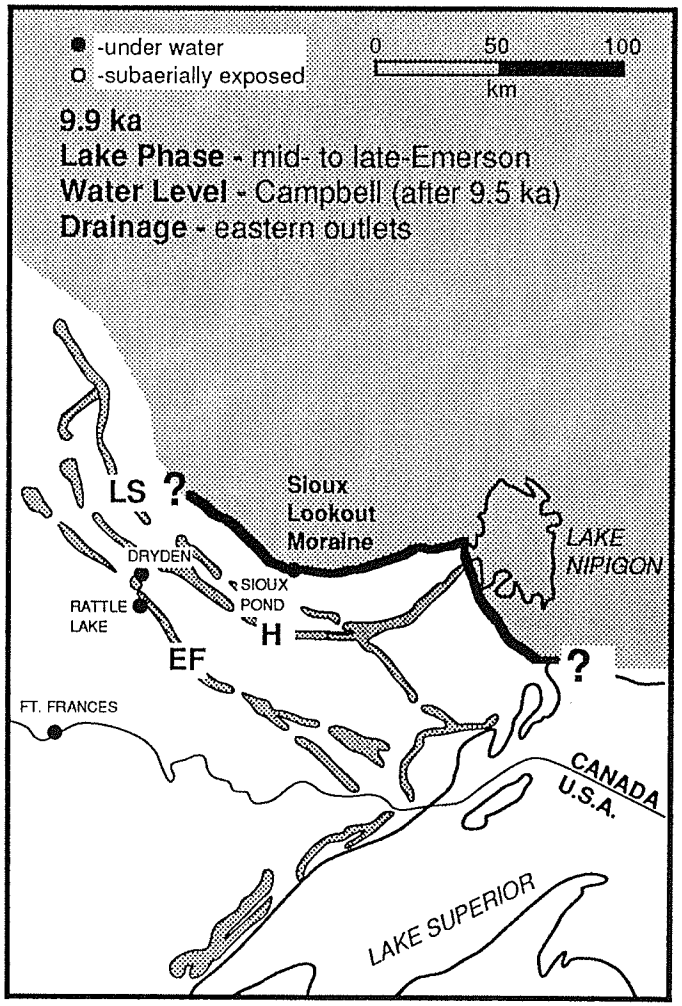

Fig. 6-3 Deglaciation and lake level history for northwestern Ontario during the later Emerson Phase of Lake Agassiz. Ice cover is stippled. H=Hartman moraine, LS=Lac Seul moraine.

Eagle-Finlayson or Hartman moraines, but Zoltai (1961) described overridden rhythmites 30 km north of the Lac Seul moraine, suggesting that surging may also have played a part in its formation.

REFERENCES CITED

Antevs, E. (1951) Glacial clay in Steep Rock Lake, Ontario, Canada; Geol. Soc. Am. Bull. 62: 1223-1262.

Arndt, B.M., (1975) Deology of Cavalier and Pembina Counties: North Dakota Geological Survey Bulletin 62 part 1,68 p.

_____ (1977) Stratigraphy of offshore sediment, Lake Agassiz - North Dakota; N. Dakota Geol. Surv. Report of Investigation 60:58 p.

Ashley, G.M. (1975) Rhythmic sedimentation in Glacial Lake Hitchcock, Massachusetts-Connecticut; in A.V. Jopling & B.C. McDonald (eds) Glaciofluvial and Glaciolacustrine Sedimentation, Soc. Econ. Pal. Min. Spec. Pub. 23:304-320.

Bajc, A.F. (1987) Quaternary Geology of the Fort Frances Area; in R.B. Barlow, M.E. Cherry, A.C. Couline, B.O. Dressler & O.L White (eds) Summary of Field Work & Other Activities 1987, Ontario Geological Survey, Misc. Paper 137:364-367

Banerjee, I. & B.C. McDonald (1975) Nature of esker sedimentation; in A.V. Jopling & B.C. McDonald (eds) Glaciofluvial and Glaciolacustrine Sedimentation, Soc. Econ. Pal. Min. Spec. Pub. 23:132-154.

Bindschadler, R. (1983) The importance of pressurized subglacial water in separation and sliding at the glacier bed; J. Glac. 29:3-19.

Biscaye, P.E. (1965) Mineralogy and sedimentation of recent deep-sea clay in the Atlantic Ocean; Geol. Soc. Am. Bull. 76:803-832.

Bjorck, S. (1985) Deglaciation chronology and revegetation in northwestern Ontario; Can. J. Earth Sci. 22:850-871.

Bjorck, S. & C.M. Keister (1983) The Emerson Phase of Lake Agassiz, independantly registered in northwestern Minnesota & northwestern Ontario: Can. J. Earth Sci. 20:1536-1542

Boothroyd, J.C. & G.M. Ashley (1975) Processes, bar morphology, and sedimentary structures on braided outwash fans, northeastern Gulf of Alaska; in A.V. Jopling & B.C. McDonald (eds) Glaciofluvial and Glaciolacustrine Sedimentation, Soc. Econ. Pal. Min. Spec. Pub. 23:304 - 320.

Boulton, G.S. (1986) Push-moraines and glacier-contact fans in marine and terrestrial environments; Sedimentology 33:677-698.

Burbidge, G.H. & B.R. Rust (1988) A Champlain Sea subwash fan at St. Lazare, Quebec; in N.R. Gadd (ed) The Late Quaternary Development of the Champlain Basin; Geol. Assoc. Can. Spec. Paper 35:47-61.

Carrol, D. (1970) Clay minerals: a guide to their x-ray identification; Geol. Soc. Am. Spec. Paper 126: 80 pp.

Carter, R.M. (1975) A discussion and classification of subaqueous mass-transport with particular application to grain-flow, slurry-flow, and fluxoturbidites; Earth Sci. Rev. 11:145-177.

Cheel, R.J. & B.R. Rust (1982) Coarse grained facies of glaciomarine deposits near Ottawa, Canada; in R. Davidson-Arnott (ed) Research in glacial, glacio-fluvial and glacio-lacustrine systems. Proc. 6th Guelph Symp. Geomorph., Geo Books, Norwich, UK:279-295.

Cherven, V.B. (1984) Early Pleistocene glacial outwash deposits in the eastern San Joaquin Valley, California: a model for humid-region alluvial fans; Sedimentology 31:823-836.

Clayton, L. (1983) Chronology of Lake Agassiz drainage to Lake Superior; in Teller, J.T. & L. Clayton (eds.) Glacial Lake Agassiz, Geol. Assoc. Can. Spec. Paper 26:291-307.

Clayton, L. & S.R. Moran (1982) Chronology of Late Wisconsonin glaciation in middle North America; Quat. Sci. Rev. 1:55 -82.

Cowan, W.R. (1987) Quaternary geology, Lake of the Woods region, northwestern Ontario, Wabigoon Lake - Gold Rock areas, Geol. Surv. Can., Open File 1697, 54pp.

_____ & D.R. Sharpe (1991) Surficial Geology Wabigoon Lake, GSC map 1774A, scale 1:100,000.

Dardis, G.F. & A.M. McCabe (1983) Facies of subglacial channel sedimentation in late-Pleistocene durmlins, Northern Ireland; Boreas 12:263-278.

Deimer, J.A. (1988) Subaqueous outwash deposits in the Ingraham ridge, Chazy, New York; Can. J. Earth Sci. 25:1384-1396.

Drever, J.I. (1973) The preparation of oriented clay mineral specimens for x-ray diffraction analysis by a filter -membrane peel technique; Amer. Mineral. 58:553-554.

Drexler, C.W., W.R. Farrand & J.D. Hughes (1983) Correlation of glacial lakes in the Superior basin with eastward discharge events from Lake Agassiz; in Teller, J.T. & L. Clayton (eds.) Glacial Lake Agassiz, Geol. Assoc. Can. Spec. Paper 26:309-329.

Duck, R.W. & J. McManus (1987) Chironomid larvae trails in proglacial lake sediments: comments; Boreas 16:322.

_____ (1984) Traces produced by chironomid larvae in sediments of an ice-contact proglacial lake; Boreas 13:89-93.

Elson, J.A. (1967) The geology of Lake Agassiz; in W.J. Mayer -Oakes (ed) Life, Land and Water, University of Manitoba Press:414 p.

Eyles, C.H. & N. Eyles (1983) Sedimentation in a large lake: a reinterpretation of the late Pleistocene stratigraphy of the Scarborough Bluffs, Ontario, Canada; Geology 11:146-152.

_____ (1984) Glaciomarine sediments of the Isle of Man as a key to late Pleistocene stratigraphic investigations in the Irish Sea Basin; Geology 12:359 -364.

Eyles, N. & A.D. Miall (1984) Glacial Facies, in R.G. Walker (ed) Facies Models, Geosci. Can. Rep. Ser. 1:15-37.

_____ & A.M. McCabe (1989) Glaciomarine facies within subglacial tunnel valleys: the sedimentary record of glacio-isostatic downwarping in the Irish Sea Basin; Sedimentology 36:431-448.

Farquharson, G.W., R.D. Hamer, & J.R. Inerson (1984) Proximal volcaniclastic sedimentation in a Cretaceous back-arc basin, northern Antarctic Peninsula, in B.P. Kokelaar & M.F. Howells (eds) Marginal Basin Geology; Volcanic and associated sedimentary and tectonic processes in modern and ancient marginal basins, The Geological Society Special Publication 16:219-232.

Fenton, M.M., S.R. Moran, J.T. Teller & L. Clayton (1983) Quaternary stratigraphy and history in the southern part of the Lake Agassiz basin; in Teller, J.T. & L. Clayton (eds.) Glacial Lake Agassiz, Geol. Assoc. Can. Spec. Paper 26:49-74.

Fisher, R.V. (1984) Submarine volcaniclastic rocks, in B.P. Kokelaar & M.F. Howells (eds) Marginal Basin Geology; Volcanic and associated sedimentary and tectonic processes in modern and ancient marginal basins, The Geological Society Special Publication 16:5-28.

_____ (1982) Debris flows and lahars, in Pyroclastic volcanism and deposits of Cenozoic intermediate to felsic volcanic islands with implications for Precambrian greenstone-belt volcanoes, L.D. Ayres (ed) Geol. Assoc. Can. Short Course 2:136-220.

Folk, R.L. (1980) Petrology of Sedimentary Rocks; Hemphill Pub. Co., Austin, Texas.

Franklin, J.M., W.H. McIlwaine, K.H. Poulsen & R.K. Wanless (1980) Stratigraphy and depositional setting of the Sibley Group, Thunder Bay District, Ontario, Canada; Can. J. Earth Sci. 17:633-651.

Fraser, G.S. & J.C. Cobb (1982) Late Wisconsinan proglacial sedimentation along the West Chicago Moraine in northereastern Illinois; J. Sed. Pet. 52:473-491.

Fyfe, G.J. (1990) The effect of water depth on ice-proximal glaciolacustrine sedimentation: Salpausselka I, southern Finland: Boreas 19:147-164.

Gagne, R.M., S.E. Pullan & J.A. Hunter (1985) A shallow seismic reflection method for use in mapping overburden stratigraphy, in Proceedings of Second International Conference on Bore- Hole and Surface Geophysical Methods and Groundwater Evaluation.

Gustavson, T.C. (1975) Sedimentation and physical limnology in proglacial Malaspina Lake, southeastern Alaska; in A.V. Jopling & B.C. McDonald (eds) Glaciofluvial and Glaciolacustrine Sedimentation, Soc. Econ. Pal. Min. Spec. Pub. 23:249-263.

_____, G.M Ashley & J.C. Boothroyd (1975) Depositional sequences in glaciolacustrine deltas; in A.V. Jopling & B.C. McDonald (eds) Glaciofluvial and Glaciolacustrine Sedimentation, Soc. Econ. Pal. Min. Spec. Pub. 23:264-280.

_____, & J.C. Boothroyd (1987) A depositional model for outwash, sediment sources, and hydrologic characteristics, Malaspina Glacier, Alaska: A modern analog of the southeastern margin of the Laurentide Ice Sheet; Geol. Soc. Amer. Bull. 99:187-200.

Harms, J.C., J.B. Southard & R.G. Walker (1982) Structures and sequences in clastic rocks; Soc. Econ. Pal. Min. Short Course 9.

Harris, K.L., S.R. Moran & L. Clayton (1974) Late Quaternary stratigraphic nomenclature, Red River Valley, North Dakota and Minnesota; N. Dakota Geol. Surv. Misc. Ser. 52:47 p.

Hebrand, M. & M. Åmark (1989) Esker formation and glacier dynamics in eastern Skåne and adjacent areas, southern Sweden: Boreas 18: 67-81.

Hein, F.J. (1982) Depositional mechanisms of deep-sea coarse clastic sediments, Cap Enrage Formation, Quebec; Can. J. Earth Sci. 19:267-287.

Henderson, P.J. (1988) Sedimentation in an esker system influenced by bedrock topography near Kingston, Ontario; Can. J. Earth Sci. 25:987-999.

Hillaire-Marcel, C., S. Occhietti & J-S. Vincent (1981) Sakami moraine, Quebec: A 500-km-long moraine without climatic control; Geology 9:210-214.

Johnston, W.A. (1915) Rainy River District, Ontario. Surficial Geology and Soils; Geol. Surv. Can. Mem. 82.

_____ (1946) Glacial Lake Agassiz with special reference to the mode of deformation of the beaches; Geol. Surv. Can. Bull. 7:20.

Jopling, A.V. & R.G. Walker (1968) Morphology and origin of ripple-drift cross-lamination, with examples from the Pleistocene of Massachusetts; J. Sed. Pet. 38:971-984.

Josenhans, H.W. & G.B.J. Fader (1989) A comparison of models of glacial sedimentations along the eastern Canadian margin: Mar. Geol. 85:273-300

Kamb, B. (1987) Glacier surge mechanism based on linked cavity configuration of the basal water conduit system; J. Geophys. Res. 92:9083-9100.

_____, C.F. Raymond, W.D. Horrison, H. Engelhardt, K.A. Echelmeyer, N. Humphrey, M.M. Brugman & T. Pfeffer (1985) Glacier surge mechanism: 1982-1983 surge of Variegated Glacier, Alaska; Science 227:469-479.

Kaszycki, C.A. (1987) A model for glacial and proglacial sedimentation in the shield terrane of southern Ontario; Can. J. Earth Sci. 24:2373-2391.

Keele, J. (1924) Preliminary report on the clay and shale deposits of Ontario; Geol. Surv. Can. Mem. 142:125-129.

Kuenen, P.H. (1951) Mechanics of varve formation and the action of turbidity currents; Geol. Foren. Forhandl. Bd. 73:69-84.

Lambert, A. & K.J. Hsu (1979) Non-annual cycles of varve-like sedimentation in Walensee, Switzerland; Sedimentology 26:453-461.

Larocque, A.C.L. (1987) Subbottom acoustic profiling of Lake Dore, Ontario: Implications for sedimentation; unpub. B.Sc. thesis, Carleton University, Ottawa.

Lemoine, R.M.J. (1989) Late glacial history, paleoecology and sedimentation in the Nipigon basin, Ontario; unpub. MSc thesis, University of Manitoba.

Lowe, D.R. (1982) Sediment gravity flows:II. Depositional models with special reference to the deposits of high -density turbidity currents; J. Sed. Pet. 52:279-297.

McCabe, A.M., G.F. Dardis & P.M. Hanvey (1984) Sedimentology of a late Plesitocene submarine-moraine complex, County Down, Northern Ireland; J. Sed. Pet. 54:716-730.

_____ (1987) Sedimentation at the margins of a late Pleistocene ice-lobe terminating in shallow marine environments, Dundalk Bay, eastern Ireland; Sedimentology 34:473-493.

_____ & N. Eyles (1988) Sedimentology of an ice-contact glaciomarine delta, Carey Valley, Northern Ireland; Sed. Geol. 59:1-14.

McDonald, B.C. & W.W. Shilts (1975) Interpretation of faults in glaciofluvial sediments; in A.V. Jopling & B.C. McDonald (eds) Glaciofluvial and Glaciolacustrine Sedimentation, Soc. Econ. Pal. Min. Spec. Pub. 23:123-131.

McLennan, S.M. (1989) Rare earth elements in sedimentary rocks: influence of provenance and sedimentary processes; in B.R. Lipin & G.A. McKay (eds.) Geochemistry and mineralogy of rare earth elements; The Min. Soc. of Am. Reviews in Min. 21:169-200.

Miall, A.D. (1984) Deltas; in R.G. Walker (ed) Facies Models, Geoscience Canada Reprint Series 1:105-118.

Middleton, G.E. & J.B. Southard (1984) Mechanics of sediment movement; Soc. Econ. Pal. Min. Short Course 3.

Minning, G.V. & D.R. Sharpe (1991) Surficial Geology Blue Lake; GSC Map 1772A, 1:100,000 scale.

Mooers, H.D. (1989) On the formation of the tunnel valleys of the Superior Lobe, Central Minnesota; Quat. Res. 32:24 -35.

Moorhouse, W.W. (1941) Geology of Eagle Lake area; Ont. Dept. Mines vol. 48 pt. IV.

Morrison, A. (1987) Chironomid larvae trails in proglacial lake sediments; Boreas 16:318-321.

Muller, G. (1967) Methods in Sedimentary Petrology, Hafner Press, New York: 283 pp.

Mustard, P.S. & J.A. Donaldson (1987) Early Proterozoic ice -proximal glaciomarine deposition: the lower Gowganda Formation at Cobalt, Ontario, Canada; Geol. Soc. Am. Bull. 98:373-387.

Nambudiri, E.M.V., J.T. Teller & W.M. Last (1980) Pre -Quaternary microfossils - a guide to errors in radiocarbon dating; Geology 8:123-126.

Nemec, W. & R.J. Steel (1984) Alluvial and coastal conglomerates: Their significant features and some comments on gravelly mass-flow deposits, in E.H. Koster & R.J. Steel (eds) Sedimentology of Gravels and Conglomerates, Can. Soc. Petrol. Geol. Memoir 10:237-258.

Nielsen, E., W.B. McKillop & J.P. McCoy (1982) The age of the Hartman moraine and the Campbell beach of Lake Agassiz in northwestern Ontario; Can. J. Earth Sci. 19:1933-1937.

Oldale, R.N. & C.J. O'Hara (1984) Glaciotectonic origin of the Massachusetts coastal end moraines and a fluctuating late Wisconsinan ice margin; Geol. Soc. Amer. Bull. 95:61-74.

Pantin, H.M. & M.R. Leeder (1987) Reverse flow in turbidity currents: the role of internal solitons; Sedimentology 34:1143-1155.

Pfirman, S.L. & A. Solheim (1989) Subglacial meltwater discharge in the open-marine tidewater glacier environment: Observations from Nordaustlandet, Svalbard Archipelago; Mar. Geol. 86:265-281.

Pickering, K.T. & R.N. Hiscott (1985) Contained (reflected) turbidity curents from the Middle Ordovician Cloridorme Formation, Quebec, Canada: an alternative to the antidune hypothesis; Sedimentology 32:373-394.

Postma, G. (1990) An analysis of the variation in delta architecture; Terra Nova 2:124-130.

Powell, R.D. & B.F. Molnia (1989) Glaciomarine sedimentary processes, facies and morphology of the south-southeast Alaska shelf and fjords; Mar. Geol. 85:359-390.

Raymond, C.F. (1987) How do glaciers surge? A review; J. Geophys. Res. 92:9121-9134.

Rittenhouse, G. (1933) A study of varve clays of northwestern Ontario; (unpub.) PhD thesis, University of Chicago.

_____ (1934) A laboratory study of an unusual series of varved clays from northern Ontario; Am. J. Sci. 28:110-120.

Rust, B.R. (1989) Ice-proximal deposits of the Champlain Sea at South Gloucester, near Ottawa, Canada; in N.R. Gadd (ed) The Late Quaternary Development of the Champlain Sea Basin; Geol. Assoc. Can. Spec. Paper 35:37-45.

_____ (1977) Mass flow deposits in a Quaternary succession near Ottawa, Canada: diagnostic criteria for subaqueous outwash; Can. J. Earth Sci. 14:175-184.

_____ & E.H. Koster (1984) Coarse alluvial deposits, in R.G. Walker (ed) Facies Models, Geoscience Canada Reprint Series 1:53-69.

_____ & R. Romanelli (1975) Late Quaternary subaqueous outwash deposits near Ottawa, Canada; in A.V. Jopling & B.C. McDonald (eds) Glaciofluvial and Glaciolacustrine Sedimentation, Soc. Econ. Pal. Min. Spec. Pub. 23:177-191.

Ruszczynska-Szenajch, H. (1982) Depositional processes of Pleistocene lowland end moraines, and their possible relation to climatic conditions; Boreas 11:249-260.

Saarnisto, M. (1974) The deglaciation history of the Lake Superior region and its climatic implications; Quat. Res. 4:316-339.

Sado, E.V. & B.F. Carswell (1987) Surficial geology of northern Ontario; Ont. Geol. Surv. Map 2518.

Satterley, J. (1960) Geology of the Dyment area; Ont. Dept. Mines vol. 69 pt. VI.

_____ (1946) Geology of the Dryden - Wabigoon area; Ont. Dept. Mines vol. 50 pt. II.

Saunderson, H.C. (1977) The sliding bed facies in esker sands and gravels: a criterion for full-pipe (tunnel) flow?; Sedimentology 24:623-638.

_____ (1975) Sedimentology of the Brampton esker and its associated deposits; an empirical test of theory; in A.V. Jopling & B.C. McDonald (eds) Glaciofluvial and Glaciolacustrine Sedimentation, Soc. Econ. Pal. Min. Spec. Pub. 23:155-176.

Sharpe, D.R. (1988) Glaciomarine fan deposition in the Champlain Sea; in N.R. Gadd (ed) The Late Quaternary Development of the Champlain Sea Basin; Geol. Assoc. Can. Spec. Paper 35:63-82.

_____ & W.R. Cowan (1990) Moraine formation in northwestern Ontario: product of subglacial fluvial and glaciolacustrine sedimentation; Can. J. Earth Sci. 27:1478- 1486.

Shaw, J. (1983) Drumlin formation related to inverted erosion marks; J. Glac. 29:461-479.

_____ (1985) Subglacial and ice marginal environments; in G.M. Ashley, J. Shaw & N.D. Smith (eds) Glacial Sedimentary Environments; Soc. Econ. Pal. Min. Short Course 16:7-84.

_____ & D. Kvill (1984) A glaciofluvial origin for drumlins of the Livingstone Lake area, Saskatchewan; Can. J. Earth Sci. 21:1442-1459.

_____ (1975) Sedimentary successions in Pleistocene ice marginal lakes; in A.V. Jopling & B.C. McDonald (eds) Glaciofluvial and Glaciolacustrine Sedimentation, Soc. Econ. Pal. Min. Spec. Pub. 23:281-303.

Smith, N.D. & G. Ashley (1985) Proglacial lacustrine environment, in G. Ashley, J. Shaw & N.D. Smith (eds) Glacial Sedimentary Environments, SEPM short course 16:135-207.

_____ (1985) Proglacial fluvial environment, in G. Ashley, J. Shaw & N.D. Smith (eds) Glacial Sedimentary Environments, SEPM short course 16:85-134.

_____ & J.P.M. Syvitski (1982) Sedimentation in a glacier-fed lake: the role of pelletization on deposition of fine-grained suspensates; J. Sed. Pet. 52:503-513.

Tanner, C.B. & M.L. Jackson (1947) Soil Sci. Soc. Amer. Proc., vol. 12:60-65.

Teller, J.T. (1976) Lake Agassiz deposits in the main offshore basin of southern Manitoba; Can. J. Earth Sci. 13:27-43.

_____ & P. Mahnic (1988) History of sedimentation in the northwestern Lake Superior basin and its relation to Lake Agassiz overflow; Can. J. Earth Sci. 25:1660-1673.

_____ & L.H. Thorleifson (1983) The Lake Agassiz - Lake Superior connection; in Teller, J.T. & L. Clayton (eds.) Glacial Lake Agassiz, Geol. Assoc. Can. Spec. Paper 26:261-290.

_____ & W.M. Last (1981) Late Quaternary history of Lake Manitoba, Canada; Quat. Res. 16:97-116.

Thomas, G.S.P. (1984a) The origin of the glacio-dynamic structure of the Bride Moraine, Isle of Man; Boreas 13:355-364.

_____ (1984b) Sedimentation of a sub-aqueous esker -delta at Strabathie, Aberdeenshire; Scott. J. Geol. 20:9-20.

Thorez, J. (1975) Phyllosilicates and clay minerals: A laboratory handbook for their x-ray diffraction analysis, Editions G. Lellote, Dison, Belgium: 579 pp.

Thorleifson, L.H. (1983) The eastern outlets of Lake Agassiz; unpub. MSc thesis, University of Manitoba.

Visser, J.N.J., J.C. Loock, & W.P. Colliston (1987) Subaqueous outwash fan and esker sandstones in the Permo -Carboniferous Dwyka Formation of South Africa; Journal of Sed. Pet. 57:467-478.

Walker, R.G. (1984) Shelf and shallow marine sands, in R.G. Walker (ed) Facies Models; Geosci. Can. Rep. Ser. 1:141-170.

_____ (1984) Turbidites and associated coarse clastic deposits, in R.G. Walker (ed) Facies Models; Geosci. Can. Rep. Ser. 1:171-188.

Wright, H.E. Jr. (1973) Tunnel valleys, glacial surges, and subglacial hydrology of the Superior Lobe, Minnesota; in R.F. Black, R.P. Goldthwait & H.B. Willman (eds) The Wisconsinan Stage, Geol. Soc. Amer. Memoir 136:251-276.

Zoltai, S.C. (1967) Eastern outlets of Lake Agassiz; in W.J. Mayer- Oakes (ed) Life, Land and Water, University of Manitoba Press:414 p.

_____ (1965) Glacial features of the Quetico - Nipigon area, Ontario; Can. J. Earth Sci. 2:247-269.

_____ (1963) Glacial features of the Canadian Lakehead area; Can. Geographer 7:101-115.

_____ (1961) Glacial history of part of northwestern Ontario; Proc. Geol. Assoc. Can. 13:61-83.

APPENDIX A

ANNOTATED GRAPHIC LOGS FOR ALL SECTIONS AND ROTASONIC BOREHOLES IN THE STUDY AREA.
SEE FIGURES 1-4 & 2-1 FOR LOCATIONS.

SECTIONS 87-1, 87-4, 87-5, 87-7, 87-12, 87-13, 87-14, 87-15, 87-16, 87-18, 87-19, AND 87-26 CONSIST ENTIRELY OF FACIES 1 SILT-CLAY RHYTHMITES, AND ARE IDENTICAL IN ALMOST ALL RESPECTS. AS SUCH, THEY ARE DESCRIBED HERE TOGETHER IN ORDER TO AVOID REPETITION. THE GRAPHIC LOGS ARE PRESENTED ON THE FOLLOWING PAGES. FOR A MORE DETAILED DESCRIPTION AND OVERVIEW OF THIS FACIES SEE CHAPTER 2.

DESCRIPTION: Silt-clay rhythmites, 0.5-5.0 cm thick, rarely up to 10 cm thick, red-clay rhythmites often present, anywhere from 8-20 red rhythmites.

LEGEND

(Note dual symbols for some lithologies)

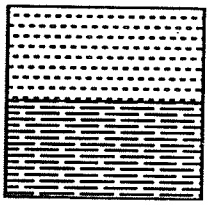

SILT-CLAY RHYTHMITES

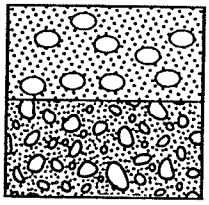

GRAVEL

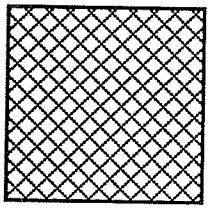

RED-CLAY RHYTHMITES

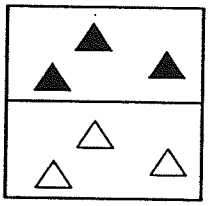

DIAMICT

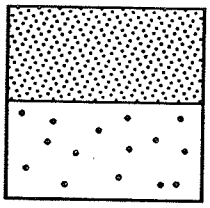

SAND/SILT

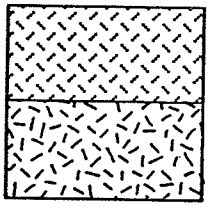

BEDROCK

CLAY BALLS

RIPPLES

TROUGH CROSSBEDS

PLANAR TABULAR CROSSBEDS

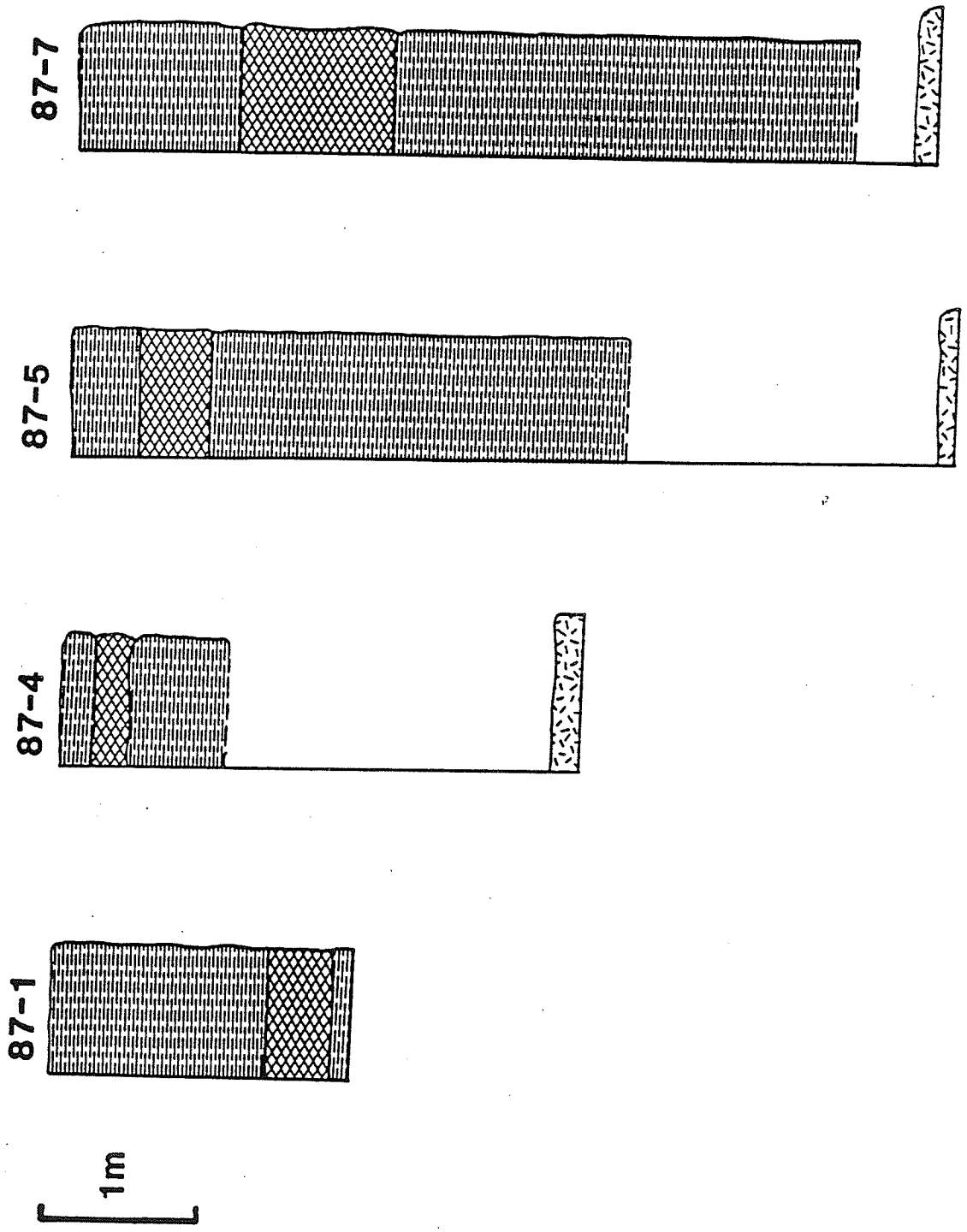
87-7
87-5
87-4
87-1
1m

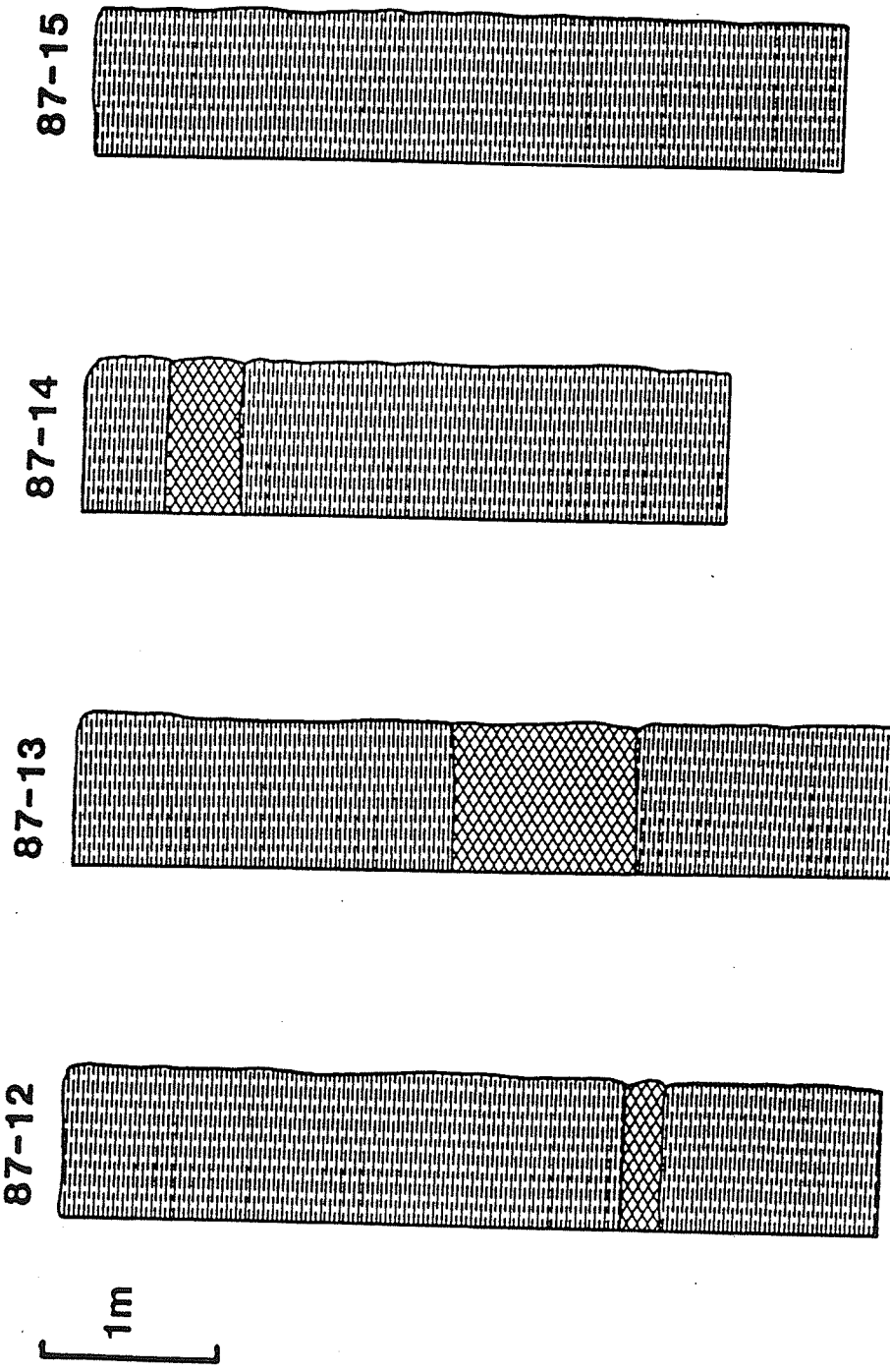
87-15
87-14
87-13
87-12
1m

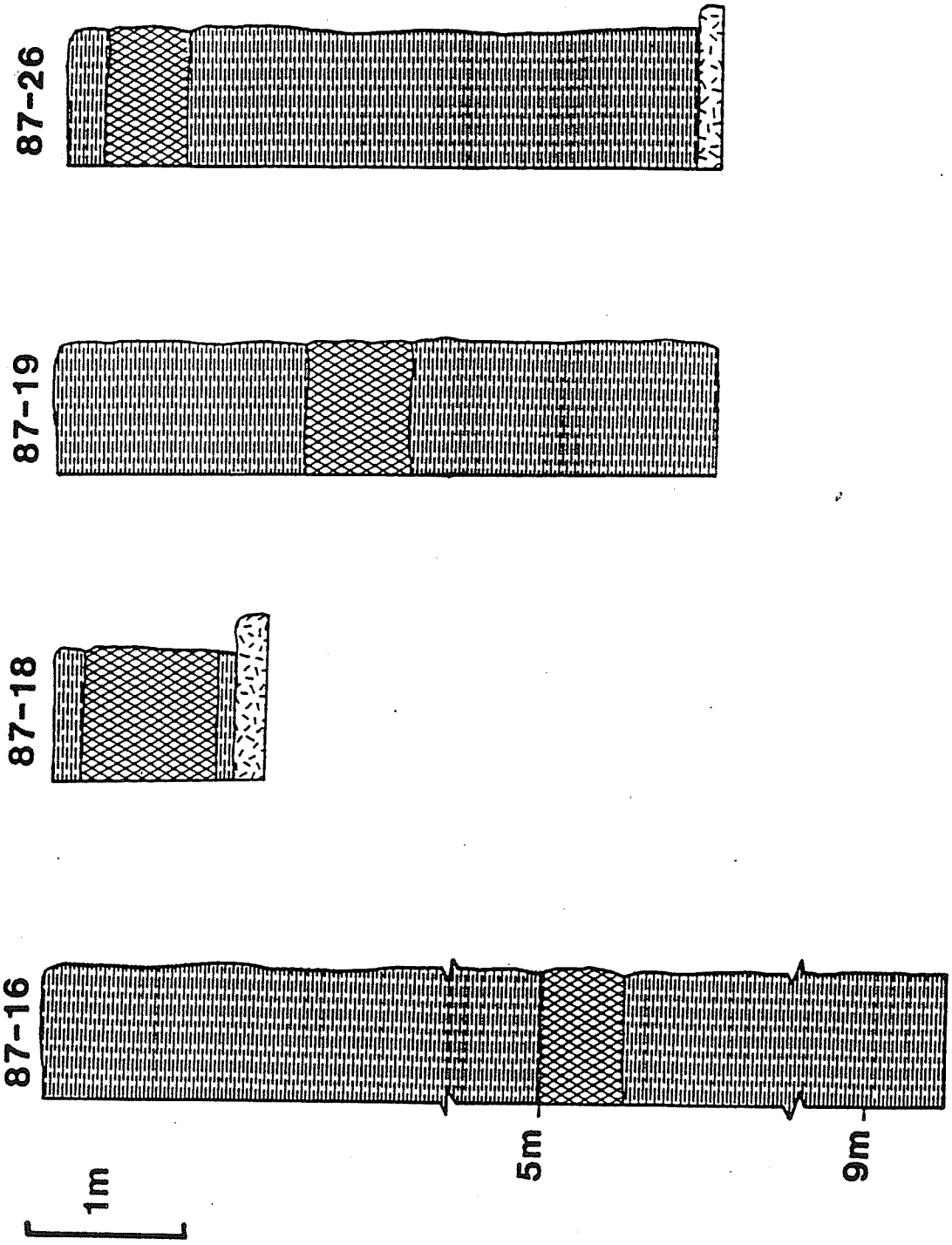
87-26
87-19
87-18
87-16
1m
5m
9m

87-8

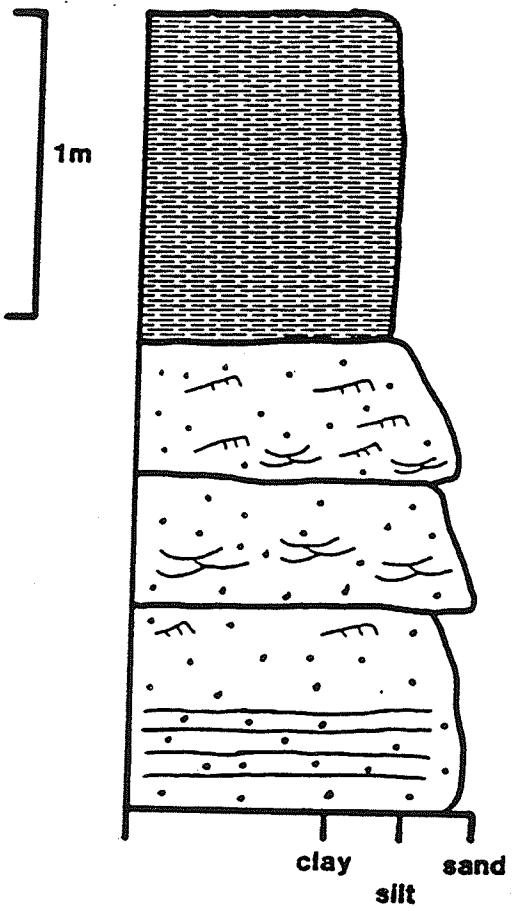

0.00-1.00m	silt-clay rhythmites, red rhythmite unit not present
1.00-1.54m	m. to f. sand with climbing ripples, horizontal laminations and minor trough crossbeds near base, thin (0.5-1.0 cm) clay laminae are present
1.54-1.92m	fining upward from well sorted m. sand to v.f. sand, abundant trough crossbeds, paleoflow 265
1.92-2.48	well sorted m. sand, horizontally laminated with ripples near top

87-9

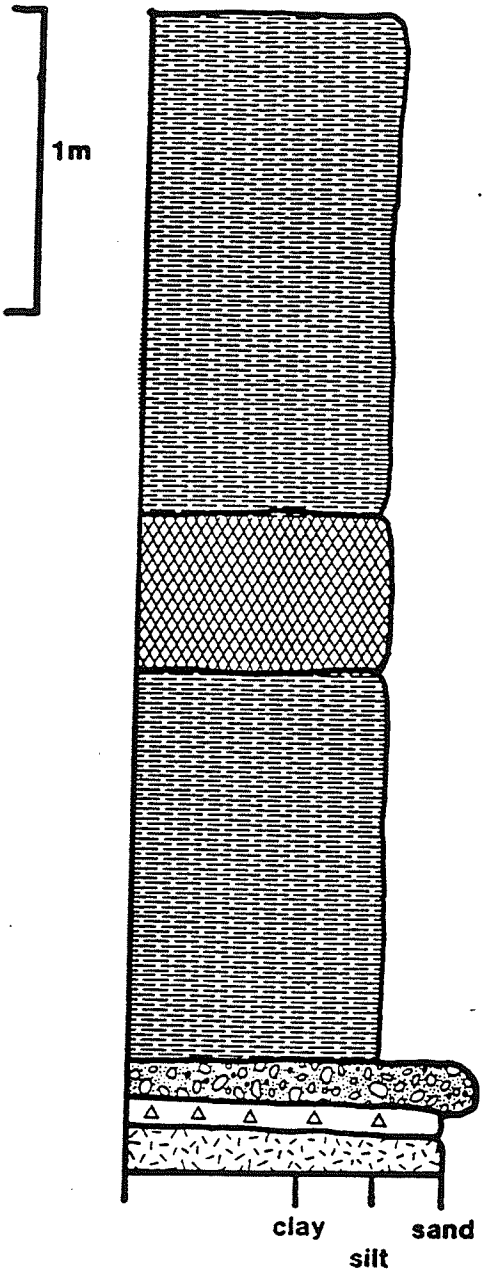

0.00-3.40m	silt-clay rhythmites, red rhythmites from 1.6 to 2.1m
3.40-3.50m	poorly sorted pebble gravel
3.50-3.60m	very hard, cemented pebbly massive diamict over bedrock striated 219

87-10

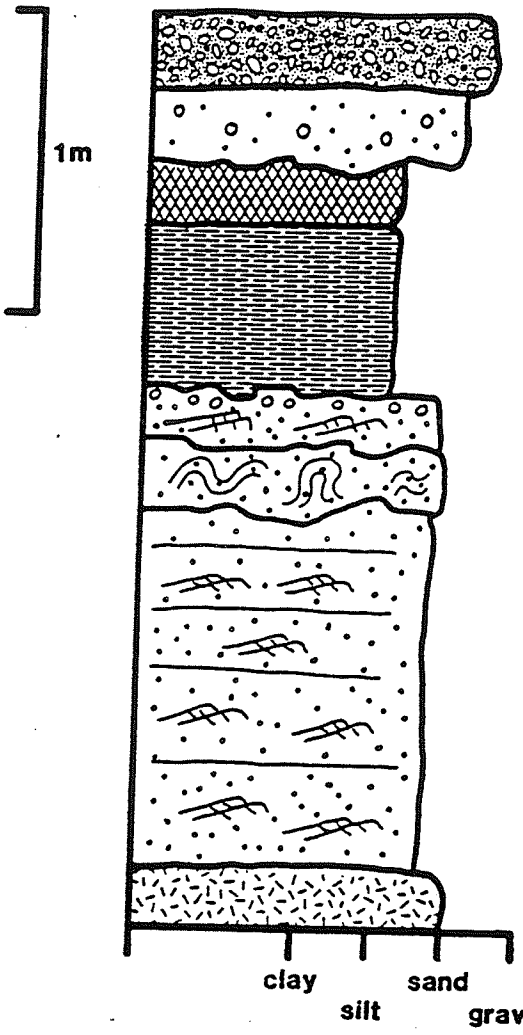

0.00-0.17m	clast-supported sandy pebble and cobble gravel, clasts subrounded
0.17-0.45m	fining upwards from c. sand with granules and small pebbles, to m. sand
0.45-1.16m	silt-clay rhythmites showing some disturbance and internal erosion surfaces, red rhythmites from 0.66 to 1.16m
1.16-1.40m	horizontally stratified to climbing rippled f. to v.f. sand
1.40-1.99m	v. disturbed f. to v.f. sand, containing occasional granules and distorted clay laminae
1.99-3.09m	well sorted m. to c. sand, planar tabular crossbedded, paleoflows 85, 88, 108, 132

87-17

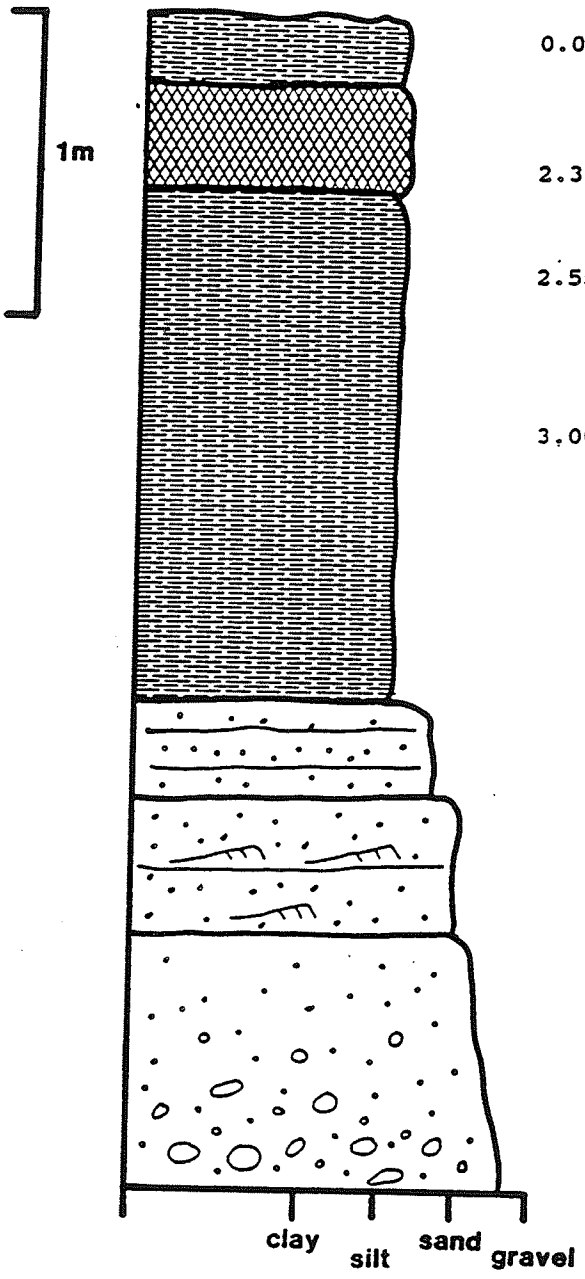

0.00-2.30m	silt-clay rhythmites, red rhythmites from 0.23 to 0.59m
2.30-2.55m	horizontally stratified f. to m. sand
2.55-3.00m	horizontally stratified and climbing rippled f. to c. sand, paleoflow 272
3.00-3.80m	fining upward from pebble and cobble gravel, to v.c. to c. massive sand

87-20

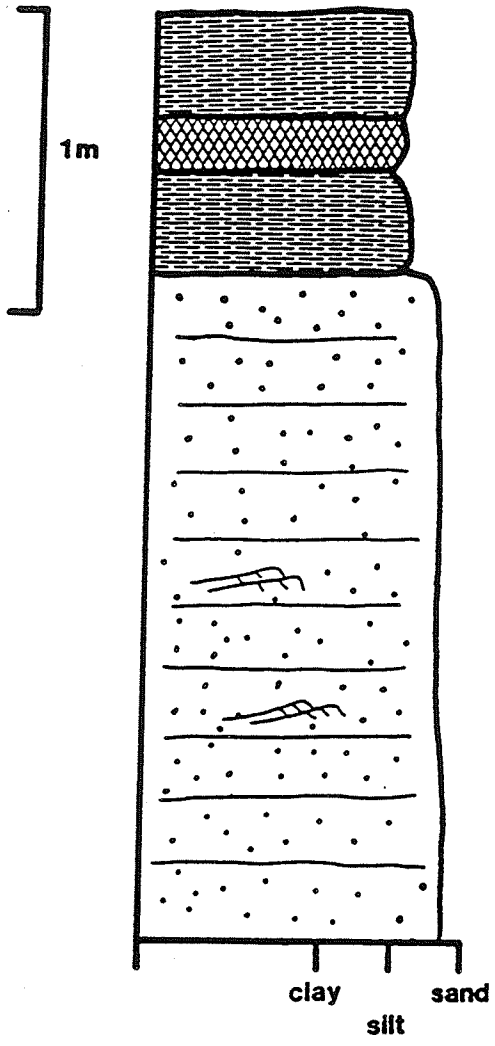

0.00-0.86m	silt-clay rhythmites, red rhythmites from 0.35 to 0.53m
0.86-3.00m	sandy rhythmites consisting of horizontally laminated to climbing rippled c. silt to f. sand (2.0 to 11.0 cm) with a 0.1 to 0.5 cm clay cap

87-21

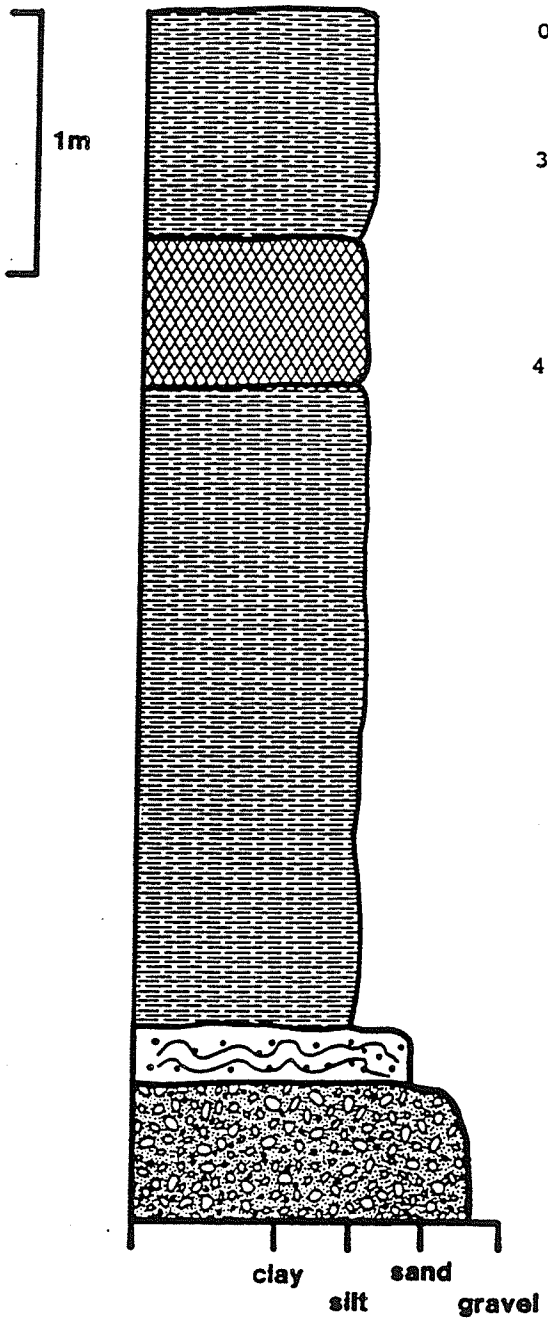

0.00-3.80	silt-clay rhythmites, red rhythmites from 0.86 to 1.43 m
3.80-4.00m	horizontally laminated v.f. to f. sand with abundant soft-sediment deformation structures
4.00-4.80m	massive sandy cobble gravel, not well exposed

87-22

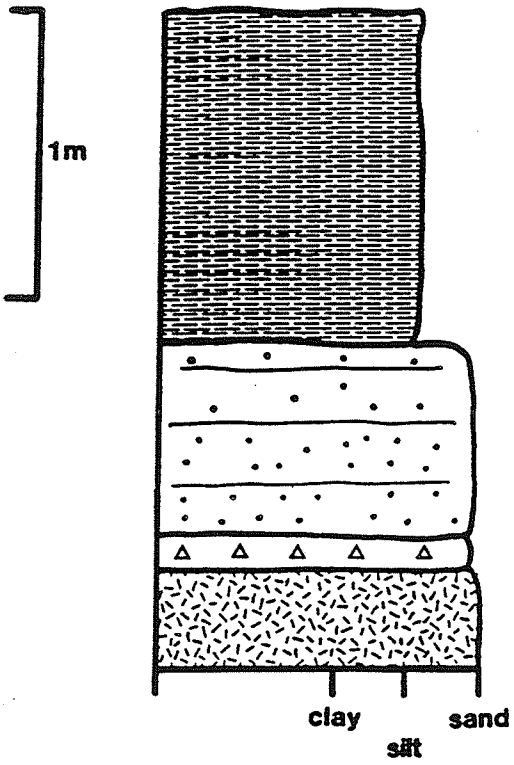

0.00-1.12m	silt-clay rhythmites, red rhythmites not present
1.12-1.72m	sandy rhythmites consisting of silty f. to v.f. horizontally laminated beds with clay caps
1.72-1.80m	sandy diamict over bedrock

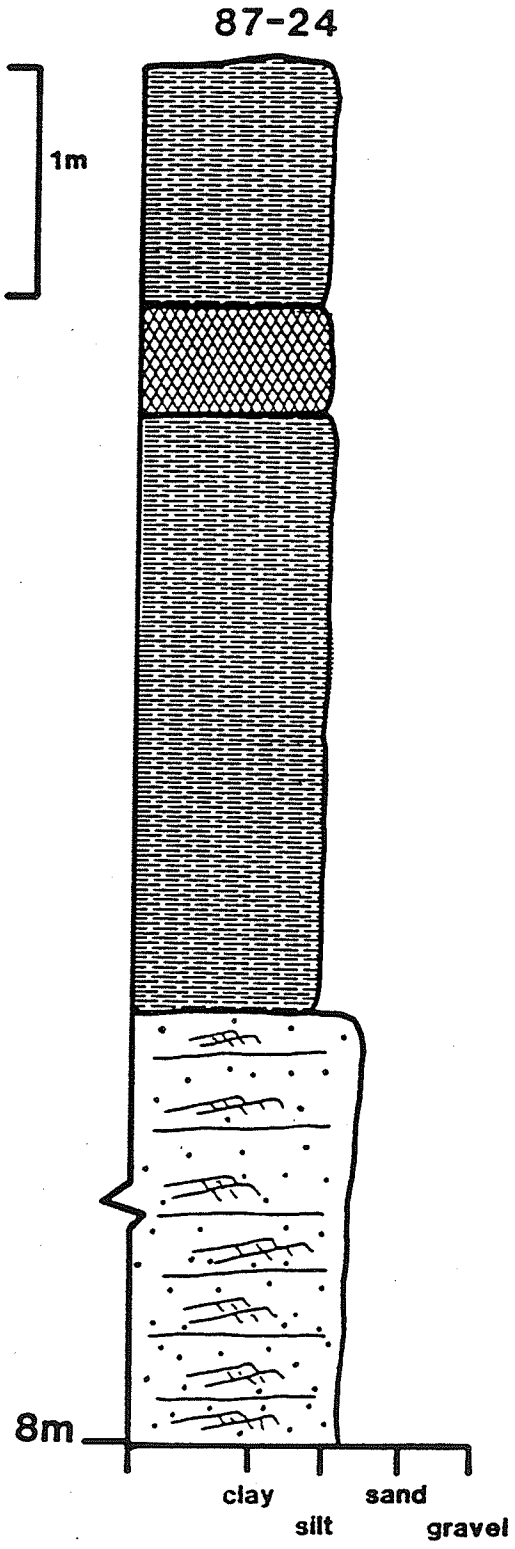

0.00-4.00m	silt-clay rhythmites, red rhythmites from 1.02-1.50m
4.00-8.00m	sand-silt rhythmites consisting of m. to v.f. sand, horizontally laminated to climbing rippled, capped with horizontally laminated to massive silt, or rarely massive clay, paleoflows 243, 262

87-25

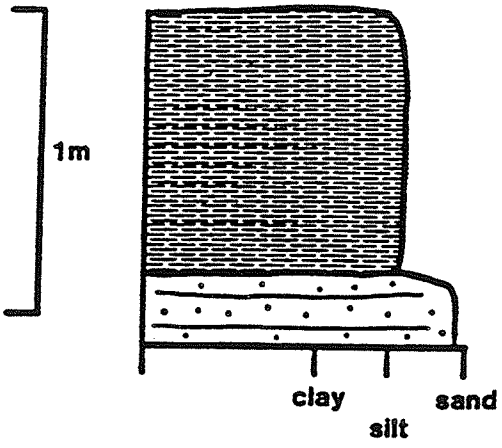

0.00-0.80m	silt-clay rhythmites, red rhythmites not present
0.80-1.10m	sandy rhythmites consisting of horizontally laminated v.f. to f. sand with massive clay cap

87-28

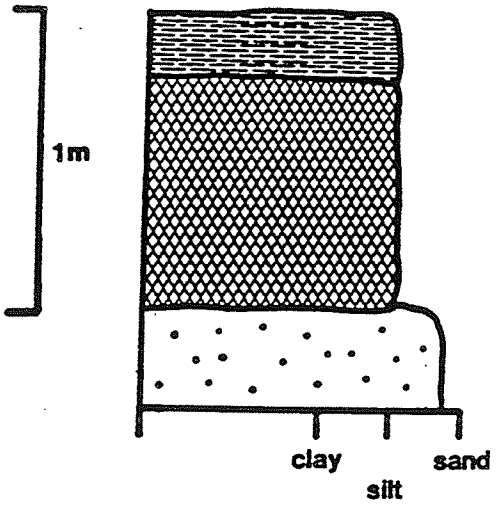

0.00-1.00m	s i l t - c l a y rhythmites, red rhythmites from 0.2-1.0m
1.00-1.20m	massive sandy silt

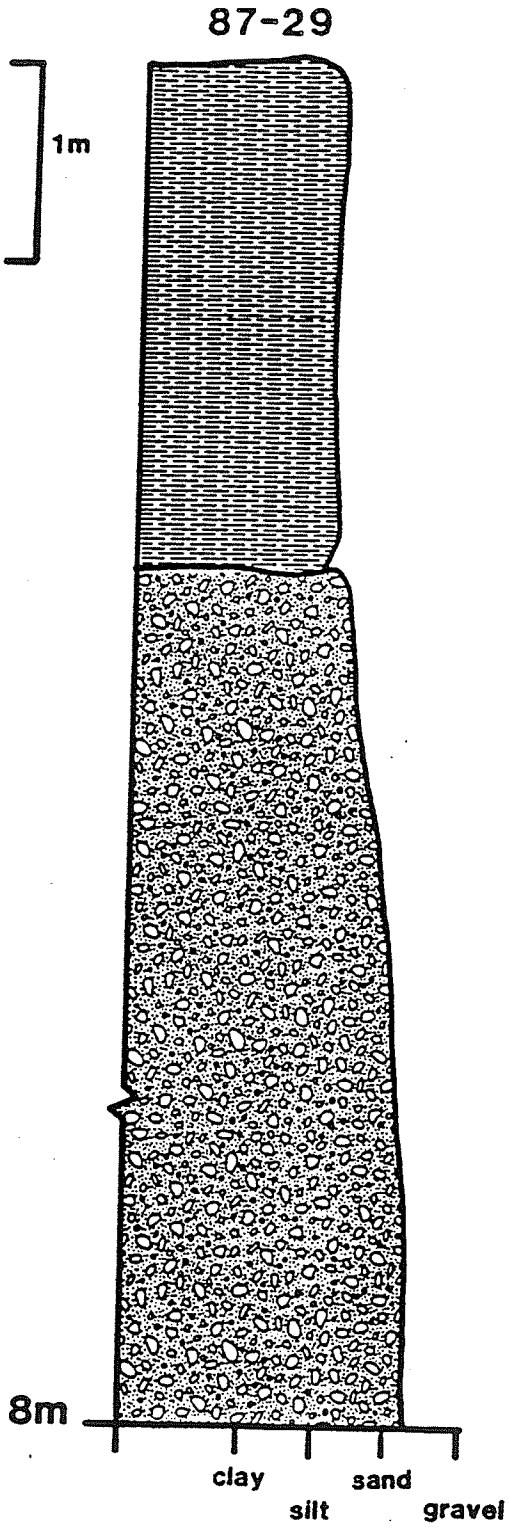

0.00-2.50m	massive red clay, becomes faintly laminated over bottom 20 cm, minor disturbance and 2 cm silt clasts
2.50-8.00m	sandy pebble and cobble gravel, crudely stratified

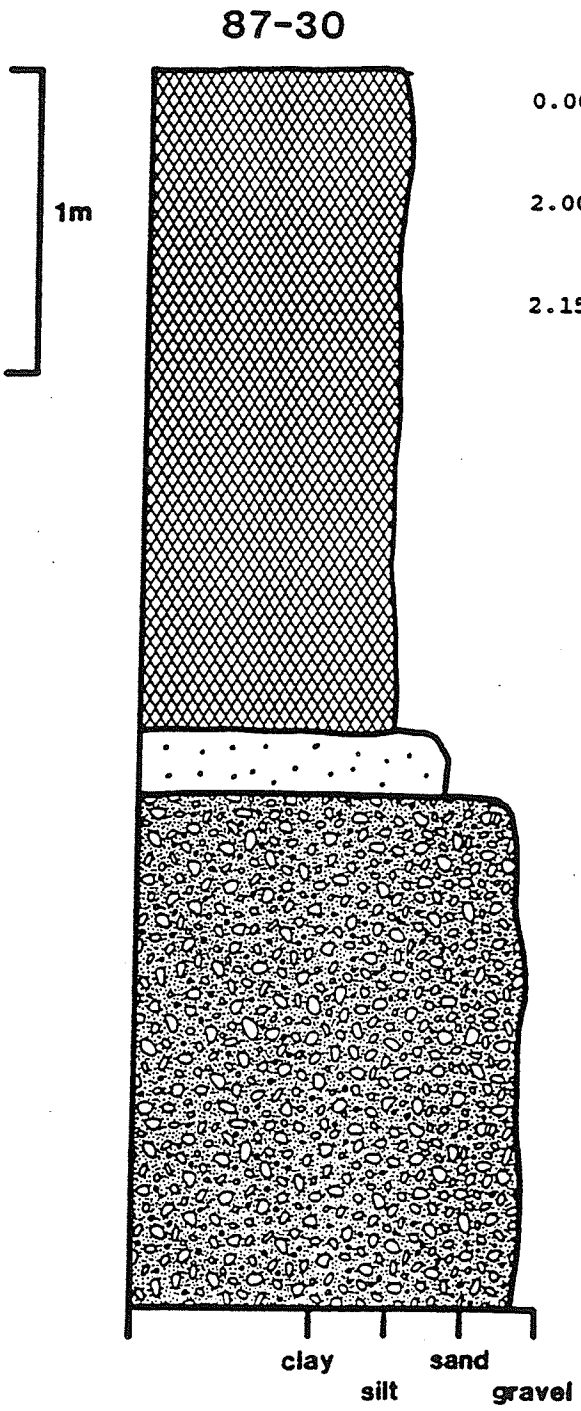

0.00-2.00m	faintly laminated to massive red clay
2.00-2.15m	horizontally laminated v.f. sand
2.15-4.00m	massive sandy pebble, cobble and boulder gravel

87-2

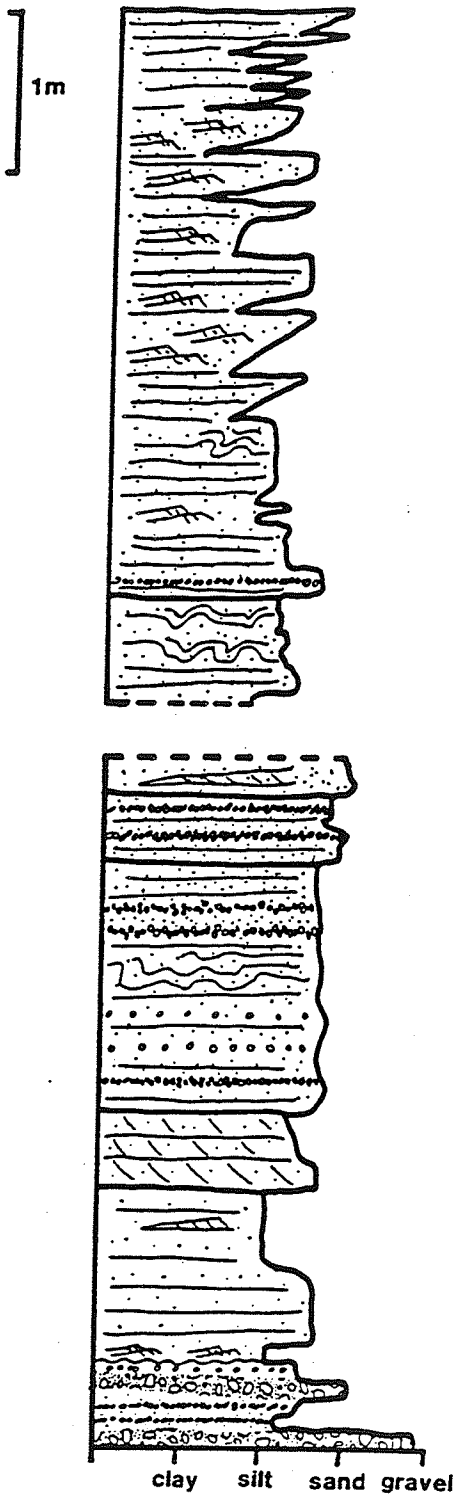

0.00-4.40m numerous fining and coarsening upward cycles ranging from c. silt to m. sand, horizontally laminated and climbing rippled, some soft-sediment deformation and minor granule to pebble horizons and clay laminae

break in section

4.40-8.65m silty v.f. to c. sand, horizontally laminated and crossbedded, minor climbing ripples, granule and pebble layers common, paleoflows 323, 243, 276, 234, 202, 216, 190 (this unit is a wedge of sediment and rests on the lee face of a gravel bar)

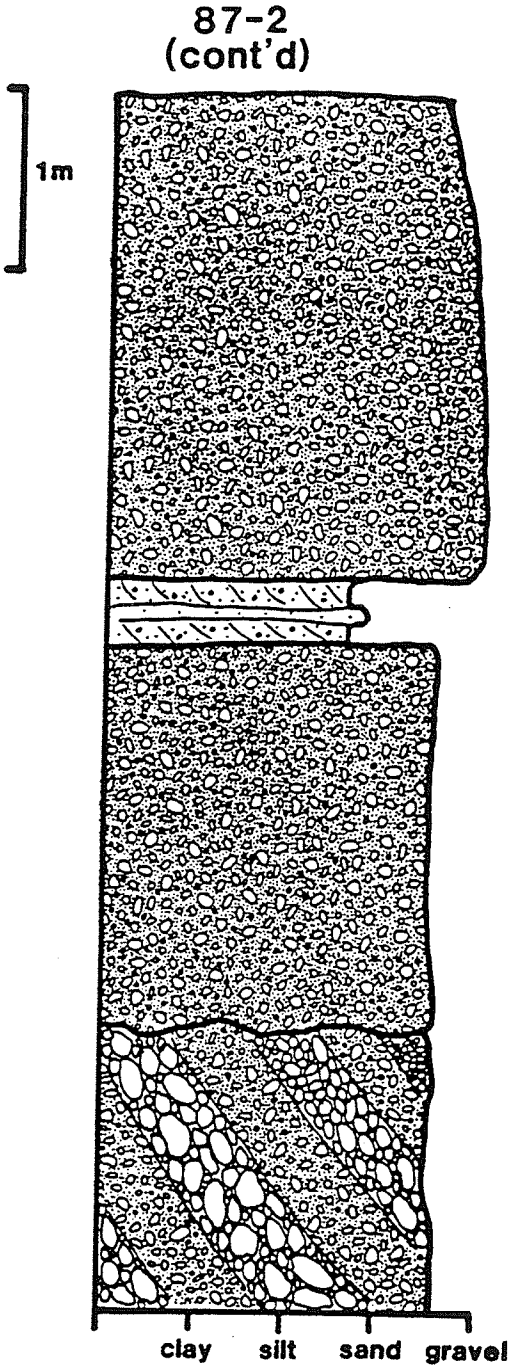

break in section	
8.65 - 11.35m	clast-supported cobble and boulder gravel, clasts up to 60 cm, sandy to granular matrix
11.35 - 11.72m	m. to c. crossbedded and horizontally laminated sand with granules on foresets
11.72 - 13.85m	clast-supported pebble and cobble gravel, clasts up to 18cm, sandy to granular matrix
13.85 - 15.38m	large-scale foresets of interbedded open- and closed-work granule, pebble and cobble gravel, clasts up to 15cm

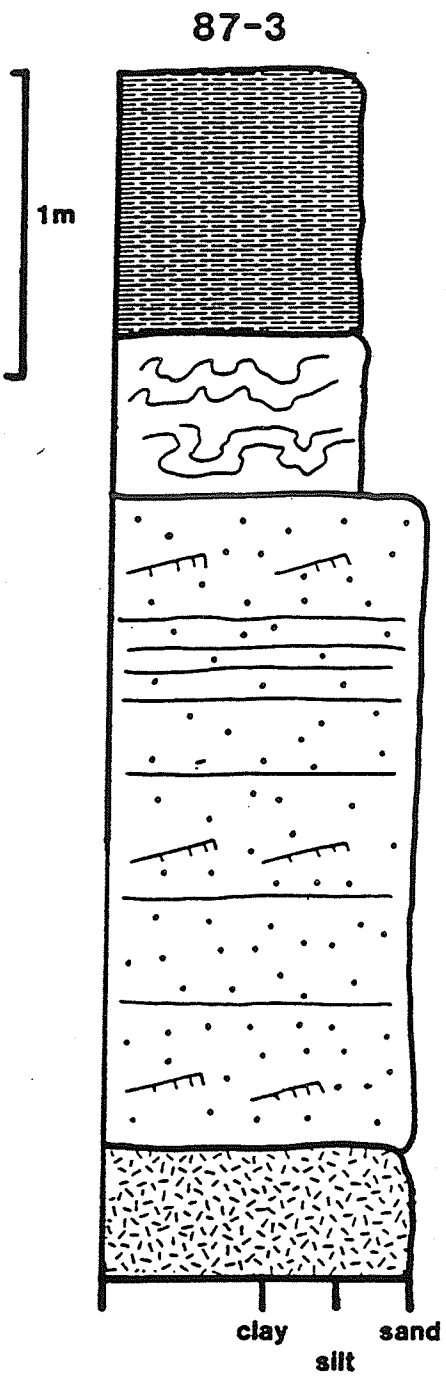

0.00-0.78m	silt-clay rhythmites, red rhythmites not present
0.78-1.28m	strongly deformed silt-clay and v.f. sand-clay rhythmites
1.28-2.12m	sandy rhythmites consisting of v.f. to f. sand, horizontally laminated to rippled, with clay caps, paleoflow 206, over bedrock striated 214

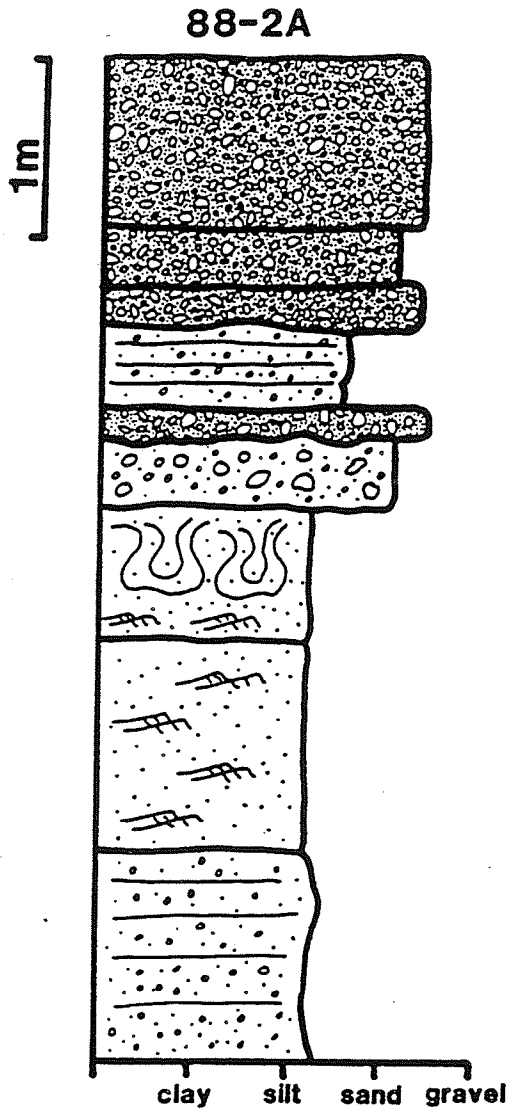

0.00-0.90m	pebble and cobble gravel, clasts subrounded and up to 13cm in size, c. sand matrix
0.90-1.20m	granule and pebble gravel
1.20-1.40m	sandy matrix-supported cobble gravel, with clasts up to 16cm
1.40-1.70m	pebbly f. to c. sand with vague horizontal laminations
1.70-1.85m	horizontally laminated f. to c. sand and granules over lag of subangular to subrounded pebbles and cobbles up to 19cm in size
1.85-2.22m	granules and pebbles up to 7cm in a f. sand matrix
2.22-2.92m	f. to v.f. sand with minor m. to c. sand, abundant climbing ripples and large (1m wide) soft-sediment deformation structures
2.92-4.02m	v.f. to f. sand, abundant climbing ripples and horizontal laminations
4.02-5.12m	interbedded v.f. to m. sand, and granules and pebbles up to 10cm in a v.f. sand matrix

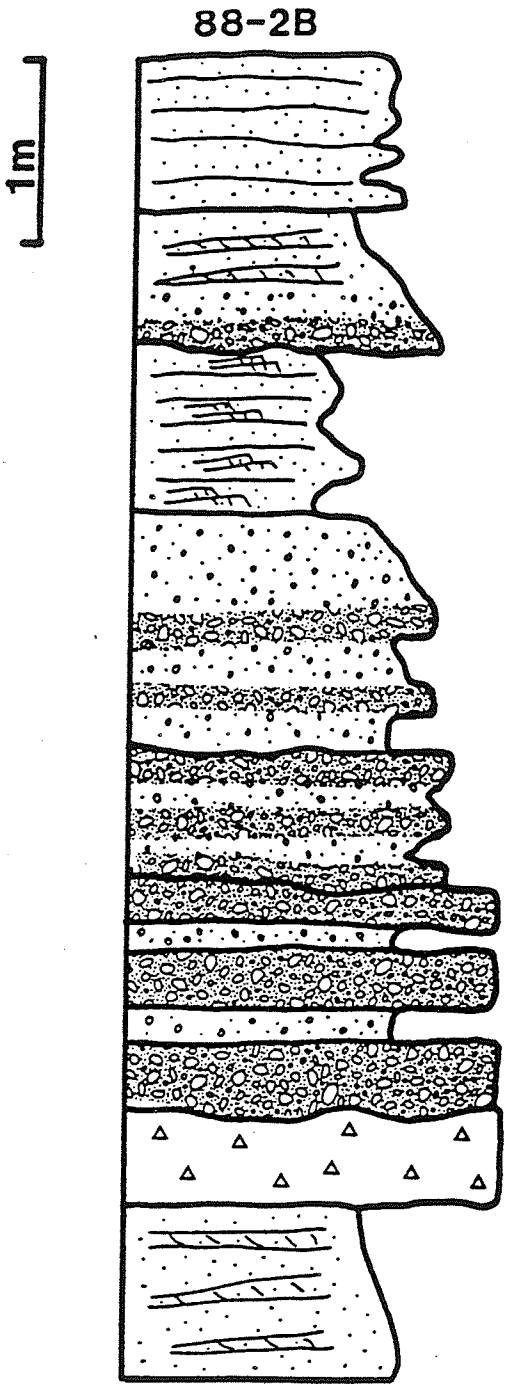

0.00-0.30m	horizontally laminated c. sand
0.30-0.80m	interstratified f., and v.c. sand
0.80-1.50m	fining upward from pebbles and cobbles in a v.c. sand matrix, to rippled pebbly m. sand
1.50-2.60m	fining upward from pebbly v.c. sand to interbedded v.c. sand and silt, horizontally stratified, abundant climbing ripples
2.60-3.60m	interstratified layers of pebbles and cobbles up to 8cm, and pebbly v.c. sand
3.60-4.30m	interstratified layers of pebbles and cobbles up to 8cm, and pebbly v.c. sand
4.30-5.50m	crudely stratified interbeds of clast-supported boulder gravel with clasts up to 60cm, and poorly sorted f. sand with pebbles up to 6cm
5.50-6.00m	cobbles and boulders up to 20cm in a massive silt-clay matrix
6.00-6.90m	fining upward from v.c. sand to m. sand, abundant horizontal laminations and minor crossbedding, paleoflow 217

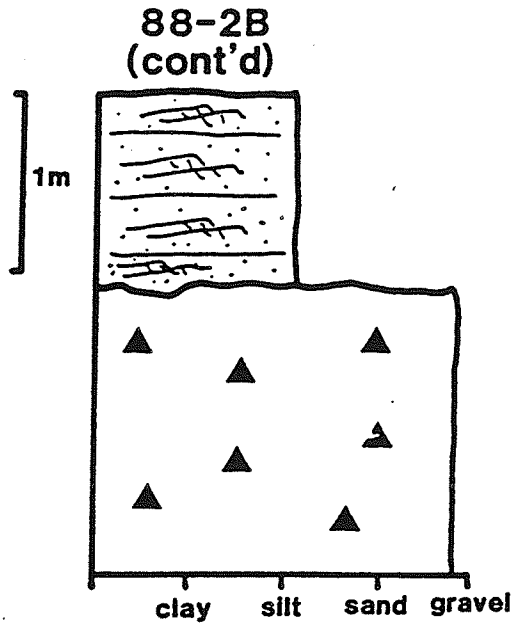

6.90-7.90m	rippled silt to v.f. sand
7.90-9.40m	pebbles and boulders up to 60 cm in a massive silty f. sand matrix

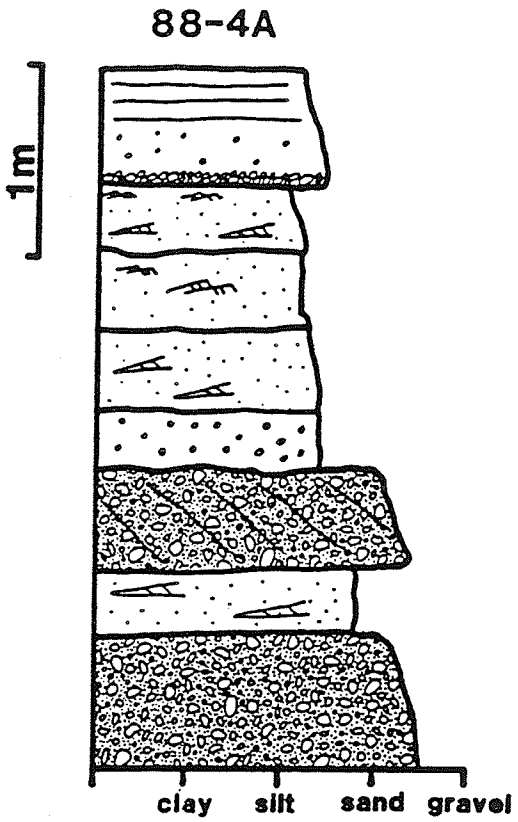

0.00-0.60m	pebbly sand, horizontally laminated with lag of cobbles at base
0.60-0.95m	planar tabular crossbedded pebbly sand, paleoflow 270
0.95-1.30m	silty f. sand, climbing ripples with 3 clay laminae
1.30-2.20m	tabular crossbedded m. sand with massive pebbly sand unit at base
2.20-2.70m	crudely crossbedded pebble to cobble gravel, sandy matrix in upper 5cm, otherwise open-work
2.70-3.05m	planar tabular crossbedded granule-rich sand, paleoflow 300

87-27

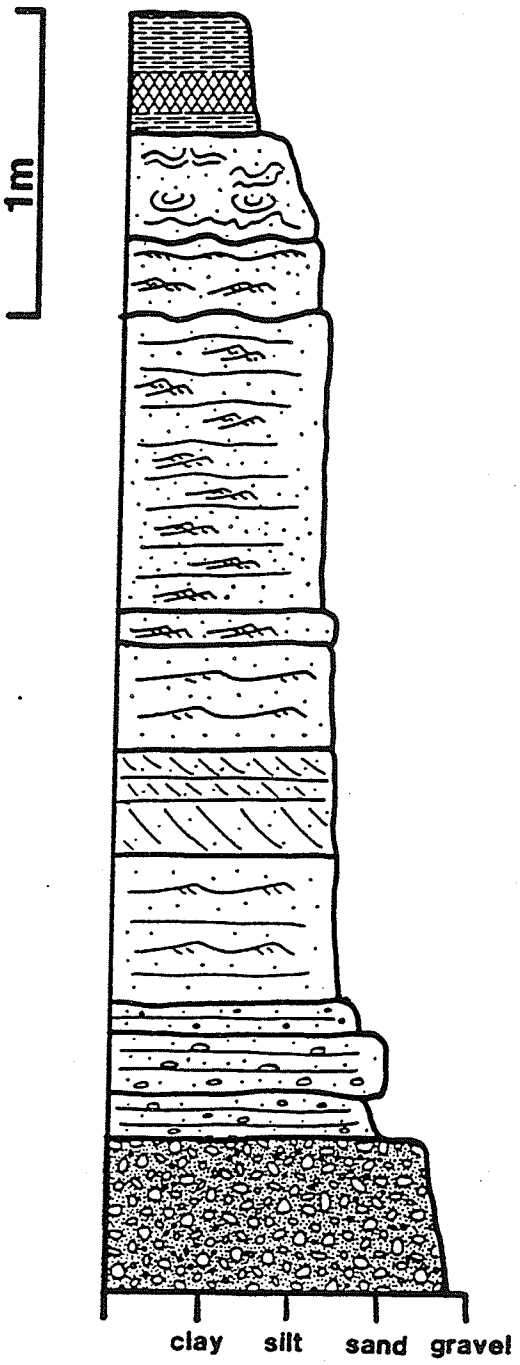

0.00-0.40m	silt-clay rhythmites, red rhythmites from 0.20-0.35m
0.40-0.75	massive to highly disturbed sandy rhythmites
0.75-1.00m	sandy rhythmites, sandy part v.f. to f. sand, horizontally laminated to climbing rippled, with clay drapes
1.00-1.98m	climbing rippled f. sand, with minor swaley laminations, paleoflow 289
1.98-2.08m	silty m. to f. sand, climbing ripples in lower 5cm
2.08-2.42m	vaguely rippled m. to c. sand
2.42-2.78m	tabular crossbedded m. to c. sand with coarser grains at base of foresets, paleoflows 282, 268, 292
2.78-3.25m	vaguely rippled m. to c. sand
3.25-3.36m	horizontally laminated m. to v.c. sand, abundant granules on laminations
3.36-3.57m	horizontally stratified pebbly c. to v.c. sand, pebbles on bedding planes
3.57-3.72m	horizontally laminated m. to c. sand with minor granules
3.72-6.00m	foreset beds composed of alternating open-work and closed-work gravels, pebbles to cobbles up to 20cm, some fining upward of clast size is apparent

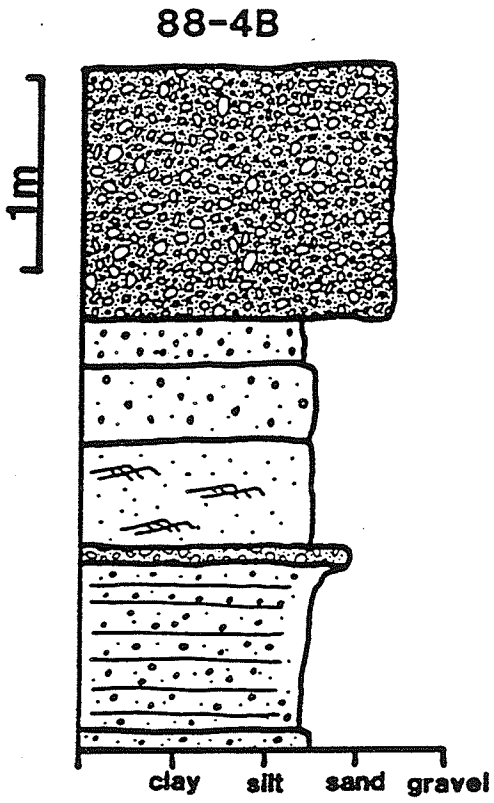

0.00-1.31m	poorly sortedsand with pebbles and cobbles supported in matrix
1.31-1.55m	poorly sorted pebbly sand
1.55-1.97m	poorly sorted pebbly sand with minor cobbles up to 7cm
1.97-2.53m	m. sand with crudely developed climbing ripples
2.53-2.57m	pebbly cobbly gravel layer, clasts up to 6cm
2.57-3.53m	finely laminated m. sand with occasional layers containing granules and pebbles, rarely cobbles
3.53-3.63m	slightly pebblym. to c. sand with faint horizontal laminations

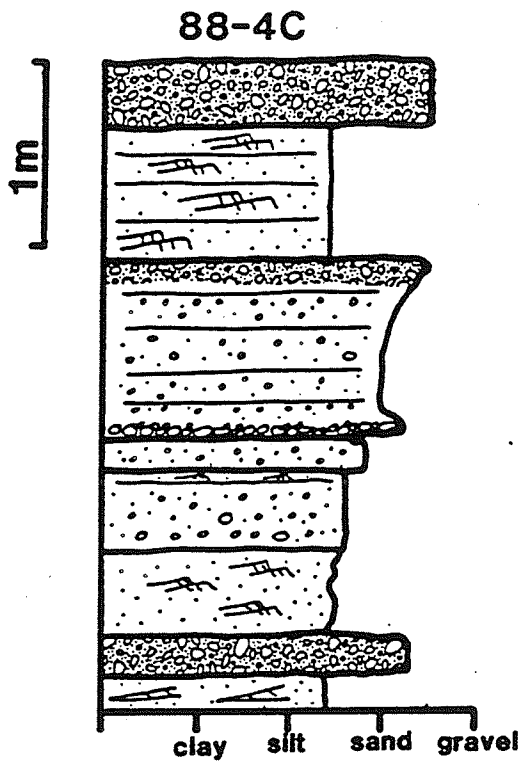

0.00-0.36m	pebbles and cobblesup to 10cm in a matrix of m. to f. sand
0.36-1.08m	interbedded silty f. tom. sand, and m. to f. sand, abundant climbing ripples, paleoflows 222, 242
1.08-1.98m	horizontally stratified c. to v.c. sand with fairly common granule, pebble, and cobble layers up to 10 cm, especially at top and bottom
1.98-3.59m	5cm silty m. to v.c. sand, very faint ripples; 17cm c. to v.c. pebbly sand with abundant granular horizons; 6cm silty m. to c. sand with granule layers, vague climbing ripples; 34cm m. to c. sand,horizontally laminated with several layers of granules and pebbles up to6cm, minor cobbles up to 14 cm
3.59-4.04m	interbedded silty m. tof. sand with abundant climbing ripples, and massive silty m. to c. sand and granules, paleoflows 208, 234, 253
4.04-4.24m	clast-supported pebbles and cobbles up to 10cm, with silty m. to f. sand matrix
4.24-4.34m	crossbedded m. to f. sand

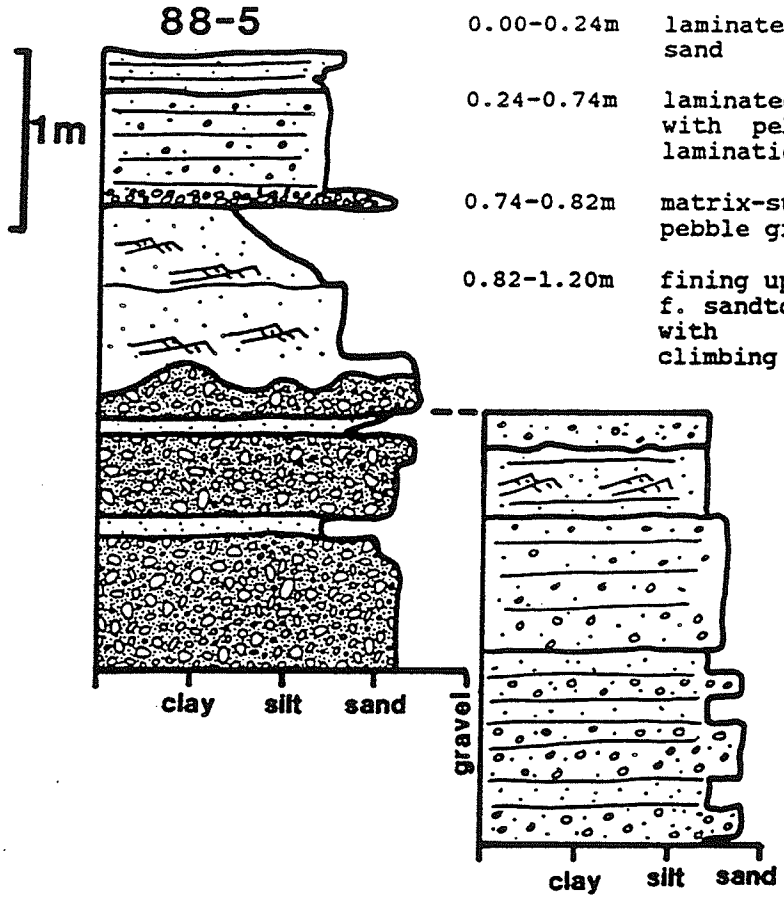

0.00-0.24m	laminated f. tom. sand
0.24-0.74m	laminated f. sand with pebbles on laminations
0.74-0.82m	matrix-supported pebble gravel
0.82-1.20m	fining upwardfrom f. sandto f. silt with abundant climbing ripples
1.20-1.60m	climbing rippled m. sand with pebbles on foresets, with drapes of v.f. to f. sand
1.60-1.80m	lag deposit of granules to 20cm cobbles
1.80-2.55m	interbeddedpebble and cobblegravel, and pebbly m.sand
2.55-3.15m	matrix-supported pebble gravel, pebblesup to 6cm, matrix f. to m. sand

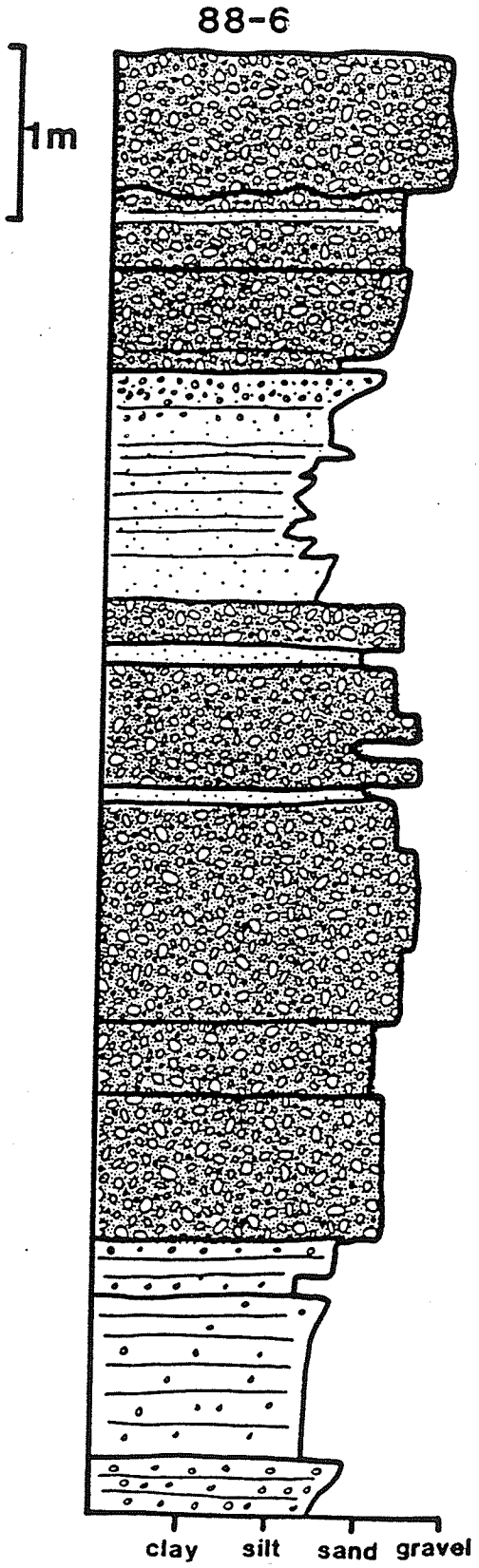

0.00–0.80m matrix-supported gravels, cobbles and boulders up to 60cm, matrix is c. to v.c. sand and granules

0.80–1.80 40cm c. to v.c. sand, granules and minor pebbles up to 5cm, vaguely stratified, pebbles concentrated in layers
40cm coarsening upward from pebbles up to 4cm in a m. to c. sand matrix, to pebbles and small cobbles up to 10cm in a m. to v.c. sand and granule matrix
40cm c. to v.c. sand with granules and minor small pebbles up to 2cm

1.80–3.10m series of coarsening and fining upward packages, 5 to 20cm thick, ranging from silt to v.c. sand and granules, horizontally stratified to massive

3.10–6.60m 139cm crudely stratified pebbles and cobbles up to 4cm, in a matrix of c. sand to granules, some beds of well rounded cobbles up to 25cm, very open matrix
52cm cobbles up to 10cm, variably clast and matrix supported, matrix from v.c. sand to small pebbles (1cm)
42cm pebbles and cobbles up to 16cm in a fairly open matrix of v.c. sand and granules, clasts lie on bedding planes with some imbrication, crude stratification
40cm pebbles up to 3cm in a c. to v.c. sand and granule matrix
80cm pebbles and cobbles up to 14cm in a fairly open matrix of c. to v.c. sand and granules

6.60–6.10m 20cm vaguely stratified m. to v.c. sand with granules and pebbles up to 4cm
11cm poorly sorted silty f. to m. sand with minor pebbles up to 2cm
90cm horizontally stratified m. to f. sand with rare small (0.5cm) pebble, coarsens slightly to c. sand near top
30cm pebbles up to 4cm in a matrix of poorly sorted f. to v.c. sand, vague laminations

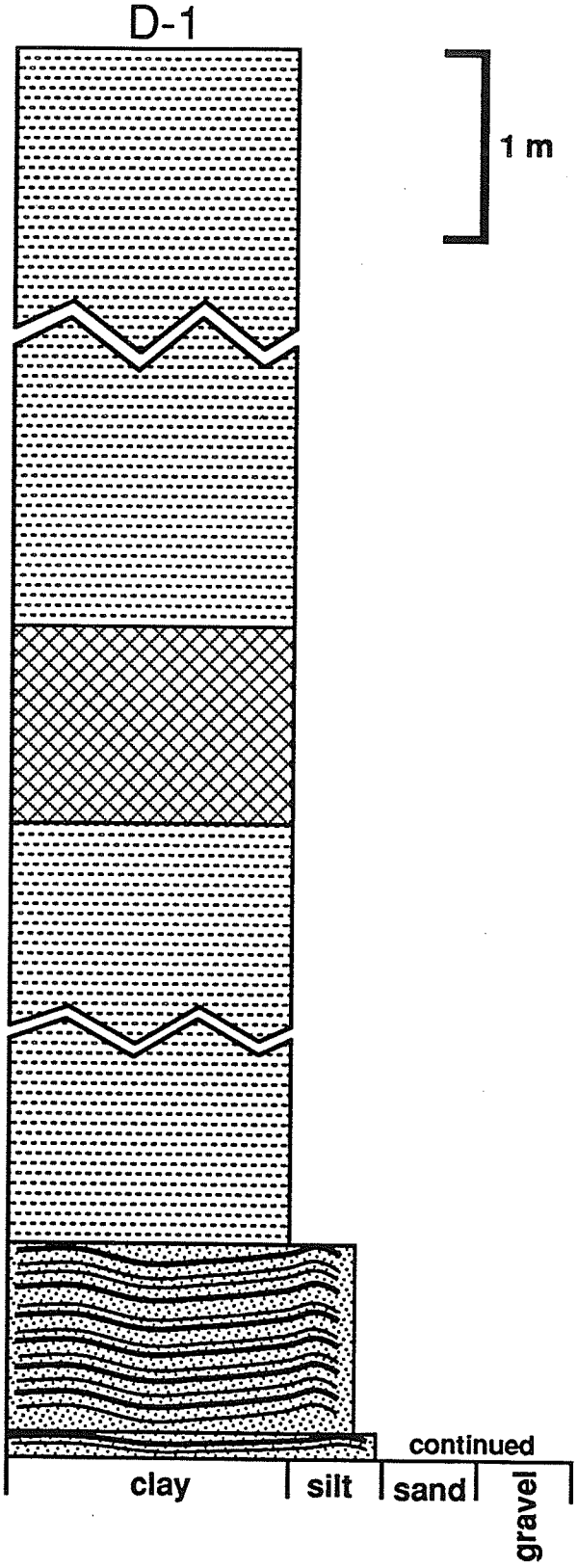

0.0-7.80 m	grey, silt-clay rhythmites, 0.5-5.0 cm thick, rarely up to 10.0 cm thick, abundant bioturbation in silt laminae
7.80-8.85 m	red clay rhythmites, similar to grey rhytmites
8.85-12.10 m	grey, silt-clay rhythmites, 0.5-5.0 cm thick, rarely up to 10.0 cm thick, abundant bioturbation in silt laminae
12.10-13.20 m	coarser and thicker silt-clay rhythmites than above
13.20-13.34 m	f. to m. sd. and clay rhythmites

D-1 (cont'd)

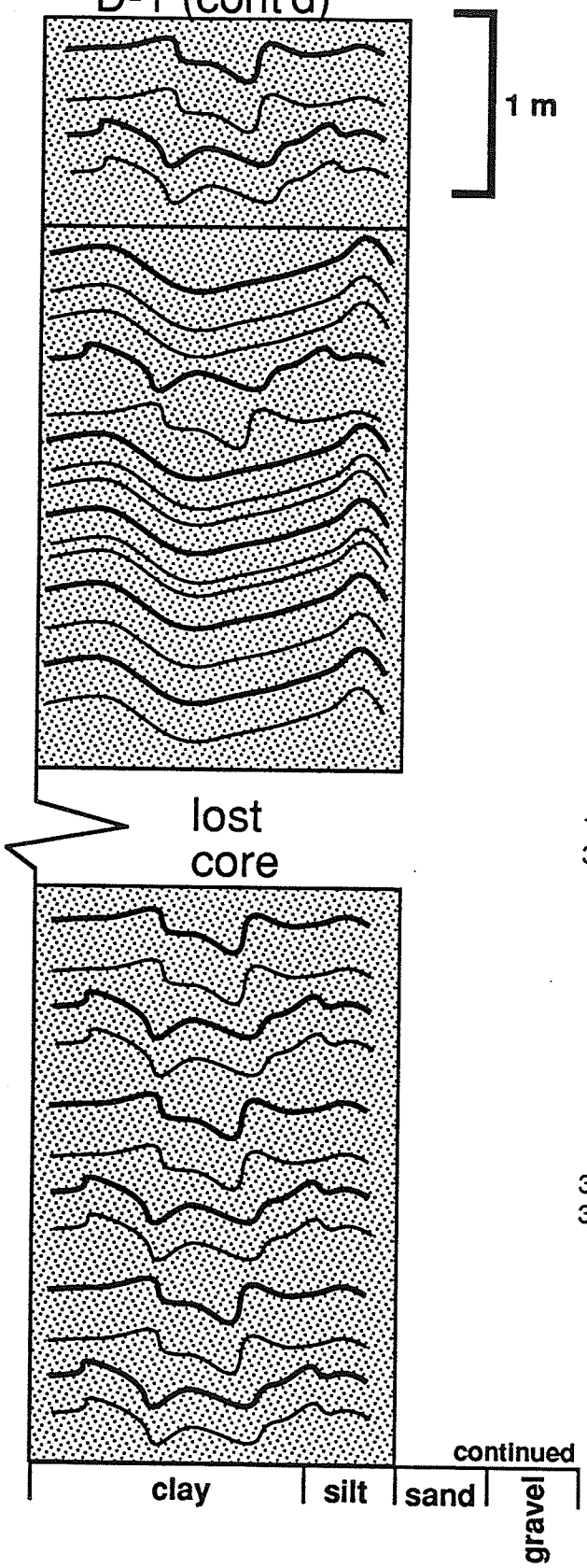

13.34-14.51m	f. to m. sd. and clay rhythmites, highly disturbed by soft-sed. deformation or drilling
14.51-17.51m	rhythmites composed of f. to m. sd. gradinging upwards to silt with a clay cap, graded portion laminated, some disturbance
17.51-31.23 m	very poor core recovery, only 1.62 m for 13.62 m drilled, sediment appears to be rhythmites like those overlying
31.23-36.54 m	very disturbed sd.-clay rhythmites

D-1 (cont'd)

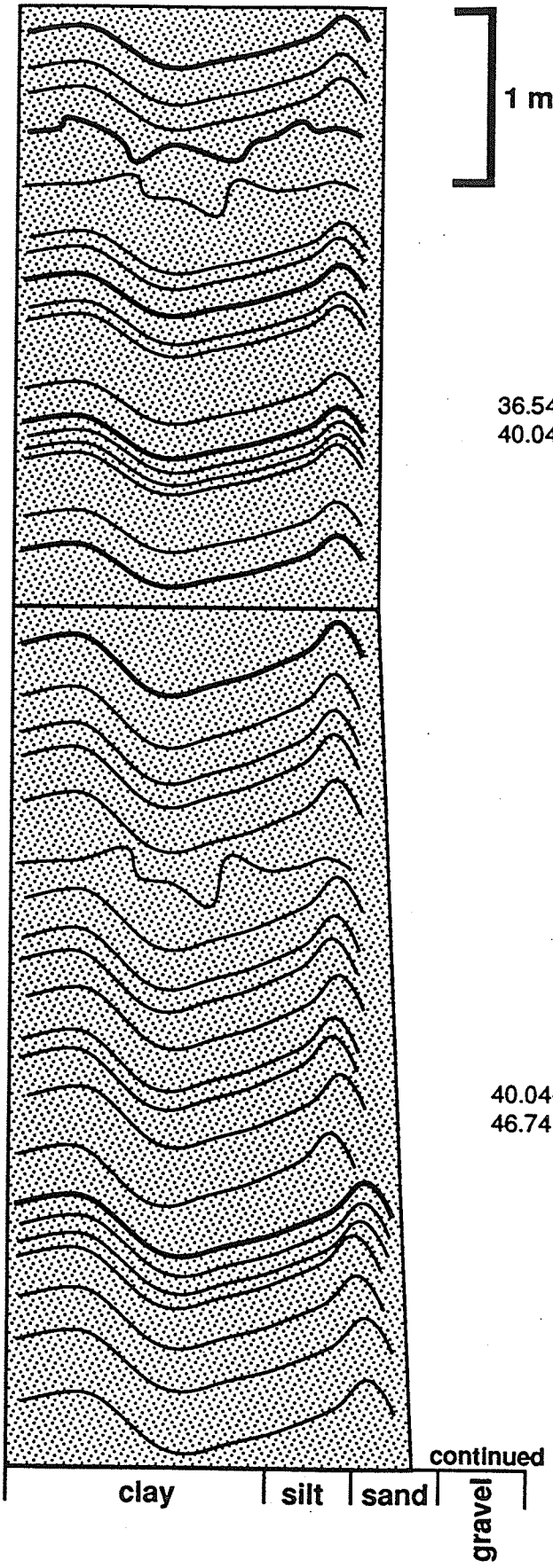

36.54-40.04 m	m.-f. sd. and clay rhythmites, rhythmites becoming thicker and coarser with depth
40.04-46.74 m	interbeds and graded beds of m. to f. sand and siltty-fine sand, rare clay laminae, sands parallel laminated, some disturbance, sequence coarsens downwards

D-1 (cont'd)

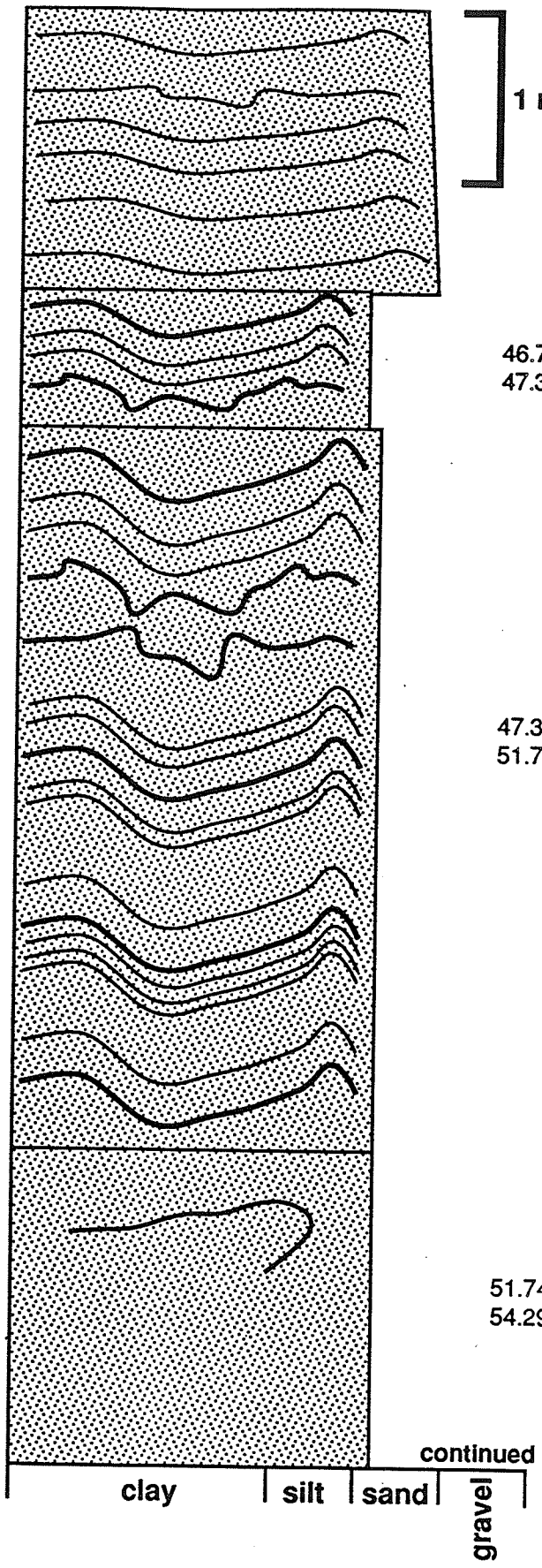

46.74- 47.34 m	sandy-silt and clay rhythmites, 4 rhythmites over 0.8 m
47.34- 51.74 m	m.-f. sd. and clay rhythmites, rhythmites becoming thicker and coarser with depth
51.74- 54.29 m	massive f. to v.f. sd with minor silt roll-ups

D-1 (cont'd)

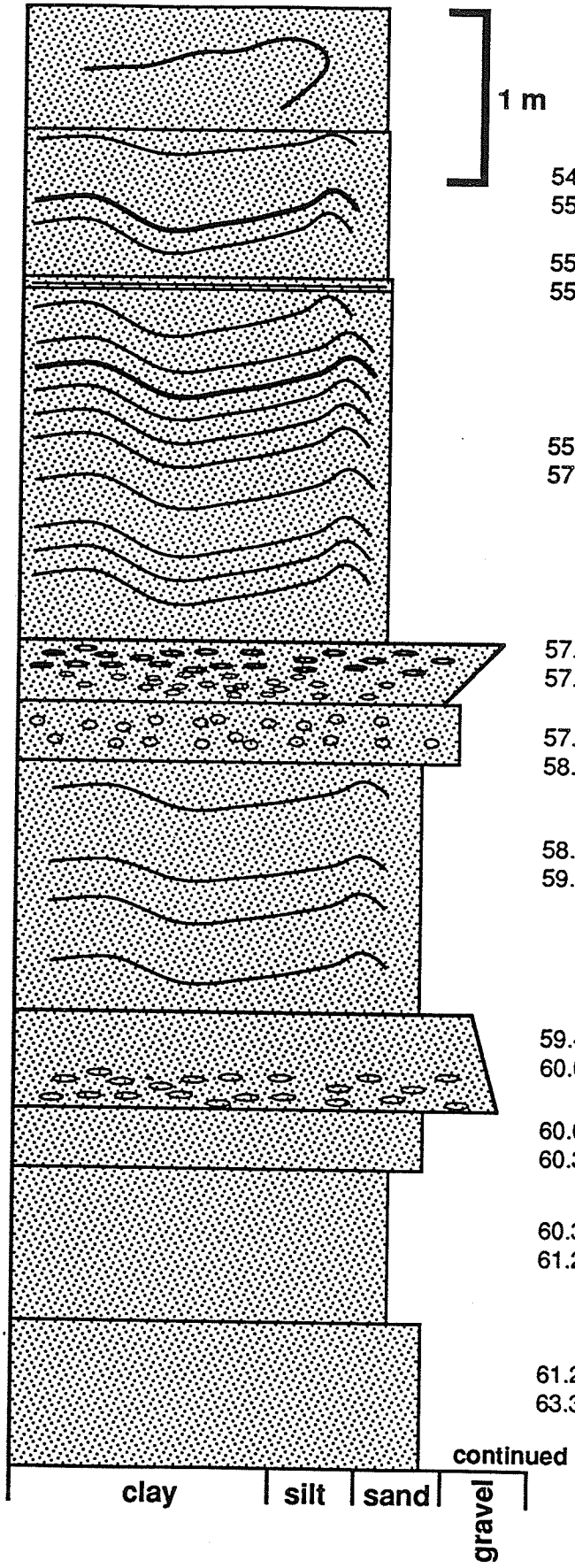

54.29-55.15 m	massive f. sand with occais. silt beds and on clay laminae
55.15-55.25 m	horizontally-laminated f. sd.
55.25-57.30 m	interbedded f. sd. and silty f. sd., one clay laminae
57.30-57.66 m	mod. well rounded, pebbly to cobbly gravel, grades down into granular c. sand
57.66-58.00 m	c. sd. with pebbles in matrix
58.00-59.45 m	interbedded f. to m. sd.
59.45-60.01 m	fine gravel fining upwards to c. sd at top, gravel well-rounded
60.01-60.36 m	massive m. to f. sd.
60.36-61.25 m	massive fine sand
61.25-63.34 m	massive m. to f. sand

D-1 (cont'd)

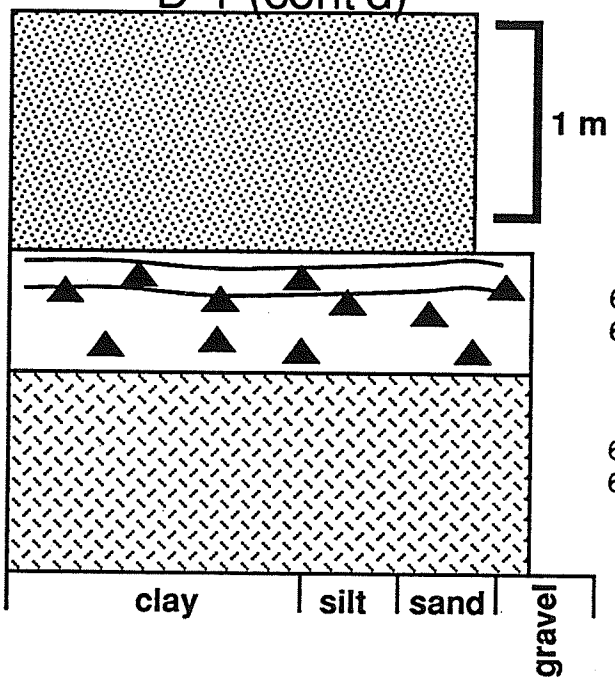

63.34-63.96 m	pebbly sandy silt diamict, massive at base, banded in upper part, common mafic pebbles
63.96-64.98 m	pegmatitic bedrock

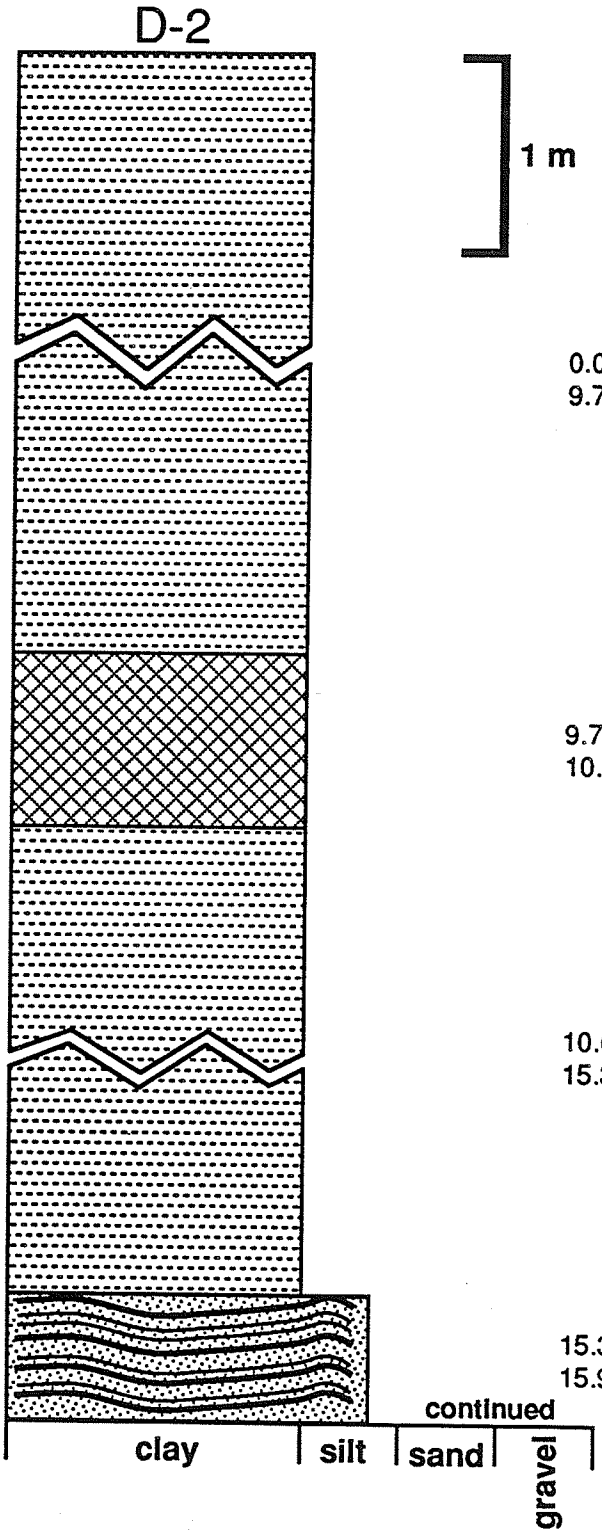

0.00- 9.70 m	grey, silt-clay rhythmites, 0.5-5.0 cm thick, rarely up to 10.0 cm thick, abundant bioturbation in silt laminae
9.70- 10.6 m	red clay rhythmites, similar to grey rhytmites
10.6- 15.3 m	grey, silt-clay rhythmites, 0.5-5.0 cm thick, rarely up to 10.0 cm thick, abundant bioturbation in silt laminae
15.3- 15.95 m	silt/f. sd. and clay rhythmites, 10.0-15.0 cm thick

D-2 (cont'd)

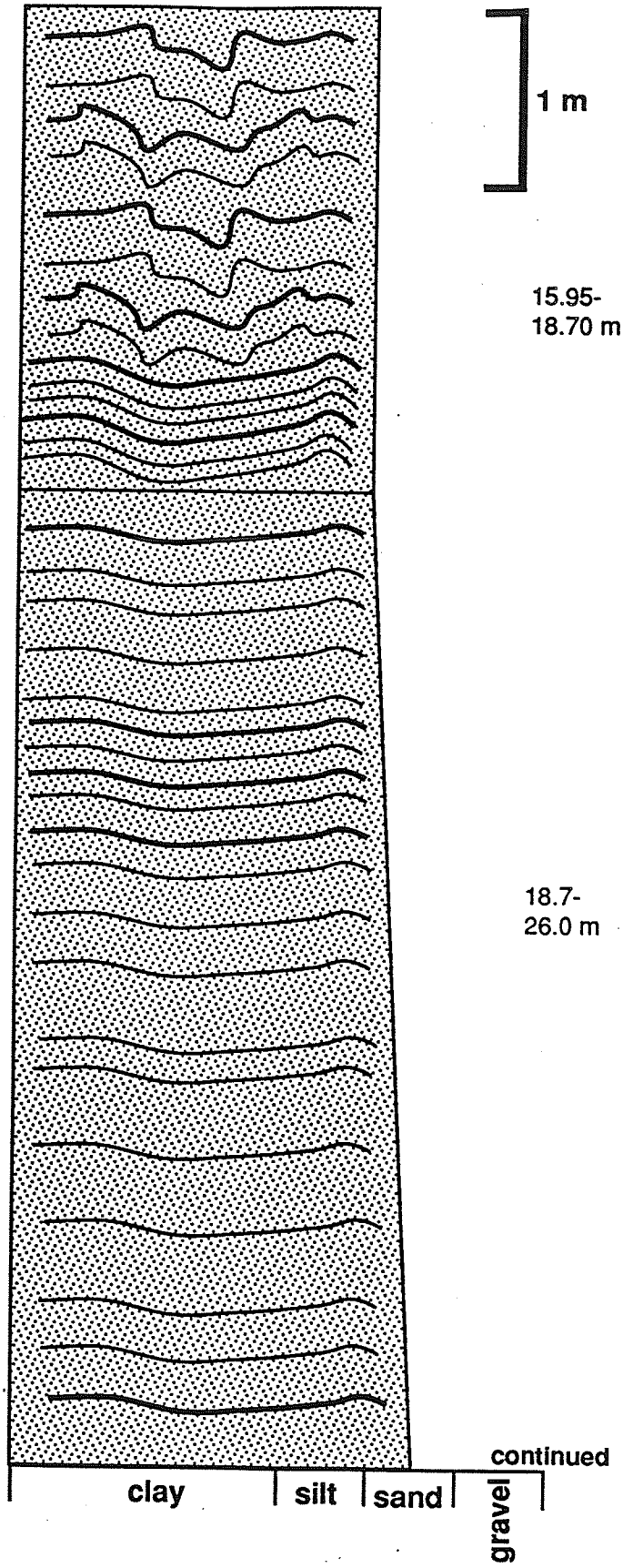

15.95-
18.70 m

f. to m. sd. and clay rhythmites, highly disturbed by soft-sed. deformation or drilling, except over bottom 1.0 m

18.7-
26.0 m

sand-silt rhythmites consisting of graded f. to c. sd. beds capped by a thin silt bed, minor clay laminae present, graded sand beds usually parallel laminated

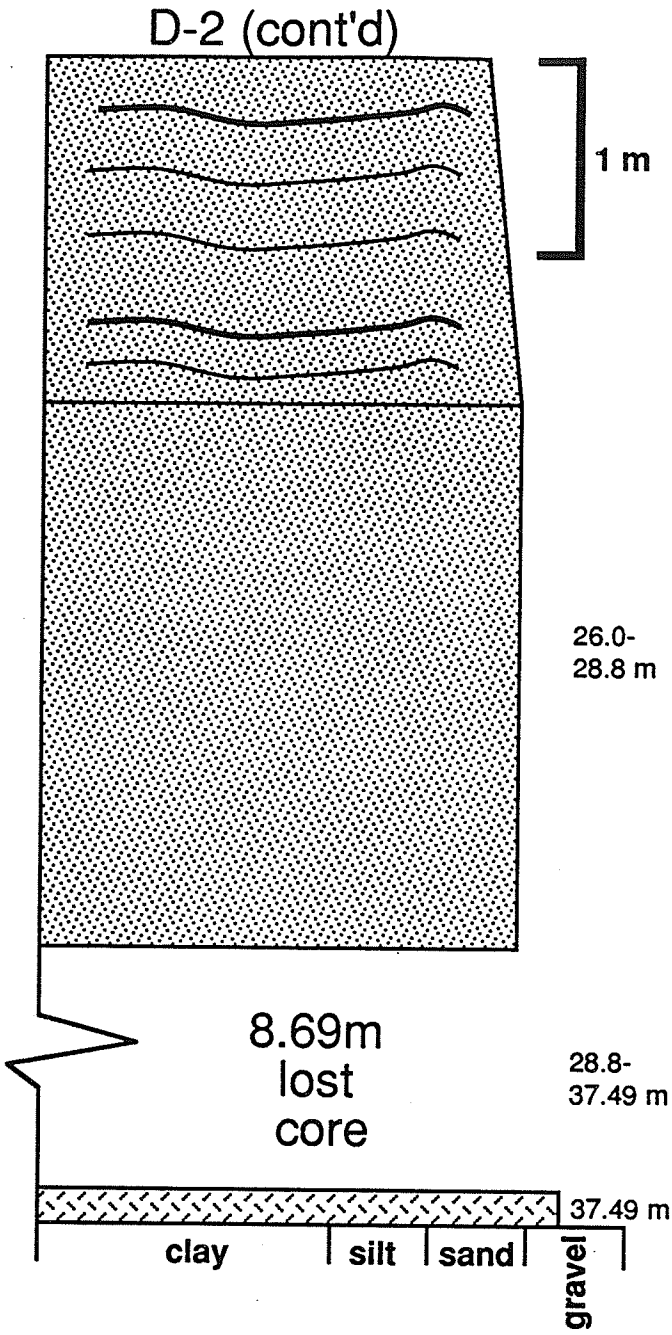

26.0-28.8 m	massive m. to c. sand
28.8-37.49 m	lost core
37.49 m	bedrock (not recovered)

D-3

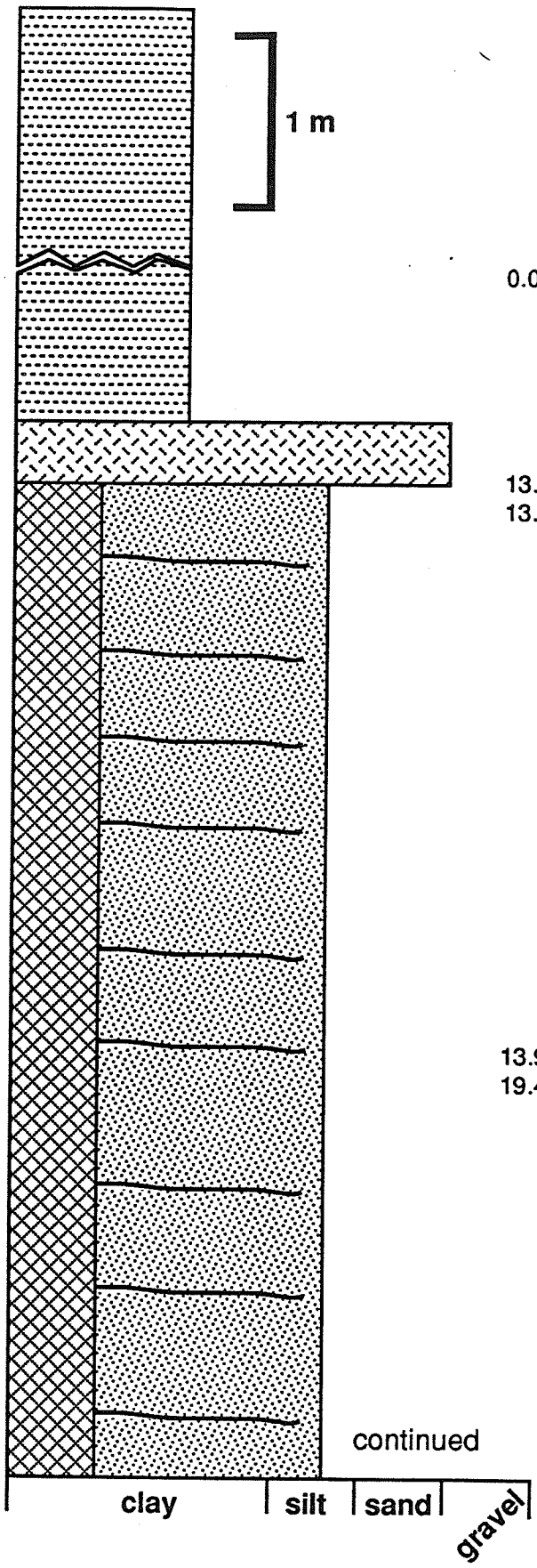

0.00-13.6 m silt-clay rhythmites, 0.5-5.0 cm thick, rarely up to 10 cm thick

13.6-13.95 m granitic boulder

13.95-19.40 m sandy rhythmites consisting of parallel-laminated c. silt to f. sand, 0.9-35.0 cm thick, with 0.5-16 cm thick red clay caps, minor bioturbation in coarse laminae

D-3 (cont'd)

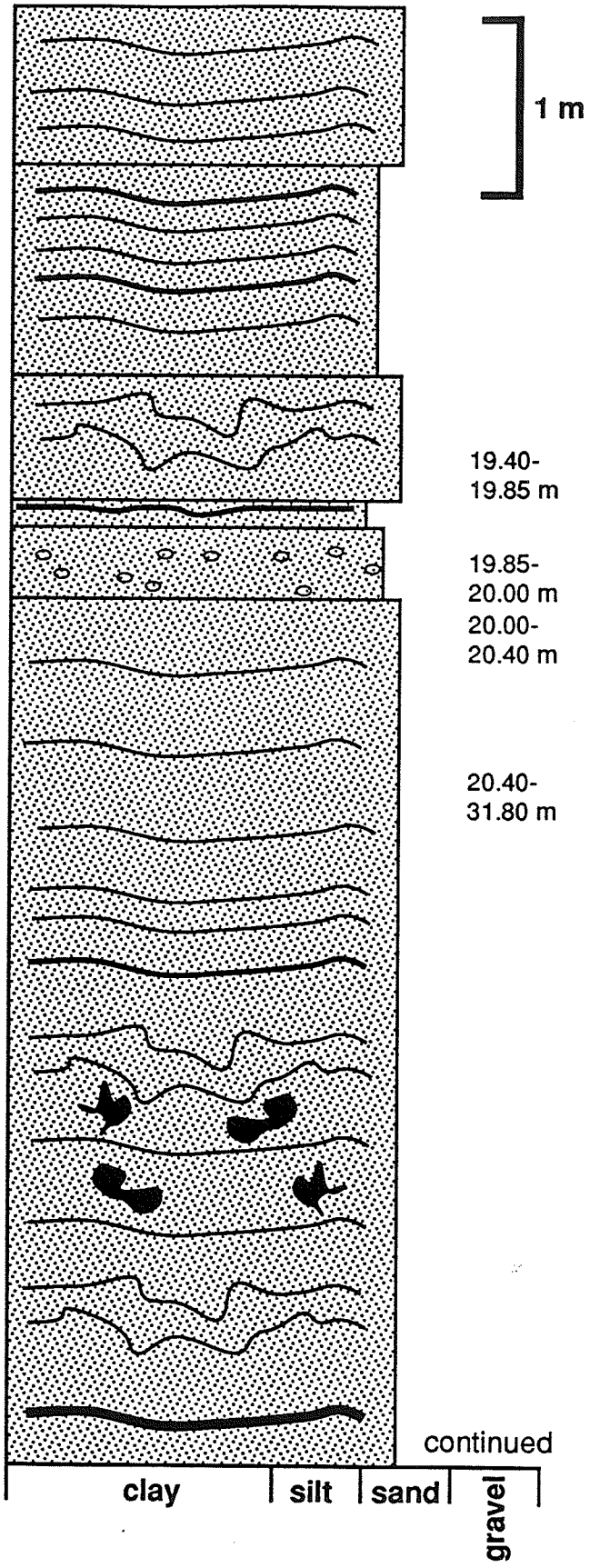

19.40-19.85 m	m. to f. sd., apparently massive but some possible highly contorted bedding
19.85-20.00 m	silty-f. sand with laminations and one clay layer
20.00-20.40 m	massive f. sand, occais. granules, poorly sorted
20.40-31.80 m	sand-silt rhythmites consisting of f. to m. sand, horizontally stratified, sometimes disturbed, 1.0-20 cm thick, capped by silt layers 0.5-10.0 cm thick, occaisonal clay laminae and clay balls or rip-ups, minor granules individual bed thicknesses difficult to determine because of soft-sediment and/or drilling-incuced disturbance in the core.

D-3 (cont'd)

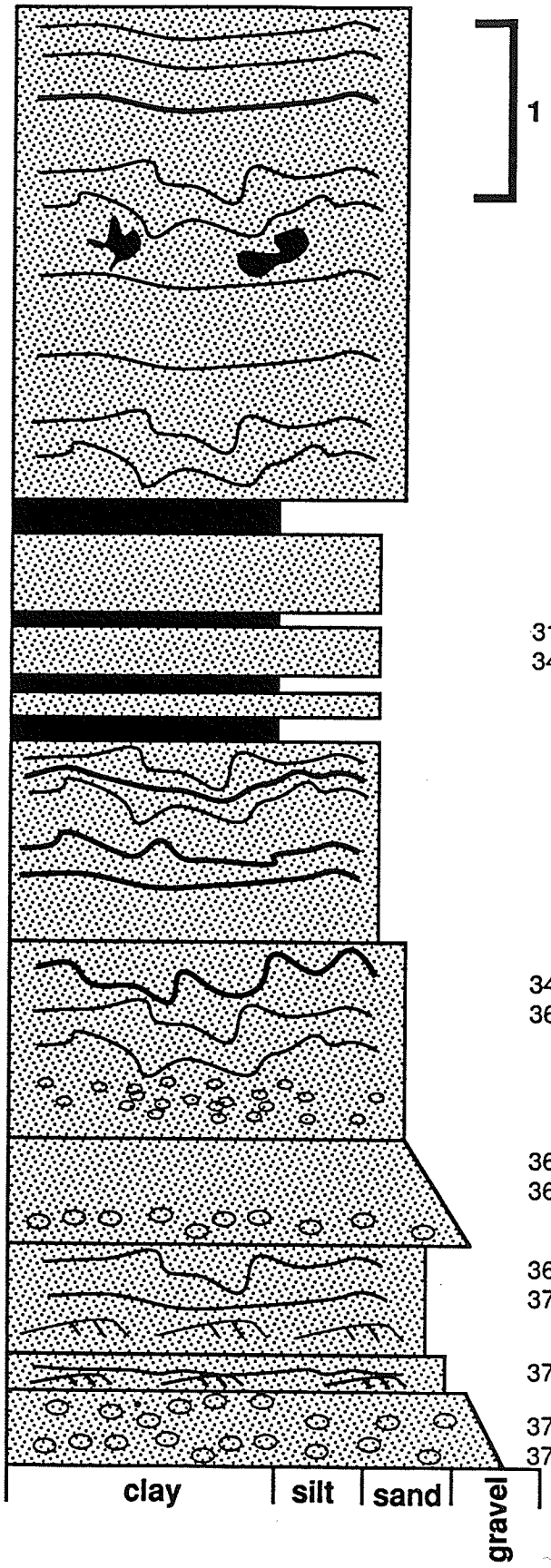

31.80-34.97 m	thick sand/silt and clay rhythmites, finely laminated to massive, abundant soft-sediment/drilling disturbance near base, some clay units up to 20 cm thick
34.97-36.08 m	-silt, silty f. sd., & fs. sd., vaguely laminated to bedded, occaisonal clay laminae, all highly disturbed
36.08-36.68 m	-pebbly c. to m. sd., grading to f.sd. at top, no pebbles at top, massive, pebbles subrounded, granitic
36.68-37.30 m	-silty-f. to f. sd., laminated at top, somewhat disturbed, apparent ripples at base
37.30-37.50 m	-m. to c. sd., massive at top, laminated, rippled at base
37.50-37.93 m	-granular to f. gravelly m. to c. sd., normally graded

continued

D-3 (cont'd)

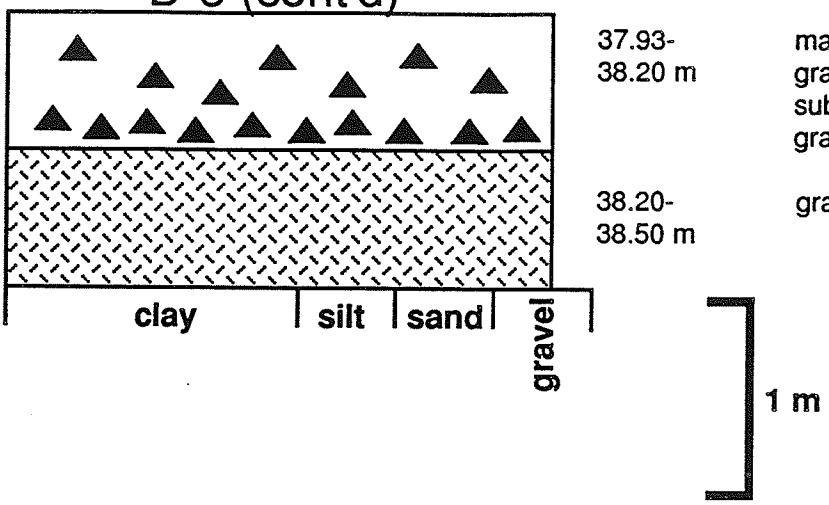

37.93-38.20 m	massive silty-sd. diamict, v. gravelly in lower 20 cm, subang. to subround. granitic pebbles
38.20-38.50 m	granitic bedrock

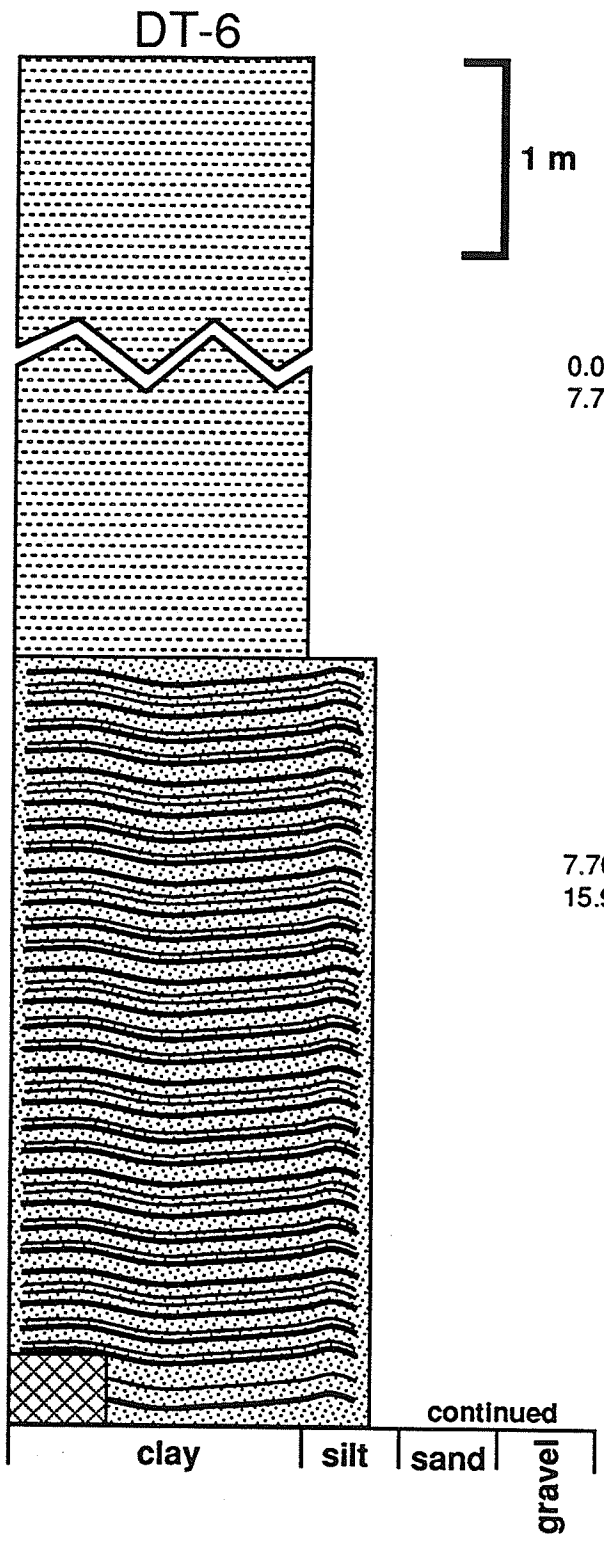

0.00- 7.70 m	grey, silt-clay rhythmites, 0.5-5.0 cm thick, rarely up to 10.0 cm thick, abundant bioturbation in silt laminae
7.70- 15.90 m	silt/f. sd. and clay rhythmites, 2.0-5.0 cm thick at top, becoming coarser (m. sand) and thicker (up to 50 cm thick) at base, note red clay caps on some rhythmites

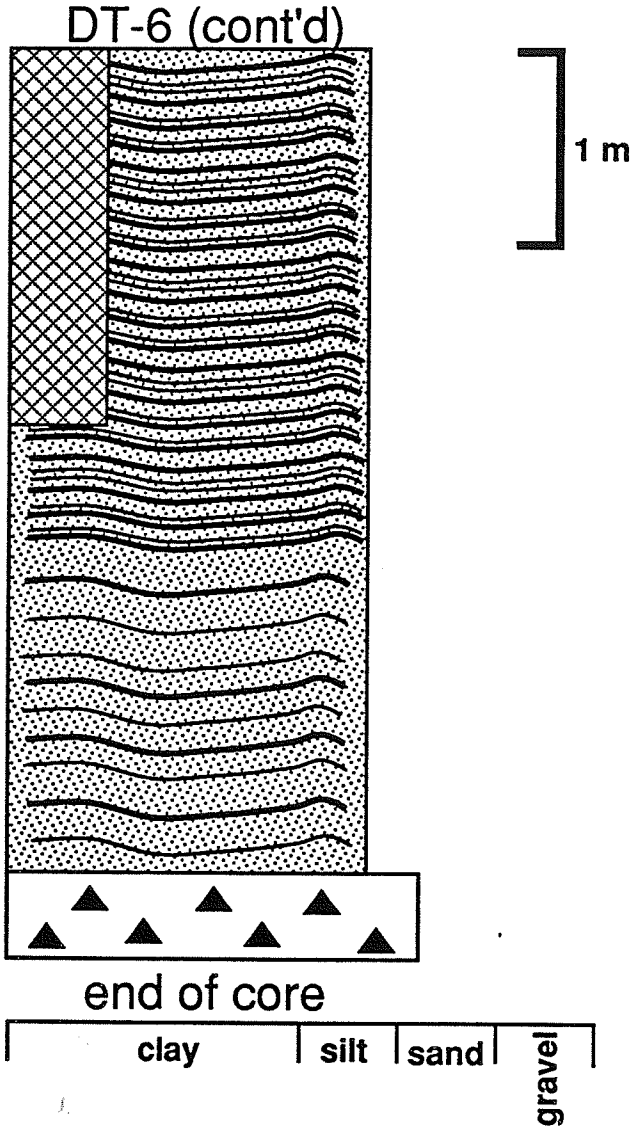

15.90-16.35 m	cobbly, silty-sand diamict, subang. to subround. clasts

APPENDIX B

DESCRIPTION OF THE SAMPLE SUITE, AND THE ANALYSES PERFORMED ON SAMPLES FROM SECTIONS 87-1, 87-19, FORT FRANCES AND THE KAMINISTIKWIA AREA.

Note in sections 87-1 and 87-19, the rhythmite numbered "0" is the lowermost red-clay rhythmite. See Fig. 2-1 for the locations of 87-1 and 87-19, and Appendix A for annotated logs of the sections.

REE -Rare Earth Elements
MIN -Quantitative clay mineralogy
C -Clay lamina
S -Silt lamina

RHYTHM NUMBER	GEO-CHEM	REE	MIN	GRAIN SIZE	DESCRIPTION
SECTION 87-19					
61	C				grey rhythmite
56	C				grey rhythmite
51	C			C	grey rhythmite
46	C,S	C	C,S	S	grey rhythmite
41	C			C	grey rhythmite
36	C,S				grey rhythmite
31	C			C	grey rhythmite
26	C,S	C	C	S	grey rhythmite
25	C			C	grey rhythmite
24	C				grey rhythmite
23	C			C	grey rhythmite
22	C				grey rhythmite
21	C			C,S	grey rhythmite
20	C				red rhythmite
19	C			C	red rhythmite
18	C				red rhythmite
17	C			C	red rhythmite
16	C				red rhythmite
15	C,S	C	C,S	C	red rhythmite
14	C				red rhythmite
13	C			C	red rhythmite
12	C				red rhythmite
11	C,S			C,S	red rhythmite
10	C,S	C			red rhythmite
9	C,S			C,S	red rhythmite
8	C				red rhythmite
7	C			C	red rhythmite
6	C				red rhythmite
5	C,S	C	C	C	red rhythmite
4	C				red rhythmite
3	C			C	red rhythmite
2	C				red rhythmite
1	C			C	red rhythmite
0	C				red rhythmite
-1	C			C	red rhythmite
-2	C				grey rhythmite
-3	C			C,S	grey rhythmite
-4	C				grey rhythmite
-5	C,S	C	C	C,S	grey rhythmite
-10	C,S				grey rhythmite
-15	C,S			C	grey rhythmite
-20	C	C	C,S		grey rhythmite
-25	C			C	grey rhythmite
-30	C				grey rhythmite
-35	C			C	grey rhythmite

RHYTHM NUMBER	GEO-CHEM	REE	MIN	GRAIN SIZE	DESCRIPTION
SECTION 87-1					
28	C				grey rhythmite
23	C				grey rhythmite
18	C				grey rhythmite
17	C				grey rhythmite
16	C				grey rhythmite
15	C				grey rhythmite
14	C				grey rhythmite
13	C				grey rhythmite
12	C				red rhythmite
11	C				red rhythmite
10	C				red rhythmite
9	C				red rhythmite
8	C				red rhythmite
7	C				red rhythmite
6	C				red rhythmite
5	C				red rhythmite
4	C				red rhythmite
3	C				red rhythmite
2	C				red rhythmite
1	C				red rhythmite
0	C				red rhythmite
-1	C				grey rhythmite
-2	C				grey rhythmite
-3	C				grey rhythmite
-4	C				grey rhythmite
-5	C				grey rhythmite
-10	C				grey rhythmite
-15	C				grey rhythmite
-20	C				grey rhythmite
-25	C				grey rhythmite
-30	C				grey rhythmite
-35	C				grey rhythmite
-40	C				grey rhythmite
-45	C				grey rhythmite
-50	C				grey rhythmite

RHYTHM NUMBER	GEO-CHEM	REE	MIN	GRAIN SIZE	DESCRIPTION
OTHER SAMPLES					
89TB 01A	C				Thunder Bay red till
89TB 01B	C	C			Thunder Bay red till
89TB 02	C				L. Kam. red clay
89TB 03A	C				L. Kam. red clay
89TB 03B	C	C	C	C	L. Kam. red clay
89TB 04	C				L. Kam. red clay
89TB 05	C				L. Kam. red clay
82-08	C				L. Kam. red clay
82-10A	C				L. Kam. red clay
82-10B	C	C	C	C	L. Kam. red clay
82-12	C				L. Kam. red clay
82-14	C				L. Kam. red clay
F-87-07	C				Ft. Frances red clay
F-88-01	C	C	C	C	Ft. Frances red clay
F-88-25	C				Ft. Frances red clay
F-1	C				Ft. Frances red clay
F-2	C				Ft. Frances red clay
NB-380	C	C	C	C	Ft. Frances red clay
NB-383	C				Ft. Frances red clay
E-165	C				Ft. Frances red clay
E-311	C				Ft. Frances red clay
E-349	C				Ft. Frances red clay

APPENDIX C

GEOCHEMICAL RESULTS FOR ANALYSES PERFORMED ON SAMPLES FROM SECTIONS 87-1, 87-19, AND THE FORT FRANCES AND KAMINISTIKWIA AREAS.

See Fig. 2-1 for locations of sections 87-1, and 87-19, Appendix A for annotated logs of the sections, and Appendix B for sample descriptions. "+61" designations refer to the rhythmite number, where rhythmite "0" is the lowermost red-clay rhythmite in sections 87-1 and 87-19.

Chemex Labs Ltd.
Analytical Chemists * Geochemists * Registered Assayers
450 MATHESON BLVD. E., UNIT 54, MISSISSAUGA,
ONTARIO, CANADA L4Z-1R5
PHONE (416) 890-0110

To: UNIVERSTIY OF MANITOBA
DEPARTMENT OF GEOLOGICAL SCIENCES
240 WALLACE BUILDING
WINNIPEG, MB
R3T 2N2

A8921113

Comments: ATTN: TIM WARMAN

CERTIFICATE A8921113

UNIVERSTIY OF MANITOBA
PROJECT :
P.O.# : FG-04187

Samples submitted to our lab in Vancouver BC.
This report was printed on 11-AUG-89.

SAMPLE PREPARATION

CHEMEX CODE	NUMBER SAMPLES	DESCRIPTION
214	114	Received sample as pulp
238	114	ICP: Aqua regia digestion

* NOTE 1:

The 32 element ICP package is suitable for trace metals in soil and rock samples. Elements for which the nitric-aqua regia digestion is possibly incomplete are: Al, Ba, Be, Ca, Cr, Ga, K, La, Mg, Na, Sr, Ti, Tl, W.

ANALYTICAL PROCEDURES

CHEMEX CODE	NUMBER SAMPLES	DESCRIPTION	METHOD	DETECTION LIMIT	UPPER LIMIT
921	114	Al %: 32 element, soil & rock	ICP-AES	0.01	15.00
922	114	Ag ppm: 32 element, soil & rock	ICP-AES	0.2	200
923	114	As ppm: 32 element, soil & rock	ICP-AES	5	10000
924	114	Ba ppm: 32 element, soil & rock	ICP-AES	10	10000
925	114	Be ppm: 32 element, soil & rock	ICP-AES	0.5	100.0
926	114	Bi ppm: 32 element, soil & rock	ICP-AES	2	10000
927	114	Ca %: 32 element, soil & rock	ICP-AES	0.01	15.00
928	114	Cd ppm: 32 element, soil & rock	ICP-AES	0.5	100.0
929	114	Co ppm: 32 element, soil & rock	ICP-AES	1	10000
930	114	Cr ppm: 32 element, soil & rock	ICP-AES	1	10000
931	114	Cu ppm: 32 element, soil & rock	ICP-AES	1	10000
932	114	Fe %: 32 element, soil & rock	ICP-AES	0.01	15.00
933	114	Ga ppm: 32 element, soil & rock	ICP-AES	10	10000
951	114	Hg ppm: 32 element, soil & rock	ICP-AES	1	10000
934	114	K %: 32 element, soil & rock	ICP-AES	0.01	10.00
935	114	La ppm: 32 element, soil & rock	ICP-AES	10	10000
936	114	Mg %: 32 element, soil & rock	ICP-AES	0.01	15.00
937	114	Mn ppm: 32 element, soil & rock	ICP-AES	5	10000
938	114	Mo ppm: 32 element, soil & rock	ICP-AES	1	10000
939	114	Na %: 32 element, soil & rock	ICP-AES	0.01	5.00
940	114	Ni ppm: 32 element, soil & rock	ICP-AES	1	10000
941	114	P ppm: 32 element, soil & rock	ICP-AES	10	10000
942	114	Pb ppm: 32 element, soil & rock	ICP-AES	2	10000
943	114	Sb ppm: 32 element, soil & rock	ICP-AES	5	10000
958	114	Sc ppm: 32 elements, soil & rock	ICP-AES	1	100000
944	114	Sr ppm: 32 element, soil & rock	ICP-AES	1	10000
945	114	Ti %: 32 element, soil & rock	ICP-AES	0.01	5.00
946	114	Tl ppm: 32 element, soil & rock	ICP-AES	10	10000
947	114	U ppm: 32 element, soil & rock	ICP-AES	10	10000
948	114	V ppm: 32 element, soil & rock	ICP-AES	1	10000
949	114	W ppm: 32 element, soil & rock	ICP-AES	10	10000
950	114	Zn ppm: 32 element, soil & rock	ICP-AES	2	10000
451	114	FeO %: Acid decomposition	TITRATION	0.01	100.0

Chemex Labs Ltd.
Analytical Chemists * Geochemists * Registered Assayers
450 MATHESON BLVD. E., UNIT 54, MISSISSAUGA,
ONTARIO, CANADA L4Z-1R5
PHONE (416) 890-9110

To: UNIVERSTIY OF MANITOBA
DEPARTMENT OF GEOLOGICAL SCIENCES
240 WALLACE BUILDING
WINNIPEG, MB
R3T 2N2
Project :
Comments: ATTN: TIM WARMAN

Date : 11-AUG-89
Invoice # : I-8921113
P.O. # : FG-04187

CERTIFICATE OF ANALYSIS A8921113

SAMPLE DESCRIPTION	PREP CODE		Al %	Ag ppm	As ppm	Ba ppm	Be ppm	Bi ppm	Ca %	Cd ppm	Co ppm	Cr ppm	Cu ppm	Fe %	Ga ppm	Hg ppm	K %	La ppm	Mg %	Mn ppm	Mo ppm
87-019 +061C	214	238	3.45	0.2	5	230	< 0.5	2	4.70	< 0.5	21	94	62	4.21	20	< 1	0.73	30	2.36	745	< 1
87-019 +056C	214	238	3.54	0.2	10	230	< 0.5	< 2	5.03	< 0.5	20	95	115	4.35	20	< 1	0.74	20	2.30	730	< 1
87-019 +051C	214	238	3.69	0.4	10	240	< 0.5	2	4.43	< 0.5	21	104	84	4.61	10	1	0.75	30	2.31	755	< 1
87-019 +046C	214	238	3.41	0.2	< 5	230	< 0.5	< 2	3.17	< 0.5	20	94	65	4.29	10	< 1	0.72	30	2.26	680	< 1
87-019 +041C	214	238	3.92	0.4	< 5	260	< 0.5	< 2	3.42	0.5	22	107	85	4.82	10	< 1	0.80	40	2.40	720	< 1
87-019 +036C	214	238	4.10	0.2	< 5	250	< 0.5	< 2	4.77	0.5	22	108	118	4.96	10	< 1	0.82	30	2.40	780	< 1
87-019 +031C	214	238	3.85	0.2	5	250	< 0.5	< 2	3.94	< 0.5	22	105	78	4.84	10	< 1	0.78	30	2.36	720	< 1
87-019 +026C	214	238	3.98	0.2	< 5	260	< 0.5	< 2	3.90	0.5	22	103	100	4.91	10	< 1	0.78	30	2.38	765	< 1
87-019 +025C	214	238	4.02	0.2	< 5	260	< 0.5	< 2	4.36	< 0.5	23	107	112	4.92	10	< 1	0.80	30	2.49	805	< 1
87-019 +024C	214	238	4.07	0.4	5	260	< 0.5	< 2	4.11	< 0.5	24	104	127	5.07	10	< 1	0.80	30	2.47	750	< 1
87-019 +023C	214	238	3.96	0.2	10	270	< 0.5	4	4.07	< 0.5	22	103	104	4.99	10	1	0.79	30	2.46	695	< 1
87-019 +022C	214	238	3.94	0.2	< 5	270	< 0.5	< 2	3.56	< 0.5	23	107	93	4.91	10	< 1	0.80	40	2.46	725	< 1
87-019 +021C	214	238	4.10	0.2	< 5	270	< 0.5	< 2	3.94	< 0.5	23	103	116	5.06	10	< 1	0.82	40	2.53	715	< 1
87-019 +020C	214	238	4.03	0.4	< 5	260	< 0.5	< 2	3.84	< 0.5	23	103	105	5.10	10	< 1	0.77	30	2.67	710	< 1
87-019 +019C	214	238	4.17	< 0.2	10	270	< 0.5	< 2	4.10	< 0.5	25	103	98	5.22	10	< 1	0.82	30	2.79	775	< 1
87-019 +018C	214	238	3.80	0.2	5	250	< 0.5	< 2	3.89	< 0.5	25	92	97	4.92	10	< 1	0.72	30	2.69	770	< 1
87-019 +017C	214	238	3.99	0.4	< 5	260	< 0.5	< 2	4.07	< 0.5	25	98	109	5.09	10	< 1	0.75	30	2.81	815	< 1
87-019 +016C	214	238	4.14	0.2	< 5	260	< 0.5	< 2	4.53	< 0.5	26	94	107	5.26	10	< 1	0.76	30	3.04	785	< 1
87-019 +015C	214	238	4.10	< 0.2	5	270	< 0.5	< 2	4.19	< 0.5	26	94	99	5.22	10	1	0.75	30	3.03	825	1
87-019 +014C	214	238	4.00	0.2	15	260	< 0.5	< 2	3.90	< 0.5	25	91	157	5.10	10	< 1	0.72	30	2.98	725	< 1
87-019 +013C	214	238	3.85	0.4	< 5	240	< 0.5	< 2	4.40	< 0.5	24	88	102	4.85	20	< 1	0.69	20	2.95	755	< 1
87-019 +012C	214	238	3.75	0.2	20	220	< 0.5	< 2	4.57	< 0.5	24	81	111	4.69	10	< 1	0.65	20	2.96	785	< 1
87-019 +011C	214	238	3.83	0.2	< 5	230	< 0.5	< 2	4.49	< 0.5	25	87	115	4.80	20	< 1	0.68	20	3.04	785	< 1
87-019 +010C	214	238	4.11	< 0.2	15	270	< 0.5	< 2	3.98	< 0.5	26	96	152	5.10	20	< 1	0.74	30	3.19	800	< 1
87-019 +009C	214	238	4.11	< 0.2	5	240	< 0.5	< 2	4.80	< 0.5	26	88	132	4.95	20	< 1	0.72	20	3.21	850	< 1
87-019 +008C	214	238	4.18	< 0.2	5	260	< 0.5	< 2	4.29	< 0.5	27	97	195	5.08	20	< 1	0.74	30	3.24	830	< 1
87-019 +007C	214	238	3.86	0.2	< 5	230	< 0.5	< 2	3.84	< 0.5	24	89	125	4.70	20	< 1	0.70	30	3.01	690	< 1
87-019 +006C	214	238	3.91	0.2	< 5	240	< 0.5	< 2	4.04	0.5	24	91	133	4.75	20	< 1	0.71	20	3.10	735	< 1
87-019 +005C	214	238	3.92	< 0.2	< 5	240	< 0.5	< 2	4.53	< 0.5	24	91	126	4.80	10	< 1	0.69	20	3.17	780	< 1
87-019 +004C	214	238	3.68	< 0.2	< 5	210	< 0.5	< 2	4.72	< 0.5	24	77	120	4.50	20	< 1	0.61	10	3.03	790	< 1
87-019 +003C	214	238	4.03	< 0.2	10	250	< 0.5	< 2	4.07	< 0.5	24	97	140	5.19	10	< 1	0.70	30	3.28	750	< 1
87-019 +002C	214	238	3.96	< 0.2	< 5	250	< 0.5	< 2	3.54	< 0.5	26	93	139	5.22	10	< 1	0.68	30	3.34	835	< 1
87-019 +001C	214	238	3.91	0.2	< 5	240	< 0.5	< 2	4.65	0.5	20	108	180	4.57	20	< 1	0.81	30	2.29	760	< 1
87-019 +000C	214	238	4.43	< 0.2	< 5	300	< 0.5	< 2	3.41	0.5	26	115	168	5.59	20	1	0.84	40	2.97	875	< 1
87-019 -001C	214	238	4.13	< 0.2	15	280	< 0.5	< 2	3.31	< 0.5	22	109	133	4.96	20	< 1	0.83	40	2.43	775	< 1
87-019 -002C	214	238	4.03	0.2	< 5	280	< 0.5	< 2	3.48	< 0.5	21	108	95	4.83	20	< 1	0.83	40	2.33	795	< 1
87-019 -003C	214	238	4.26	< 0.2	< 5	280	< 0.5	< 2	4.45	< 0.5	23	115	79	5.10	20	< 1	0.87	30	2.44	840	< 1
87-019 -004C	214	238	4.15	< 0.2	15	270	< 0.5	< 2	4.54	< 0.5	21	114	76	4.97	20	< 1	0.86	30	2.49	785	< 1
87-019 -005C	214	238	3.89	< 0.2	< 5	240	< 0.5	< 2	4.46	< 0.5	21	110	90	4.72	20	< 1	0.78	30	2.29	755	< 1
87-019 -010C	214	238	4.16	< 0.2	< 5	270	< 0.5	2	4.93	< 0.5	20	117	102	4.92	10	< 1	0.86	30	2.41	730	< 1

CERTIFICATION : B. Cargi

Chemex Labs Ltd.
Analytical Chemists * Geochemists * Registered Assayers
450 MATHESON BLVD. E., UNIT 54, MISSISSAUGA, ONTARIO, CANADA L4Z-1R5
PHONE (416) 890-0110

To: UNIVERSTIY OF MANITOBA
DEPARTMENT OF GEOLOGICAL SCIENCES
240 WALLACE BUILDING
WINNIPEG, MB
R3T 2N2
Project :
Comments: ATTN: TIM WARMAN

**Page No. :1-B
Tot. Pages: 3
Date :11-AUG-89
Invoice # :I-8921113
P.O. # :FG-04187

CERTIFICATE OF ANALYSIS A8921113

SAMPLE DESCRIPTION	PREP CODE		Na %	Ni ppm	[illegible] ppm	Pb ppm	Sb ppm	Mo ppm	Sr ppm	Ti %	Tl ppm	U ppm	V ppm	W ppm	Zn ppm	FeO %
87-019 +061C	214	238	0.07	51	520	2	5	10	56	0.24	< 10	< 10	80	< 10	106	1.61
87-019 +056C	214	238	0.06	54	470	< 2	5	10	56	0.23	< 10	< 10	81	< 10	118	1.97
87-019 +051C	214	238	0.07	56	460	8	< 5	10	52	0.24	< 10	< 10	83	< 10	116	1.66
87-019 +046C	214	238	0.07	49	480	4	< 5	9	45	0.24	< 10	< 10	79	< 10	106	1.98
87-019 +041C	214	238	0.08	53	450	8	< 5	11	50	0.26	< 10	< 10	85	< 10	120	1.99
87-019 +036C	214	238	0.08	56	440	2	< 5	12	57	0.26	< 10	< 10	88	< 10	126	1.92
87-019 +031C	214	238	0.08	53	450	2	5	11	51	0.25	< 10	< 10	85	< 10	116	1.87
87-019 +026C	214	238	0.08	53	450	4	< 5	11	51	0.24	< 10	< 10	85	< 10	120	1.74
87-019 +025C	214	238	0.09	55	460	8	< 5	12	55	0.25	< 10	< 10	86	< 10	124	1.72
87-019 +024C	214	238	0.09	56	440	6	< 5	12	52	0.24	< 10	< 10	84	< 10	126	1.74
87-019 +023C	214	238	0.09	56	440	14	5	11	52	0.24	< 10	< 10	83	< 10	122	1.89
87-019 +022C	214	238	0.09	54	460	2	5	11	51	0.26	< 10	< 10	84	< 10	120	1.88
87-019 +021C	214	238	0.09	57	460	2	< 5	12	53	0.26	< 10	< 10	85	< 10	124	1.86
87-019 +020C	214	238	0.09	61	440	6	< 5	12	50	0.24	< 10	< 10	84	< 10	120	1.90
87-019 +019C	214	238	0.10	58	460	6	5	13	54	0.25	< 10	< 10	90	< 10	118	1.82
87-019 +018C	214	238	0.09	53	440	< 2	< 5	12	49	0.22	< 10	< 10	80	< 10	112	1.81
87-019 +017C	214	238	0.09	58	450	6	< 5	12	50	0.22	< 10	< 10	82	< 10	114	1.69
87-019 +016C	214	238	0.10	60	450	< 2	< 5	13	52	0.21	< 10	< 10	81	< 10	114	1.35
87-019 +015C	214	238	0.11	64	480	6	5	13	51	0.21	< 10	< 10	86	< 10	112	1.51
87-019 +014C	214	238	0.10	59	470	< 2	5	12	48	0.20	< 10	< 10	82	< 10	120	1.54
87-019 +013C	214	238	0.09	54	460	10	< 5	12	48	0.19	< 10	< 10	81	< 10	106	1.08
87-019 +012C	214	238	0.09	51	450	< 2	5	11	48	0.18	< 10	< 10	80	< 10	100	1.79
87-019 +011C	214	238	0.10	57	470	< 2	5	12	50	0.19	< 10	< 10	83	< 10	106	1.46
87-019 +010C	214	238	0.12	65	500	4	10	12	51	0.21	< 10	< 10	91	< 10	118	1.34
87-019 +009C	214	238	0.10	60	500	2	< 5	12	52	0.19	< 10	< 10	84	< 10	110	1.39
87-019 +008C	214	238	0.12	67	480	2	5	13	51	0.21	< 10	< 10	91	< 10	124	1.40
87-019 +007C	214	238	0.11	56	450	6	< 5	11	46	0.19	< 10	< 10	81	< 10	104	1.39
87-019 +006C	214	238	0.11	56	430	< 2	< 5	12	47	0.20	< 10	< 10	83	< 10	108	1.23
87-019 +005C	214	238	0.11	62	480	2	5	12	50	0.18	< 10	< 10	82	< 10	104	1.18
87-019 +004C	214	238	0.10	54	480	6	< 5	11	49	0.15	< 10	< 10	74	< 10	98	1.50
87-019 +003C	214	238	0.11	63	430	< 2	5	12	48	0.21	< 10	< 10	85	< 10	114	1.61
87-019 +002C	214	238	0.11	66	480	14	5	11	45	0.21	< 10	< 10	85	< 10	114	1.48
87-019 +001C	214	238	0.08	54	450	8	< 5	10	57	0.24	< 10	< 10	87	< 10	140	1.86
87-019 +000C	214	238	0.11	63	460	14	< 5	12	52	0.27	< 10	< 10	106	< 10	142	1.71
87-019 -001C	214	238	0.10	60	450	4	5	11	51	0.27	< 10	< 10	98	< 10	132	2.20
87-019 -002C	214	238	0.09	58	490	2	< 5	10	52	0.26	< 10	< 10	95	< 10	124	1.99
87-019 -003C	214	238	0.08	59	450	8	5	11	57	0.26	< 10	< 10	100	< 10	126	1.92
87-019 -004C	214	238	0.09	59	490	8	5	11	58	0.26	< 10	< 10	98	< 10	124	2.01
87-019 -005C	214	238	0.07	53	440	6	5	10	54	0.23	< 10	< 10	93	< 10	120	1.93
87-019 -010C	214	238	0.09	57	450	12	< 5	11	61	0.25	< 10	< 10	90	< 10	128	2.07

CERTIFICATION : B. Caghi

Chemex Labs Ltd.
Analytical Chemists * Geochemists * Registered Assayers
450 MATHESON BLVD. E., UNIT 54, MISSISSAUGA, ONTARIO, CANADA L4Z-1R5
PHONE (416) 890-0310

To: UNIVERSTIY OF MANITOBA
DEPARTMENT OF GEOLOGICAL SCIENCES
240 WALLACE BUILDING
WINNIPEG, MB
R3T 2N2

Project :
Comments: ATTN: TIM WARMAN

Date :11-AUG-89
Invoice # :I-8921113
P.O. # :FG-04187

CERTIFICATE OF ANALYSIS A8921113

SAMPLE DESCRIPTION	PREP CODE		Al %	Ag ppm	As ppm	Ba ppm	Be ppm	Bi ppm	Ca %	Cd ppm	Co ppm	Cr ppm	Cu ppm	Fe %	Ga ppm	Hg ppm	K %	La ppm	Mg %	Mn ppm	Mo ppm
87-019 -015C	214	238	3.78	0.2	15	260	< 0.5	< 2	4.23	< 0.5	21	105	122	4.60	10	< 1	0.81	30	2.28	770	< 1
87-019 -020C	214	238	4.05	< 0.2	< 5	270	< 0.5	< 2	3.62	0.5	25	99	146	5.46	10	< 1	0.73	30	3.25	795	< 1
87-019 -025C	214	238	4.16	< 0.2	< 5	270	< 0.5	< 2	4.74	< 0.5	22	113	137	5.09	10	< 1	0.86	30	2.44	810	< 1
87-019 -030C	214	238	3.81	0.2	< 5	250	< 0.5	< 2	4.14	< 0.5	21	103	89	4.72	10	< 1	0.81	30	2.32	755	< 1
87-019 -035C	214	238	3.80	0.2	< 5	260	< 0.5	< 2	3.91	0.5	22	103	113	4.70	10	< 1	0.80	40	2.28	855	< 1
87-001 +033C	214	238	2.98	0.2	5	180	< 0.5	< 2	2.02	< 0.5	18	82	47	4.00	10	< 1	0.52	50	1.95	715	2
87-001 +028C	214	238	3.25	< 0.2	5	190	< 0.5	< 2	2.98	< 0.5	18	88	48	4.28	10	< 1	0.58	40	2.15	760	5
87-001 +023C	214	238	3.68	< 0.2	< 5	230	< 0.5	< 2	3.45	< 0.5	21	99	75	4.78	10	< 1	0.66	40	2.48	825	< 1
87-001 +018C	214	238	3.06	< 0.2	10	190	< 0.5	< 2	4.06	< 0.5	18	79	60	3.91	10	1	0.54	30	2.30	730	4
87-001 +017C	214	238	4.06	0.4	15	270	< 0.5	< 2	3.95	< 0.5	24	100	84	5.05	20	1	0.76	40	2.68	840	< 1
87-001 +016C	214	238	3.98	0.4	< 5	270	< 0.5	4	3.81	0.5	25	100	74	4.95	20	< 1	0.75	40	2.65	810	< 1
87-001 +015C	214	238	3.86	0.6	< 5	270	< 0.5	8	3.53	< 0.5	24	96	76	4.81	20	< 1	0.73	40	2.57	795	< 1
87-001 +014C	214	238	3.77	0.4	< 5	250	< 0.5	< 2	3.88	< 0.5	24	91	73	4.76	20	1	0.70	30	2.65	735	< 1
87-001 +013C	214	238	4.24	0.2	< 5	280	< 0.5	< 2	4.11	< 0.5	25	100	89	5.36	20	2	0.77	30	3.06	805	< 1
87-001 +012C	214	238	3.99	0.4	< 5	270	< 0.5	4	4.30	< 0.5	25	91	86	5.08	20	1	0.72	30	2.94	800	< 1
87-001 +011C	214	238	4.10	0.4	10	270	< 0.5	2	4.98	< 0.5	26	95	86	5.14	20	1	0.73	20	3.00	780	< 1
87-001 +010C	214	238	3.98	0.2	< 5	260	< 0.5	< 2	5.38	< 0.5	25	86	90	4.98	20	1	0.68	10	3.03	805	< 1
87-001 +009C	214	238	3.92	0.2	< 5	250	< 0.5	< 2	5.34	< 0.5	25	81	88	4.96	10	< 1	0.65	10	3.17	820	< 1
87-001 +008C	214	238	4.13	0.2	< 5	270	< 0.5	4	5.63	< 0.5	26	86	98	5.15	10	< 1	0.69	10	3.23	880	< 1
87-001 +007C	214	238	4.15	0.2	< 5	270	< 0.5	< 2	5.46	< 0.5	27	86	94	5.16	20	< 1	0.70	10	3.21	845	< 1
87-001 +006C	214	238	3.72	0.2	10	230	< 0.5	< 2	5.22	< 0.5	25	77	83	4.75	10	< 1	0.58	10	2.96	820	< 1
87-001 +005C	214	238	3.74	< 0.2	< 5	240	< 0.5	< 2	6.60	0.5	24	75	87	4.77	10	1	0.57	< 10	3.05	800	< 1
87-001 +004C	214	238	3.71	< 0.2	< 5	240	< 0.5	< 2	6.56	0.5	24	81	91	4.88	10	1	0.57	< 10	3.16	780	< 1
87-001 +003C	214	238	3.76	0.2	20	250	< 0.5	2	4.99	< 0.5	25	81	91	4.99	10	< 1	0.57	20	3.20	770	< 1
87-001 +002C	214	238	2.96	< 0.2	< 5	180	< 0.5	< 2	6.56	< 0.5	18	62	71	3.91	10	< 1	0.42	< 10	2.75	630	4
87-001 +001C	214	238	3.76	0.2	< 5	240	< 0.5	2	5.52	0.5	25	80	85	4.78	10	< 1	0.59	10	3.26	880	< 1
87-001 000C	214	238	3.08	< 0.2	< 5	200	< 0.5	2	5.42	< 0.5	18	82	48	3.79	10	< 1	0.55	10	2.23	620	4
87-001 -001C	214	238	3.59	0.2	< 5	250	< 0.5	< 2	6.07	< 0.5	20	100	54	4.26	20	< 1	0.69	10	2.27	720	< 1
87-001 -002C	214	238	4.05	0.2	20	280	< 0.5	< 2	6.54	< 0.5	21	111	59	4.74	20	< 1	0.79	10	2.40	740	1
87-001 -003C	214	238	3.82	< 0.2	< 5	270	< 0.5	2	6.03	< 0.5	21	102	58	4.51	20	< 1	0.74	10	2.30	715	< 1
87-001 -004C	214	238	4.17	0.4	< 5	280	< 0.5	2	5.01	0.5	23	108	61	4.91	20	< 1	0.85	30	2.38	825	< 1
87-001 -005C	214	238	4.03	0.2	5	270	< 0.5	< 2	4.95	< 0.5	21	103	62	4.79	20	< 1	0.82	30	2.30	795	< 1
87-001 -010C	214	238	3.34	0.2	< 5	250	< 0.5	2	2.97	< 0.5	18	86	49	4.02	10	< 1	0.67	40	2.03	680	6
87-001 -015C	214	238	3.75	0.4	< 5	260	< 0.5	2	4.55	< 0.5	20	98	55	4.44	20	< 1	0.75	30	2.28	770	< 1
87-001 -020C	214	238	3.66	0.2	10	250	< 0.5	< 2	4.37	< 0.5	20	93	51	4.43	20	< 1	0.75	30	2.40	745	< 1
87-001 -025C	214	238	3.03	0.2	< 5	190	< 0.5	< 2	6.51	< 0.5	17	84	44	3.66	20	< 1	0.60	< 10	2.17	700	2
87-001 -030C	214	238	3.42	0.2	15	220	< 0.5	< 2	4.31	< 0.5	19	91	47	4.15	20	< 1	0.67	30	2.31	745	6
87-001 -035C	214	238	3.13	0.2	< 5	200	< 0.5	2	4.56	< 0.5	18	85	49	3.85	20	< 1	0.61	20	2.25	710	4
87-001 -040C	214	238	2.33	< 0.2	5	140	< 0.5	< 2	4.47	< 0.5	15	71	57	3.02	10	1	0.44	20	1.99	595	< 1
87-001 -045C	214	238	2.72	0.2	< 5	170	< 0.5	< 2	3.03	< 0.5	17	81	39	3.50	10	< 1	0.52	30	1.98	670	< 1

CERTIFICATION : B. Caughlin

Chemex Labs Ltd.
Analytical Chemists * Geochemists * Registered Assayers
450 MATHESON BLVD., E., UNIT 54, MISSISSAUGA, ONTARIO, CANADA L4Z-1R5
PHONE (416) 890-0310

To: UNIVERSTIY OF MANITOBA
DEPARTMENT OF GEOLOGICAL SCIENCES
240 WALLACE BUILDING
WINNIPEG, MB
R3T 2N2
Project :
Comments: ATTN: TIM WARMAN

Date : 11-AUG-89
Invoice # : I-8921113
P.O. # : FG-04187

CERTIFICATE OF ANALYSIS A8921113

SAMPLE DESCRIPTION	PREP CODE		Na %	Ni ppm	P ppm	Pb ppm	Sb ppm	Sc ppm	Sr ppm	Ti %	Tl ppm	U ppm	V ppm	W ppm	Zn ppm	FeO %
87-019 -015C	214	238	0.08	55	460	14	< 5	10	55	0.25	< 10	< 10	86	< 10	126	1.74
87-019 -020C	214	238	0.11	64	430	6	5	12	47	0.24	< 10	< 10	88	< 10	122	1.38
87-019 -025C	214	238	0.09	57	480	10	5	11	60	0.25	< 10	< 10	91	< 10	136	1.51
87-019 -030C	214	238	0.09	52	500	10	< 5	10	57	0.25	< 10	< 10	87	< 10	120	1.94
87-019 -035C	214	238	0.09	52	490	10	< 5	10	55	0.24	< 10	< 10	82	< 10	124	1.44
87-001 +033C	214	238	0.08	46	540	8	5	9	42	0.23	< 10	< 10	73	< 10	88	1.81
87-001 +028C	214	238	0.07	49	420	12	5	9	44	0.22	< 10	< 10	75	< 10	92	1.73
87-001 +023C	214	238	0.09	57	480	8	< 5	11	50	0.25	< 10	< 10	83	< 10	106	1.58
87-001 +018C	214	238	0.09	48	480	8	< 5	9	52	0.22	< 10	< 10	72	< 10	88	1.62
87-001 +017C	214	238	0.11	62	450	4	10	12	53	0.24	< 10	< 10	89	< 10	114	1.96
87-001 +016C	214	238	0.12	59	500	2	< 5	12	54	0.25	< 10	< 10	86	< 10	110	1.82
87-001 +015C	214	238	0.11	61	470	12	< 5	12	52	0.24	< 10	< 10	85	< 10	110	1.76
87-001 +014C	214	238	0.10	52	440	2	< 5	12	50	0.22	< 10	< 10	80	< 10	104	1.96
87-001 +013C	214	238	0.12	62	470	2	5	13	53	0.23	< 10	< 10	91	< 10	114	1.69
87-001 +012C	214	238	0.11	62	450	2	< 5	13	52	0.22	< 10	< 10	83	< 10	108	1.21
87-001 +011C	214	238	0.11	67	420	12	5	13	53	0.21	< 10	< 10	85	< 10	108	1.04
87-001 +010C	214	238	0.11	62	460	10	5	13	54	0.19	< 10	< 10	79	< 10	100	1.37
87-001 +009C	214	238	0.12	59	500	10	< 5	13	54	0.19	< 10	< 10	82	< 10	98	1.62
87-001 +008C	214	238	0.11	68	460	6	< 5	13	53	0.18	< 10	< 10	81	< 10	102	1.38
87-001 +007C	214	238	0.11	65	470	12	5	13	54	0.18	< 10	< 10	82	< 10	102	1.43
87-001 +006C	214	238	0.09	63	440	4	< 5	11	50	0.16	< 10	< 10	73	< 10	94	1.42
87-001 +005C	214	238	0.10	60	460	4	< 5	11	54	0.15	< 10	< 10	72	< 10	94	1.29
87-001 +004C	214	238	0.11	59	470	8	5	12	56	0.17	< 10	< 10	75	< 10	96	1.43
87-001 +003C	214	238	0.12	64	460	8	5	12	51	0.18	< 10	< 10	78	< 10	100	1.79
87-001 +002C	214	238	0.10	44	460	< 2	< 5	10	54	0.15	< 10	< 10	67	< 10	74	1.49
87-001 +001C	214	238	0.11	62	450	< 2	< 5	11	53	0.17	< 10	< 10	73	< 10	92	1.67
87-001 000C	214	238	0.09	48	470	< 2	< 5	9	58	0.20	< 10	< 10	73	< 10	86	1.99
87-001 -001C	214	238	0.09	49	400	8	5	10	62	0.23	< 10	< 10	84	< 10	102	2.03
87-001 -002C	214	238	0.10	57	420	14	5	11	67	0.25	< 10	< 10	91	< 10	112	2.02
87-001 -003C	214	238	0.09	53	390	14	10	11	63	0.24	< 10	< 10	87	< 10	108	2.11
87-001 -004C	214	238	0.11	57	430	10	< 5	12	63	0.26	< 10	< 10	92	< 10	114	2.02
87-001 -005C	214	238	0.09	57	410	6	5	11	60	0.25	< 10	< 10	89	< 10	112	1.87
87-001 -010C	214	238	0.10	49	490	2	5	9	49	0.24	< 10	< 10	78	< 10	96	1.80
87-001 -015C	214	238	0.10	50	430	4	< 5	11	57	0.25	< 10	< 10	83	< 10	108	1.82
87-001 -020C	214	238	0.09	56	470	2	5	10	57	0.26	< 10	< 10	85	< 10	108	2.12
87-001 -025C	214	238	0.07	44	430	< 2	5	9	58	0.22	< 10	< 10	72	< 10	88	1.76
87-001 -030C	214	238	0.08	47	450	6	5	10	53	0.24	< 10	< 10	84	< 10	100	2.02
87-001 -035C	214	238	0.08	45	480	2	5	9	53	0.23	< 10	< 10	79	< 10	92	1.89
87-001 -040C	214	238	0.06	38	480	8	10	7	46	0.19	< 10	< 10	62	< 10	74	1.81
87-001 -045C	214	238	0.07	43	560	4	5	8	44	0.21	< 10	< 10	71	< 10	84	2.02

CERTIFICATION : B. Caghi

Chemex Labs Ltd.
Analytical Chemists * Geochemists * Registered Assayers
450 MATHESON BLVD. E., UNIT 54, MISSISSAUGA, ONTARIO, CANADA L4Z-1R5
PHONE (416) 890-0310

To : UNIVERSTIY OF MANITOBA
DEPARTMENT OF GEOLOGICAL SCIENCES
240 WALLACE BUILDING
WINNIPEG, MB
R3T 2N2
Project :
Comments: ATTN: TIM WARMAN

Date : 11-AUG-89
Invoice # : I-8921113
P.O. # : FG-04187

CERTIFICATE OF ANALYSIS A8921113

SAMPLE DESCRIPTION	PREP CODE		Al %	Ag ppm	As ppm	Ba ppm	Be ppm	Bi ppm	Ca %	Cd ppm	Co ppm	Cr ppm	Cu ppm	Fe %	Ga ppm	Hg ppm	K %	La ppm	Mg %	Mn ppm	Mo ppm
87-001 -050C	214	238	2.89	0.2	< 5	190	0.5	4	3.15	< 0.5	17	82	55	3.71	20	< 1	0.60	40	2.10	680	2
87-019 +046S	214	238	1.55	< 0.2	< 5	100	< 0.5	4	5.50	< 0.5	10	53	28	2.12	10	< 1	0.34	10	2.07	430	< 1
87-019 +036S	214	238	1.21	< 0.2	5	70	< 0.5	< 2	6.08	< 0.5	8	43	23	1.76	10	< 1	0.24	< 10	2.11	380	< 1
87-019 +026S	214	238	1.24	0.2	< 5	70	< 0.5	< 2	6.16	< 0.5	8	43	25	1.73	10	< 1	0.26	< 10	2.13	400	< 1
87-019 +015S	214	238	1.78	< 0.2	< 5	110	0.5	< 2	5.56	< 0.5	12	56	179	2.46	10	< 1	0.33	< 10	2.20	580	< 1
87-019 +011S	214	238	1.12	< 0.2	< 5	70	< 0.5	< 2	5.26	< 0.5	8	39	43	1.68	10	< 1	0.21	< 10	1.94	385	< 1
87-019 +010S	214	238	1.32	< 0.2	< 5	80	< 0.5	2	4.83	< 0.5	11	43	110	1.93	10	1	0.24	< 10	1.92	460	< 1
87-019 +009S	214	238	1.08	< 0.2	< 5	70	< 0.5	4	5.34	< 0.5	7	37	23	1.65	10	1	0.19	< 10	1.97	350	< 1
87-019 +005S	214	238	1.09	< 0.2	< 5	60	< 0.5	2	5.68	< 0.5	7	39	75	1.63	10	< 1	0.19	< 10	2.05	365	< 1
87-019 -005S	214	238	1.04	< 0.2	< 5	60	< 0.5	2	5.18	< 0.5	7	38	56	1.55	10	< 1	0.21	< 10	1.89	360	< 1
87-019 -010S	214	238	0.98	< 0.2	< 5	60	< 0.5	2	6.07	< 0.5	8	36	27	1.49	10	< 1	0.19	< 10	2.04	400	1
87-019 -015S	214	238	1.37	< 0.2	10	90	< 0.5	2	5.62	< 0.5	10	46	57	1.92	10	1	0.31	< 10	1.97	435	< 1
89TB 01A	214	238	2.57	< 0.2	10	200	< 0.5	< 2	4.39	< 0.5	22	62	121	5.53	10	2	0.38	10	2.60	1005	6
89TB 01B	214	238	2.14	0.2	10	160	< 0.5	< 2	3.88	< 0.5	21	57	100	5.25	10	< 1	0.26	10	2.16	1085	1
89TB 02	214	238	3.27	< 0.2	5	220	< 0.5	< 2	6.74	< 0.5	24	71	120	4.31	10	< 1	0.45	< 10	3.01	765	< 1
89TB 03A	214	238	3.28	< 0.2	10	240	< 0.5	< 2	4.75	< 0.5	23	79	105	4.22	10	< 1	0.55	10	3.06	665	< 1
89TB 03B	214	238	3.32	< 0.2	5	230	< 0.5	2	6.21	< 0.5	24	75	108	4.39	10	< 1	0.51	< 10	3.05	730	< 1
89TB 04	214	238	3.37	< 0.2	15	230	< 0.5	< 2	6.70	< 0.5	23	73	87	4.41	10	< 1	0.52	< 10	3.13	755	< 1
89TB 05	214	238	3.96	0.2	< 5	310	< 0.5	< 2	5.31	< 0.5	28	81	132	5.13	20	< 1	0.68	10	3.44	880	< 1
82-08	214	238	3.44	< 0.2	5	280	< 0.5	2	6.04	< 0.5	26	79	112	4.69	10	1	0.53	< 10	3.29	785	< 1
82-10A	214	238	3.12	< 0.2	< 5	220	< 0.5	< 2	6.33	0.5	21	71	116	4.21	< 10	< 1	0.52	< 10	3.37	630	6
82-10B	214	238	3.10	< 0.2	20	220	< 0.5	< 2	6.26	< 0.5	20	67	116	4.11	< 10	3	0.52	< 10	3.33	625	5
82-12	214	238	3.33	< 0.2	< 5	210	< 0.5	< 2	7.07	< 0.5	20	68	153	4.21	< 10	< 1	0.50	< 10	3.08	640	< 1
82-14	214	238	3.61	< 0.2	5	300	< 0.5	< 2	5.97	< 0.5	23	78	127	5.00	< 10	< 1	0.55	< 10	3.57	800	< 1
P-87-07	214	238	3.42	0.2	< 5	200	< 0.5	< 2	1.79	< 0.5	20	68	97	4.47	< 10	< 1	0.36	30	2.96	785	< 1
P-88-01	214	238	1.67	< 0.2	< 5	180	< 0.5	< 2	6.06	< 0.5	17	41	67	2.33	< 10	2	0.30	< 10	3.41	1450	< 1
P-88-25	214	238	2.50	0.2	< 5	150	< 0.5	< 2	3.75	< 0.5	16	58	69	3.42	< 10	< 1	0.43	10	3.32	590	< 1
P-1	214	238	3.04	< 0.2	< 5	210	< 0.5	< 2	6.41	< 0.5	18	62	136	4.20	< 10	< 1	0.41	< 10	3.03	630	4
P-2	214	238	3.07	< 0.2	< 5	220	< 0.5	< 2	5.33	0.5	18	68	130	4.24	< 10	< 1	0.42	< 10	2.85	635	4
NB-380	214	238	4.71	< 0.2	< 5	280	< 0.5	< 2	0.66	1.0	35	100	142	6.16	< 10	< 1	0.43	40	2.16	630	< 1
NB-383	214	238	4.57	< 0.2	< 5	260	< 0.5	< 2	0.85	< 0.5	26	100	195	5.84	< 10	< 1	0.65	50	2.91	920	< 1
E-165	214	238	3.55	< 0.2	10	190	< 0.5	< 2	1.02	< 0.5	33	77	115	4.66	< 10	2	0.50	30	2.27	445	< 1
E-311	214	238	3.63	< 0.2	< 5	230	< 0.5	< 2	3.14	< 0.5	21	80	155	4.75	< 10	1	0.48	20	3.18	825	< 1
E-349	214	238	2.76	< 0.2	< 5	150	< 0.5	2	0.75	< 0.5	17	58	64	3.66	< 10	1	0.33	50	1.49	410	< 1

CERTIFICATION : B. Caughlin

Chemex Labs Ltd.
Analytical Chemists * Geochemists * Registered Assayers
450 MATHESON BLVD. E., UNIT 54, MISSISSAUGA, ONTARIO, CANADA L4Z-1R5
PHONE (416) 890-0310

To: UNIVERSTIY OF MANITOBA
DEPARTMENT OF GEOLOGICAL SCIENCES
240 WALLACE BUILDING
WINNIPEG, MB
R3T 2N2
Project :
Comments: ATTN: TIM WARMAN

**Page No. : 3-B
Tot. Pages: 3
Date : 11-AUG-89
Invoice # : I-8921113
P.O. # : FG-04187

CERTIFICATE OF ANALYSIS A8921113

SAMPLE DESCRIPTION	PREP CODE		Na %	Ni ppm	P ppm	Pb ppm	Sb ppm	Sc ppm	Sr ppm	Ti %	Tl ppm	U ppm	V ppm	W ppm	Zn ppm	FeO %
87-001 -050C	214	238	0.08	46	520	10	< 5	8	47	0.22	< 10	< 10	74	10	94	1.86
87-019 +046S	214	238	0.05	24	590	2	< 5	6	54	0.17	< 10	< 10	49	10	50	1.54
87-019 +036S	214	238	0.04	21	580	< 2	< 5	5	54	0.15	< 10	< 10	42	10	38	1.43
87-019 +026S	214	238	0.04	17	560	4	5	5	54	0.15	< 10	< 10	41	10	38	1.25
87-019 +015S	214	238	0.07	31	630	2	5	7	55	0.18	< 10	< 10	59	10	78	1.62
87-019 +011S	214	238	0.04	20	590	< 2	10	4	45	0.13	< 10	< 10	41	< 10	38	1.46
87-019 +010S	214	238	0.05	23	600	10	5	5	44	0.14	< 10	< 10	46	< 10	54	1.50
87-019 +009S	214	238	0.04	18	570	< 2	5	4	45	0.13	< 10	< 10	41	< 10	32	1.36
87-019 +005S	214	238	0.04	17	560	< 2	5	4	48	0.13	< 10	< 10	41	< 10	42	1.09
87-019 -005S	214	238	0.03	16	560	2	5	4	46	0.13	< 10	< 10	39	< 10	40	1.32
87-019 -010S	214	238	0.03	15	590	6	< 5	4	52	0.14	< 10	< 10	37	10	32	1.19
87-019 -015S	214	238	0.04	20	610	< 2	5	5	52	0.16	< 10	< 10	45	< 10	52	1.32
89TB 01A	214	238	0.11	53	620	6	5	9	41	0.15	< 10	< 10	93	10	108	1.84
89TB 01B	214	238	0.09	47	580	6	< 5	8	36	0.13	< 10	< 10	81	20	98	1.81
89TB 02	214	238	0.09	53	510	< 2	5	11	56	0.15	< 10	< 10	77	10	86	1.21
89TB 03A	214	238	0.10	55	480	< 2	5	10	51	0.13	< 10	< 10	72	10	94	1.73
89TB 03B	214	238	0.08	53	480	12	< 5	10	55	0.14	< 10	< 10	76	10	88	1.22
89TB 04	214	238	0.09	55	560	8	5	11	59	0.15	< 10	< 10	78	10	86	1.12
89TB 05	214	238	0.11	65	540	< 2	< 5	12	48	0.16	< 10	< 10	87	10	108	1.76
82-08	214	238	0.11	60	490	8	< 5	11	50	0.16	< 10	< 10	89	10	92	1.44
82-10A	214	238	0.12	50	530	2	< 5	10	73	0.15	< 10	< 10	69	10	90	2.40
82-10B	214	238	0.11	52	490	6	5	10	72	0.14	< 10	< 10	65	10	88	2.15
82-12	214	238	0.09	51	490	< 2	5	10	56	0.15	< 10	< 10	65	< 10	94	1.38
82-14	214	238	0.13	60	480	2	< 5	12	50	0.17	< 10	< 10	78	10	100	1.68
F-87-07	214	238	0.05	57	450	8	< 5	10	33	0.12	< 10	< 10	74	< 10	90	1.18
F-88-01	214	238	0.02	46	450	6	< 5	5	51	0.05	< 10	< 10	50	< 10	64	0.66
F-88-25	214	238	0.05	45	480	6	< 5	8	43	0.08	< 10	< 10	57	< 10	92	1.20
F-1	214	238	0.11	48	480	4	5	10	54	0.15	< 10	< 10	69	< 10	88	1.39
F-2	214	238	0.10	47	440	4	5	10	49	0.13	< 10	< 10	62	< 10	88	1.22
NB-380	214	238	0.04	62	290	2	< 5	14	36	0.17	< 10	< 10	93	< 10	98	0.75
NB-383	214	238	0.08	75	380	4	< 5	14	53	0.19	< 10	< 10	82	< 10	110	1.06
E-165	214	238	0.08	63	500	4	< 5	11	36	0.13	< 10	< 10	74	< 10	120	1.33
E-311	214	238	0.08	55	460	< 2	< 5	11	47	0.14	< 10	< 10	72	10	100	1.25
E-349	214	238	0.04	54	520	6	< 5	8	26	0.08	< 10	< 10	58	< 10	76	1.02

CERTIFICATION : B. Caglioni

Samples 87-19 clay units	Fe as FeO %	Fe3+ %	Fe3+ as Fe2O3 %	Fe2O3:FeO
87-019 +061C	5.43	3.82	4.24	2.63
87-019 +056C	5.61	3.64	4.04	2.05
87-019 +051C	5.95	4.29	4.76	2.87
87-019 +046C	5.53	3.55	3.95	1.99
87-019 +041C	6.22	4.23	4.69	2.36
87-019 +036C	6.40	4.48	4.97	2.59
87-019 +031C	6.24	4.37	4.85	2.60
87-019 +026C	6.33	4.59	5.10	2.93
87-019 +025C	6.35	4.63	5.14	2.99
87-019 +024C	6.54	4.80	5.33	3.06
87-019 +023C	6.44	4.55	5.05	2.67
87-019 +022C	6.33	4.45	4.94	2.63
87-019 +021C	6.53	4.67	5.18	2.79
87-019 +020C	6.58	4.68	5.19	2.73
87-019 +019C	6.73	4.91	5.45	3.00
87-019 +018C	6.35	4.54	5.04	2.78
87-019 +017C	6.57	4.88	5.41	3.20
87-019 +016C	6.79	5.44	6.03	4.47
87-019 +015C	6.73	5.22	5.80	3.84
87-019 +014C	6.58	5.04	5.59	3.63
87-019 +013C	6.26	5.18	5.75	5.32
87-019 +012C	6.05	4.26	4.73	2.64
87-019 +011C	6.19	4.73	5.25	3.60
87-019 +010C	6.58	5.24	5.82	4.34
87-019 +009C	6.39	5.00	5.55	3.99
87-019 +008C	6.55	5.15	5.72	4.09
87-019 +007C	6.06	4.67	5.19	3.73
87-019 +006C	6.13	4.90	5.44	4.42
87-019 +005C	6.19	5.01	5.56	4.71
87-019 +004C	5.81	4.31	4.78	3.19
87-019 +003C	6.70	5.09	5.64	3.51
87-019 +002C	6.73	5.25	5.83	3.94
87-019 +001C	5.90	4.04	4.48	2.41
87-019 +000C	7.21	5.50	6.11	3.57
87-019 -001C	6.40	4.20	4.66	2.12
87-019 -002C	6.23	4.24	4.71	2.37
87-019 -003C	6.58	4.66	5.17	2.69
87-019 -004C	6.41	4.40	4.89	2.43
87-019 -005C	6.09	4.16	4.62	2.39
87-019 -010C	6.35	4.28	4.75	2.29
87-019 -015C	5.93	4.19	4.66	2.68
87-019 -020C	7.04	5.66	6.29	4.56
87-019 -025C	6.57	5.06	5.61	3.72
87-019 -030C	6.09	4.15	4.61	2.37
87-019 -035C	6.06	4.62	5.13	3.56

Samples	Fe as FeO %	Fe3+ %	Fe3+ as Fe2O3 %	Fe203:FeO
87-19 silt units				
87-019 +046S	2.73	1.19	1.33	0.86
87-019 +036S	2.27	0.84	0.93	0.65
87-019 +026S	2.23	0.98	1.09	0.87
87-019 +015S	3.17	1.55	1.72	1.06
87-019 +011S	2.17	0.71	0.78	0.54
87-019 +010S	2.49	0.99	1.10	0.73
87-019 +009S	2.13	0.77	0.85	0.63
87-019 +005S	2.10	1.01	1.12	1.03
87-019 -005S	2.00	0.68	0.75	0.57
87-019 -010S	1.92	0.73	0.81	0.68
87-019 -015S	2.48	1.16	1.28	0.97
T-Bay red till				
89TB 01A	7.13	5.29	5.88	3.19
89TB 01B	6.77	4.96	5.51	3.04
L. Kam red clay				
89TB 02	5.56	4.35	4.83	3.99
89TB 03A	5.44	3.71	4.12	2.38
89TB 03B	5.66	4.44	4.93	4.04
89TB 04	5.69	4.57	5.07	4.53
89TB 05	6.62	4.86	5.39	3.06
82-08	6.05	4.61	5.12	3.55
82-10A	5.43	3.03	3.36	1.40
82-10B	5.30	3.15	3.50	1.63
82-12	5.43	4.05	4.50	3.26
82-14	6.45	4.77	5.29	3.15
Ft. Fran. red clay				
F-87-07	5.77	4.59	5.09	4.31
F-88-01	3.01	2.35	2.60	3.95
F-88-25	4.41	3.21	3.57	2.97
F-1	5.42	4.03	4.47	3.22
F-2	5.47	4.25	4.72	3.87
NB-380	7.95	7.20	7.99	10.65
NB-383	7.53	6.47	7.19	6.78
E-165	6.01	4.68	5.20	3.91
E-311	6.13	4.88	5.41	4.33
E-349	4.72	3.70	4.11	4.03

Chemex Labs Ltd.
Analytical Chemists * Geochemists * Registered Assayers
450 MATHESON BLVD. E., UNIT 14, MISSISSAUGA,
ONTARIO, CANADA L4Z-1R5
PHONE (416) 890-9611

To: UNIVERSITY OF MANITOBA
DEPARTMENT OF GEOLOGICAL SCIENCES
240 WALLACE BUILDING
WINNIPEG, MB
R3T 2N2
Project :
Comments: ATTN: TIM WARMAN

Date 13-SEP-89
Invoice # I-8921114
P O # FG-04187

CERTIFICATE OF ANALYSIS A8921114

SAMPLE DESCRIPTION	PREP CODE		Ce NAA ppm	Dy NAA ppm	Er NAA ppm	Eu NAA ppm	Gd NAA ppm	Ho NAA ppm	La NAA ppm	Lu NAA ppm	Nd NAA ppm	Pr NAA ppm	Sm NAA ppm	Tb NAA ppm	Th NAA ppm	Tm NAA ppm	U NAA ppm	Yb NAA ppm
87-019 +046C	299	—	44	2	< 20	0.3	< 50	< 1	26	0.1	24	< 10	3.1	0.5	10.0	< 1	< 1	1.0
87-019 +026C	299	—	48	3	< 20	0.6	< 50	< 1	33	0.1	28	< 20	3.7	0.5	11.0	< 1	< 1	1.2
87-019 +015C	299	—	42	4	< 20	0.9	< 50	3	30	0.3	23	< 15	4.3	0.2	11.0	< 1	< 1	1.5
87-019 +010C	299	—	51	4	< 20	0.7	< 50	< 1	28	0.2	23	< 15	4.0	0.3	10.0	< 1	1	1.3
87-019 +005C	299	—	55	4	< 20	0.8	< 50	< 1	28	0.3	21	< 20	4.3	0.3	9.0	< 1	< 1	1.4
87-019 -005C	299	—	57	3	< 20	0.7	< 50	< 1	33	0.2	26	< 20	4.1	0.2	11.0	< 1	< 1	0.9
87-019 -020C	299	—	46	2	< 20	0.5	< 50	< 1	28	0.2	22	< 20	3.5	0.2	10.0	< 1	< 1	0.9
89TB-01B	299	—	43	3	< 20	0.8	< 50	< 1	20	0.3	11	< 15	3.5	0.2	5.0	< 1	1	1.3
89TB-03B	299	—	51	5	< 20	0.7	< 50	< 1	25	0.3	17	< 20	4.4	0.2	7.0	< 1	< 1	1.7
82-10B	299	—	51	4	< 20	0.8	< 50	< 1	26	0.3	18	< 15	4.4	0.2	7.0	< 1	1	1.6
P-88-1	299	—	38	4	< 20	0.7	< 50	< 1	22	0.2	13	< 15	3.0	0.3	5.0	< 1	< 1	1.4
NB-380	299	—	58	5	< 20	0.9	< 50	< 1	28	0.3	17	< 5	4.0	0.4	8.0	< 1	< 1	1.3

CERTIFICATION :

APPENDIX D

CLAY MINERALOGY RESULTS FOR SAMPLES FROM SECTION 87-19 AT DRYDEN, AND SELECTED SAMPLES FROM FORT FRANCES AND THE KAMINISTIKWIA AREA.

See Fig. 2-1 for location of section 87-19, Appendix A for an annotated log of the section, and Appendix B for a description of the samples. Sample numbers ending in "C" are clay laminae, and those ending in "S" are silt laminae from the Facies 1 rhythmites in section 87-19.

CLAY MINERALOGY (RHYTHMITES AND MASSIVE CLAYS)

SAMPLE NUMBER	COLOUR	% KAOL	% CHL	% ILL	% EXP	COMMENTS
87-19 46C	GREY	0.1	21.8	57.6	20.2	A,C
87-19 26C	GREY	1.0	17.2	59.1	22.6	A,C
87-19 15C	RED	1.7	20.6	57.6	20.1	A,C
87-19 05C	RED	7.0	15.6	58.7	18.6	A,B,C
87-19 -05C	GREY	3.2	15.9	62.5	18.3	A,B,C
87-19 -20C	GREY	0.0	16.4	50.6	32.9	A,C
87-19 46S	GREY	0.0	17.9	61.7	20.3	C
87-19 15S	RED	1.2	16.7	64.8	17.9	A,C
87-19 -20S	GREY	3.3	13.3	65.9	17.6	A,C
89TB-03B	RED	0.5	22.8	60.9	15.7	A,C
82-10B	RED	0.0	37.2	55.9	6.9	A,C
F88-01	RED	0.0	23.1	61.9	14.9	A,B,C
NB-380	RED	3.9	13.6	68.9	17.6	A,B,C

A - smectite
B - mixed layer illite-smectite,
chlorite-smectite,
vermiculite-swelling chlorite,
or vermiculite-smectite
C - mixed layer chlorite-swelling chlorite

89TB-03B	KAMINISTIKWIA AREA
82-10B	KAMINISTIKWIA AREA
F88-01	FORT FRANCES
NB-380	FORT FRANCES

::

APPENDIX E

GRAIN SIZE DATA FOR SAMPLES FROM SECTION 87-19, FORT FRANCES, AND THE KAMINISTIKWIA AREA.

See Fig. 2-1 for location of 87-19, Appendix A for an annotated log of the section, and Appendix B for a description of the samples.

RHYTHMITE NUMBER	84th PERCENTILE (microns)	50th PERCENTILE (microns)	16th PERCENTILE (microns)	GRAPHIC MEAN SIZE (microns)
Dryden clay laminae				
+51C	1.60	0.56	0.16	0.52
+41C	1.50	0.52	0.14	0.48
+31C	1.40	0.42	0.11	0.40
+25C	1.40	0.46	0.11	0.41
+23C	1.50	0.56	0.16	0.51
+21C	0.70	0.20	0.08	0.22
+19C	1.40	0.50	0.13	0.45
+17C	1.40	0.50	0.17	0.49
+15C	1.40	0.56	0.18	0.52
+13C	0.98	0.33	0.15	0.36
+11C	1.10	0.42	0.13	0.39
+09C	1.60	0.60	0.18	0.56
+07C	1.20	0.54	0.19	0.50
+05C	0.94	0.40	0.14	0.37
+03C	1.10	0.60	0.29	0.58
+01C	1.70	0.56	0.17	0.54
-01C	1.40	0.50	0.12	0.44
-03C	1.80	0.54	0.14	0.51
-05C	1.40	0.46	0.11	0.41
-15C	1.70	0.52	0.13	0.49
-25C	1.20	0.40	0.10	0.36
-35C	1.40	0.46	0.11	0.41
Dryden silt laminae				
+46S	6.40	2.70	0.44	1.97
+26S	7.40	3.70	0.70	2.68
+21S	6.20	2.90	0.46	2.02
+11S	7.20	3.80	1.10	3.11
+09S	7.80	4.20	1.40	3.58
-03S	6.40	3.10	0.82	2.53
-05S	7.40	3.90	0.72	2.75
Kaministikwia samples				
82-10B	1.90	0.72	0.21	0.66
89TB-03B	1.50	0.60	0.18	0.55
Fort Frances samples				
F88-01	5.10	0.80	0.13	0.81
NB-380	1.20	0.42	0.1	0.37